PARAMETER-UNIFORM NUMERICAL METHODS FOR SINGULARLY PERTURBED CONVECTION-DIFFUSION BOUNDARY-VALUE PROBLEMS USING ADAPTIVE GRID

by

JUGAL MOHAPATRA

DEPARTMENT OF MATHEMATICS

INDIAN INSTITUTE OF TECHNOLOGY GUWAHATI

GUWAHATI-781039, INDIA

February, 2010

PARAMETER-UNIFORM NUMERICAL METHODS FOR SINGULARLY PERTURBED CONVECTION-DIFFUSION BOUNDARY-VALUE PROBLEMS USING ADAPTIVE GRID

A thesis submitted

in partial fulfillment of the requirements

for the degree of

DOCTOR OF PHILOSOPHY

by

Jugal Mohapatra

(Roll Number: 05612303)

to the

DEPARTMENT OF MATHEMATICS

INDIAN INSTITUTE OF TECHNOLOGY GUWAHATI

February, 2010

DECLARATION

It is certified that the work contained in this thesis entitled **"Parameter-Uniform Numerical Methods for Singularly Perturbed Convection-Diffusion Boundary-Value Problems using Adaptive Grid"** has done by me, under the supervision of **Dr. Natesan Srinivasan**, Associate professor, Department of Mathematics, Indian Institute of Technology Guwahati for the award of the degree of Doctor of Philosophy and this work has not been submitted elsewhere for a degree.

February, 2010

Jugal Mohapatra
Roll No. 05612303
Department of Mathematics
Indian Institute of Technology Guwahati

CERTIFICATE

It is certified that the work contained in this thesis entitled **"Parameter-Uniform Numerical Methods for Singularly Perturbed Convection-Diffusion Boundary-Value Problems using Adaptive Grid"** by **Jugal Mohapatra,** a student of Department of Mathematics, Indian Institute of Technology Guwahati, for the award of the degree of Doctor of Philosophy has been carried out under my supervision and this work has not been submitted elsewhere for a degree.

February, 2010

Dr. Natesan Srinivasan
Associate professor
Department of Mathematics
Indian Institute of Technology Guwahati

To

My Parents

Acknowledgement

First and foremost, I would like to express my deep and sincere gratitude to my thesis supervisor, **Dr. S. Natesan** for guiding me through my research; his careful guidance, constructive criticisms and valuable suggestions proved very stimulating and helpful. I am deeply indebted to him for his utmost care and making me feel free to express my views. Without his help, the work could not have been accomplished. Special thanks to his family for making me feel at home.

I owe my thanks to the members of my doctoral committee Prof. D. C. Dalal and Prof. R. K. Sinha and Dr. S. N. Bora for their helpful criticism and in overseeing the advancement of my work. I take this opportunity to express my gratitude to all the faculty members of the Department of Mathematics who have offered help directly or indirectly at different stages during my research work. My sincere thanks are due to Mr. Santanu for his technical support, Mr. Sridhar and Mr. Manoj of mathematics department for their assistance in all official matters.

Special thanks to Professor S. Pattanayak, Director, Institute of Mathematics and Applications, Bhubaneswar for his constant support during my M.Sc and encouraging me for pursing Ph. D.

I gladly acknowledge the Indian Institute of Technology Guwahati and the Council of Scientific and Industrial Research (CSIR) for providing fellowship during the period of my Ph.D. programme.

I take this opportunity to convey my gratefulness to my friends and co-researchers for all their timely help, encouragement and support. My love and thanks to have friends like Bibhas, Biswajit, Debajit, Gowri, Jyo, Laxmidhar, Murali, Nihar, Pratibhamoy, Raju, Ravi, Safique, Sanjeeb, Sasmita, Shubh, Smruti, Subash, Sunil and Tarakanta. I acknowledge their company for making my life at IIT Guwahati a great pleasure. My heartfelt thanks to "Dada" (my senior Kaushik) for his friendship, care and valuable suggestions throughout.

This work would have not been possible without the strong moral support and the unfailing faith of my parents (my mother Mrs. Sarita Mohapatra and my father Mr. Purna Chandra Mohapatra) that has sustained me throughout this endeavour. They have been a source of inspiration throughout my life and I dedicate this thesis to them. Special thanks to my nephew "GUDDU" who reminds me my childhood; his sweet smile and innocent questions kept me inspiring to move forward. I would like to convey my deepest love to my brother "Bimal", my sister "Mamata" and my brother-in-law "Bishnu" for all their care and affection that I can not forget in my whole life.

Last but not the least, thanks to my dear "Ladly" who shares a part of my soul and is always with me in every step of this journey and beyond.

February, 2010

With Regards

Jugal Mohapatra

Abstract

This thesis provides some efficient numerical techniques for solving singularly perturbed convection-diffusion boundary-value problems exhibiting boundary layers. These singular perturbation problems (SPPs) are described by differential equations in which the highest derivative is multiplied by an arbitrarily small parameter ε known as "singular perturbation parameter". This leads to the occurrence of boundary layers, which are basically thin regions in the neighbourhood of the boundary of the domain, where the gradients of the solutions steepen as the perturbation parameter ε tends to zero. Due to this layer phenomena, it is very difficult and also a challenging task to provide ε-uniform numerical methods *i.e.,* methods in which the approximate solution converges to the exact solution independently with respect to the perturbation parameter, measured in the supremum norm.

The convergence properties of some ε-uniform numerical methods are developed and analyzed in this thesis for solving SPPs using nonuniform grids. Especially two types of nonuniform grids are discussed here. They are the well-known piecewise-uniform *Shishkin mesh* and the newly developed *adaptive grid* which is based on the equidistribution of a strictly positive monitor function depending on the solution. These nonuniform grids are so chosen as to give a numerical solution that is uniformly accurate with respect to the singular perturbation parameter.

This thesis consists of eight chapters. Chapter 1 contains the general introduction and it also provides the motivation and objective for solving SPPs. Chapter 2 presents a brief discussion on the generation of the Shishkin mesh and the adaptive grid and proposes an algorithm for the practical implementation of an adaptive remeshing strategy. A model convection-diffusion problem is solved using the upwind scheme on this adaptively generated grid formed by the arc-length monitor function. Here, the first-order accurate global solution *via* interpolation and the first-order approximation to the normalized flux are found out on this adaptively generated grid and also their uniform convergence analysis is carried out in the whole domain. The monitor function remains the same irrespective of the location of the boundary layer (on left or right) of the domain which shows the advantage of using such kind of adaptive grid over the Shishkin mesh. Again, the same monitor function is used in Chapter 3 for solving a model convection-diffusion problem with Robin boundary conditions and achieves the optimal rate of convergence in the discrete supremum norm.

The adaptive grid idea is then extended for solving the singularly perturbed differential-difference equations with the delay and the shift terms, for the first time in the literature in Chapters 4 and 5. The error analysis is carried out for the classical upwind scheme on the adaptive grid and an optimal first-order convergence is obtained.

Next, two higher-order methods are discussed for solving the singularly perturbed delay differential equations on the Shishkin mesh namely: *the Richardson extrapolation technique* (a post-processing technique) and *the defect-correction method* in Chapters 6 and 7, respectively, which give almost second-order convergence improving the almost first-order convergence of the upwind scheme.

Finally, Chapter 8 summarizes the results obtained by this thesis. It also provides a few possible extensions of the adaptive grid idea with the post-processing techniques and contains some numerical experiments for supporting the proposal.

Contents

NOMENCLATURE

SPP	Singular Perturbation Problem
SPDDE	Singularly Perturbed Differential-Difference Equation
BVP	Boundary-Value Problem
FMM	Fitted Mesh Method
ODE	Ordinary Differential Equation
PDE	Partial Differential Equation
$\mathbb{R}$	Set of real numbers
ε	Singular perturbation parameter
δ and η	Delay and shift parameter
C	Generic positive constant independent of $\varepsilon, \delta, \eta, h, x_j$
$O(\cdot)$, $o(\cdot)$	Landau order symbols
N	Number of mesh intervals
x, x_i, x_j	Independent variables
h_i, h_j	Mesh width of a nonuniform mesh
$u(x), u_\varepsilon(x)$	Solution of continuous problem
U_i, U_i^N, U^N	Numerical solution
Ω	Open interval $(0, 1)$
$\overline{\Omega}$	Closed interval $[0, 1]$
$\partial\Omega$	Boundary of the domain Ω
$\Omega^N, \overline{\Omega}^N$	Discrete domain
$\mathcal{C}^{(k)}(\Omega), \mathcal{C}^{(k)}(\bar{\Omega})$	k times continuously differentiable functions in the respective domain
$\lvert\cdot\rvert$	Absolute value
$\lVert\cdot\rVert$ or $\lVert\cdot\rVert_D$	Supremum norm over the domain D
$L, L_\varepsilon, \mathscr{L}_\varepsilon, \mathfrak{L}_\varepsilon$	Differential operators
$L^N, L_\varepsilon^N, \mathscr{L}_\varepsilon^N, \mathfrak{L}_\varepsilon^N$	Difference operators
D^+, D^-	Forward and backward difference operators
$D^0, D^\pm$	Central and modified central difference operators
$E_\varepsilon^N, E^N, G_\varepsilon^N, G^N, \mathscr{E}_\varepsilon^N$	Maximum point-wise errors
$r_\varepsilon^N, r^N, q_\varepsilon^N, q^N, \mathscr{R}_\varepsilon^N$	Rates of convergence

List of Figures

List of Tables

Chapter 1

Introduction

1.1 Singular Perturbation Problem

The study of singular perturbation problems (SPPs) are so important as they arise in several branches of engineering and applied mathematics. Typical examples include high Reynold's number flow in fluid dynamics, heat transport problems with large Pécklet number, modelling the problems in mathematical biology and semi-conductor devices where the edge effects are important. These problems are often described by differential equations which are parameter-dependent problems and are known as singular perturbation problems (SPP). For example, the Navier-Stokes equations of fluid dynamics

$$\frac{\partial(u^2+p)}{\partial x}+\frac{\partial(uv)}{\partial y}=\frac{1}{Re}\left(\frac{\partial^2 u}{\partial x^2}+\frac{\partial^2 u}{\partial y^2}\right) \tag{1.1.1}$$

with some suitable initial and boundary conditions where u, v are velocity component along x, y directions and p is the pressure, is a well-known example of SPP for large Reynolds number 'Re' *i.e.,* for $Re \gg 1$. The Reynolds number 'Re' is proportional to the length scale, the velocity scale and inversely proportional to the kinematic viscosity of the fluid. Considering the flow of water, where the velocity of the flow is very large, such that, $Re \geq 10^3$, then the problem poses considerable amount of numerical difficulties due to the presence of a thin layer surrounding the rigid wall.

Another area in which these types of problems arise is the modelling of the semi–conductor devices where the governing equations are given by

$$\begin{cases} v''(x) = d(x) - p(x). \\ \\ \lambda p''(x) + v'(x)p'(x) + \big(d(x) - p(x)\big)p(x) = 0. \end{cases} \tag{1.1.2}$$

Here, v is the electrostatic potential, p is the density of positive charged holes, d is the dopant density of negative charges and $0 < \lambda \ll 1$ is a small diffusion coefficient. The equations (1.1.1) and (1.1.2) are often referred as convection-diffusion equations. Several other examples can be found in the book of Morton [63] and in the survey articles of Lagerstrom and Casten [52], Kadalbajoo

and Patidar ([37], [38]). Another class of equations that can be singularly perturbed is the reaction-diffusion class; mostly found in mathematical biology, forming the coloured patterns of the skins of animals and in evolution of chemical reactions. A large number of such examples (though not considered in this thesis) can be found in the book of Murray [64].

The birth of singular perturbation problems occurred at the Third International Congress of Mathematicians in Heidelberg in 1904. Prandtl's seven page report published in the proceedings [80] innovated the subject called the *boundary layer theory* and gave an explanation that how a quantity as small as the viscosity of common fluids such as water and air could play a crucial role in determining their flow. Prandtl proved that the flow about a body can be treated by dividing it into two regions: a very thin layer in proximity to the body (which he called the boundary layer) where the frictional effects are prominent, and the remaining as the outside region. On the basis of this hypothesis, Prandtl emphasized the importance of viscous flows without delving into the mathematical complexities involved. The boundary layer theory became the foundation stone for modern fluid dynamics. However, the word "*singular perturbations*" was first used in the work of Friedrichs and Wasow [30], a paper on nonlinear vibrations presented at New York University. Though Prandtl introduced the terminology boundary layer, it got much greater generality in the substantial work of Wasow [99].

A differential equation becomes singularly perturbed when the magnitude of the highest derivative is dominated by the lower order terms and is often attributed to a small parameter (ε) multiplying the highest derivative. The small parameter is called the *singular perturbation parameter*. So it is natural to pose a question about the role of ε, where $0 < \varepsilon \ll 1$. Singular perturbation are manifested in the solution of differential equation as steep, thin layers at the boundaries and interior of the domain across which the dependent variable undergoes very rapid changes. These narrow regions frequently adjoin the boundaries usually referred as boundary layers in fluid mechanics, edge layers in solid mechanics, transition point in quantum mechanics and skin layers in electrical applications. It is well-known that the solution of SPP has a multiscale character as it varies rapidly within the boundary layer and behaves smoothly away from these layers. A direct numerical solution of the SPP is difficult due to the presence of thin boundary layer. Therefore, it is desirable to develop numerical methods, more precisely ε-uniform that solve the singularly perturbed differential equations effectively. This is indeed the reason why the methods of singular perturbation are of practical interest.

Numerical analysis and asymptotic analysis are the two principal approaches for solving SPPs. The numerical analysis tries to provide quantitative information about a particular problem, whereas the asymptotic analysis tries to gain insight into the qualitative behavior of a family of problems and only semi-quantitative information about any particular member of the family. Numerical methods are intended for a broad class of problems and to minimize demands upon the

problem solver. Asymptotic methods treat comparatively restricted class of problems and require the problem solver to have some understanding of the behavior of the solution. Since the mid-1960s, singular perturbations have flourished, the subject is now commonly a part of graduate students training in applied mathematics and in many fields of engineering. Numerous good textbooks have appeared in this area which either dealt with the asymptotic approach or with the numerical ones. Some of the books dealt with both of these. The list is quite long but we mention a few of them. They are Bender and Orszag [10], Dingle [20], Doolan et al. [21], Eckhaus ([23], [24]), Erdelyi [25], Farrell et al.[28], Hemker and Miller [35], Holmes [36], Kaplaun [44], Kevorkian and Cole([47], [48]), Miller et al. [62], Nayfeh ([73], [74]) and Roos et al. [84].

Mathematicians and engineers study the behavior of the analytical solution of SPPs through asymptotic expansion technique as ε goes to zero. This is the principle analytical approach to enter insight the qualitative properties of these multi-scale problems. A straightforward perturbation expansion using an asymptotic series in the small parameter ε leads to differential equations of lower order than the original governing equation. In consequence not all of the boundary or initial conditions can be satisfied by the perturbation expansion. The technique for overcoming this difficulty is to combine the straightforward expansion known as the *outer expansion* valid away from the boundary layer, with an expansion called the *inner expansion* valid within a layer adjacent to this boundary where the boundary condition is not satisfied. The inner expansion associated within the boundary layer region is expressed in terms of a stretched variable rather than the original independent variable, which takes account of the scale of certain derivative terms. The inner and outer expansions are matched over a region located at the edge of the boundary layer using the method of matched asymptotic expansions. Note that one has to know the width and the location of the boundary layer before solving the problem which can be obtained using the principle of least degeneracy by Van Dyke [22]. For more details, one can refer to the books of Bush [13], Lagerstrom [51], O' Malley ([75], [76]) and the survey articles of Lagerstrom and Casten [52] and Smith [88].

Most contemporary numerical methods (standard finite difference/element/volume methods) are not robust and layer-resolving when applied to solve SPPs on uniform meshes. By saying that standard or classical finite difference methods, we mean numerical methods that have been applied successfully to problems which are not singularly perturbed. Due to the presence of steep gradients in the analytical solution, inaccurate numerical solutions are obtained whenever the classical numerical methods are used to solve SPPs with boundary or interior layers on uniform meshes . In this context, careful numerical experiments ([28], [61]) show that the classical methods fail to decrease the maximum point-wise error as the mesh is refined, until the mesh parameter and the perturbation parameter have the same order of magnitude. This contradicts the natural expectation that the error of a numerical method decreases while the mesh is refined. Also, from the practical point

of view, this assumption is not acceptable due to the fact that when ε becomes very small, *i.e.,* its size is of the order of 10^{-8} or 10^{-10}, an undesirably large (ε-dependent) number of mesh points are required to achieve an accurate numerical solution thus resulting a vast computational cost. This drawback motivates to develop ε-uniform numerical methods *i.e.,* methods in which the error constant and the order of convergence are independent of the perturbation parameter. Therefore, in the study of SPPs, the most challenging job is to develop such ε-uniform numerical methods.

In the construction of ε-uniform numerical methods, two approaches generally been taken to date. A finite difference method has two major ingredients: the finite difference operator L^N that is used to approximate the differential operator L and the mesh Ω^N that replaces the continuous domain Ω. The first of these ε-uniform methods involve replacing the standard finite difference operator by an operator which reflects the singularly perturbed nature of the differential operator. Such finite difference operators are referred as fitted finite difference operators and they may be constructed by choosing their coefficient so that some or all of the exponential functions are in the null space of the differential operator. Such exponentially fitted finite difference operator and a standard mesh (which in practise is often a uniform mesh) are referred as *fitted operator methods*. Such fitted operator methods were first suggested in Allen et al. [19] for solving the problem of the flow of a viscous fluid past a cylinder. One can find an extensive amount of ε-uniform fitted operator methods in Berger et al. ([11], [12]), Stynes and O'Riordan [91] and in the books of Doolan et al. [21] and Miller et al. [62]. However, Farrell [27] proved that in some cases the fitted finite difference operator is required only in a neighborhood of the layers, while a standard finite difference operator can be used on the mesh points in rest part of the domain.

The second successful approach to the construction of ε-uniform numerical methods involves the use of standard finite difference operators on a special mesh condensed in the boundary or interior layers. Such methods are referred as *fitted mesh methods*. The fitted mesh method utilizes special nonuniform meshes condensed around the layer region and hence, a recognized technique for solving SPPs overcoming the limitation of the classical methods. These *fitted mesh methods* have an extra advantage over the *fitted operator methods* due to their easy implementation and extension to solve higher dimensional and nonlinear problems. This idea is widely used to solve a broad class of problem due to the fact that the accuracy of the fitted mesh methods depends only on the number of nodes and is independent of the value of the small parameter. The underlying idea is to construct a piecewise-uniform mesh, that is a mesh which is the union of finite number of uniform meshes having different mesh sizes inside and outside the layers. If the location and the width of the boundary layer are known, then highly accurate piecewise-uniform mesh known as the *Shishkin mesh* can be easily constructed. These uniform fitted meshes were first introduced by Shishkin [86] and the corresponding numerical methods are further developed and shown ε-uniform in ([28], [84]). Different approaches involving complicated redistribution of mesh points have been taken by

several other authors ([5], [33]) but none has the simplicity of the piecewise-uniform Shishkin mesh.

The above two approaches are based on the *a priori* knowledge of the solution before solving the original problem which is not always available. For solving SPPs, the aim is to cluster automatically the grid points within the boundary layer. A commonly used technique for determining the grid points that they equidistribute a positive function of the solution over the domain. (see, for example Pereyra and Sewel [79], Russell and Christiansen [85] and White [100]). The positive function is known as the *monitor function* and has to be approximated from the numerical solution of the original problem. The adaptive grid approach has the advantage that it can be applied using little or no *a priori* information about the width and the location of the boundary layer. The monitor function automatically detects the presence of the boundary layers together with their location and width and distribute mesh points accordingly if layers are of different thickness. This equidistributed grid is exponentially stretched within the boundary layers and therefore, responsible for an improved rate of convergence compared to the related piecewise-uniform Shishkin mesh. Hence, for solving singular perturbation problems, an obvious choice of adaptive criterion is therefore the solution gradient. Now-a-days, these *adaptive grid* methods are established as a valuable computational technique in approximating effectively the solutions of problems with boundary (or interior) layers.

1.2 Objective and Motivation

The main theme of this thesis revolves around developing, analyzing and optimizing the ε-uniform upwind based fitted mesh methods resolving the convection-dominated boundary-value problems (BVP) using the above two kinds of nonuniform grids namely; the piecewise-uniform *Shishkin mesh* and the newly developed *adaptive grid*. A brief survey of the literature illustrating the motivation behind the work carried out in this thesis, are presented below:

Over the last few decades, the numerical solutions of SPPs have received much attention. The literature of approximating the solutions of convection–diffusion problems is large and many finite difference/element/volume methods have been proposed to approximate the solutions. One may refer the books ([21], [62], [84], [87]) and the articles ([1], [27], [49], [58], [60], [61], [83], [88], [90], [92]) and the references therein. Also one can refer the articles ([6], [67], [68], [69], [70], [95], [96]) where Natesan and his collaborators have made a significant contribution to the field of SPP by developing several initial and parallel boundary-value techniques for solving singularly perturbed BVPs. Most of the articles cited above used the piecewise-uniform Shishkin mesh to approximate the solution of convection-diffusion BVPs. At the same time, several authors ([7], [8], [9], [15], [16], [50], [59], [81], [82]) used the adaptive grid for solving convection-diffusion problems, where the upwind finite difference scheme is applied on a nonuniform mesh formed by equidistributing a positive monitor function depending on the solution. All of them show the first-order convergence

of the numerical solution measured in the discrete maximum norm. However, there are less number of research articles for approximating the global solution. Recently, Clavero et al. [17] and Natesan et al. [66] used a hybrid finite difference scheme for obtaining the global solution for a class of reaction-diffusion problems using the Shishkin mesh. In this context, one can naturally ask: *"Can we extend the idea of adaptive grid approach for obtaining an uniformly accurate global solution for singularly perturbed convection-diffusion BVPs ?"*

Many researchers used finite difference methods for approximating the unwieghted and the ε-weighted derivatives (in the literature, it is also known as the *normalized flux*) of the solution. Such approximations are desirable in certain applications, for example, the normal derivatives are required to compute the skin friction coefficients and to calculate the stress intensity factors. There are only a few articles that consider the finite difference approximations of the derivatives of the solutions of the convection-diffusion BVPs. Ervin and Layton [26] approximated the unweighted derivative of the convection-diffusion problem only outside the boundary layer using the uniform mesh. Kopteva and Stynes [49] used special kind of nonuniform meshes namely, the piecewise-uniform Shishkin mesh and the Bakhvalov mesh to derive the derivative approximation on the entire domain where the model equation is in the conservative form. Here, the same question can be asked *"whether the upwind scheme on the adaptively generated grid can be used for approximating both the normalized flux and the global normalized flux for such convection-diffusion problems ?"*.

Recently, Cai and Liu ([14]) used a class of conservative difference schemes on the uniform mesh for approximating the solution of convection-diffusion problems with Robin type boundary conditions which is difficult to implement. Natesan et al. ([65], [71]) solved the reaction-diffusion problem with mixed boundary conditions using the Shishkin mesh. At the same time, Ansari and Hegarty ([4]) used the piecewise-uniform Shishkin mesh to solve the mixed BVP and derived an approximation to the solution which is of almost first-order *i.e.,* first-order upto a logarithmic factor. Therefore, the natural question is: *"Can we develop a uniformly convergent numerical scheme which is more accurate (optimal) for solving singularly perturbed convection-diffusion BVP with mixed type boundary conditions using the adaptive grid ?"*

Singularly perturbed differential-difference equations (SPDDE) are widespread in many mathematical models of biophysics and mechanics where the delay and the shift terms play an important role in modelling the real-life phenomena ([54], [55], [89], [93]). Problems of this type occur when the future depends not only on the immediate present, but also on the past history of the system under consideration. Such problems are sometimes addressed as two-parameter problems. Lange and Miura ([53]-[57]) provided an asymptotic approach to solve SPDDE having both the delay and the shift terms and showed that the effect of the small delay and the shift terms on the solution cannot be neglected. The computation of the solution of delay differential equations has been a great challenge and of great importance due to the appearance of such equations in mathematical

modelling of biological problems. Amiraliyev and Erdogan [2] proposed a numerical scheme to solve an initial value problem having only the delay term. Now it is desirable to develop uniformly convergent numerical methods for solving singularly perturbed differential-difference boundary value problems. Patidar and Sharma ([77], [78]) used a non-standard finite difference scheme for solving such kind of equations where as Kadalbajoo et al. ([39], [40], [41], [42]) applied the fitted operator methods or the piecewise-uniform Shishkin mesh for solving these type of problems. So far no result exists, where the adaptive grid technique is used for solving SPDDE. This raises the same question of *using the adaptive grid approach for solving SPDDE having only the delay term and having both the delay and the shift terms.*

Next, in view of increasing the accuracy of numerical methods with less complexity, we draw our attention to construct and analyze two simple post-processing techniques that can be applied to the standard upwind scheme for solving singularly perturbed delay differential equations on the Shishkin mesh. The Richardson extrapolation technique, a well-known post-processing technique which provides a better approximation to the exact solution obtained by averaging the numerical solutions computed on two embedded meshes. This method has been studied in the literature by a few researchers ([29], [45], [98]). But their analysis based on the direct expansion of the upwind solution, is found to be complicated. However, Natividad and Stynes [72] provided a comparatively easier analysis to deal with the Richardson extrapolation for singulary perturbed convection-diffusion BVP. In this thesis, the Richardson extrapolation technique is studied by extending their analysis for solving the singularly perturbed delay differential equation. It is shown both theoretically and computationally that how the solution after extrapolation converges uniformly with respect to the perturbation parameter in the discrete supremum norm with an accuracy of almost order two.

Finally, another kind of post-processing technique namely; the defect-correction method for solving the singularly perturbed delay differential equations on the Shishkin mesh is discussed. The defect-correction method has been studied by many researchers ([31], [32], [34]) for solving singulary perturbed convection-diffusion BVP with only one parameter. By applying their technique for singularly perturbed delay differential equations, it is proved that the defect-correction method gives almost second-order convergence improving the almost first-order convergence of the upwind scheme.

1.3 Preliminaries

This section introduces some basic definitions, notations and conventions which will be used throughout the thesis.

First of all, Ω denotes a bounded open interval in $\mathbb{R}$ and is given by $\Omega = (0, 1)$. For any non-negative integer k, $\mathcal{C}^k(\Omega)$ denotes the space of all functions whose derivatives are continuous upto

order k on Ω. In the analysis, the standard supremum norm $\|\cdot\|$ or $\|\cdot\|_D$ is used, which is defined by

$$\|g\| = \sup_{\xi \in D} |g(\xi)|,$$

for a function g on some domain D. It is a convention that when the domain is obvious, or of no particular significance, D is omitted. For any discrete function ϕ_i, define the norm $\|\cdot\|_*$ as

$$\|\phi\|_* = \max_{i=1,\ldots,N-1} \left| \sum_{j=i}^{N-1} h_{j+1}\phi_i \right|.$$

Note that

$$\|\phi\|_* \leq \|\phi\| \quad \text{and} \quad \|D^-\phi\|_* \leq 2\|\phi\|,$$

where D^- is the backward difference operator defined below.

Now, the standard finite difference operators are defined which will be used for describing the difference schemes in the subsequent chapters. Consider an arbitrary nonuniform mesh $\overline{\Omega}^N = \{x_j\}_{j=0}^N$ given by

$$\overline{\Omega}^N = \{0 = x_0 < x_1 < x_2 < \ldots < x_{N-1} < x_N = 1\}.$$

Let us denote $h_j = x_j - x_{j-1},\ j = 1, \ldots, N$. For a mesh function Z_j, the forward, backward and central difference operators D^+, D^- and D^0 are given as:

$$D^+Z_j = \frac{Z_{j+1} - Z_j}{h_{j+1}}, \quad D^-Z_j = \frac{Z_j - Z_{j-1}}{h_j}, \quad D^0Z_j = \frac{Z_{j+1} - Z_{j-1}}{h_{j+1} + h_j},$$

respectively. In addition, we also define a modified central difference operator $D^\pm$ and the second-order finite difference operator D^+D^- in the following manner:

$$D^\pm Z_j = \frac{h_j D^+Z_j + h_{j+1}D^-Z_j}{h_j + h_{j+1}}, \quad D^+D^-Z_j = \frac{2}{h_j + h_{j+1}}\left(\frac{Z_{j+1} - Z_j}{h_{j+1}} - \frac{Z_j - Z_{j-1}}{h_j}\right).$$

Throughout this thesis C denotes a generic positive constant independent of the grid points x_j and the parameter ε and the number of mesh intervals N which can take different values at different places, even in the same argument. But a subscripted C (*i.e.,* C_1) is a fixed constant. Also, we assume that

$$\varepsilon \leq CN^{-1} \tag{1.3.1}$$

as is generally the case of discretization of the SPPs. It is worthwhile to mention that this assumption is not a restriction in practical situation. This inequality is used in the proof of some theorems. If $\varepsilon > N^{-1}$, then in practice the model problems considered in this thesis are not difficult to solve computationally.

Finally, this section is concluded by introducing the following definitions to be used throughout the thesis. One can refer the books ([28], [84], [94]) for further discussions on the following definitions.

Definition 1.3.1. ***Boundary layer*** *is defined as that region of the independent variables where the dependent variables change rapidly.*

Definition 1.3.2. *A sequence of order functions* $\delta_n(\varepsilon),\ n = 0, 1, \ldots$ *is called* **an asymptotic sequence** *if for* $n = 0, 1, \ldots,\ \delta_{n+1} = o(\delta_n),\ as\ \varepsilon \to 0.$

Definition 1.3.3. *The sum* $\sum_{n=0}^{m} a_n f_n(\varepsilon)$ *with constant coefficient* a_n *is called* **an asymptotic series** *if* $f_n(\varepsilon),\ n = 0, 1, \ldots, m$ *is an asymptotic sequence.*

To measure the performance and the robustness of a numerical method, let us introduce the concept of uniform accuracy.

Definition 1.3.4. **ε-uniform numerical method:** *Consider a family of mathematical problems parameterized by a parameter* ε*, where* ε *lies in the semi-open interval* $0 < \varepsilon \ll 1$*. Assume that each problem in the family has a unique solution denoted by* u_ε *and that of each* u_ε *is approximated by a sequence of numerical solution* $U_\varepsilon, \overline{\Omega}^N$ *where* U_ε *is defined on the discrete space* $\overline{\Omega}^N$ *and* N *is the discretization parameter. Now the numerical solution* U_ε *is said to converge* ε*-uniformly to the exact solution* u_ε*, if there exist a positive integer* N_0 *and positive numbers 'C' and* p*, where* N_0, C, p *all are independent of* ε *such that for all* $N \geq N_0$

$$\sup_{0<\varepsilon\ll 1} \|U_\varepsilon - u_\varepsilon\| \leq CN^{-p}.$$

Here p *is called the* ε*-uniform rate of convergence and* C *is called the* ε*-uniform error constant.*

The above definition may be interpreted as follows. If a numerical method is ε-uniform convergent, then for all values of $0 < \varepsilon \leq 1$, no matter how small, the pointwise error at the mesh points is never greater than CN^{-p}, for all values of $N \geq N_0$. Notice that since C, p and N_0 are independent of ε, it follows that the upper bound on the error is independent of ε.

The choice of the maximum norm for the measurement of the error is due to the need to measure the error in the very small subdomains in which the boundary (or interior) layer occurs. Other norms, such as the root mean square, involve the averages of the error which smooth out the rapid changes in the solutions and therefore, may fail to capture the local behaviour of the errors in these layers. Further discussion on the choice of the norm can be found in the book of Miller et al. [62].

Definition 1.3.5. *A matrix* $\mathbf{A} = (a_{i,j}) \in \mathbb{R}^{n\times n}$ *is an* M*-matrix if* $\mathbf{A}$ *is nonsingular,* $\mathbf{A}^{-1} \geq 0$ *and* $a_{i,j} \leq 0 \quad \forall i \neq j,\ 1 \leq i, j \leq n.$

Lastly, we define the **Landau's order symbol** O **(big-oh) and** o **(small-oh)** which are used in this thesis.

Definition 1.3.6. *Let $f(\varepsilon)$ and $g(\varepsilon)$ be two real valued functions and $0 < \varepsilon \leq \varepsilon_0 \ll 1$. The expression $f(\varepsilon) = O(g(\varepsilon))$ as $\varepsilon \to 0$ means that there exists some positive constant C, ε_0 such that in $(0, \varepsilon_0]$,*

$$|f(\varepsilon)| \leq C|g(\varepsilon)|, \qquad as \quad \varepsilon \to 0.$$

Similarly, the expression $f(\varepsilon) = o(g(\varepsilon))$ as $\varepsilon \to 0$ means

$$\lim_{\varepsilon \to 0} \frac{f(\varepsilon)}{g(\varepsilon)} = 0.$$

To simplify the notation, we also set $g_j = g(x_j)$ for any function g, while g_j^N denotes an approximation of g at x_j.

1.4 Model Problems

Here, in this section, the model problems considered in this thesis are briefly described. But to have a clear idea, we elaborately provide these model problems with suitable boundary conditions at the beginning of the subsequent chapters.

The following four types of model problems are considered and their concise description are given below:

1.4.1 Singularly perturbed convection-diffusion Dirichlet boundary-value problems

Consider the following singularly perturbed BVP:

$$\begin{cases} Lu(x) \equiv -\varepsilon u''(x) - a(x)u'(x) + b(x)u(x) = f(x), \ x \in \Omega = (0,1), \\ u(0) = s_0, \quad u(1) = s_1, \end{cases} \tag{1.4.1}$$

where $0 < \varepsilon \ll 1$ is a small parameter, the functions $a(x), b(x), f(x)$ are sufficiently smooth and s_0, s_1 are given constants. Further, we assume that

$$a(x) \geq \alpha > 0 \ \text{ and } \ b(x) \geq 0, \qquad \forall x \in \overline{\Omega}.$$

Under these assumptions, the BVP (1.4.1) has a unique solution which exhibits a boundary layer of width $O(\varepsilon)$ at $x = 0$.

1.4.2 Singularly perturbed convection-diffusion problems with Robin boundary conditions

Consider the following form of singularly perturbed mixed BVP:

$$\begin{cases} Lu(x) \equiv -\varepsilon u''(x) - a(x)u'(x) + b(x)u(x) = f(x), \ x \in \Omega = (0,1), \\ B_0 u(0) \equiv \beta_1 u(0) - \beta_2 \varepsilon u'(0) = s_0, \quad B_1 u(1) \equiv \lambda_1 u(1) + \lambda_2 u'(1) = s_1, \end{cases} \tag{1.4.2}$$

where $0 < \varepsilon \ll 1$ is a small parameter, the functions $a(x), b(x), f(x)$ are sufficiently smooth such that $a(x) \geq \alpha > 0,\ b(x) \geq 0$ and s_0, s_1 are given constants. Further, we assume that the constants satisfy

$$\beta_1, \beta_2 \geq 0,\ \beta_1 + \beta_2 > 0,\ \lambda_1 > 0 \quad \text{and} \quad \lambda_2 \geq 0.$$

Under these assumptions, the BVP (1.4.2) admits a unique solution exhibiting a boundary layer near $x = 0$.

1.4.3 Singularly perturbed delay differential equations

Here, we consider the following singularly perturbed delay differential equation:

$$\begin{cases} \mathcal{L}_\varepsilon u_\varepsilon(x) \equiv -\varepsilon u_\varepsilon''(x) - a(x)u_\varepsilon'(x-\delta) + b(x)u_\varepsilon(x) = f(x), \quad x \in \Omega = (0,1), \\ u_\varepsilon(x) = \gamma(x), \quad -\delta \leq x \leq 0, \qquad u_\varepsilon(1) = \lambda\,, \end{cases} \tag{1.4.3}$$

where $0 < \varepsilon \ll 1$ is a small parameter and the delay parameter δ is such that $0 < \delta < 1$, which is of $o(\varepsilon)$. The functions $a(x), b(x), f(x)$ and $\gamma(x)$ are sufficiently smooth and λ is a given constant. It is also assumed that $a(x) > 0,\ b(x) \geq 0, \forall x \in \overline{\Omega}$. Under these assumptions, the problem (1.4.3) has a unique solution which exhibits a boundary layer at $x = 0$.

When $\delta = 0$, the differential equation (1.4.3) becomes a singularly perturbed differential equation with a single parameter ε as given in (1.4.1). Depending on the sign of $a(x)$, *i.e.,* if $a(x) > 0$ (or $a(x) < 0$), a boundary layer is located at left (or right) end of the domain. The layer is maintained for sufficiently small δ with $\delta \neq 0$ and $\delta = o(\varepsilon)$. Lange and Miura ([53]-[57]) provided an asymptotic approach for solving the SPDDE having both the delay and the shift terms and showed that the effect of the small delay and the small shift terms can not be neglected. For $\delta = \kappa\varepsilon > 0$, where κ is sufficiently small, we follow the same technique done in ([53], [56]). To tackle the delay term, we expand the delay term through the Taylor's series expansion assuming sufficient smoothness condition on the solution of (1.4.3) so that the BVP (1.4.3) reduces to a standard singular perturbation problem.

1.4.4 Singularly perturbed differential-difference equations

Consider the following SPDDE in the domain $\Omega = (0,1)$:

$$\begin{cases} \mathbb{L}_\varepsilon u_\varepsilon(x) \equiv -\varepsilon u_\varepsilon''(x) - p(x)u_\varepsilon'(x) - \alpha(x)u_\varepsilon(x-\delta) + q(x)u_\varepsilon(x) - \beta(x)u_\varepsilon(x+\eta) = F(x), \\ u_\varepsilon(x) = \phi(x), \quad -\delta \leq x \leq 0, \\ u_\varepsilon(x) = \gamma(x), \quad 1 \leq x \leq 1+\eta, \end{cases} \tag{1.4.4}$$

where $0 < \varepsilon \ll 1$ is the perturbation parameter, the functions $p(x), \alpha(x), q(x), \beta(x)\ F(x), \phi(x)$ and $\gamma(x)$ are sufficiently smooth functions and the delay parameter δ and the shift parameter η are such that $0 < \delta, \eta \ll 1$, both are of $o(\varepsilon)$.

Here, we follow the same technique as done in [53], [56] and expand the delay and the shift terms through Taylor's series expansion assuming sufficient smoothness condition on the solution of (1.4.4) so that the BVP (1.4.4) reduces to a standard singular perturbation problem.

1.5 Outline of the Thesis

This thesis consists of eight chapters. **Chapter** 1 is devoted to the general introduction along with the historical background of the related work done in the field of SPP. In particular, it provides the motivation and objective for solving SPPs and also the preliminaries to be used in the thesis. The rest of the thesis is organized as follows:

In **Chapter** 2, the BVP (1.4.1) is solved by applying the upwind scheme for obtaining the solution and the global normalized flux on a suitable nonuniform mesh which is formed by equidistributing the arc-length monitor function depending on the numerical solution. It is shown that the discrete solution obtained by the upwind scheme and the global solution obtained *via* interpolation converge uniformly with respect to the perturbation parameter ε. In addition, the uniform first-order convergence of the weighted derivative of the numerical solution on this nonuniform mesh and the uniform convergence of the global normalized flux on the whole domain are proved. Our results are compared with the Shishkin mesh results which shows the advantage of using such adaptive grid.

The singularly perturbed Robin BVP (1.4.2) is solved in **Chapter** 3 by applying the upwind scheme on the adaptive grid based on the equidistribution principle. The error analysis for the numerical solution is carried out and it is shown that the error converges at the rate of first-order, independent of the singular perturbation parameter. Numerical results obtained for some examples show that the proposed scheme is of first-order accurate.

The rest part of the thesis is solely devoted to the study of the numerical schemes for singularly perturbed differential-difference equations.

In **Chapter** 4, a numerical method is proposed to solve the problem of type (1.4.3) which comprises of the upwind finite difference scheme on the adaptive grid. The adaptive grid is formed with the help of a positive monitor function which contains the first derivative of the solution. The error analysis for the numerical solution is carried out which shows the ε-uniform convergence of the proposed method. From the theoretical and numerical results presented, one can conclude that the errors converge at the rate of first-order, independent of the small perturbation parameters. Hence if the mesh is generated adaptively, it is possible to obtain approximate solutions that converge

uniformly without depending on the small parameters.

In **Chapter** 5, the idea of adaptive grid technique discussed in Chapter 4 is extended to solve the SPDDE having both the delay and the shift terms of the form (1.4.4). The maximum principle, stability results and some *a priori* estimates on the solution and its derivatives are established. The upwind finite difference discretization is used on the adaptive grids and the bounds for the local truncation error and the maximum point-wise errors are derived. It is shown both theoretically and numerically that the proposed scheme is of ε-uniformly convergent and of first-order accurate.

In the following two chapters, two higher-order methods are discussed which improve the accuracy of the standard upwind scheme applied on the piecewise-uniform Shishkin mesh to the singularly perturbed delay differential equation of the form (1.4.3).

Chapter 6 deals with the study of a post-processing technique known as the Richardson extrapolation technique for solving the singularly perturbed delay differential equation of the type (1.4.3). The Richardson extrapolation technique is a well-known postprocessing method where two computed solutions are approximated by an average quantity to provide a better approximation. First, the BVP (1.4.3) is solved on the piecewise-uniform Shishkin mesh by the upwind finite difference scheme to get the numerical solution U^N and the convergence analysis is carried out to obtain the optimal error of order of convergence *i.e.*, $O(N^{-1}\ln N)$. By keeping the transition parameter fixed on the Shishkin mesh, the solution U^{2N} using $2N$ number of mesh intervals is calculated. Then the Richardson extrapolation technique is implemented. It is proved both theoretically and computationally that after extrapolation, the rate of convergence of the upwind scheme is raised from almost first-order *i.e.*, $O(N^{-1}\ln N)$ to almost second-order *i.e.*, $O(N^{-2}\ln^2 N)$.

Chapter 7 is devoted to the study of a defect-correction method based on the finite difference scheme for solving the singularly perturbed delay differential equation of type (1.4.3) on the Shishkin mesh. The BVP (1.4.3) is solved first by using the upwind finite difference scheme and then by the defect-correction method. The defect-correction method combines the stability of the upwind scheme and the higher-order convergence of the central differences scheme. It is shown both theoretically and numerically that by using the defect-correction method, the rate of convergence of the upwind scheme is increased from almost first-order to almost second-order *i.e.,* from $O(N^{-1}\ln N)$ to $O(N^{-2}\ln^3 N)$.

Finally, **Chapter** 8 is concerned with a brief summary of the results highlighting the contribution made by this thesis. It also provides various ideas for the scope of future investigation.

Extensive numerical experiments are conducted to support the theoretical findings and also to demonstrate the accuracy of the proposed numerical methods. The computational results for the corresponding examples are presented in the numerical section at the end of each chapter of this thesis in the form of graphs and tables validating the analytical results that are derived.

Chapter 2

Parameter-Uniform Numerical Method for Global Solution and Global Normalized Flux of Singularly Perturbed Convection-Diffusion Problem

This chapter deals with the analysis of an upwind scheme for obtaining the global solution and the global normalized flux for convection-diffusion two-point boundary-value problems exhibiting boundary layers. The numerical solution is obtained using the upwind scheme on a suitable nonuniform mesh formed by equidistributing the arc-length monitor function. It is shown that the discrete solution obtained by the upwind scheme and the global solution obtained *via* interpolation converges uniformly with respect to the perturbation parameter measured in the discrete supremum norm. In addition, the first-order convergence of the global normalized flux *i.e.,* the errors in the derivatives which are weighted by the small diffusion coefficient, on this nonuniform mesh is proved.

2.1 Introduction

Consider the following singularly perturbed boundary-value problem (BVP):

$$\begin{cases} Lu(x) \equiv -\varepsilon u''(x) - a(x)u'(x) + b(x)u(x) = f(x), \quad x \in \Omega = (0,1), \\ u(0) = s_0, \qquad u(1) = s_1, \end{cases} \tag{2.1.1}$$

where $0 < \varepsilon \ll 1$ is a small singular perturbation parameter, the functions $a(x), b(x), f(x)$ are sufficiently smooth and s_0, s_1 are the given constants. Further, we assume that $2\alpha^* \geq a(x) > 2\alpha > 0$ and $b(x) \geq 0$. Under these assumptions, the BVP (2.1.1) has a unique solution which exhibits a layer of width $O(\varepsilon)$ at $x = 0$.

This chapter is organized as follows: Section 2.2 recalls the pertinent properties of the solution $u(x)$ of (2.1.1) and provides *a priori* bounds on the analytical solution and its derivatives. The

generation of the nonuniform meshes in particular, the Shishkin mesh and the adaptive grid is discussed in Section 2.3. Section 2.4 describes the upwind scheme and some technical results that are used later. The estimates for the local truncation error, the bounds for the weighted derivative errors and the convergence analysis of the numerical solution obtained by the upwind scheme on the adaptive grid are proved in Section 2.5. The convergence of the global solution *via* interpolation and the error in the global normalized flux are also discussed in the same section. Finally, Section 2.6 gives some numerical examples that confirm the theoretical error estimates.

2.2 Continuous Problem

This section presents the maximum principle, the stability estimate and *a priori* bounds on the analytical solution of the BVP (2.1.1).

Lemma 2.2.1. (Maximum Principle) *Let $\mathcal{V}$ be a smooth function satisfying $\mathcal{V}(0) \geq 0,\ \mathcal{V}(1) \geq 0$ and $L\mathcal{V}(x) \geq 0,\ \forall x \in\ \Omega$. Then $\mathcal{V}(x) \geq 0,\ \forall x \in\ \overline{\Omega}$.*

Proof. Let $x^* \in \overline{\Omega}$ be such that $\mathcal{V}(x^*) = \min \mathcal{V}(x), x \in \overline{\Omega}$ and assume that $\mathcal{V}(x^*) < 0$. Clearly $x^* \notin \{0, 1\}$ and $\mathcal{V}'(x^*) = 0$ and $\mathcal{V}''(x^*) \geq 0$. Now consider

$$L\mathcal{V}(x^*) \equiv -\varepsilon \mathcal{V}''(x^*) - a(x^*)\mathcal{V}'(x^*) + b(x^*)\mathcal{V}(x^*) < 0$$

which is a contradiction to our assumption. Hence $\mathcal{V}(x) \geq 0, \forall x \in\ \overline{\Omega}$. ∎

An immediate consequence of the maximum principle is the following stability estimate.

Lemma 2.2.2. *If u is the solution of the boundary value problem (2.1.1), then*

$$\|u\| \ \leq\ \alpha^{-1}\|f\| + \max\{|s_0|, |s_1|\}. \tag{2.2.1}$$

Proof. Consider the following barrier function

$$\psi^{\pm}(x) = \left[\left(\frac{1-x}{\alpha}\right)\|f\| + \max\left\{|s_0|, |s_1|\right\}\right] \pm u(x).$$

It is easy to check that $\psi^{\pm}(x) \geq 0$ at $x = 0, 1$. Now from (2.1.1), we have

$$\begin{aligned}
L\psi^{\pm}(x) &= -\varepsilon\big(\psi^{\pm}(x)\big)'' - a(x)\big(\psi^{\pm}(x)\big)' + b(x)\psi^{\pm}(x) \\
&= \frac{a(x)}{\alpha}\|f\| + b(x)\left[\left(\frac{1-x}{\alpha}\right)\|f\| + \max\{|s_0|, |s_1|\}\right] \pm Lu(x) \\
&\geq \big[\|f\| \pm f(x)\big] + b(x)\left[\left(\frac{1-x}{\alpha}\right)\|f\| + \max\{|s_0|, |s_1|\}\right] \\
&\geq 0.
\end{aligned}$$

Thus by applying the maximum principle (Lemma 2.2.1), we can conclude that $\psi^{\pm}(x) \geq 0, \forall x \in \overline{\Omega}$, which is the required result. ∎

Lemma 2.2.3. *The solution $u(x)$ of the BVP (2.1.1) and its derivatives satisfy the following bounds:*

$$|u^{(k)}(x)| \leq C\Big(1+\varepsilon^{-k}\exp(-\alpha x/\varepsilon)\Big), \quad k=0,1,2,3, \qquad x\in\overline{\Omega}. \tag{2.2.2}$$

Proof. One can prove this lemma by following the method of proof given in Lemma 8.1 of [62]. ∎

The solution $u(x)$ of (2.1.1) is decomposed into regular and singular parts as follows:

$$u(x) = v(x) + w(x). \tag{2.2.3}$$

Now $v(x)$ can be written in an asymptotic expansion as

$$v(x) = v_0(x) + \varepsilon v_1(x) + \varepsilon^2 v_2(x),$$

where v_0, v_1 and v_2 are respectively the solutions of the following problems:

$$\begin{cases} a(x)v_0'(x) - b(x)v_0(x) = -f(x), & v_0(1) = s_1, \\ a(x)v_1'(x) - b(x)v_1(x) = -v_0''(x), & v_1(1) = 0, \\ Lv_2(x) = v_1''(x), & v_2(0) = 0, \quad v_2(1) = 0. \end{cases} \tag{2.2.4}$$

Hence, the regular component of the solution satisfies the BVP:

$$Lv(x) = f(x), \quad v(0) = v_0(0) + \varepsilon v_1(0), \quad v(1) = s_1, \tag{2.2.5}$$

and the singular component satisfies:

$$Lw(x) = 0, \quad |w(0)| \leq C, \quad w(1) = 0, \tag{2.2.6}$$

where $w(0)$ depends on v and its derivatives which are bounded uniformly in ε.

Lemma 2.2.4. *For sufficiently small ε and $0 \leq k \leq 3$, the derivatives of v and w satisfy the following bounds:*

$$\begin{aligned} |v^{(k)}(x)| &\leq C\big(1+\varepsilon^{3-k}\big), \\ |w^{(k)}(x)| &\leq C\varepsilon^{-k}\exp\left(-\alpha x/\varepsilon\right), \quad \forall x\in\overline{\Omega}. \end{aligned} \tag{2.2.7}$$

Proof. The proof can be found in [28]. ∎

2.3 Generation of Nonuniform Grids

In this section, two nonuniform meshes are discussed; namely the piecewise-uniform Shishkin mesh and the adaptive grid and also provides an adaptive algorithm for practical implementation.

2.3.1 The Shishkin mesh

Consider the domain $\overline{\Omega} = [0, 1]$ and let $N \geq 4$ be an even positive integer. For the singularly perturbed convection-diffusion problem (2.1.1) with boundary layer at $x = 0$, the simplest construction of the piecewise-uniform Shishkin mesh is to divide the domain $\overline{\Omega}$ into two subdomains $[0, \sigma)$ and $[\sigma, 1]$. Here, the transition parameter σ can be chosen by taking

$$\sigma = \min\left\{\frac{1}{2}, \sigma_0 \varepsilon \ln N\right\},$$

where σ_0 depends on the bound of the convection coefficients $a(x)$ (see [28], [62], [87]). Now in each subdomain, a uniform mesh with $N/2$ mesh intervals is placed such that the piecewise-uniform mesh is of the form

$$\overline{\Omega}_\sigma^N = \{x_i | x_i = 2i\sigma/N,\ i \leq N/2,\ x_i = x_{i-1} + 2(1-\sigma)/N,\ N/2 < i\}.$$

Note that σ depends on both ε, N and on α which is the lower bound on the convective coefficient $a(x)$ defined in the model equation. A piecewise uniform mesh is slightly more complex than the uniform mesh because it is simply two uniform meshes glued together at a carefully chosen transition point. One can note that the piecewise-uniform fitted mesh reduces to a uniform mesh if $\sigma = 1/2$ which occurs when $N \geq \exp(\alpha/2\varepsilon)$. So in the analysis, we will assume that $\sigma = \sigma_0 \varepsilon \ln N$ otherwise N^{-1} will exponentially smaller than ε which is very unlikely in practise.

Similarly in the case when the boundary layer is at $x = 1$, the piecewise-uniform Shishkin mesh can be constructed with the transition point located at $1 - \sigma$. Geometrically, one can see the Shishkin meshes for the left and right boundary layers in Figures 2.1 and 2.2, respectively.

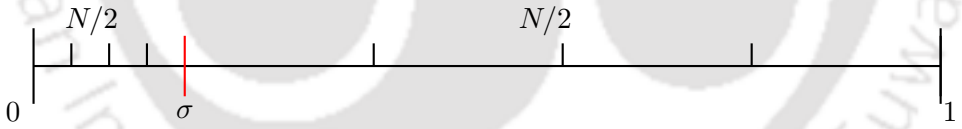

Figure 2.1: Shishkin mesh with $N = 8$ for left layer.

Figure 2.2: Shishkin mesh with $N = 8$ for right layer.

2.3.2 The adaptive grid

Let $M\big(u(x), x\big)$ be a strictly positive, L^1- integrable function on Ω. A commonly-used technique in the adaptive grid generation is based on the idea of equidistribution of the grid points. A grid

$\overline{\Omega}^N$ is said to be equidistributing, if

$$\int_{x_{j-1}}^{x_j} M\big(u(s),s\big)ds = \int_{x_j}^{x_{j+1}} M\big(u(s),s\big)ds, \quad j=1,\ldots,N-1, \tag{2.3.1}$$

where $M\big(u(x),x\big) > 0$ is called the monitor function. Equivalently, (2.3.1) can be expressed as

$$\int_{x_{j-1}}^{x_j} M\big(u(s),s\big)ds = \frac{1}{N}\int_0^1 M\big(u(s),s\big)ds, \quad j=1,\ldots,N. \tag{2.3.2}$$

For practical purposes, it is common to use the monitor functions which are bounded away from zero to maintain a sensible distribution of mesh points throughout the domain. The region of the domain where the monitoring function is large, the mesh spacing will be small and vice versa. One may think of this monitoring function being a measure for solving the local difficulty in solving SPPs. Hence the monitoring functions are so chosen that it depends upon the solution directly and on the BVP indirectly.

Here, the following arc-length monitor function is considered

$$M\big(u(x),x\big) = \sqrt{1+(u'(x))^2}, \tag{2.3.3}$$

which is bounded below by unity. The optimal choice of the monitor function depends on the problem being solved, the numerical discretization being used, and the norm of the error that is to be minimized. In practice, the monitor function is often based on a simple function of the derivatives of the unknown solution. For more details about the equidistribution principle and the choice of the monitor functions, one can refer the articles ([8], [58], [59]).

Remark 2.3.1. *One desirable property of the monitor function is that there exist some positive constants $C_1 \le C_2$ such that*

$$C_1 \le M(u(x),x) \quad \text{and} \quad \int_0^1 M(u(x),x)dx \le C_2.$$

Now combining the above with (2.3.2), we have $h_j \le (C_2/C_1)N^{-1}, \quad j=1,\ldots,N-1.$

To simplify the treatment, we construct the monitor function (2.3.3) in terms of the exact solution of (2.1.1). Now equidistribution can also be thought of as giving rise to a mapping $x = x(\xi)$ relating a computational coordinate $\xi \in [0,1]$ to the physical coordinate $x \in [0,1]$ defined by

$$\int_0^{x(\xi)} M\big(u(s),s\big)ds = \xi\int_0^1 M\big(u(s),s\big)ds = \xi\ell, \tag{2.3.4}$$

where ℓ is the length of u over $\overline{\Omega}$. Now

$$\frac{dx}{d\xi} = \frac{\ell}{\sqrt{1+(u'(x))^2}}\ .$$

More precisely, we have

$$x_j = \int_0^{\xi_j} \frac{\ell}{\sqrt{1+u'(s)^2}} ds, \quad \xi_j = \frac{j}{N}, \quad j = 0, \ldots, N. \tag{2.3.5}$$

Hence, the step sizes of the mesh are given by

$$h_j = x_j - x_{j-1} = \int_{\xi_{j-1}}^{\xi_j} \frac{\ell}{\sqrt{1+(u'(s))^2}} ds \quad j = 1, \ldots, N. \tag{2.3.6}$$

For truly adaptive algorithm, the monitoring function has to be approximated from the numerical solution. Let U_j^N be the piecewise linear interpolant of the knots $(x_j, u(x_j))$. From the equidistribution principle (2.3.1), we have

$$\left[1 + (D^- U_j^N)^2\right] dx^2 = (\ell d\xi)^2 .$$

Now we can construct the mesh from (2.3.2) as the solution of the following nonlinear system of equations:

$$\begin{cases} (x_{j+1} - x_j)^2 + (U_{j+1}^N - U_j^N)^2 = (x_j - x_{j-1})^2 + (U_j^N - U_{j-1}^N)^2, \ j = 1, \ldots, N-1, \\ x_0 = 0, \quad x_N = 1. \end{cases}$$

In other words, find $\{x_i, u_i^N\}$ with $\{u_i^N\}$ computed from the $\{x_i\}$ by means the discrete scheme (2.4.1) such that

$$\underbrace{\sqrt{|u_i^N - u_{i-1}^N|^2 + |x_i - x_{i-1}|^2}}_{\text{arc-length between } x_{i-1} \text{ and } x_i} = \frac{1}{N} \underbrace{\sum_{j=1}^{N} \sqrt{|u_i^N - u_{i-1}^N|^2 + |x_i - x_{i-1}|^2}}_{\text{total arc-length}} \quad \forall\ i.$$

The above equation can be written in the form

$$h_i M_i = \frac{1}{N} \sum_{j=1}^{N} h_j M_j \quad \text{for } i = 1, 2, \ldots, N \quad \text{where} \quad M_i = \sqrt{1 + [D^- u_i^N]^2} \tag{2.3.7}$$

The system of equations (2.4.1) and (2.3.7) are solved simultaneously to obtain the solution U_j^N and the grids x_j.

2.3.3 Practical implementation

The following algorithm gives an idea how to generate the adaptive grid in the computer.

Adaptive algorithm

Step-1 Initialize mesh: The uniform mesh $\{0, 1/N, 2/N, \ldots, 1\}$ is taken as the initial mesh.

Step-2 For each $k = 0, 1, 2 \ldots$, assuming that the mesh $x_i^{(k)}$ is given, compute the numerical solution $u_i^{(k)}$ using the discrete scheme. Let $h_i^{(k)} = x_i^{(k)} - x_{i-1}^{(k)}$ for each i. Now calculate

$$l_i^{(k)} = h_i^{(k)} \sqrt{1 + \left(D^- u_i^{(k)}\right)^2} = \sqrt{\left(u_i^{(k)} - u_{i-1}^{(k)}\right)^2 + \left(h_i^{(k)}\right)^2}$$

be the arc-length between the points $\left(x_{i-1}^{(k)}, u_{i-1}^{(k)}\right)$ and $\left(x_i^{(k)}, u_i^{(k)}\right)$ in the piecewise continuous solution $u_i^{(k)}$. Then the total arc-length of the solution curve $u_i^{(k)}$ is

$$\mathscr{L}^{(k)} := \sum_{i=1}^{N} l_i^{(k)} = \sum_{i=1}^{N} \sqrt{\left(u_i^{(k)} - u_{i-1}^{(k)}\right)^2 + \left(h_i^{(k)}\right)^2}.$$

Step-3 Test mesh: Let C_0 be a user-chosen constant with $C_0 > 1$ (see Remark 2.3.2) . If

$$\frac{\max l_i^{(k)}}{\mathscr{L}^{(k)}} \leq \frac{C_0}{N}, \tag{2.3.8}$$

holds true, then go to step-5. Otherwise, continue to Step-4.

Step-4 Generate new mesh by equidistributing arc-length of current computed solution. Choose the grid points $\{0 = x_0^{(k+1)} < x_1^{(k+1)} < x_2^{(k+1)} < \ldots < x_N^{(k+1)} = 1\}$ such that for each i, the distance from $(x_{i-1}^{(k+1)}, u_{i-1}^{(k+1)})$ and $(x_i^{(k+1)}, u_i^{(k+1)})$, measured along the polygonal solution curve $u_i^{(k)}$, equals $\mathscr{L}^{(k)}/N$. This clearly determines the $x_i^{(k+1)}$ uniquely. Now the new mesh is given by $\{x_i^{(k+1)}\}$. Return to Step-2.

Step-5 Set the final mesh and the solution as $\{x_0^* < x_1^* < x_2^* < \ldots < x_N^*\} = \{x_i^{k+1}\}$ and $u_i^* = u^{k+1}$. Then **STOP**.

Remark 2.3.2. *Instead of (2.3.8), one can use the following stopping criterion*

$$\frac{\max_i l_i^{(k)}}{\min_i l_i^{(k)}} \leq C_0, \tag{2.3.9}$$

as if (2.3.9) holds true, then

$$\mathscr{L}^{(k)} = \sum_{i=1}^{N} l_i^{(k)} \geq N \min_i l_i^{(k)} \geq (N/C_0) \max_i l_i^{(k)}$$

which is equivalent to (2.3.8). Similarly the constant C_0 satisfies $C_0 > 1$ and $C_0 \approx 1$. The larger is C_0, the fewer iterations needed in the algorithm, but the final error bound increases with C_0. One can refer ([7], [50]) for more details about the adaptive algorithms and their stopping criterion.

Theorem 2.3.3. *(Existence of a solution to the equidistribution problem) For each $\varepsilon \in (0, 1]$ and each positive integer N, there exists a mesh that provides a solution to the equidistribution problem which equidistributes the discrete arc-length monitor function of (2.3.7) for the model problem (2.1.1).*

Proof. The detailed proof is given in [50]. ∎

Lemma 2.3.4. *If the mesh $\overline{\Omega}^N$ is generated by (2.3.7), then*

- *There are $O(N)$ grid points inside the boundary layer $(0, x_{_K})$. Moreover, $h_j \le C\varepsilon$ for $j \le K$.*
- *There are $O(1)$ grid points inside the transition region $(x_{_K}, x_{_J})$ where $O(1)$ is independent of ε and N.*
- *There are $O(N)$ grid points inside the regular region $(x_{_J}, 1)$ and $h_j \le CN^{-1}$ for $j \ge J+1$, where $|u'(x)| \gg 1$ if $x < x_{_J}$ and $|u'(x)| = O(1)$ if $x > x_{_J}$.*

Proof. The proof can be found in [82]. ∎

2.4 Discrete Problem

The upwind finite difference scheme for the BVP (2.1.1) takes the form

$$\begin{cases} L^N U_j^N \equiv -\varepsilon D^+ D^- U_j^N - a_j D^+ U_j^N + b_j U_j^N = f_j\,, \quad 1 \le j \le N-1, \\ U_0^N = s_0, \quad U_N^N = s_1\ . \end{cases} \tag{2.4.1}$$

Equation (2.4.1) can be expressed in the following form of system of algebraic equations

$$\begin{cases} -r_j^- U_{j-1}^N + r_j^c U_j^N - r_j^+ U_{j+1}^N = f_j, \quad j = 1, \ldots, N-1, \\ U_0^N = s_0, \quad U_N^N = s_1\,, \end{cases} \tag{2.4.2}$$

where

$$r_j^- = \frac{2\varepsilon}{h_j(h_j + h_{j+1})}, \quad r_j^c = \frac{2\varepsilon}{h_j h_{j+1}} + \frac{a_j}{h_{j+1}} + b_j, \quad r_j^+ = \frac{2\varepsilon}{h_{j+1}(h_j + h_{j+1})} + \frac{a_j}{h_{j+1}}\ .$$

In the tri-diagonal system (2.4.2), the off-diagonal entries have the following properties:

$$r_j^- > 0,\ r_j^+ > 0, \quad j = 1, \ldots, N-1,$$

and

$$r_j^c + r_j^- + r_j^+ \ge 0, \quad \text{for} \quad j = 1, \ldots, N-1, \tag{2.4.3}$$

which imply that the stiffness matrix is an M-matrix.

Now we have to find the bound of the truncation error. Set

$$A\phi(x) = \varepsilon\phi'(x) + a(x)\phi(x). \tag{2.4.4}$$

In the discrete form, the above upwind scheme (2.4.1) can be written as

$$L^N U_j^N \equiv \big(- D^+(A^N) + b_j \big) U_j^N = f_j, \tag{2.4.5}$$

where the discrete operator A^N (corresponding to the continuous operator A) is defined by

$$A^N\phi_j = \varepsilon D^-\phi_j + a_j\phi_j. \tag{2.4.6}$$

Now from (2.1.1) and (2.4.4), we obtain

$$\frac{1}{h_{j+1}}\int_{x_j}^{x_{j+1}} f(x)dx = -D^+(A^N U_j^N) + b_j U_j^N. \tag{2.4.7}$$

So from (2.4.5) and (2.4.7), we have

$$\left| f_j - \frac{1}{h_{j+1}}\int_{x_j}^{x_{j+1}} f(x)dx \right| \le CN^{-1}. \tag{2.4.8}$$

The truncation error is defined by

$$\tau_j \equiv L^N(U_j^N - u(x_j)) = D^+\left[A^N U_j^N - Au(x_j)\right] + \left[f_j - \frac{1}{h_{j+1}}\int_{x_j}^{x_{j+1}} f(x)dx\right]. \tag{2.4.9}$$

Using the decomposition (2.2.3), we have

$$A^N U_j^N - Au(x_j) = \varepsilon[D^- U_j^N - u'(x_j)] = \varepsilon[D^- V_j^N - v'(x_j)] + \varepsilon[D^- W_j^N - w'(x_j)] =: \varepsilon\mu_j + \eta_j, \tag{2.4.10}$$

where V_j^N and W_j^N are the discrete approximations of $v(x_j)$ and $w(x_j)$, respectively. Applying the mean-value theorem and using (2.2.7), we get the following:

$$|\mu_j| = |D^- V_j^N - v'(x_j)| \le Ch_j \le CN^{-1}, \tag{2.4.11}$$

and

$$|\eta_j| = \varepsilon|D^- W_j^N - w'(x_j)| \le C\left\{ \min\left\{\frac{h_j}{\varepsilon}, 1\right\} \exp\left(\frac{-\alpha x_{j-1}}{\varepsilon}\right)\right\}. \tag{2.4.12}$$

Lemma 2.4.1. *For the truncation error τ_j defined by $\tau_j = \varepsilon D^+\mu_j + D^+\eta_j + O(N^{-1})$, the following inequality holds:*

$$\|\tau_j\|_* \le C \max_{1\le j\le N}\left\{ \min\left\{\frac{h_j}{\varepsilon}, 1\right\} \exp\left(\frac{-\alpha x_{j-1}}{\varepsilon}\right)\right\} + CN^{-1}. \tag{2.4.13}$$

Proof. Using the bounds of η_j and μ_j given by (2.4.11) and (2.4.12) in (2.4.10) and combining with (2.4.8), we shall obtain the required estimate. ∎

2.5 Error Analysis

2.5.1 Local truncation error

In order to obtain the bound of the local truncation error, the following lemmas are required.

Lemma 2.5.1. *For any $\psi \in \mathcal{C}^3(\overline{\Omega})$, we have*

$$\begin{aligned}
\left|\left(D^+ - \frac{d}{dx}\right)\psi(x_j)\right| &\leq \frac{1}{x_{j+1}-x_j}\int_{x_j}^{x_{j+1}} (x_{j+1}-s)\psi''(s)ds\,, \\
\left|\left(D^+D^- - \frac{d^2}{dx^2}\right)\psi(x_j)\right| &\leq \frac{1}{x_{j+1}-x_{j-1}}\left[\frac{1}{h_{j+1}}\int_{x_j}^{x_{j+1}} (x_{j+1}-s)^2\psi'''(s)ds\right. \\
&- \left.\frac{1}{h_j}\int_{x_{j-1}}^{x_j} (s-x_{j-1})^2\psi'''(s)ds\right].
\end{aligned} \tag{2.5.1}$$

Proof. One can find the complete proof of this lemma in [Lemma 4.1 of [62]]. ∎

Lemma 2.5.2. *The truncation error defined in (2.4.9) has the following bound:*

$$|\tau_j| \leq \frac{C}{\varepsilon N}\exp\left(\frac{-\alpha x_j}{\varepsilon}\right). \tag{2.5.2}$$

Proof. Using the Taylor series expansion and (2.5.1), the truncation error (2.4.9) can be expressed as

$$\begin{aligned}
\tau_j = \frac{-\varepsilon}{h_j+h_{j+1}}\left[\frac{1}{h_{j+1}}\int_{x_j}^{x_{j+1}}(x_{j+1}-s)^2u'''(s)ds - \frac{1}{h_j}\int_{x_{j-1}}^{x_j}(s-x_{j-1})^2u'''(s)ds\right] \\
+\frac{a_j}{h_{j+1}}\int_{x_j}^{x_{j+1}}(x_{j+1}-s)u''(s)ds,
\end{aligned} \tag{2.5.3}$$

from which we obtain the following bound

$$|\tau_j| < \varepsilon\int_{x_{j-1}}^{x_{j+1}}|u'''(s)|ds + C\int_{x_{j-1}}^{x_{j+1}}|u''(s)|ds. \tag{2.5.4}$$

If we invoke the derivative bounds of the continuous solution (2.2.2) in the first term, the above expression becomes

$$|\tau_j| < C\int_{x_{j-1}}^{x_{j+1}}|u''(s)|ds. \tag{2.5.5}$$

From (2.3.5), we have

$$|\tau_j| \;\leq\; C\ell\int_{\xi_{j-1}}^{\xi_{j+1}}\frac{|u''(x)|}{\sqrt{1+u'(x)^2}}d\xi \;\leq\; \frac{C}{\varepsilon}\int_{\xi_{j-1}}^{\xi_{j+1}}\frac{|u'(x)|}{\sqrt{1+u'(x)^2}}d\xi. \tag{2.5.6}$$

From Lemma 2.2.3, we know that $|u'(x)| = O(1/\varepsilon)$. Using this bound of the solution, we can get constants C_3 and C_4 such that

$$\frac{C_3}{\varepsilon}\exp\left(\frac{-\alpha^* x}{\varepsilon}\right) \leq u'(x) \leq \frac{C_4}{\varepsilon}\exp\left(\frac{-\alpha x}{\varepsilon}\right),$$

holds. Now (2.5.6) can be written as

$$\begin{aligned}
|\tau_j| &\leq \frac{C}{\varepsilon}\int_{\xi_{j-1}}^{\xi_{j+1}}\frac{\frac{C_4}{\varepsilon}\exp\left(\frac{-\alpha x}{\varepsilon}\right)}{\sqrt{1+(\frac{C_3}{\varepsilon})^2\exp\left(\frac{-2\alpha^* x}{\varepsilon}\right)}}d\xi \\
&\leq \frac{C}{\varepsilon N}\frac{\frac{C_4}{\varepsilon}\exp\left(\frac{-\alpha x_j}{\varepsilon}\right)}{\sqrt{1+(\frac{C_3}{\varepsilon})^2\exp\left(\frac{-2\alpha^* x_j}{\varepsilon}\right)}} \\
&\leq R_j\exp\left(\frac{-\omega x_j}{\varepsilon}\right),
\end{aligned} \tag{2.5.7}$$

where $0 < \omega < 1$ is independent of ε, N and $R_j = \dfrac{C}{\varepsilon N} \dfrac{(C_4/\varepsilon)\exp\left(-(\alpha-\omega)x_j/\varepsilon\right)}{\sqrt{1+(C_3/\varepsilon)^2\exp\left(-2\alpha^* x_j/\varepsilon\right)}}$.

Let us denote by $y_j = (C/\varepsilon)\exp\left(-\alpha x_j/\varepsilon\right)$, $g(y) = y/\sqrt{1+y^2}$, which is an increasing function in $[0, y^*]$, where $y^* = \sqrt{(1-\omega)/\omega}$. Since $\omega = O(1)$, we have $y^* = O(\omega)$ and hence $g(y^*) = O(1)$. Therefore, we can express

$$R_j \leq \frac{C}{\varepsilon N} g(y_j) \leq \frac{C}{\varepsilon N} g(y^*) \leq \frac{C}{\varepsilon N} \ ,$$

and hence,

$$|\tau_j| \leq \frac{C}{\varepsilon N} \exp\left(\frac{-\alpha x_j}{\varepsilon}\right),$$

which is the required result. ∎

Let us define the piecewise $(0,1)$-Padé approximation of $\exp(-\alpha x_j/\varepsilon)$ by

$$S_0 = 1, \quad S_j = \prod_{k=1}^{j} \left(1 + \frac{\alpha h_k}{\varepsilon}\right)^{-1}, \quad j = 1, \ldots, N, \tag{2.5.8}$$

then

$$S_j \geq \exp\left(\frac{-\alpha x_j}{\varepsilon}\right).$$

Define the parameter $\sigma = \varepsilon \ln N$, then $\exp(-\sigma/\varepsilon) = N^{-1}$. In other words, we can say that

$$\left(1 + \frac{H}{\varepsilon}\right)^{-1} \approx \exp\left(\frac{-H}{\varepsilon}\right), \quad \text{if} \quad \frac{H}{\varepsilon} \ll 1.$$

2.5.2 Convergence of the numerical solution

Before deriving the error estimate for the numerical solution, here some lemmas are provided which are the prerequisites for the main result.

Lemma 2.5.3. *(**Discrete Comparison Principle**) If $L^N \mathcal{V}_j < L^N \mathcal{Z}_j$ for $1 \leq j \leq N-1$ with $\mathcal{V}_0 < \mathcal{Z}_0$ and $\mathcal{V}_N < \mathcal{Z}_N$, then $\mathcal{V}_j < \mathcal{Z}_j$ for $0 \leq j \leq N$.*

Proof. From (2.4.3), it is clear that the matrix associated with the discrete operator L^N is an M-matrix and therefore has a positive inverse. Hence, the result follows. ∎

Lemma 2.5.4. *The mesh functions S_j satisfy the following property: for $j = 1, \ldots, N-1$, there exists a constant C, such that*

$$L^N S_j \geq \frac{C}{\max\{\varepsilon, h_{j+1}\}} S_j \ . \tag{2.5.9}$$

Proof. From the definition of S_j, it is clear that

$$\frac{S_j - S_{j-1}}{h_j} = -\frac{\alpha}{\varepsilon} S_j \ .$$

Now

$$\begin{aligned} L^N S_j &= -\frac{2\varepsilon}{h_j + h_{j+1}} \left[\frac{S_{j+1} - S_j}{h_{j+1}} - \frac{S_j - S_{j-1}}{h_j} \right] - a_j \left[\frac{S_{j+1} - S_j}{h_{j+1}} \right] + b_j S_j \\ &\geq -\frac{2\alpha h_{j+1}}{(h_j + h_{j+1})} \left[\frac{S_j - S_{j+1}}{h_{j+1}} \right] + \frac{\alpha\, a_j}{\varepsilon} S_{j+1} \\ &= \left(\frac{\alpha}{\varepsilon + \alpha h_{j+1}} \right) \left[a_j - \frac{2\alpha h_{j+1}}{(h_j + h_{j+1})} \right] S_j \\ &\geq \frac{C}{\max\{\varepsilon, h_{j+1}\}} S_j \ . \end{aligned}$$

Therefore, (2.5.9) is proved. ∎

The following lemma provides the two-sided bound for S_j, which will be used later.

Lemma 2.5.5. *The grid functions S_j defined in (2.5.8) satisfy*

$$\exp\left(\frac{-\alpha x_j}{\varepsilon}\right) < S_j < C \exp\left(\frac{-\alpha x_j}{\varepsilon}\right), \quad j = 1, \ldots, N-1. \tag{2.5.10}$$

Proof. We can express the nodes x_j as

$$x_j = \sum_{k=1}^{j} h_k \ .$$

Therefore,

$$\exp\left(-\frac{\alpha x_j}{\varepsilon}\right) = \exp\left(\sum_{k=1}^{j} \frac{-\alpha h_k}{\varepsilon}\right) = \prod_{k=1}^{j} \exp\left(-\frac{\alpha h_k}{\varepsilon}\right).$$

For any real value of $\lambda > 0$, we have $\exp(-\lambda) < (1+\lambda)^{-1}$. Therefore,

$$\exp\left(-\frac{\alpha x_j}{\varepsilon}\right) < \prod_{k=1}^{j} \left(1 + \frac{\alpha h_k}{\varepsilon}\right)^{-1} \leq S_j.$$

Now we have to find the upper bound for S_j. We know from (2.3.6) that

$$\begin{aligned} h_j &= \int_{\xi_{j-1}}^{\xi_j} \frac{\ell}{\sqrt{1 + (u'(s))^2}} ds \\ &\leq \int_{\xi_{j-1}}^{\xi_j} \frac{\ell}{u'(x)} ds \\ &\leq \frac{\ell}{N u'(x_j)}. \end{aligned}$$

From (2.2.2), we can see that

$$|u'(x_j)| \leq C\varepsilon^{-1}\exp\left(\frac{-\alpha x_j}{\varepsilon}\right).$$

Hence, we have

$$h_j \leq \frac{\varepsilon\ell}{\alpha N}\exp\left(\frac{\alpha x_j}{\varepsilon}\right). \tag{2.5.11}$$

Observe that

$$\ln\Big[\prod_{k=1}^{j}\left(1+\frac{\alpha h_k}{\varepsilon}\right)\Big] \;\geq\; \sum_{k=1}^{j}\Big[\frac{\alpha h_k}{\varepsilon}-\frac{1}{2}\Big(\frac{\alpha h_k}{\varepsilon}\Big)^2\Big] \geq \frac{\alpha x_j}{\varepsilon}-\frac{1}{2}\sum_{k=1}^{j}\Big(\frac{\alpha h_k}{\varepsilon}\Big)^2. \tag{2.5.12}$$

Now using (2.5.11) and for some $\tilde{x}$ in the layer region *i.e.*, $\tilde{x}\in(0,x_{_K})$, we can write

$$\sum_{j=1}^{K}\Big(\frac{\alpha h_j}{\varepsilon}\Big)^2 \leq C\varepsilon^{-1}N^{-1}\sum_{k=1}^{j}\exp\left(\frac{\alpha h_k}{\varepsilon}\right) \leq C\varepsilon^{-1}N^{-1}\int_0^{\tilde{x}}\exp\left(\frac{\alpha s}{\varepsilon}\right)ds \leq C\,.$$

Then, from (2.5.11) and (2.5.12), we obtain

$$\prod_{k=1}^{j}\left(1+\frac{\alpha h_k}{\varepsilon}\right)^{-1} \leq C\exp\left(\frac{-\alpha x_j}{\varepsilon}\right),$$

and hence

$$S_j \leq C\exp\left(\frac{-\alpha x_j}{\varepsilon}\right),$$

and hence, the proof is done. ∎

The following theorem shows the ε-uniform convergence of the upwind scheme.

Theorem 2.5.6. *Let $u(x)$ and U_j^N be respectively the exact solution of (2.1.1) and the discrete solution of (2.4.1) on the grids defined by (2.3.2). Then, the following ε-uniformly error estimate holds:*

$$\max_{0\leq j\leq N}|u(x_j)-U_j^N| \leq CN^{-1}. \tag{2.5.13}$$

Proof. We already know from Lemma 2.5.2, the bound of the truncation error is given by

$$|\tau_j| \leq \frac{C}{\varepsilon N}\exp\left(\frac{-\alpha x_j}{\varepsilon}\right).$$

Let us apply the discrete comparison principle (Lemma 2.5.3) to the barrier function $\mathcal{W}_j$ defined by

$$\mathcal{W}_j = CN^{-1}(1+S_j), \quad j=0,\ldots,N.$$

The truncation error τ_j and the nodal error e_j are related by $L^Ne_j=\tau_j$. Using (2.5.10), we have for $j=1,\ldots,N-1$,

$$L^Ne_j=\tau_j \;\leq\; \frac{C}{\varepsilon N}\exp\Big(-\frac{\alpha x_j}{\varepsilon}\Big) \leq \frac{C}{\varepsilon N}S_j \leq \frac{C}{\varepsilon N}L^NS_j \leq L^N\mathcal{W}_j\,.$$

Since $e_0 \le \mathcal{W}_0$ and $e_N \le \mathcal{W}_N$, we conclude that

$$e_j \le \mathcal{W}_j \le CN^{-1}, \quad j = 0, \ldots, N.$$

Now the same argument can be repeated with e_j being replaced by $-e_j$ and hence we have

$$|e_j| \le CN^{-1}, \quad j = 0, \ldots, N.$$

which is the required result. ∎

2.5.3 Error in the normalized flux

In this section, the bounds on the ε-weighted derivative errors $\{\varepsilon E_j\}$ are derived. E_j is defined by $E_j = D^- e_j = (e_j - e_{j-1})/h_j$, where e_j denotes the pointwise errors.

Before deriving the bound of the weighted derivatives, the following lemmas are proved.

Lemma 2.5.7. *Let the mesh functions z_j and ϕ_j satisfy $L^N z_j = \phi_j$ for $j = 1, \ldots, N-1$ with $z_0 = z_N = 0$, then*

$$\|z\| \le \frac{2\|\phi\|_*}{\alpha} \quad \text{and} \quad \varepsilon \|D^- z\| \le \left(2 + \frac{2\alpha}{\alpha^*}\right) \|\phi\|_*$$

Proof. One can refer [49] for the proof. ∎

Lemma 2.5.8. *For $j = 1, \ldots, N$, there exist positive constants C_5 and C_6 such that if*

$$S_j \ge C_5 \varepsilon, \tag{2.5.14}$$

for some j, then

$$M_j = M(U_j^N, x_j) \ge |D^- U_j^N| \ge \frac{C_6 S_j}{\varepsilon}. \tag{2.5.15}$$

Proof. We have $u = v + w$, where $|v'(x)| \le C$ and $|w'(x)| \le w(0)\varepsilon^{-1} \exp(-x/\varepsilon)$. If $S_j \ge C_5\varepsilon$, then we have $S_j/(C_5\varepsilon) \ge 1$. We know that the total arc length ℓ is of $O(1)$ and does not change dramatically. Now

$$1 \le \ell = \sum_{j=1}^{N} \sqrt{|U_j - U_{j-1}|^2 + |x_j - x_{j-1}|^2} \le C_2, \tag{2.5.16}$$

where $C_2 = 1 + 2\|f\|$. If $\exp(-x/\varepsilon) \ge C_5\varepsilon$ for some x, then using the bounds of $|v'(x)|$ and $|w'(x)|$, we can claim that

$$|u'(x)| \ge C\varepsilon^{-1} \exp(-x/\varepsilon).$$

Now combining $M_j \ge |D^- U_j^N|$ with the above inequality, we can find a constant C_6 such that (2.5.15) holds. ∎

Let $\lambda_j = C_2/(C_6 S_j N)$. Using the assumptions $\varepsilon \le CN^{-1}$ and (2.5.14), it is easy to check that $|\lambda_j| \le C$.

Lemma 2.5.9. *Let $\varepsilon \leq CN^{-1}$, then*

(*i*) *For any $[t_1, t_2] \subseteq [0, x_j]$ such that $\ell[t_1, t_2] = \ell/N$, where $\ell[t_1, t_2]$ represents the arc-length of the solution curve in $[t_1, t_2]$, then we have $|t_2 - t_1| \leq \varepsilon\lambda_j$.*

(*ii*) *If $x_i \geq \varepsilon\lambda_j$, then $\ell[0, x_j] \geq \ell/N$.*

Proof. We know from the definition that

$$\begin{aligned} \ell[t_1, t_2] &= \int_{t_1}^{t_2} \sqrt{1 + u'(s)^2} ds \\ &\geq |t_2 - t_1| \min_{1 \leq j \leq N} |D^- U_j^N|. \end{aligned}$$

Again for $j \leq i$, $S_j \geq S_i$ and $S_i \geq C_5\varepsilon$, so $S_j \geq C_5\varepsilon$. Now using Lemma 2.5.8, we have

$$\ell[t_1, t_2] \geq |t_2 - t_1| \frac{C_6 S_j}{\varepsilon}. \tag{2.5.17}$$

Given that $[t_1, t_2] \subseteq [0, x_j]$ and $\ell[t_1, t_2] = \ell/N$. Hence using (2.5.16) and (2.5.17), we can write

$$|t_2 - t_1| \leq \frac{\varepsilon \ell[t_1, t_2]}{C_6 S_j} = \frac{\varepsilon \ell}{C_6 S_j N} \leq \varepsilon \lambda_j.$$

(*ii*) Set $[t_1, t_2] = [0, x_j]$. From (2.5.17), we have

$$\ell[0, x_j] \geq \frac{x_j C_6 S_j}{\varepsilon} \geq C_6 \lambda_j S_j = \frac{C_5}{N} \geq \frac{\ell}{N},$$

and hence, the lemma is proved. ∎

Lemma 2.5.10. *There exists a constant C independent of ε such that*

$$\min\left\{\frac{h_j}{\varepsilon}, 1\right\} \exp\left(\frac{-\alpha x_{j-1}}{\varepsilon}\right) \leq CN^{-1},$$

holds.

Proof. Let J be the largest value of j such that $x_{J-1} \leq \sigma - C_7\varepsilon$. In other words, we have

$$x_{j-1} \leq \sigma - C_7\varepsilon < x_J < \sigma - (C_7 - C_8)\varepsilon, \tag{2.5.18}$$

where C_7, C_8 satisfy

$$C_7 > C_8 \geq \frac{C_2}{C_5 C_6} \quad \text{and} \quad \exp(C_7 - C_8) > C_5(1 + C_2). \tag{2.5.19}$$

We know that

$$S_J \geq \exp\left(\frac{-x_J}{\varepsilon}\right) \geq \exp\left(\frac{-[\sigma - (C_7 - C_8)\varepsilon]}{\varepsilon}\right) \geq \frac{\exp(C_7 - C_8)}{N}.$$

Combing (2.5.19) with the assumption $\varepsilon < N^{-1}$, we have $S_{_J} \geq C_2/N \geq C_5\varepsilon$. So

$$x_{_J} > \sigma - C_7\varepsilon = \varepsilon(\ln N - C_7) \geq C_8\varepsilon. \tag{2.5.20}$$

For sufficiently large N, combining (2.5.18) and (2.5.19), we have

$$\varepsilon\lambda_{_J} = \frac{C_2\varepsilon}{C_6 S_{_J} N} \leq \frac{C_2\varepsilon}{C_2 C_6} \leq C_8\varepsilon. \tag{2.5.21}$$

We know that $|\lambda_{_J}| \leq C_7$, so we can write

$$x_{j-1} \leq \sigma - (C_7 + C_8)\varepsilon = (\sigma - C_7\varepsilon) - C_8\varepsilon. \tag{2.5.22}$$

From (2.5.18) and (2.5.20), we obtain $x_{j-1} \leq x_{_J} - \varepsilon\lambda_{_J}$. As $x_{j-1} < x_{_J}$. Now we can have

$$h_{j-1} = x_j - x_{j-1} = x_{_J} - x_{j-1} \leq \varepsilon\lambda_{_J} \leq C_7\varepsilon. \tag{2.5.23}$$

Now combining (2.5.22) and (2.5.23), we get $x_j \leq \sigma - C_7\varepsilon$. Since $j < J$, then $S_j \geq S_{_J}$ and combining with (2.5.23), we obtain $h_j \leq \varepsilon\lambda_j = C_1\varepsilon/C_6 S_j N$. Since $S_j \geq \exp(-\alpha x_j/\varepsilon)$, we can write

$$\frac{h_j}{\varepsilon}\exp\left(\frac{-\alpha x_{j-1}}{\varepsilon}\right) \leq \frac{C_2}{C_6 N}\exp\left(\frac{\alpha(x_j - x_{j-1})}{\varepsilon}\right).$$

Using (2.5.23) in the above expression, we get

$$\frac{h_j}{\varepsilon}\exp\left(\frac{-\alpha x_{j-1}}{\varepsilon}\right) \leq CN^{-1}. \tag{2.5.24}$$

Since $\exp(-\sigma/\varepsilon) = N^{-1}$. So from (2.5.22),

$$\begin{aligned}\exp\left(\frac{-x_{j-1}}{\varepsilon}\right) &= N^{-1}\exp\left(\frac{\sigma - x_{i-1}}{\varepsilon}\right) \\ &\leq N^{-1}\exp(C_7 + C_8) \leq CN^{-1}.\end{aligned} \tag{2.5.25}$$

Finally, combining (2.5.24) and (2.5.25), we can conclude that

$$\left\{\min\left\{\frac{h_j}{\varepsilon}, 1\right\}\exp\left(\frac{-\alpha x_{j-1}}{\varepsilon}\right)\right\} \leq CN^{-1}, \tag{2.5.26}$$

and this completes the proof. ∎

The bound for the ε-weighted error between the computed and the actual derivatives of the solution of (2.1.1) is given in the following theorem.

Theorem 2.5.11. *There exists a constant C independent of ε and mesh points such that*

$$\max_{1\leq j\leq N} \varepsilon|D^- U_j^N - u'(x_j)| \leq CN^{-1}.$$

Proof. We know that $L^N e_j = \tau_j$. From Lemma 2.4.1, we have

$$\varepsilon\|E\| \leq C|\tau_j| \leq C \max_{j=1,\ldots,N} \left\{ \min\left\{ \frac{h_j}{\varepsilon}, 1 \right\} \exp\left(\frac{-\alpha x_{j-1}}{\varepsilon} \right) \right\} + CN^{-1}. \tag{2.5.27}$$

By using the inequality (2.5.26) in (2.5.27), we obtain the desired estimate. ∎

2.5.4 Convergence of the global solution

The estimate given in Theorem 2.5.6 shows that the classical upwind scheme applied on the equidistributed grids is uniformly first-order accurate at all the mesh points. The global approximation to the exact solution is obtained by interpolating the numerical solution at the mesh points using the piecewise constant or the piecewise linear functions. It is shown that these global approximations are uniformly first-order accurate throughout the domain.

Theorem 2.5.12. *Let $\widetilde{u}(x)$ be the piecewise constant or piecewise linear interpolant of the solution U_j^N for the difference scheme (2.4.1) obtained on the grid (2.3.7). Then the global error satisfies the ε-uniform estimate*

$$\|u(x) - \widetilde{u}(x)\| \leq CN^{-1}. \tag{2.5.28}$$

Proof. Let $\widetilde{u}(x)$ denotes the piecewise polynomial interpolant of degree k with either $k = 0$ or $k = 1$ where $x \in (x_{j-1}, x_j)$. Then

$$\widetilde{u}(x) = \begin{cases} U_j^N \chi_j(x), & k = 0, \\ U_{j-1}^N \phi_{j-1}(x) + U_j^N \phi_j(x), & k = 1, \end{cases} \tag{2.5.29}$$

where

$$\chi_j(x) = \begin{cases} 1, & \text{if } x \in (x_{j-1}, x_j), \\ 0, & \text{otherewise}, \end{cases}$$

and $\phi_{j-1}(x)$, $\phi_j(x)$ are Lagrange's interpolating polynomials of first degree given by

$$\phi_{j-1}(x) = \frac{x_j - x}{x_j - x_{j-1}}, \quad \phi_j(x) = \frac{x - x_{j-1}}{x_j - x_{j-1}}.$$

For $k = 0$, we have

$$\begin{aligned} \widetilde{u}(x) - u(x) &= U_j^N \chi_j(x) - u(x_j) + u(x_j) - u(x) \\ &= U_j^N - u(x_j) + \int_x^{x_j} u'(s)ds. \end{aligned}$$

For $k = 1$, we have

$$\begin{aligned} \widetilde{u}(x) - u(x) &= U_{j-1}^N \phi_{j-1}(x) + U_j^N \phi_j(x) - u(x) \\ &= [U_{j-1}^N - u(x_{j-1})]\phi_{j-1}(x) + [U_j^N - u(x_j)]\phi_j(x) - \\ &\qquad -\phi_{j-1}(x) \int_{x_{j-1}}^{x} u'(s)ds + \phi_j(x) \int_x^{x_j} u'(s)ds. \end{aligned}$$

Using Theorem 2.5.6, we can conclude that

$$|\widetilde{u}(x)-u(x)| \leq \begin{cases} CN^{-1}+\displaystyle\int_x^{x_j}|u'(s)|ds, & \text{if } k=0,\\ CN^{-1}+C\displaystyle\int_{x_{j-1}}^{x_j}|u'(s)|ds, & \text{if } k=1. \end{cases}$$

Now we have to find the bound for the integral

$$I_j=\int_{x_{j-1}}^{x_j}|u'(s)|ds\ .$$

Using (2.2.7) and the equidistribution principle (2.3.2), we may conclude that

$$\begin{aligned} I_j &\leq C\varepsilon^{-1}\int_{x_{j-1}}^{x_j}\exp(-\alpha s/m\varepsilon)ds\\ &\leq \int_{x_{j-1}}^{x_j}\sqrt{1+(u'(s))^2}ds=\frac{1}{N}\int_0^1 M(u(s),s)ds\\ &\leq \frac{C\ell}{N}\leq CN^{-1}. \end{aligned}$$

Hence, the desired result follows. ∎

2.5.5 Error in the global normalized flux

The bound given in Theorem 2.5.11 provides the estimate for the pointwise error in the normalized flux defined by $\varepsilon u'(x)$. The following theorem proves the uniform convergence estimate for the global normalized flux.

Theorem 2.5.13. *Let $u(x)$ be the solution of (2.1.1) and $\widetilde{u}(x)$ be the global solution defined as in (2.5.29). Then, the error of the normalized flux satisfies*

$$\varepsilon|u'(x_j)-\widetilde{u}'(x_j)|\leq CN^{-1},\quad j=0,\ldots,N. \tag{2.5.30}$$

Proof. For constant interpolant, we can get the required bound using Theorem 2.5.11. Now for the case of linear interpolant defined in (2.5.29), we have

$$\widetilde{u}'(x_j)=\frac{U_j^N-U_{j-1}^N}{h_j}.$$

Using the Taylor series expansion, we obtain that

$$\varepsilon|u'(x_j)-\widetilde{u}'(x_j)|\leq\frac{C\varepsilon}{h_j}\left[|u(x_{j-1})-U_{j-1}^N|+|u(x_j)-U_j^N|\right]+C\varepsilon h_j|u''(\xi)|, \tag{2.5.31}$$

where $\xi\in(x_{j-1},x_j)$. Now we distinguish the following two cases.

Case (i)**:** $h_j = O(\varepsilon)$ (*i.e.,* for the mesh points inside the layer region). Using the bound for the error given in Theorem 2.5.6, the inequality (2.5.31) can be bounded as

$$\varepsilon|u'(x_j) - \widetilde{u}'(x_j)| \leq CN^{-1} + C\varepsilon^2|u''(\xi)|.$$

Now using the bound of $u(x)$ given in Lemma 2.2.3, we can obtain the required estimate, *i.e.,*

$$\varepsilon|u'(x_j) - \widetilde{u}'(x_j)| \leq CN^{-1}.$$

Case (ii)**:** On the other hand, when $h_j \leq CN^{-1}$ (*i.e.,* for the mesh points outside the layer region), using Theorem 2.5.6, we obtain

$$\varepsilon|u'(x_j) - \widetilde{u}'(x_j)| \leq CN^{-1} + C\varepsilon N^{-1}|u''(\xi)|.$$

Finally, using the assumption $\varepsilon \leq CN^{-1}$ and the bound given in Lemma 2.2.3, we can obtain the desired result. ∎

2.6 Numerical Results

In this section to validate the theoretical results, the proposed numerical scheme is applied to several test problems with constant and variable coefficients having left and right boundary layers. For comparison purposes, the numerical solution obtained by the upwind differences scheme on the piecewise-uniform Shishkin mesh are used.

Example 2.6.1. *Consider the test problem*

$$\begin{cases} -\varepsilon u''(x) - u'(x) + u(x) = 0, \quad x \in (0,1), \\ u(0) = 0, \quad u(1) = 1. \end{cases}$$

The exact solution is given by

$$u(x) = \frac{\exp(m_1 x) - \exp(m_2 x)}{\exp(m_1) - \exp(m_2)}, \quad \text{where} \quad m_{1,2} = \frac{-1 \pm \sqrt{1+4\varepsilon}}{2\varepsilon}.$$

This BVP has a boundary layer in the left end at $x = 0$.

Example 2.6.2. *Consider the variable coefficient problem*

$$\begin{cases} -\varepsilon u''(x) - \big(1 + x(1-x)\big)u'(x) = f(x), \quad x \in (0,1), \\ u(0) = 0, \quad u(1) = 0, \end{cases}$$

where $f(x)$ is chosen in such that its solution $u(x)$ is of the form

$$u(x) = \frac{1 - \exp(-x/\varepsilon)}{1 - \exp(-1/\varepsilon)} - \cos\left(\frac{\pi}{2}(1-x)\right).$$

The above problem has a boundary layer at the left side of the domain near $x = 0$.

Example 2.6.3. *Consider the variable coefficient problem*

$$\begin{cases} -\varepsilon u''(x) + \big(1 + x(1-x)\big)u'(x) = f(x), \quad x \in (0,1), \\ u(0) = 0, \quad u(1) = 0. \end{cases}$$

Now $f(x)$ is chosen in such a way that its solution $u(x)$ is of the form

$$u(x) = \frac{1 - \exp(-(1-x)/\varepsilon)}{1 - \exp(-1/\varepsilon)} - \cos\left(\frac{\pi x}{2}\right).$$

The above problem has a boundary layer at the right side of the domain near $x = 1$.

For any value of N and ε, the exact maximum pointwise errors E_ε^N and the corresponding rates of convergence are calculated by

$$E_\varepsilon^N = \max_{0 \le j \le N} |u(x_j) - U_j^N| \quad \text{and} \quad r_\varepsilon^N = \log_2\left(\frac{E_\varepsilon^N}{E_\varepsilon^{2N}}\right),$$

where u is the exact solution and U_j^N is the numerical solution obtained by using N mesh intervals in the domain $\overline{\Omega}^N$.

Now we would like to see the errors associated with the global solution and with the weighted derivatives. To do that, we calculate the maximum errors at the midpoints $x_j^* = (x_j + x_{j+1})/2$ of the corresponding adaptive mesh. The errors associated with the global solution and the corresponding rates of convergence are obtained by

$$\widetilde{E}_\varepsilon^N = \max_{x_j^* \in \overline{\Omega}^N} \varepsilon |u(x_j^*) - \widetilde{u}(x_j^*)| \quad \text{and} \quad \widetilde{r}_\varepsilon^N = \log_2\left(\frac{\widetilde{E}_\varepsilon^N}{\widetilde{E}_\varepsilon^{2N}}\right),$$

where $u(x)$ is the exact solution and $\widetilde{u}(x)$ is the global solution as defined in (2.5.29). Similarly, we can define the pointwise errors associated with the normalized flux as

$$D_\varepsilon^N = \max_{1 \le j \le N} \varepsilon |u'(x_j) - D^- U_j^N| \quad \text{and} \quad p_\varepsilon^N = \log_2\left(\frac{D_\varepsilon^N}{D_\varepsilon^{2N}}\right),$$

and the global error for the normalized flux as

$$\widetilde{D}_\varepsilon^N = \max_{x_j^* \in \overline{\Omega}^N} \varepsilon |u'(x_j^*) - \widetilde{u}'(x_j^*)| \quad \text{and} \quad \widetilde{p}_\varepsilon^N = \log_2\left(\frac{\widetilde{D}_\varepsilon^N}{\widetilde{D}_\varepsilon^{2N}}\right).$$

Figure 2.3(a) represents the movement of mesh after each iteration and Figure 2.3(b) shows the final computed mesh corresponding to the solution of Example 2.6.1. It is clear from these two figures that the mesh starts to move towards the boundary layer and clusters as many points required for the layer region. Also we plot similar graphs in the case when the boundary layer is located at the right *i.e.,* for Example 2.6.3. In Figure 2.6(a) the movement of the mesh towards right is presented and the final mesh is shown in Figure 2.6(b). These figures help us to conclude

that we can construct suitable non-uniform mesh through the same monitor function as defined in (2.3.3) even in the case of right boundary layer.

Figures 2.4(a) and 2.4(b) represent the global solution along with the exact solution and the corresponding error obtained on the adaptive grid for Example 2.6.2, respectively. Similarly Figures 2.5(a) and 2.5(b) show the normalized flux and the corresponding error.

In Table 2.1 and Table 2.2, the maximum pointwise error and the corresponding order of convergence for the solution and it derivatives respectively, are presented for Example 2.6.1. Similar results are shown in Table 2.3 and Table 2.4 for Example 2.6.2 which clearly show that the proposed method is ε-uniform convergent of order one. But for small values of ε, the rate of convergence becomes very slow due to the effect of high condition number of the coefficient matrix. As the condition number is directly proportional to square of N and inversely proportional to ε, hence for small values of ε the condition number is very high resulting the coefficient matrix nearly singular. One can refer [59] for more details on this argument. The same argument is also valid for the results in the subsequent chapters. At the same time if we use W_j^N (see [7]) instead of U_j^N as given in (2.3.7), we can get better results for non-homogeneous problems which is shown in Table 2.9.

The computational results using the adaptive mesh are also compared with the numerical results using the Shishkin mesh which are shown in Table 2.5 and in Table 2.6 for $\varepsilon = 1e-3$ and $\varepsilon = 1e-6$ for Example 2.6.2. From these results, one can observe that the adaptive mesh produces errors almost of the same order as produced by using the Shishkin mesh. The advantage of this approach is that without any prior knowledge of the location of the boundary layer, we are able to generate an appropriate nonuniform mesh suitable for the layer type problems.

2.7 Conclusion

In this chapter, the analysis of an upwind scheme for obtaining the global solution and the normalized flux for singularly perturbed BVPs of the form (2.1.1) is presented. The solution is obtained on a suitable nonuniform adaptive grids based on the equidistribution principle and the global solution is obtained using the constant or piecewise liner interpolants. The error analysis for the ε-weighted error of the derivatives for both the numerical solution and the global solution are carried out. It is shown that the errors converge at the rate of first-order, independent of the singular perturbation parameter. Numerical results obtained for some examples show that the proposed scheme is of first-order accurate. Hence, the key result established here is that the global solution and the global normalized flux computed on the adaptive grids are uniformly convergent with respect to the perturbation parameter.

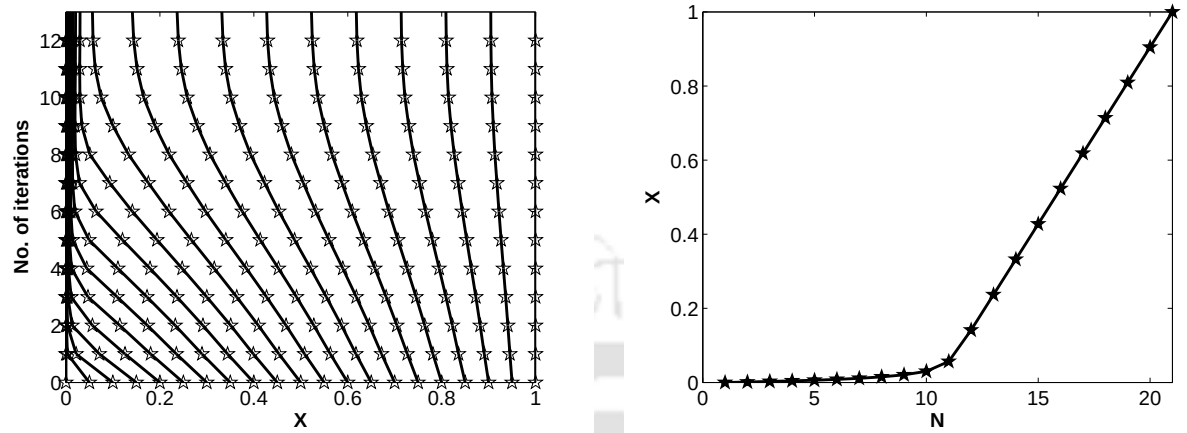

(a) Mesh movement toward left. *(b) Final computed mesh.*

Figure 2.3: *Movements of mesh towards left with* $\varepsilon = 1e-2$ *and* $N = 20$ *for Example 2.6.1.*

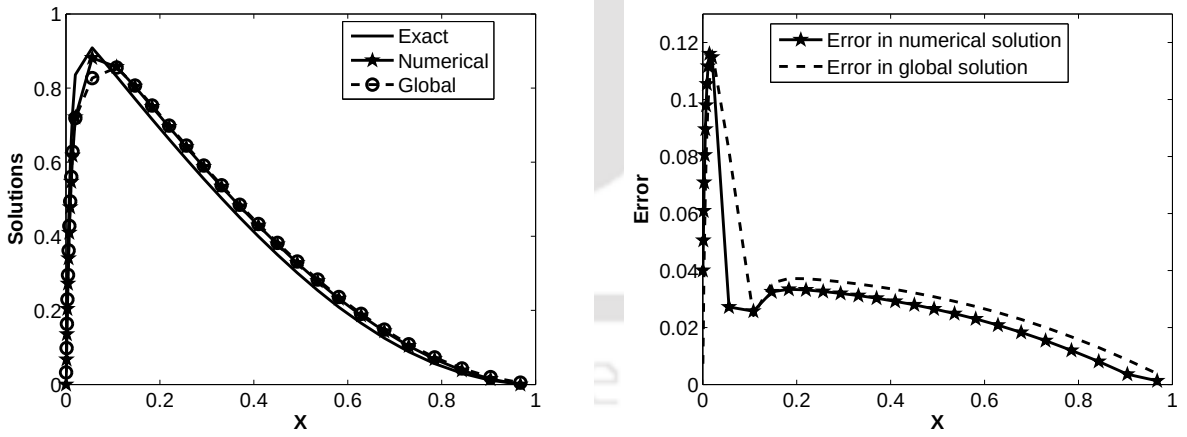

(a) Solution. *(b) Error.*

Figure 2.4: *Numerical solution and the global solution with the exact solution and the corresponding errors for Example 2.6.2 with* $\varepsilon = 1e-2$ *and* $N = 32$.

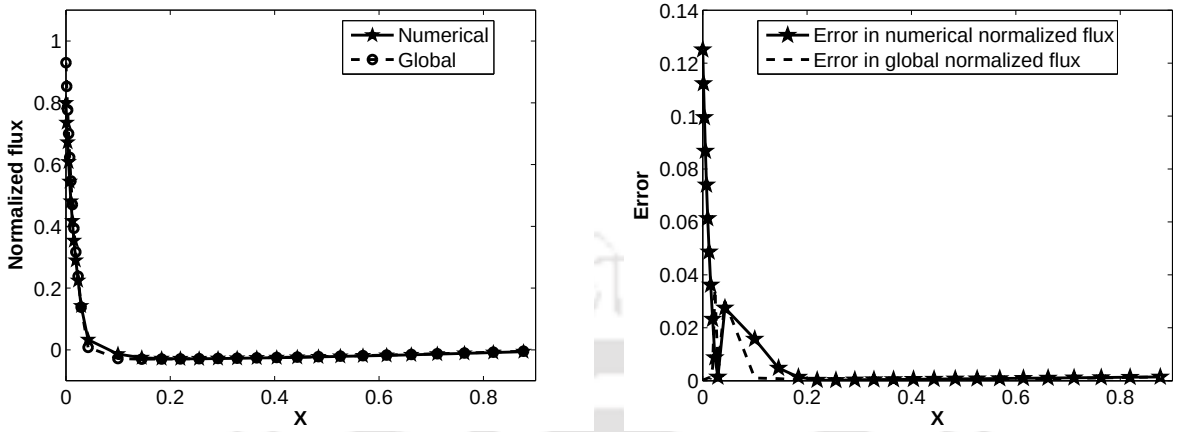

(a) Normalized flux. *(b) Error in the normalized flux.*

Figure 2.5: *Normalized flux and the error in the normalized flux for Example 2.6.2 with* $\varepsilon = 1e-2$ *and* $N = 32$.

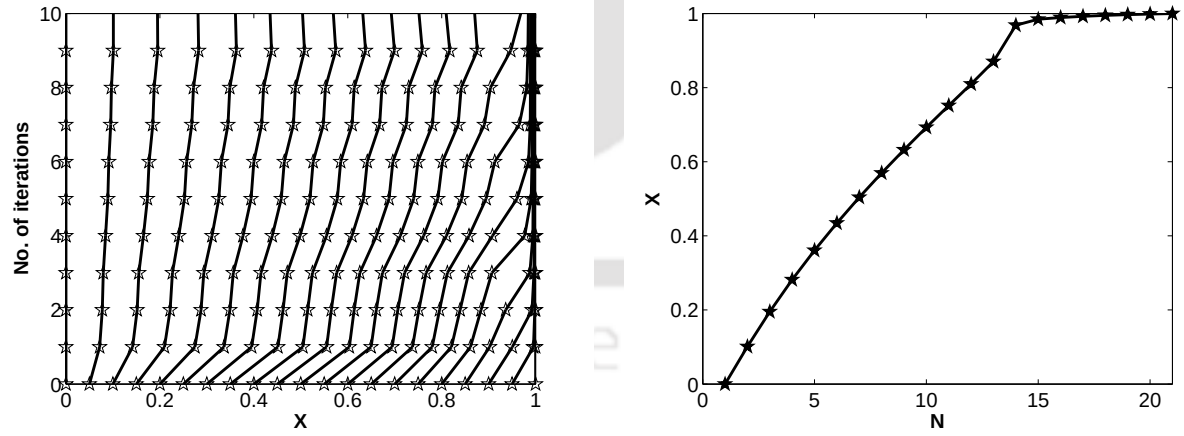

(a) Mesh movement toward right. *(b) Final computed mesh.*

Figure 2.6: *Movements of mesh towards right for Example 2.6.3 with* $\varepsilon = 1e-2$ *and* $N = 20$.

Table 2.1: *Maximum errors and the corresponding rate of convergence for Example 2.6.1.*

ε		Number of intervals N					
		32	64	128	256	512	1024
1	E_ε^N	1.8581e-3	9.3979e-4	4.7263e-4	2.3702e-4	1.1868e-4	5.9385e-5
	r_ε^N	0.9834	0.9916	0.9957	0.9978	0.9989	
	$\widetilde{E}_\varepsilon^N$	1.9822e-3	9.7129e-4	4.8056e-4	2.3900e-4	1.1918e-4	5.9509e-5
	$\widetilde{r}_\varepsilon^N$	1.0291	1.0152	1.0077	1.0039	1.0019	
$1e-2$	E_ε^N	8.8525e-2	4.9365e-2	2.9749e-2	1.3796e-2	7.7305e-3	3.8790e-3
	r_ε^N	0.8426	0.7306	1.1086	0.8355	0.9949	
	$\widetilde{E}_\varepsilon^N$	9.1050e-2	4.9969e-2	2.9920e-2	1.3839e-2	7.7417e-3	3.8818e-3
	$\widetilde{r}_\varepsilon^N$	0.8656	0.7399	1.1124	0.8379	0.9959	
$1e-4$	E_ε^N	1.1167e-1	6.3034e-2	3.6250e-2	2.0689e-2	1.1791e-2	6.2814e-3
	r_ε^N	0.8250	0.7981	0.8090	0.8111	0.9085	
	$\widetilde{E}_\varepsilon^N$	1.1439e-1	6.3899e-2	3.6486e-2	2.0754e-2	1.1809e-2	6.2860e-3
	$\widetilde{r}_\varepsilon^N$	0.8400	0.8084	0.8140	0.8134	0.9096	
$1e-8$	E_ε^N	1.1267e-1	6.6210e-2	3.8084e-2	2.0875e-2	1.1736e-2	6.5254e-3
	r_ε^N	0.7670	0.7978	0.8674	0.8308	0.8467	
	$\widetilde{E}_\varepsilon^N$	1.1542e-1	6.7138e-2	3.8327e-2	2.0939e-2	1.1753e-2	6.5302e-3
	$\widetilde{r}_\varepsilon^N$	0.7817	0.8087	0.8721	0.8331	0.8478	

Table 2.2: *Maximum errors associated with the normalized flux and the corresponding rate of convergence for Example 2.6.1.*

ε		Number of intervals N					
		32	64	128	256	512	1024
1	D_ε^N	9.0413e-3	4.6545e-3	2.3611e-3	1.1891e-3	5.9669e-4	2.9888e-4
	p_ε^N	0.9579	0.9791	0.9896	0.9948	0.9974	
	$\widetilde{D}_\varepsilon^N$	8.8040e-3	4.5960e-3	2.3466e-3	1.1855e-3	5.9579e-4	2.9866e-4
	$\widetilde{p}_\varepsilon^N$	0.9378	0.9698	0.9851	0.9926	0.9963	
$1e-2$	D_ε^N	1.3050e-1	7.3835e-2	4.3398e-2	2.0703e-2	1.1352e-2	5.7057e-3
	p_ε^N	0.8217	0.7667	1.0678	0.8669	0.9924	
	$\widetilde{D}_\varepsilon^N$	1.2532e-1	7.2484e-2	4.3023e-2	2.0614e-2	1.1328e-2	5.6998e-3
	$\widetilde{p}_\varepsilon^N$	0.7899	0.7526	1.0615	0.8638	0.9909	
$1e-4$	D_ε^N	1.5698e-1	9.0000e-2	5.1245e-2	2.8758e-2	1.6067e-2	8.4818e-3
	p_ε^N	0.8026	0.8125	0.8335	0.8399	0.9216	
	$\widetilde{D}_\varepsilon^N$	1.5055e-1	8.8314e-2	5.0791e-2	2.8635e-2	1.6033e-2	8.4730e-3
	$\widetilde{p}_\varepsilon^N$	0.7696	0.7981	0.8268	0.8367	0.9201	
$1e-8$	D_ε^N	1.5808e-1	9.3570e-2	5.3303e-2	2.8969e-2	1.6007e-2	8.7534e-3
	p_ε^N	0.7565	0.8118	0.8797	0.8558	0.8708	
	$\widetilde{D}_\varepsilon^N$	1.5161e-1	9.1824e-2	5.2831e-2	2.8844e-2	1.5973e-2	8.7443e-3
	$\widetilde{p}_\varepsilon^N$	0.7234	0.7975	0.8731	0.8527	0.8692	

Table 2.3: *Maximum errors and the corresponding rate of convergence for Example 2.6.2.*

ε		Number of intervals N					
		32	64	128	256	512	1024
1	E_ε^N	1.8695e-3	9.3934e-4	4.7082e-4	2.3570e-4	1.1792e-4	5.8979e-5
	r_ε^N	0.9929	0.9964	0.9982	0.9991	0.9995	
	$\widetilde{E}_\varepsilon^N$	2.0127e-3	9.7526e-4	4.7981e-4	2.3795e-4	1.1848e-4	5.9120e-5
	$\widetilde{r}_\varepsilon^N$	1.0453	1.0233	1.0118	1.0060	1.0032	
$1e-2$	E_ε^N	1.0544e-1	5.5846e-2	3.3356e-2	1.5908e-2	8.4806e-3	4.0269e-3
	r_ε^N	0.9169	0.7434	1.0682	0.9075	1.0745	
	$\widetilde{E}_\varepsilon^N$	1.1674e-1	5.6885e-2	3.3642e-2	1.5981e-2	8.4993e-3	4.0315e-3
	$\widetilde{r}_\varepsilon^N$	1.0372	0.7577	1.0739	0.9109	1.0760	
$1e-4$	E_ε^N	1.0115e-1	7.8402e-2	3.5465e-2	2.4687e-2	1.3366e-2	7.2825e-3
	r_ε^N	0.3675	1.1445	0.5226	0.8851	0.8761	
	$\widetilde{E}_\varepsilon^N$	1.0446e-1	7.9705e-2	3.5759e-2	2.4782e-2	1.3391e-2	7.2892e-3
	$\widetilde{r}_\varepsilon^N$	0.3901	1.1563	0.5290	0.8879	0.8774	
$1e-8$	E_ε^N	1.0148e-1	7.8716e-2	3.5681e-2	2.4508e-2	1.3250e-2	7.1047e-3
	r_ε^N	0.3664	1.1415	0.5418	0.8872	0.8991	
	$\widetilde{E}_\varepsilon^N$	1.0481e-1	8.0018e-2	3.5977e-2	2.4604e-2	1.3276e-2	7.1113e-3
	$\widetilde{r}_\varepsilon^N$	0.3893	1.1532	0.5482	0.8900	0.9006	

Table 2.4: *Maximum errors associated with the normalized flux and the corresponding rate of convergence for Example 2.6.2.*

ε		Number of intervals N					
		32	64	128	256	512	1024
1	D_ε^N	8.1040e-3	4.2931e-3	2.2058e-3	1.1176e-3	5.6242e-4	2.8212e-4
	p_ε^N	0.9166	0.9607	0.9809	0.9906	0.9953	
	$\widetilde{D}_\varepsilon^N$	8.0120e-3	4.2878e-3	2.2065e-3	1.1180e-3	5.6256e-4	2.8216e-4
	$\widetilde{p}_\varepsilon^N$	0.9019	0.9585	0.9809	0.9908	0.9955	
$1e-2$	D_ε^N	1.5561e-1	8.4682e-2	4.9688e-2	2.4250e-2	1.2815e-2	6.1740e-3
	p_ε^N	0.8778	0.7692	1.0349	0.9202	1.0535	
	$\widetilde{D}_\varepsilon^N$	1.4837e-1	8.2838e-2	4.9172e-2	2.4126e-2	1.2782e-2	6.1662e-3
	$\widetilde{p}_\varepsilon^N$	0.8409	0.7525	1.0273	0.9164	1.0517	
$1e-4$	D_ε^N	1.5008e-1	1.1044e-1	5.2416e-2	3.4431e-2	1.8471e-2	9.9343e-3
	p_ε^N	0.4425	1.0751	0.6063	0.8984	0.8948	
	$\widetilde{D}_\varepsilon^N$	1.4232e-1	1.0792e-1	5.1836e-2	3.4249e-2	1.8423e-2	9.9215e-3
	$\widetilde{p}_\varepsilon^N$	0.3992	1.0579	0.5979	0.8945	0.8929	
$1e-8$	D_ε^N	1.5045e-1	1.1075e-1	5.2675e-2	3.4229e-2	1.8343e-2	9.7373e-3
	p_ε^N	0.4419	1.0722	0.6219	0.9000	0.9136	
	$\widetilde{D}_\varepsilon^N$	1.4266e-1	1.0823e-1	5.2090e-2	3.4048e-2	1.8295e-2	9.7248e-3
	$\widetilde{p}_\varepsilon^N$	0.3985	1.0550	0.6134	0.8961	0.9117	

Table 2.5: *Comparison of numerical results with the Shishkin mesh for Example 2.6.2.*

N		$\varepsilon = 1e-3$		$\varepsilon = 1e-6$	
		Shishkin mesh	**Adaptive grid**	**Shishkin mesh**	**Adaptive grid**
64	E_ε^N	2.9727e-2	5.9218e-2	2.9662e-2	6.0498e-2
	r_ε^N	0.6307	0.4734	0.6315	0.7764
	$\widetilde{E}_\varepsilon^N$	3.2816e-2	6.0233e-2	3.2746e-2	6.1490e-2
	$\widetilde{r}_\varepsilon^N$	0.6873	0.4860	0.6878	0.7879
128	E_ε^N	1.9200e-2	4.2652e-2	1.9147e-2	3.5320e-2
	r_ε^N	0.7041	0.9632	0.7042	0.5356
	$\widetilde{E}_\varepsilon^N$	2.0379e-2	4.3006e-2	2.0329e-2	3.5616e-2
	$\widetilde{r}_\varepsilon^N$	0.7453	0.9695	0.7455	0.5421
256	E_ε^N	1.1785e-2	2.1877e-2	1.1752e-2	2.4365e-2
	r_ε^N	0.7594	0.9396	0.7595	0.8601
	$\widetilde{E}_\varepsilon^N$	1.2157e-2	2.1963e-2	1.2125e-2	2.4459e-2
	$\widetilde{r}_\varepsilon^N$	0.7799	0.9425	0.7800	0.8629
512	E_ε^N	6.9618e-3	1.1406e-2	6.9421e-3	1.3423e-2
	r_ε^N	0.7976	0.9339	0.7976	0.8808
	$\widetilde{E}_\varepsilon^N$	7.0807e-3	1.1428e-2	7.0613e-3	1.3449e-2
	$\widetilde{r}_\varepsilon^N$	0.8087	0.9354	0.8088	0.8823

Table 2.6: *Comparison of flux results with the Shishkin mesh for Example 2.6.2.*

N		$\varepsilon = 1e-3$		$\varepsilon = 1e-6$	
		Shishkin mesh	**Adaptive grid**	**Shishkin mesh**	**Adaptive grid**
64	D_ε^N	6.8247e-2	8.8884e-2	6.8135e-2	9.0495e-2
	r_ε^N	0.4742	0.5556	0.4744	0.7924
	$\widetilde{D}_\varepsilon^N$	4.4718e-2	8.6834e-2	4.4621e-2	8.8382e-2
	$\widetilde{p}_\varepsilon^N$	0.1888	0.5376	0.1887	0.7743
128	D_ε^N	4.9129e-2	6.0476e-2	4.9041e-2	5.2252e-2
	r_ε^N	0.6147	0.9532	0.6147	0.6168
	$\widetilde{D}_\varepsilon^N$	3.9233e-2	5.9823e-2	3.9151e-2	5.1673e-2
	$\widetilde{p}_\varepsilon^N$	0.4670	0.9451	0.4669	0.6084
256	D_ε^N	3.2085e-2	3.1236e-2	3.2026e-2	3.4074e-2
	r_ε^N	0.7101	0.9433	0.7101	0.8781
	$\widetilde{D}_\varepsilon^N$	2.8383e-2	3.1071e-2	2.8327e-2	3.3894e-2
	$\widetilde{p}_\varepsilon^N$	0.6301	0.9394	0.6299	0.8742
512	D_ε^N	1.9613e-2	1.6244e-2	1.9577e-2	1.8539e-2
	r_ε^N	0.7734	0.9428	0.7733	0.8987
	$\widetilde{D}_\varepsilon^N$	1.8340e-2	1.6202e-2	1.8305e-2	1.8491e-2
	$\widetilde{p}_\varepsilon^N$	0.7294	0.9409	0.7293	0.8968

Table 2.7: *Maximum errors and the corresponding rate of convergence for Example 2.6.3.*

ε		Number of intervals N					
		32	64	128	256	512	1024
$1e-4$	E_ε^N	1.0115e-1	7.8402e-2	3.5465e-2	2.4687e-2	1.3366e-2	7.2825e-3
	r_ε^N	0.3675	1.1445	0.5226	0.8852	0.8761	
	$\widetilde{E}_\varepsilon^N$	1.0446e-1	7.9705e-2	3.5759e-2	2.4782e-2	1.3391e-2	7.2892e-3
	$\widetilde{r}_\varepsilon^N$	0.3902	1.1563	0.5290	0.8880	0.8775	
$1e-8$	E_ε^N	1.0148e-1	7.8716e-2	3.5681e-2	2.4508e-2	1.3249e-2	7.1137e-3
	r_ε^N	0.3664	1.1415	0.5419	0.8874	0.8972	
	$\widetilde{E}_\varepsilon^N$	1.0481e-1	8.0018e-2	3.5977e-2	2.4603e-2	1.3274e-2	7.1204e-3
	$\widetilde{r}_\varepsilon^N$	0.3893	1.1532	0.5483	0.8902	0.8986	

Table 2.8: *Maximum errors associated with the normalized flux and the corresponding rate of convergence for Example 2.6.3.*

ε		Number of intervals N					
		32	64	128	256	512	1024
$1e-4$	D_ε^N	1.3338e-1	1.0508e-1	5.1166e-2	3.4044e-2	1.8369e-2	9.9073e-3
	p_ε^N	0.3440	1.0383	0.5878	0.8901	0.8907	
	$\widetilde{D}_\varepsilon^N$	1.2571e-1	1.0257e-1	5.0586e-2	3.3862e-2	1.8321e-2	9.8945e-3
	$\widetilde{p}_\varepsilon^N$	0.2934	1.0198	0.5791	0.8861	0.8888	
$1e-8$	D_ε^N	1.3369e-1	1.0539e-1	5.1416e-2	3.3844e-2	1.8240e-2	9.7210e-3
	p_ε^N	0.3432	1.0354	0.6033	0.8918	0.9079	
	$\widetilde{D}_\varepsilon^N$	1.2598e-1	1.0287e-1	5.0832e-2	3.3663e-2	1.8192e-2	9.7084e-3
	$\widetilde{p}_\varepsilon^N$	0.2924	1.0170	0.5946	0.8878	0.9060	

Table 2.9: *Maximum point-wise errors E_ε^N and the rate of convergence r_ε^N for using W_j^N in stead of U_j^N for Example 2.6.3.*

ε		Number of intervals N					
		32	64	128	256	512	1024
$1e-4$	E_ε^N	6.0288e-2	3.5673e-2	2.2023e-2	1.3126e-2	7.6032e-3	4.3006e-3
	r_ε^N	0.7570	0.6958	0.7466	0.7877	0.8221	
$1e-8$	E_ε^N	6.9285e-2	4.3067e-2	2.5913e-2	1.5339e-2	8.8619e-3	5.0083e-3
	r_ε^N	0.6859	0.7329	0.7565	0.7915	0.8233	

Chapter 3

Numerical Solution of a Singularly Perturbed Robin Boundary–Value Problem

This chapter analyzes the upwind finite difference scheme for a class of singularly perturbed convection-diffusion BVPs with Robin boundary conditions. The solution is obtained on a suitable nonuniform mesh, formed by equidistributing the arc-length monitor function. It is shown that the method converges uniformly in the discrete supremum norm with respect to the perturbation parameter. Moreover, an optimal first-order convergence *i.e.,* error of the order $O(N^{-1})$ is shown.

3.1 Introduction

This chapter considers the following form of the singularly perturbed Robin BVP:

$$\begin{cases} Lu(x) \equiv -\varepsilon u''(x) - a(x)u'(x) + b(x)u(x) = f(x), \ x \in \Omega = (0,1), \\ B_0u(0) \equiv \beta_1 u(0) - \beta_2 \varepsilon u'(0) = s_0, \quad B_1u(1) \equiv \lambda_1 u(1) + \lambda_2 u'(1) = s_1, \end{cases} \tag{3.1.1}$$

where $0 < \varepsilon \ll 1$ is a small singular perturbation parameter, the functions $a(x), b(x), f(x)$ are sufficiently smooth and s_0, s_1 are given constants. Further, we assume that the coefficients are such that

$$\alpha^* \geq a(x) > \alpha > 0, \ \ b(x) \geq 0 \quad \forall \ x \in \overline{\Omega}$$

and the constants satisfy

$$\beta_1, \beta_2 \geq 0, \ \beta_1 + \beta_2 > 0, \ \lambda_1 > 0, \ \lambda_2 \geq 0.$$

Under these assumptions, the BVP (3.1.1) has a unique solution which exhibits a layer behavior near $x = 0$.

An outline of this chapter is as follows. The next section provides *a priori* bounds on the analytical solution of (3.1.1) and its derivatives; in particular, a decomposition into regular and singular components is derived. In Section 3.3, we describe the upwind scheme, the generation of the

adaptive grid and some results on this equidistributing grid that are used later. The convergence analysis of the numerical solution obtained by the upwind scheme is discussed in Section 3.4. Finally, Section 3.5 gives a few numerical examples that confirm our theoretical estimates.

3.2 Continuous Problem

This section provides the maximum principle, the stability estimate and the bounds of the solution of the BVP (3.1.1).

Lemma 3.2.1. (Maximum Principle) *Let $\mathcal{V}$ be a smooth function satisfying $B_0\mathcal{V}(0) \geq 0,\ B_1\mathcal{V}(1) \geq 0$ and $L\mathcal{V}(x) \geq 0,\ \forall x \in\ \Omega$. Then $\mathcal{V}(x) \geq 0,\ \forall x \in\ \overline{\Omega}$.*

Proof. Let $x^* \in \overline{\Omega}$ be such that $\mathcal{V}(x^*) = \min \mathcal{V}(x), x \in \overline{\Omega}$ and assume that $\mathcal{V}(x^*) < 0$. Clearly $x^* \neq 1$. Now consider the three cases: $\lambda_2 = 0, \lambda_1/\lambda_2 > \alpha/2\varepsilon$ and $\lambda_1/\lambda_2 < \alpha/\varepsilon$.
Case (i)**:** If $\lambda_2 = 0$, from the boundary condition, we have $\mathcal{V}(1) \geq 0$. Define the auxiliary function $\mathcal{W}(x) = \mathcal{V}(x)\exp(\alpha x/2\varepsilon)$. Now for $x^* \in \Omega$, then $\mathcal{W}'(x^*) = 0$ and $\mathcal{W}''(x^*) \geq 0$ and thus $L\mathcal{V}(x) < 0$ which contradicts our hypothesis. The only possibility is that $x^* = 0$, which means that $\mathcal{W}(0) < 0$ and $\mathcal{W}'(0) \geq 0$. Using the auxiliary function we can conclude that $\mathcal{V}(0) < 0$ and $\mathcal{V}'(0) \geq 0$, which is also a contradiction.
Case (ii)**:** Let $\lambda_1/\lambda_2 > \alpha/2\varepsilon$. If $x^* = 1$, then the minimum of $\mathcal{W}(x)$ also occurs at $x = 1$, and thus $\mathcal{W}(1) < 0,\ \mathcal{W}'(1) \leq 0$. From this it follows that $\mathcal{V}'(1) \leq -(\alpha/2\varepsilon)\mathcal{V}(1)$ and since $\lambda_1/\lambda_2 > \alpha/2\varepsilon$ we have $\mathcal{V}'(1) < -(\lambda_1/\lambda_2)\mathcal{V}(1)$ which violates our hypothesis. If $x^* \in \Omega$, then $L\mathcal{V}(x^*) < 0$ which again contradicts our hypothesis. So the only possibility left out is that $\mathcal{W}(x)$ attains its minimum at $x = 0$ which can be discarded by the same argument as given in the first case.
Case (iii)**:** Finally, if $\lambda_1/\lambda_2 \leq \alpha/\varepsilon$, define the auxiliary function $\mathcal{W}(x) = \mathcal{V}(x)\exp(\lambda_1 x/2\lambda_2)$. By giving a similar argument we can conclude $x^* \neq 1$. If $x^* \in \Omega$, then $L\mathcal{V}(x^*) < 0$ which contradicts our hypothesis. Thus the only possibility left is that $x^* = 0$, which can be excluded as before. ∎

Now *a priori* bounds for the solution and its derivatives of the BVP (3.1.1) are established.

Lemma 3.2.2. *If u is the solution of the boundary value problem (3.1.1), then we have the the following stability estimate:*

$$\|u\| \ \leq\ \alpha^{-1}\left(1 + \frac{\lambda_1}{\lambda_2}\right)\|f\| + C\left(\frac{|s_0|}{\beta_1 + \alpha\beta_2} + \frac{|s_1|}{\lambda_1}\right). \tag{3.2.1}$$

Proof. Consider the following barrier function

$$\psi^{\pm}(x) = \frac{|s_0|}{(\beta_1 + \alpha\beta_2) - \beta_1(1 - \lambda_2\alpha/\lambda_1\varepsilon)e^{-\alpha/\varepsilon}}\left(e^{-\alpha x/\varepsilon} - \left(1 - \frac{\lambda_2\alpha}{\lambda_1\varepsilon}\right)e^{-\alpha/\varepsilon}\right)$$
$$+\frac{|s_1|}{\lambda_1} + \alpha^{-1}\|f\|\left(1 + \frac{\lambda_2}{\lambda_1} - x\right) \pm u(x).$$

It is easy to check that $\beta_1\psi^{\pm}(0)-\varepsilon\beta_2(\psi^{\pm})'(0)\geq 0$ and $\lambda_1\psi^{\pm}(1)+\lambda_2(\psi^{\pm})'(1)\geq 0$. Now from (3.1.1) for $x\in\Omega$, we have $L\psi^{\pm}(x)\geq 0$. Hence, by applying the maximum principle as given in Lemma 3.2.1, we can conclude that $\psi^{\pm}(x)\geq 0, \forall x\in\overline{\Omega}$, which is our desired result. ∎

Lemma 3.2.3. *The derivatives $u^{(k)}$ of the solution u of (3.1.1) satisfy the following bounds:*

$$\begin{aligned}\|u^{(k)}\| &\leq C\varepsilon^{-k}\max\{\|f\|,\|u\|\}, \qquad k=1,2,\\ \|u^{(3)}\| &\leq C\varepsilon^{-3}\max\{\|f\|,\|f'\|,\|u\|\},\end{aligned} \tag{3.2.2}$$

where C depends only on the bounds of the coefficients and their derivatives.

Proof. The proof is analogous to the one as given in [28]. Note that

$$\int_0^x \big(f(t)-b(t)u(t)+a(t)u'(t)\big)\,dt \leq \|f\|+C\|u\|, \tag{3.2.3}$$

where C depends on $\|a\|,\|b\|,\|a'\|$ and $\|b'\|$. Using the mean-value theorem [18], there exists a $z\in(0,\varepsilon)$ such that $|\varepsilon u'(z)|\leq 2\|u\|$. Integrating the BVP (3.1.1), we have

$$\varepsilon(u'(x)-u'(0)) = \int_0^x \big(f(t)-b(t)u(t)+a(t)u'(t)\big)\,dt. \tag{3.2.4}$$

Combining (3.2.3) and (3.2.4), we have

$$|\varepsilon u'(x)| \leq \|f\|+C\|u\|,$$

which gives the required result for $k=1$. Again from the BVP (3.1.1), we have

$$\varepsilon u'' = bu-au'-f \quad \text{and} \quad \varepsilon u''' = \big(bu-au'-f\big)',$$

which gives successively the required bounds on the second and third derivatives. ∎

In order to derive the ε-uniform error estimate, we require sharper bounds on the derivatives of the solution, for this, we decompose the solution of (3.1.1) into regular and singular parts as follows:

$$u(x) = v(x)+w(x). \tag{3.2.5}$$

Now $v(x)$ can be written in an asymptotic expansion as

$$v(x) = v_0(x)+\varepsilon v_1(x)+\varepsilon^2 v_2(x),$$

where v_0, v_1 and v_2 are respectively the solutions of the following differential equations:

$$\begin{cases} a(x)v_0'(x)-b(x)v_0(x) = -f(x), & \lambda_1 v_0(1)+\lambda_2 v_0'(1) = s_1,\\ a(x)v_1'(x)-b(x)v_1(x) = -v_0''(x), & \lambda_1 v_1(1)+\lambda_2 v_1'(1) = 0,\\ Lv_2(x) = v_1''(x), & \beta_1 v_2(0)+\beta_2 v_2'(0) = 0, \quad \lambda_1 v_2(1)+\lambda_2 v_2'(1) = 0. \end{cases} \tag{3.2.6}$$

Hence, the regular component of the solution satisfies the BVP:

$$\begin{cases} Lv(x) = f(x), \\ \beta_1 v(0) - \varepsilon\beta_2 v'(0) = \beta_1 v_0(0) - \varepsilon\beta_2 v_0'(0) + \varepsilon\big(\beta_1 v_1(0) - \varepsilon\beta_2 v_1'(0)\big), \\ \lambda_1 v(1) + \lambda_2 v'(1) = s_1, \end{cases} \tag{3.2.7}$$

and the singular component satisfies:

$$\begin{cases} Lw(x) = 0, \\ \beta_1 w(0) - \varepsilon\beta_2 w'(0) = s_0 - \big(\beta_1 v(0) - \varepsilon\beta_2 v'(0)\big), \\ \lambda_1 w(1) + \lambda_2 w'(1) = 0. \end{cases} \tag{3.2.8}$$

In the following lemma, we obtain bounds for the components of the solution and their derivatives.

Lemma 3.2.4. *For sufficiently small ε and $0 \le k \le 3$, the derivatives of v and w satisfy the following bounds:*

$$\begin{aligned} |v^{(k)}(x)| &\le C\big(1 + \varepsilon^{2-k}\big), \\ |w^{(k)}(x)| &\le C\varepsilon^{-k}\exp\left(-\alpha x/\varepsilon\right), \quad \forall x \in \overline{\Omega}. \end{aligned} \tag{3.2.9}$$

Proof. The proof is given in [4]. ∎

3.3 Numerical Scheme and Nonuniform Grids

3.3.1 Discrete problem

Consider the difference approximation of (3.1.1) on a nonuniform grid $\overline{\Omega}^N = \{x_j\}_{j=0}^N$ and denote $h_j = x_j - x_{j-1}$. The upwind finite difference scheme for (3.1.1) takes the form

$$\begin{cases} L^N U_j^N \equiv -\varepsilon D^+ D^- U_j^N - a_j D^+ U_j^N + b_j U_j^N = f_j\,, \quad 1 \le j \le N-1, \\ B_0^N U_0^N \equiv \beta_1 U_0^N - \beta_2 \varepsilon D^+ U_0^N = s_0, \quad B_1^N U_N^N \equiv \lambda_1 U_N^N + \lambda_2 D^- U_N^N = s_1. \end{cases} \tag{3.3.1}$$

Equation (3.3.1) can be expressed in the following form of system of algebraic equations

$$\begin{cases} -r_j^- U_{j-1}^N + r_j^c U_j^N - r_j^+ U_{j+1}^N = f_j, \quad j = 1, \ldots, N-1, \\ r_0^c U_0^N + r_0^+ U_1^N = s_0, \qquad r_N^- U_{N-1}^N + r_N^c U_N^N = s_1, \end{cases} \tag{3.3.2}$$

where

$$\begin{cases} r_j^- = \dfrac{2\varepsilon}{h_j(h_j + h_{j+1})}, \quad r_j^c = \dfrac{2\varepsilon}{h_j h_{j+1}} + \dfrac{a_j}{h_{j+1}} + b_j, \quad r_j^+ = \dfrac{2\varepsilon}{h_{j+1}(h_j + h_{j+1})} + \dfrac{a_j}{h_{j+1}}, \\ r_0^c = \beta_1 + \dfrac{\varepsilon\beta_2}{h_1}, \; r_0^+ = -\dfrac{\varepsilon\beta_2}{h_1}, \; r_N^- = -\dfrac{\lambda_2}{h_N}, \quad r_N^c = \lambda_1 + \dfrac{\lambda_2}{h_N}\,. \end{cases} \tag{3.3.3}$$

In the tri-diagonal system (3.3.3), the off-diagonal entries have the following properties:

$$r_0^+ < 0\,, r_N^- < 0 \quad \text{and} \quad r_j^- > 0,\ r_j^+ > 0, \quad j = 1, \ldots, N-1,$$

and

$$r_j^c + r_j^- + r_j^+ \geq 0, \quad \text{for} \quad j = 1, \ldots, N-1, \tag{3.3.4}$$

which imply that the stiffness matrix is an M-matrix.

Lemma 3.3.1. (Discrete Comparison Principle) *Let L^N be the upwind finite difference operator as defined in (3.3.1) and let Ω^N be an arbitrary mesh of $N+1$ mesh points. If $\mathcal{V}_j$ be any mesh function satisfying $\beta_1\mathcal{V}_0 - \varepsilon\beta_2 D^+\mathcal{V}_0 \geq 0$, $\lambda_1\mathcal{V}_N + \lambda_2 D^-\mathcal{V}_N \geq 0$ and $L^N\mathcal{V}_j \geq 0$, $\quad 1 \leq j \leq N-1$, then $\mathcal{V}_j \geq 0$ for $0 \leq j \leq N$.*

Proof. Here, we consider the two cases: $\beta_2 = 0$ and $\beta_2 \neq 0$.

Case (i)**:** If $\beta_2 = 0$, then from the left boundary condition, we have $\mathcal{V}_0 \geq 0$. Define $\mathcal{V}_k = \min_j \mathcal{V}_j < 0$. Now $D^+\mathcal{V}_k \geq 0$ and $D^+D^-\mathcal{V}_k \geq 0$, which results $L^N\mathcal{V}_k \leq 0$. To avoid such contradiction, we must take $\mathcal{V}_k = \mathcal{V}_{k-1} = \mathcal{V}_{k+1} < 0$. By repeating this argument we reach at $\mathcal{V}_0 < 0$ which is a contradiction.

Case (ii)**:** When $\beta_2 \neq 0$. Define a mesh function as $\mathcal{W}_j = \big(1 + (\beta_1 h_j)/(\beta_2\varepsilon)\big)\mathcal{V}_j$. Consider $\mathcal{W}_k = \min_j\{\mathcal{W}_j\}$. Assuming $\mathcal{V}_k < 0$ implies $\mathcal{W}_k < 0$. Note that if $k = N$, then $D^-\mathcal{V}_N \leq 0$ and also $\mathcal{V}_N < 0$ which violates the right hand side boundary condition and hence $k \neq N$. We thus have two remaining possibilities.

First, suppose $k = 0$, so that $\mathcal{W}_0 = \min_j\{\mathcal{W}_j\}$. Using the left boundary conditions, we get $\mathcal{W}_1 \leq \mathcal{W}_0$ and since $\mathcal{W}_0$ is the minimum, we have $\mathcal{W}_1 = \mathcal{W}_0$. Repeating the same argument, we can reach at $\mathcal{W}_N = \mathcal{W}_0$ which means $D^+\mathcal{V}_{N-1} = 0$ and $D^-\mathcal{V}_N = 0$. So we have the right boundary condition as $\lambda_1\mathcal{V}_N + \lambda_2 D^-\mathcal{V}_N \leq 0$ which contradicts the hypothesis.

Finally, suppose $0 < k < N$ for which $V_k = \min_j\{\mathcal{V}_j\} < 0$ be the minimum, then $D^+\mathcal{V}_k \geq 0$ and $D^+D^-\mathcal{V}_k \geq 0$ which gives $L^N\mathcal{V}_k \leq 0$. To avoid this contradiction, we can take $\mathcal{V}_k = \mathcal{V}_{k-1} = \mathcal{V}_{k+1} < 0$ which is again a contradiction to the right hand side boundary condition. ∎

3.3.2 Grid equidistribution

Here, we consider the arc-length monitor function

$$M\big(u(x), x\big) = \sqrt{1 + (u'(x))^2}, \tag{3.3.5}$$

which is bounded below by unity.

Now the nonuniform mesh can be constructed as the solution of the following nonlinear system of equations:

$$\begin{cases} (x_{j+1}-x_j)^2+(U_{j+1}^N-U_j^N)^2=(x_j-x_{j-1})^2+(U_j^N-U_{j-1}^N)^2,\ j=1,\ldots,N-1. \\ x_0=0, \quad x_N=1. \end{cases} \tag{3.3.6}$$

The system of equations (3.3.1) and (3.3.6) are solved simultaneously to obtain the solution U_j^N and the grids x_j. One can refer Section 2.3 of Chapter 2 for details of the adaptive algorithm.

3.4 Error Analysis

3.4.1 Local truncation error

The local truncation error of the difference scheme (3.3.1) at the grid x_j is given by

$$\tau_j = L^N U_j^N - Lu(x_j), \tag{3.4.1}$$

where u and U_j^N denote the solutions of (3.1.1) and (3.3.1) respectively.

Lemma 3.4.1. *The truncation error defined in (3.4.1) has the following bound:*

$$|\tau_j| \le \frac{C}{\varepsilon N}\exp\left(\frac{-\alpha x_{j-1}}{\varepsilon}\right). \tag{3.4.2}$$

Proof. The proof is similar to the proof as given in Lemma 2.5.2 of Chapter 2. ∎

In the following lemma, we wish to find the bound of the discrete solution. For simplicity, a constant coefficient version without the zeroth order term of (3.1.1) is considered.

Lemma 3.4.2. *The solution of the constant coefficient problem given by*

$$\begin{cases} -\varepsilon D^+D^-\Phi_j-\alpha D^+\Phi_j=0\,, \quad 1\le j\le N-1, \\ \beta_1\Phi_0-\beta_2\varepsilon D^+\Phi_0=1, \qquad \lambda_1\Phi_N+\lambda_2 D^-\Phi_N=0. \end{cases} \tag{3.4.3}$$

on a uniform mesh or on the nonuniform mesh Ω^N satisfies $|\Phi_j|\le C$ and $D^+\Phi_j\le 0, \quad \forall\ 1\le j\le N-1$.

Proof. Assume that the mesh is uniform, then $h_j=h=N^{-1}$. The solution of the difference equation (3.4.3) is of the form

$$\Phi_j=\frac{\mu^{N-j}+(\alpha\lambda_2/\lambda_1\varepsilon)-1}{[\beta_1(\mu^N+(\alpha\lambda_2/\lambda_1\varepsilon)-1)-\beta_2\mu^{N-1}]}, \text{ where } \mu=1+\frac{\alpha h}{\varepsilon},$$

and therefore

$$D^+\Phi_j=\frac{\mu^{N-j-1}}{\varepsilon[\beta_1(\mu^N+(\alpha\lambda_2/\lambda_1\varepsilon)-1)-\beta_2\mu^{N-1}]}\le 0. \tag{3.4.4}$$

Now, consider the case, when the mesh is nonuniform, then the solution is of the form

$$\Phi_j = \frac{\mu_j^{N-j} + (\lambda_2\alpha/\lambda_1\varepsilon) - 1}{\mu_j^N + (\lambda_2\alpha/\lambda_1\varepsilon) - 1}, \quad \text{where} \quad \mu_j = 1 + \frac{\alpha h_j}{\varepsilon}.$$

Applying the forward difference operator, we obtain

$$D^+\Phi_j = \frac{\alpha\mu^{N-j-1}}{\varepsilon\left[\mu^N + (\alpha\lambda_2/\lambda_1\varepsilon) - 1\right]} \leq 0. \tag{3.4.5}$$

Combining (3.4.4) and (3.4.5), we have the desired result. ∎

Analogous to the continuous case, the discrete solution U_j^N can be decomposed into the sum

$$U_j^N = V_j^N + W_j^N, \tag{3.4.6}$$

where V_j^N and W_j^N are, respectively, the solutions of the problems:

$$\begin{cases} L^N V_j^N = f_j, \quad x_j \in \Omega^N, \\ \beta_1 V_0^N - \varepsilon\beta_2 D^+ V_0^N = \beta_1 v(0) - \varepsilon\beta_2 v'(0), \\ \lambda_1 V_N^N + \lambda_2 D^- V_N^N = \lambda_1 v(1) + \lambda_2 v'(1), \end{cases} \tag{3.4.7}$$

and

$$\begin{cases} L^N W_j^N = 0, \quad x_j \in \Omega^N, \\ \beta_1 W_0^N - \varepsilon\beta_2 D^+ W_0^N = \beta_1 w(0) - \varepsilon\beta_2 w'(0), \\ \lambda_1 W_N^N + \lambda_2 D^- W_N^N = 0. \end{cases} \tag{3.4.8}$$

Now we will obtain the error estimates for each of these components separately.

Lemma 3.4.3. *The error in the regular component of the numerical solution is obtained as*

$$|V_j^N - v(x_j)| \leq CN^{-1}, \quad \forall x_j \in \Omega^N,$$

where V_j^N is the solution of (3.4.7) and v is the solution of (3.2.7).

Proof. Consider the local truncation error

$$L^N V_j^N - Lv(x_j) = -\varepsilon\left(\frac{d^2}{dx^2} - D^+D^-\right)v(x_j) - a_j\left(\frac{d}{dx} - D^+\right)v(x_j).$$

Then, by using the bounds given in Lemma 2.5.1 and in (3.2.9), we have

$$|L^N V_j^N - Lv(x_j)| \leq \frac{\varepsilon}{3}(x_{j+1} - x_{j-1})\|v^{(3)}\| + \frac{a_j}{2}(x_{j+1} - x_j)\|v^{(2)}\| \leq CN^{-1}.$$

Let us use the mesh function

$$\Psi^{\pm}(x_j) = CN^{-1}\left(\phi_j + \frac{1}{\lambda_1}\right) \pm (V_j^N - v)(x_j),$$

where ϕ_j is the solution of the constant coefficient problem

$$\begin{cases} -\varepsilon D^+D^-\phi_j - \alpha D^+\phi_j + b\phi_j = f_j\,, \quad 1 \le j \le N-1, \\ \beta_1\phi_0 - \beta_2\varepsilon D^+\phi_0 = 1, \qquad \lambda_1\phi_N + \lambda_2 D^-\phi_N = 0. \end{cases} \tag{3.4.9}$$

Using the bounds given in Lemma 3.2.4 and in Lemma 2.5.1, the following inequalities hold:

$$|\beta_1(V_0^N - v(0)) - \varepsilon\beta_2(D^+V_0^N - v'(0))| \le CN^{-1},$$

$$|\lambda_1(V_0^N - v(1)) + \lambda_2(D^-V_N^N - v'(1))| \le CN^{-1}.$$

Now by choosing C large enough, we can show that $\beta_1\Psi_0^{\pm} - \varepsilon\beta_2 D^+\Psi_0^{\pm} \ge 0$ and $\lambda_1\Psi_N^{\pm} + \lambda_2 D^-\Psi_N^{\pm} \ge 0$ and $L^N\Psi^{\pm}(x_j) \ge 0$. Hence, by applying the discrete comparison principle as given in Lemma 3.3.1, the result follows. ∎

Lemma 3.4.4. *The error in the singular component of the numerical solution is obtained as*

$$|W_j^N - w(x_j)| \le CN^{-1}, \quad \forall x_j \in \Omega^N,$$

where W_j^N is the solution of (3.4.8) and w is the solution of (3.2.8).

Proof. Using the bounds given in Lemma 3.2.4, the following inequalities holds:

$$\begin{aligned} |\beta_1(W_0^N - w(0)) - \varepsilon\beta_2(D^+W_0^N - w'(0))| &= |\varepsilon\beta_2(D^+W_0^N - w'(0))| \\ &\le \left|\frac{\varepsilon}{h}\int_0^h (s-h)w''(s)ds\right| \\ &\le CN^{-1}. \end{aligned}$$

Similarly, we can show that

$$|\lambda_1(W_N^N - w(1)) + \lambda_2(D^-W_N^N - w'(1))| \le CN^{-1}.$$

First, we consider the case of uniform mesh. Using the bounds given in Lemma 3.2.4, the truncation error corresponding to the singular part is

$$|L^NW_j^N - Lw(x_j)| \le C\varepsilon^{-1}(x_{j+1} - x_{j-1})\exp(-\alpha x_{j-1}/\varepsilon) \le C\varepsilon^{-1}N^{-1}\exp(-\alpha x_{j-1}/\varepsilon). \tag{3.4.10}$$

We employ the barrier function

$$\chi^{\pm}(x_j) = \frac{C\exp(2\tau h/\varepsilon)}{\tau(\alpha-\tau)}\varepsilon^{-1}N^{-1}\left(\gamma_j + \frac{1}{\lambda_1}\right) \pm \left(W_j^N - w(x_j)\right),$$

where τ is a constant with $0 < \tau < \alpha$ and γ_j is the solution of the problem (3.4.9). By choosing C large enough such that $\chi^{\pm}(x_j)$ satisfy the discrete comparison principle as given in Lemma 3.3.1 and using the fact $\gamma_j \le C$, we can conclude that

$$\left(W_j^N - w(x_j)\right) \le \frac{C\exp(2\tau h/\varepsilon)}{\tau(\alpha-\tau)}\varepsilon^{-1}N^{-1}\gamma_j \le CN^{-1}. \tag{3.4.11}$$

Now consider the mesh to be nonuniform. Using Lemma 2.3.4 (of Chapter 2), the domain Ω^N is broadly divided into two subdomains $[0, x_{_K})$ and $[x_{_K}, 1]$. We wish to find the error in both the subdomains separately.

First, consider the points inside the regular region *i.e.*, $x_j \in [x_{_K}, 1]$. Using the triangle inequality, we have

$$|W_j^N - w(x_j)| \leq |W_j^N| + |w(x_j)|.$$

We know from Lemma 3.2.4 that $|w(x_j)| \leq C \exp(-\alpha x_j/\varepsilon) \leq CN^{-1}$. It remains to find the bound for $|W_j^N|$. Let us consider the constant coefficient problem (assuming $b(x) \equiv 0$)

$$-\varepsilon D^+D^-Y_j - \alpha D^+Y_j = 0\,, \quad 1 \leq j \leq N-1,$$
$$Y_0 = 1, \qquad \lambda_1 Y_N + \lambda_2 D^-Y_N = 0.$$

The above problem has the solution of the form

$$Y_j = \frac{\mu_j^{N-j} + (\lambda_2\alpha/\lambda_1\varepsilon) - 1}{\mu_j^N + (\lambda_2\alpha/\lambda_1\varepsilon) - 1}, \quad \text{where} \quad \mu_j = 1 + \alpha h_j/\varepsilon. \tag{3.4.12}$$

From Lemma 2.3.4, we know that if $h_j \in [x_{_K}, 1]$, then $h_j \leq CN^{-1}$. Now using the fact that $(1 + (2\ln N)/N)^{-N/2} \leq 2N^{-1}$, we obtain

$$\frac{\alpha}{\varepsilon}\mu_j^{-N/2} \leq 2. \tag{3.4.13}$$

So

$$-\frac{\varepsilon}{\alpha}D^+Y_K = \frac{\mu_j^{K-1}}{\mu_j^K + (\lambda_2\alpha/\lambda_1\varepsilon) - 1} \geq \frac{1}{\mu_j}\left[\frac{1}{1 + (\lambda_2\alpha/\lambda_1\varepsilon)\mu_j^{-N/2}}\right].$$

Combining the above inequality with (3.4.13), we get

$$-\frac{\varepsilon}{\alpha}D^+Y_K = \frac{1}{\mu_j}\left[\frac{\lambda_1}{\lambda_1 + 2\lambda_2}\right]. \tag{3.4.14}$$

Using (3.4.13) and (3.4.14) in (3.4.12), we obtain

$$Y_j \leq CN^{-1}\left(1 + \frac{2\lambda_2}{\lambda_1}\right),$$

and note that $D^+Y_j \leq 0$. Consider the barrier function

$$\xi^{\pm}(x_j) = |\beta_1 W_0^N - \varepsilon\beta_2 D^+W_0^N|Y_j \pm W_j^N,$$

then $\beta_1\xi_0^{\pm} - \varepsilon\beta_2 D^+\xi_0^{\pm} \geq 0$, $\lambda_1\xi_N^{\pm} + \lambda_2 D^-\xi_N^{\pm} \geq 0$ and in addition, $L^N\xi_j^{\pm} \geq 0$. Thus applying the discrete comparison principle, we have

$$|W_j^N| \leq |\beta_1 W_0^N - \varepsilon\beta_2 D^+W_0^N|Y_j \leq CN^{-1}.$$

Finally, it remain to show the bound of the error for $x_j \in [0, x_{_K})$. The proof is similar to the case of uniform mesh except we use the discrete comparison principle on $[0, x_{_K})$. Analogously, let us take the mesh function

$$\eta^{\pm}(x_j) = \frac{Ce^{2\tau h/\varepsilon}}{\tau(\alpha-\tau)}\varepsilon^{-1}N^{-1}\left(Z_j + \frac{1}{\lambda_1}\right) \pm (W_j^N - w)(x_j),$$

where τ is a constant with $0 < \tau < \alpha$ and Z_j is the solution of the following problem:

$$\begin{cases} -\varepsilon D^+D^-Z_j - \tau D^+Z_j = 0\,, \quad 1 \le j \le K, \\ \beta_1 Z_0 - \beta_2\varepsilon D^+Z_0 = 1, \qquad \lambda_1 Z_K + \lambda_2 D^-Z_K = 0. \end{cases} \tag{3.4.15}$$

Now the solution is

$$Z_j = \frac{\mu^{K-j} + (\lambda_2\tau/\lambda_1\varepsilon) - 1}{\mu^K + (\lambda_2\tau/\lambda_1\varepsilon) - 1}, \quad \text{where} \quad \mu = 1 + \tau h_j/\varepsilon.$$

and we can see that

$$D^+Z_j = -\frac{\mu^{K-j-1}}{\varepsilon[\mu^K + (\lambda_2\tau/\lambda_1\varepsilon) - 1]} \le 0.$$

Note that $\beta_1\eta_0^{\pm} - \beta_2\varepsilon D^+\eta_0^{\pm} \ge 0$, $\lambda_1\eta_K^{\pm} + \lambda_2 D^-\eta_K^{\pm} \ge 0$ and $L^N\eta_j^{\pm} \ge 0$; therefore applying the discrete comparison principle as given in Lemma 3.3.1, we can have $\eta_j^{\pm} \ge 0$. Hence, for $x_j \in [0, x_{_K})$, we have

$$|W_j^N - w(x_j)| \le CN^{-1}, \tag{3.4.16}$$

and hence, this completes the proof of the lemma. ∎

The above error estimates for the regular and the singular component of the numerical solution now lead to the following error estimate.

Theorem 3.4.5. *If u is the solution of problem (3.1.1) and U_j^N is the solution of (3.3.1) on the mesh defined by (3.3.6), then we have*

$$\max_{0\le j\le N} |u(x_j) - U_j^N| \le CN^{-1}.$$

Proof. From (3.2.5) and (3.4.6), we have

$$|u(x_j) - U_j^N| \le |v(x_j) - V_j^N| + |w(x_j) - W_j^N|.$$

Using the error bounds for the regular and singular components given in Lemmas 3.4.3 and 3.4.4 respectively, we obtain the desired bound. ∎

3.5 Numerical Results

In this section to validate the theoretical results, the proposed numerical scheme is applied to several test problems with constant and variable coefficients. The results obtained on the adaptive grid are also compared with the numerical results obtained by using the upwind difference scheme on the piecewise-uniform Shishkin mesh.

Example 3.5.1. *Consider the test problem*

$$\begin{cases} -\varepsilon u''(x) - u'(x) + u(x) = 0, \quad x \in (0,1), \\ u(0) - \varepsilon u'(0) = 1, \quad u(1) + u'(0) = 1. \end{cases}$$

The exact solution is given by

$$u(x) = C_1 \exp(m_1 x) + C_2 \exp(m_2 x), \quad \text{where} \quad m_{1,2} = \frac{-1 \pm \sqrt{1+4\varepsilon}}{2\varepsilon},$$

and

$$C_1 = \frac{\varepsilon m_2 - 1 - (1+m_2)\exp(m_2)}{(1+m_1)(1-\varepsilon m_2)\exp(m_1) - (1+m_2)(1-\varepsilon m_1)\exp(m_2)},$$

$$C_2 = \frac{\varepsilon m_1 - 1 - (1+m_1)\exp(m_1)}{(1+m_1)(1-\varepsilon m_2)\exp(m_1) - (1+m_2)(1-\varepsilon m_1)\exp(m_2)}.$$

This BVP has a boundary layer in the left end at $x = 0$.

Example 3.5.2. *Consider the variable coefficient problem*

$$\begin{cases} \varepsilon u''(x) + \dfrac{1}{1+x} u'(x) = x + 1, \quad x \in (0,1), \\ u(0) - \varepsilon u'(0) = 1, \quad u(1) + u'(0) = 1. \end{cases}$$

The solution $u(x)$ is of the form

$$u(x) = \frac{(x+1)^3}{6\varepsilon + 3} + C_3 \left[\frac{(x+1)^{1-1/\varepsilon}}{\varepsilon - 1} - \frac{2^{1-1/\varepsilon}}{\varepsilon - 1} - \frac{2^{-1/\varepsilon}}{\varepsilon} \right] + \left[1 - \frac{20}{6\varepsilon + 3} \right].$$

where

$$C_3 = \frac{(19 + 3\varepsilon)/(6\varepsilon + 3)}{((1 - 2^{1-1/\varepsilon})(\varepsilon - 1) - 2^{-1/\varepsilon}/\varepsilon) - 1}$$

The above problem has a boundary layer at the left side of the domain near $x = 0$.

For boundary layer on the left, the piecewise-uniform Shishkin mesh $\overline{\Omega}_\sigma^N$ can be constructed by using the idea discussed in Section 2.3 of Chapter 2.

For any value of N and ε, the maximum pointwise errors E_ε^N and the ε-uniform errors E^N are calculated by

$$E_\varepsilon^N = \max_{0 \le j \le N} |u(x_j) - U_j^N| \quad \text{and} \quad E^N = \max_{0 < \varepsilon \le 1} E_\varepsilon^N, \tag{3.5.1}$$

where u is the exact solution and U_j is the numerical solution obtained by using N mesh intervals in the domain $\overline{\Omega}^N$. The corresponding rate of convergence are calculated by

$$r_\varepsilon^N = \log_2\left(\frac{E_\varepsilon^N}{E_\varepsilon^{2N}}\right) \quad \text{and} \quad r^N = \log_2\left(\frac{E^N}{E^{2N}}\right). \tag{3.5.2}$$

Figures 3.1(a) and 3.1(b) represent the numerical solution along with the exact solution and the corresponding error obtained on the adaptive grid for Example 3.5.1 respectively. In Table 3.1 and Table 3.3, the maximum pointwise error and the corresponding order of convergence of the solution for Examples 3.5.1 and 3.5.2 respectively, are presented which clearly shows that the proposed method is ε-uniform convergent of order one.

The computational results using the adaptive grid are compared to the numerical results using the Shishkin mesh and are shown in Table 3.2 with $\varepsilon = 1e-3$ and $\varepsilon = 1e-6$ for Example 3.5.1. From these results, one can observe that adaptive mesh produces better results than that produced by using the Shishkin mesh. The advantage of this approach is that without any prior knowledge of the location and the width of the boundary layer, we are able to generate an appropriate nonuniform mesh suitable for the layer type problems.

3.6 Conclusion

In this chapter, the analysis of an upwind scheme is presented of obtaining the solution of singularly perturbed mixed BVPs of the form (3.1.1) on a suitable nonuniform adaptive grid based on the equidistribution principle. The error analysis for the numerical solution is carried out and it is shown that the error converges at the rate of first-order, independently of the singular perturbation parameter. Numerical results obtained for some examples show that the proposed scheme is of first-order accurate, independent of the perturbation parameter.

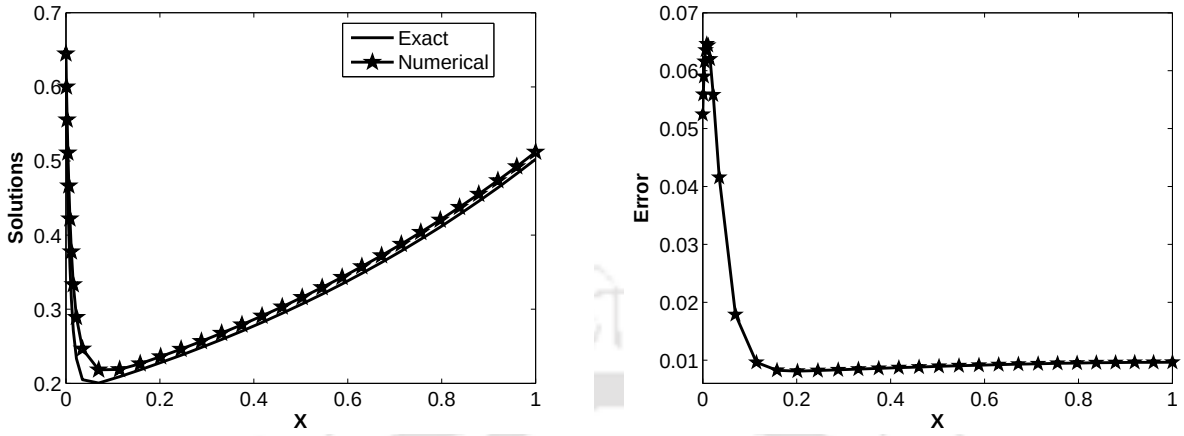

(a) Solution. *(b) Error.*

Figure 3.1: *Numerical solution with the exact solution and the corresponding error for Example 3.5.1 with* $\varepsilon = 1e-2$ *and* $N = 32$.

Table 3.1: *Maximum point-wise errors* E_ε^N *and the rate of convergence* r_ε^N *for Example 3.5.1.*

ε		Number of intervals N					
		32	64	128	256	512	1024
1	E_ε^N	1.0908e-2	5.4606e-3	2.7320e-3	1.3664e-3	6.8332e-4	3.4169e-4
	r_ε^N	0.9982	0.9991	0.9996	0.9998	0.9999	
$1e-2$	E_ε^N	6.4626e-2	3.5456e-2	1.8811e-2	9.7417e-3	4.9658e-3	2.5126e-3
	r_ε^N	0.9596	0.9786	0.9890	0.9944	0.9972	
$1e-4$	E_ε^N	8.0792e-2	4.7244e-2	2.6781e-2	1.4919e-2	8.1599e-3	4.4533e-3
	r_ε^N	0.7741	0.8189	0.8441	0.8705	0.8737	
$1e-6$	E_ε^N	8.1147e-2	4.7652e-2	2.7158e-2	1.5176e-2	8.3265e-3	4.6297e-3
	r_ε^N	0.7680	0.8112	0.8396	0.8660	0.8468	
$1e-8$	E_ε^N	8.1160e-2	4.7663e-2	2.7162e-2	1.5180e-2	8.3289e-3	4.6307e-3
	r_ε^N	0.7679	0.8113	0.8394	0.8660	0.8469	
	E^N	**8.1160e-2**	**4.7663e-2**	**2.7162e-2**	**1.5180e-2**	**8.3289e-3**	**4.6307e-3**
	r^N	**0.7679**	**0.8113**	**0.8394**	**0.8660**	**0.8469**	

Table 3.2: *Comparison of numerical results with the Shishkin mesh for Example 3.5.1.*

N	$\varepsilon = 1e-3$		$\varepsilon = 1e-6$	
	Shishkin mesh	**Adaptive grid**	**Shishkin mesh**	**Adaptive grid**
32	7.8107e-2	7.8136e-2	7.8268e-2	8.1147e-2
	0.6516	0.8007	0.6524	0.7680
64	4.9720e-2	4.4855e-2	4.9795e-2	4.7652e-2
	0.7204	0.8438	0.7209	0.8112
128	3.0176e-2	2.4991e-2	3.0212e-2	2.7158e-2
	0.7732	0.8756	0.7734	0.8396
256	1.7657e-2	1.3621e-2	1.7675e-2	1.5176e-2
	0.8113	0.9099	0.8114	0.8660
512	1.0062e-2	7.2494e-3	1.0071e-2	8.3265e-3
	0.8385	0.9395	0.8386	0.8468

Table 3.3: *Maximum point-wise errors E_ε^N and the rate of convergence r_ε^N for Example 3.5.2.*

ε		Number of intervals N					
		32	64	128	256	512	1024
	E_ε^N	5.5687e-1	3.0267e-1	1.5959e-1	8.3796e-2	4.4184e-2	2.2633e-2
$1e-2$	r_ε^N	0.8796	0.9234	0.9294	0.9234	0.9651	
	E_ε^N	5.8701e-1	3.1851e-1	1.7697e-1	9.5507e-2	4.9720e-2	2.6464e-2
$1e-4$	r_ε^N	0.8820	0.8478	0.8899	0.9418	0.9098	
	E_ε^N	5.8750e-1	3.1914e-1	1.7698e-1	9.5516e-2	4.9982e-2	2.6729e-2
$1e-8$	r_ε^N	0.8804	0.8506	0.8898	0.9344	0.9030	
	E^N	**5.8750e-1**	**3.1914e-1**	**1.7698e-1**	**9.5516e-2**	**4.9982e-2**	**2.6729e-2**
	r^N	**0.8804**	**0.8506**	**0.8898**	**0.9344**	**0.9030**	

Chapter 4

A Uniformly Accurate Finite Difference Approximation for Singularly Perturbed Delay Differential Equation

Adaptive grid methods are established as a valuable computational technique in approximating effectively the solutions of problems with boundary or interior layers. This chapter presents the analysis of an upwind scheme for singularly perturbed delay differential equation on a grid which is formed by equidistributing the arc-length monitor function. It is shown that the discrete solution obtained converges uniformly with respect to the perturbation parameter. Numerical experiments illustrate in practice the result of convergence proved theoretically.[1]

4.1 Introduction

Consider the following singularly perturbed delay differential equation

$$\begin{cases} \mathcal{L}_\varepsilon u_\varepsilon(x) \equiv -\varepsilon u_\varepsilon''(x) - a(x)u_\varepsilon'(x-\delta) + b(x)u_\varepsilon(x) = f(x), \quad x \in \Omega = (0,1), \\ u_\varepsilon(x) = \gamma(x), \quad -\delta \le x \le 0, \qquad u_\varepsilon(1) = \lambda\,, \end{cases} \tag{4.1.1}$$

where $0 < \varepsilon \ll 1$ is a small parameter and the delay parameter δ is such that $0 < \delta \ll 1$, which is of $o(\varepsilon)$. The functions $a(x), b(x), f(x)$ and $\gamma(x)$ are sufficiently smooth and λ is a constant. It is also assumed that $b(x) \ge \beta > 0, \forall x \in \overline{\Omega}$. Depending upon the sign of $a(x)$, *i.e.,* if $a(x) > 0$ (or $a(x) < 0$), a boundary layer is located at the left (or right) end of the domain. The layer is maintained for sufficiently small δ with $\delta \neq 0$ and $\delta = o(\varepsilon)$.

The BVP (4.1.1) is sometimes addressed as a two-parameter problem. The argument for small delay problems are widespread in many mathematical models of biophysics and mechanics where the delay term plays an important role in modelling the real-life phenomena [89]. Lange and

[1]Some portion of this chapter is published in *Numer. Math. Theory Methods Appl., Vol-3(1), pp.1–22, 2010.*

Miura ([53]-[57]) provided an asymptotic approach to BVPs of type (4.1.1). By considering several examples, they have shown that the effect of the small delay on the solution cannot be neglected. From the numerical point of view, Kadalbajoo et al. ([40], [42], [43]) used the piecewise-uniform Shishkin mesh for solving the BVP of type (4.1.1) whereas Patidar and Sharma ([77], [78]) used the non-standard finite difference scheme for solving the singularly perturbed delay differential equation. So far, no result exists in the literature where the adaptive grid is used to solve the delay differential equations. Here, our aim is to propose a numerical method comprising of upwind finite difference scheme on an adaptively generated grid for solving the BVP (4.1.1) and to carry out the convergence analysis.

Without loss of generality, we assume that $a(x) > 0$. If $\delta \equiv 0$, then the BVP (4.1.1) reduces to a singularly perturbed differential equation with boundary layer at $x = 0$. In this case, the outer solution is given by

$$u_\varepsilon(x) = \lambda \exp\left[\int_x^1 \frac{b(t)}{a(t)} dt\right] + O(\varepsilon), \qquad \text{as } \varepsilon \to 0,$$

which converges uniformly in x to the solution of (4.1.1) on $0 \le x_0 \le x \le 1$. In order to find the solution in the layer region, one can follow the standard procedure of singular perturbation analysis by introducing a new variable $\bar{x} = x/\varepsilon$, which yields a solution

$$\bar{u}_\varepsilon(\bar{x}) = \Gamma + (\gamma(0) - \Gamma)\exp(-a(0)\bar{x}) + O(\varepsilon),$$

where $\Gamma = \lambda \exp\left[\int_0^1 \frac{b(t)}{a(t)} dt\right]$ in the region $0 < \bar{x} < \infty$ as $\varepsilon \to 0$.

For $\delta = \kappa\varepsilon > 0$, where κ is sufficiently small, we follow the technique as done in ([53], [56]). To tackle the delay term, we expand the delay argument through Taylor's series expansion assuming sufficient smoothness condition on the solution of (4.1.1) so that the BVP (4.1.1) reduces to a standard singular perturbation problem. Here in this thesis, we focus on this particular case. But for large κ, there may be oscillations in the solution which grow exponentially. A WKB method is developed in [54] to solve such kind of problems and is not discussed here. Now, expanding the delay term, we obtain

$$u'_\varepsilon(x - \delta) = u'_\varepsilon(x) - \delta u''_\varepsilon(x) + \ldots, \qquad \text{as } \delta \to 0. \tag{4.1.2}$$

Now using the first two terms of the expansion (4.1.2) in the BVP (4.1.1), we have the following BVP:

$$\begin{cases} L_\varepsilon u(x) \equiv -\big(\varepsilon - \delta a(x)\big)u''(x) - a(x)u'(x) + b(x)u(x) = f(x), \quad x \in \Omega, \\ u(x) = \gamma(x), \qquad -\delta \le x \le 0, \qquad u(1) = \lambda\,. \end{cases} \tag{4.1.3}$$

It is worthwhile to mention that the BVP (4.1.3) is an approximate differential equation to the original equation (4.1.1). Since (4.1.3) is an approximation of (4.1.1), we have used $u(x)$ as a

different notation for $u_\varepsilon(x)$. For convenience, we have taken $\gamma(x) \equiv$ constant (see [53], [56]). Also, we assume that $a(x) \geq \alpha > 0, \forall x \in \overline{\Omega}$. Under these assumptions, the problem (4.1.3) has a unique solution and it exhibits layer behavior on the left side of the domain at $x = 0$.

If the delay term is sufficiently small, then we expect that $u(x)$ provides a good approximation to $u_\varepsilon(x)$. The crucial question is for what order of magnitude of δ for small ε, does $u(x)$ as a solution of (4.1.3) provide a leading order approximation to the solution $u_\varepsilon(x)$ of (4.1.1). We answer this question by following two approaches; firstly by an *asymptotic approach* and secondly by a *numerical approach*.

Lange and Miura have done a rigorous study in their articles ([53], [54], [56]). One can see the details of the following argument in ([54], [56]). Here, the asymptotic approach is applied to a constant coefficient homogeneous problem *i,e.,* by setting $a(x) \equiv \alpha,\ b(x) \equiv \beta$ and $f(x) \equiv 0$.

Consider the following singularly perturbed delay differential equation

$$\begin{cases} -\varepsilon y_\varepsilon''(x) - \alpha y_\varepsilon'(x-1) + \beta y_\varepsilon(x) = 0, \quad 0 < x < t \\ y_\varepsilon(x) = \phi, \quad -\delta \leq x \leq 0, \qquad y_\varepsilon(t) = \lambda\,, \end{cases} \tag{4.1.4}$$

where $0 < \varepsilon \ll 1$, $1 < t < 2$ and α, β, ϕ, λ are specified constants. The BVP (4.1.4) can be solved by following the method of stepwise integration. Let $y_{_A}(x)$ and $y_{_B}(x)$ denote the solution on the intervals $[0, 1]$ and $[1, t]$ respectively. So $y_{_A}(x)$ must solve the problem

$$\begin{cases} -\varepsilon y_{_A}''(x) - \alpha y_{_A}'(x) = -\beta\phi, \quad 0 < x < 1 \\ y_{_A}(0) = \phi, \end{cases} \tag{4.1.5}$$

while $y_{_B}$ satisfies

$$\begin{cases} -\varepsilon y_{_B}''(x) = -\alpha y_{_A}'(x) - \beta y_{_A}, \quad 1 < x < t \\ y_{_B}(t) = \lambda\,. \end{cases} \tag{4.1.6}$$

Furthermore, $y_{_A}(x)$ and $y_{_B}(x)$ satisfy the continuity condition

$$y_{_A}(1) = y_{_B}(1) \quad \text{and} \quad y_{_A}'(1^-) = y_{_B}'(1^+). \tag{4.1.7}$$

Now, we follow the standard procedure of asymptotic analysis for solving the BVP (4.1.5) by introducing a new stretching variable $x_1 = x/\varepsilon$ which implies that $y_{_A}(x_1) = y(\varepsilon x)$. Setting

$$y_{_A}(x) \sim \sum_{j=0}^{\infty} y_{A,j}(x_1)\varepsilon^j, \quad as \quad \varepsilon \to 0,$$

the solution of BVP (4.1.5) is of the form

$$y_{_A}(x_1) = d_1 + (\phi - d_1)\exp(-\alpha x_1)\,.$$

where d_1 is an arbitrary constant. Similarly, for solving the BVP (4.1.6), let us introduce $x_2 = (x-1)/\varepsilon$ such that $y_{_B}(x_2) = y(1+\varepsilon x_2)$. Setting

$$y_{_B}(x) \sim \sum_{j=0}^{\infty} y_{B,j}(x_2)\varepsilon^j \qquad \varepsilon \to 0,$$

we find the solution of the BVP (4.1.6) as

$$y_{_B}(x_2) = d_2(d_1-\phi)x_2\exp(-\alpha x_2) + d_3\,,$$

where d_2 and d_3 are the constants of integration. Now for our purposes, it is sufficient to record the leading-order behavior of the solution which shows that

$$y(x) = \begin{cases} y_{_A}(x_1) = d_1 + (\phi - d_1)\exp(-\alpha x_1) + O(\varepsilon) + O(\varepsilon\exp(-1/\varepsilon)), & 0 \le x \le 1 \\ y_{_B}(x_2) = d_2(d_1-\phi)x_2\exp(-\alpha x_2) + d_3 + O(\varepsilon) + O(\varepsilon\exp((1-x)/\varepsilon)), & 1 \le x \le t \end{cases} \tag{4.1.8}$$

Finally, the arbitrary constants d_1, d_2 and d_3 can be found out by using the boundary conditions and continuity conditions (4.1.7).

Now it remains to answer "*for what order of magnitude of δ for small ε, does $u(x)$ as a solution of (4.1.3) provide a leading order approximation to the solution $u_\varepsilon(x)$ of (4.1.1)*". To answer this, let us take $\delta(\varepsilon) = \tau\varepsilon^p$ where $p > 0$ will be determined later. Now (4.1.3) can be written as

$$-\varepsilon\big(1+\alpha\mu\varepsilon^{p-1}\big)u''(x) - \alpha u'(x) + \beta u(x) = 0. \tag{4.1.9}$$

Then the exact solution of (4.1.9) is of the form

$$u(x) = \exp(Ax)[C_1\cos(Bx) + C_2\sin(Bx)],$$

where

$$A = \frac{\alpha}{2\varepsilon(1+\alpha\mu\varepsilon^{p-1})}, \quad B = \frac{\sqrt{\alpha^2 + 4\beta\varepsilon(1+\alpha\mu\varepsilon^{p-1})}}{2\varepsilon(1+\alpha\mu\varepsilon^{p-1})}.$$

For all $p \ge 1$, A and B are of $O(\varepsilon^{-1})$; therefore $\delta^n u^{(n)}$ is of $O(\varepsilon^{n(p-1)})$ if C_1 and C_2 are constants and are of $O(1)$. It is also known that for a singular perturbation problem, the derivatives $u^{(n)}$ of the solution are of order $O(\varepsilon^{-n})$ and if δ is of the same order of ε, then the higher-order terms in the expansion of (4.1.2) cannot be neglected. In other words, for $p = 1$, all higher-order derivative terms that have been omitted from (4.1.3) upon expansion of the delay term given by (4.1.2) are of the same order of magnitude of those that have been kept. Since the approximated differential equation (4.1.3) of (4.1.1) is of $O(\delta^2 u_\varepsilon''')$ which will at least give us $O(\varepsilon)$ order approximation by choosing $m \ge 2$.

Secondly, to justify that the approximation (4.1.3) is a valid approximation, we follow the idea proposed by Amiraliyev and Erdogan [2] for solving singularly perturbed initial-value problems with delay term. Extending their technique, the original BVP (4.1.1) can be solved numerically by the direct scheme given below:

$$\begin{cases} \mathcal{L}_\varepsilon^N \mathscr{U}_j \equiv -\varepsilon D^+ D^- \mathscr{U}_j - a_j \mathscr{U}_{j-N} + b_j \mathscr{U}_j = f_j\,, \quad 1 \le j \le N-1, \\ \mathscr{U}_0 = \gamma(0), \quad \mathscr{U}_N = \lambda, \end{cases} \tag{4.1.10}$$

where $\mathscr{U}_{j-N} = \gamma_j$. Here, the delay term is approximated numerically. The numerical solution of the BVP (4.1.10) with large number of mesh points is treated as the exact solution of the original BVP (4.1.1). The numerical solution obtained by the proposed method is compared with the numerical solution of the BVP (4.1.10).

In order to calculate the maximum point-wise error $\mathscr{E}_\varepsilon^N$ and the rate of convergence $\mathscr{R}_\varepsilon^N$, the idea of interpolation is used. Define $\widehat{\mathscr{U}}^{8192}$ as the piecewise linear interpolation to $\mathscr{U}_j$ of (4.1.10) in Ω_N. Define

$$\mathscr{E}_\varepsilon^N = \max_{x_i \in \overline{\Omega}^N} |U^N - \widehat{\mathscr{U}}^{8192}| \quad \text{and} \quad \mathscr{R}_\varepsilon^N = \log_2\left(\frac{\mathscr{E}_\varepsilon^N}{\mathscr{E}_\varepsilon^{2N}}\right),$$

where U^N is the numerical solution obtained by our proposed method (4.3.1).

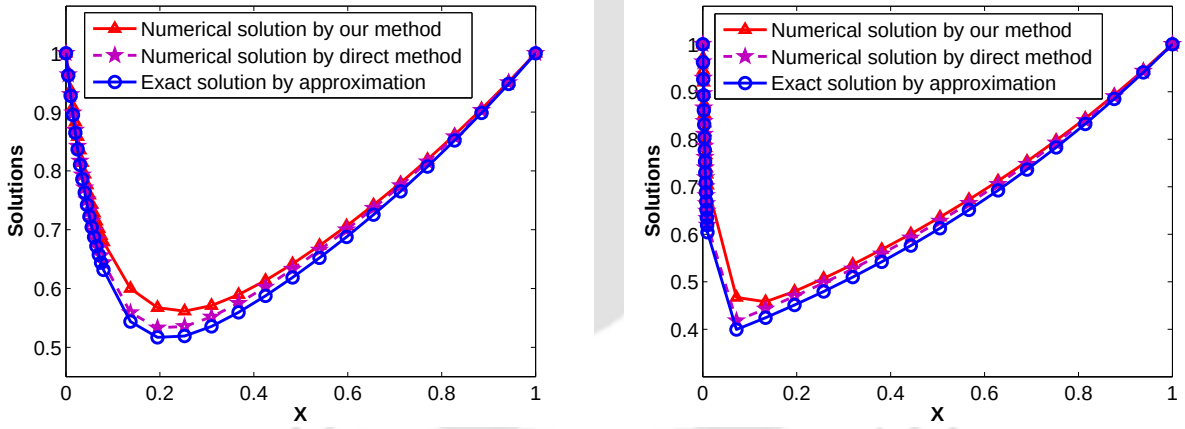

(a) $\varepsilon = 1e-01$. *(b)* $\varepsilon = 1e-02$.

Figure 4.1: *Comparison of solutions with* $N = 32$ *and* $\delta = 1e-08$.

The solution of the proposed method (4.3.1) is compared with the solution of (4.1.10) in Figure 4.1 and in Table 4.1. From these graphs and numerical results, one can conclude that the solution obtained by the proposed scheme (4.3.1) very well approximates the solution of (4.1.1) by the direct scheme (4.1.10).

Hence, in summary of the constant coefficient case, one can conclude that the solution of the approximated equation (4.1.3) provides a leading order solution to (4.1.1) up to δ which is of $o(\varepsilon)$.

Table 4.1: *Maximum point-wise errors* $\mathscr{E}_\varepsilon^N$ *and the rate of convergence* $\mathscr{R}_\varepsilon^N$ *for Example 4.5.1.*

ε	Number of intervals N					
	16	32	64	128	256	512
$1e-4$	5.7746e-2	3.6758e-2	2.0382e-2	1.0942e-2	5.6674e-3	2.8852e-3
	0.6516	0.8508	0.8974	0.9491	0.9740	
$1e-8$	8.9448e-2	7.3965e-2	6.3698e-2	4.4727e-2	2.5882e-2	1.4098e-2
	0.2742	0.2156	0.5101	0.7892	0.8764	

A description of the contents of this chapter is as follows. Section 4.2 establishes the maximum principle for the differential operator, stability result and some *a priori* estimates on the solution and its derivatives. Section 4.3 presents the upwind finite difference discretization and generation of the non-uniform grids through equidistribution principle. A bound for the local truncation error is obtained in Section 4.4 and the error analysis is carried out which leads to the main theoretical result namely the ε-uniform convergence in the maximum norm. Finally, several numerical examples are provided in Section 4.5 to illustrate the applicability of the present method with maximum point-wise error and the rate of convergence are shown in terms of tables and figures. This chapter ends with Section 4.6 that summarizes the main conclusion.

4.2 Continuous Problem

This section studies the bounds of the solution of BVP (4.1.3) and its derivatives which will be used later to derive the ε-uniform error estimates.

4.2.1 Properties of the solution and its derivatives

Lemma 4.2.1. (Maximum Principle) *Let v be a smooth function satisfying $v(0) \geq 0,\ v(1) \geq 0$ and $L_\varepsilon v(x) \geq 0,\ \forall x \in \Omega,$ then $v(x) \geq 0,\ \forall x \in \overline{\Omega}$.*

Proof. Let $x^* \in \overline{\Omega}$ be such that $v(x^*) = \min_{x\in\overline{\Omega}} v(x)$ and assume that $v(x^*) < 0$. Clearly $x^* \notin \{0,1\}$ and $v'(x^*) = 0$ and $v''(x^*) \geq 0$. Now consider

$$L_\varepsilon v(x^*) \equiv -\big(\varepsilon - \delta a(x^*)\big)v''(x^*) - a(x^*)v'(x^*) + b(x^*)v(x^*) < 0,$$

which is a contradiction to our assumption. Hence $v(x) \geq 0, \forall x \in \overline{\Omega}$. ∎

An immediate consequence of the maximum principle is the following stability estimate.

Lemma 4.2.2. *If u is the solution of BVP (4.1.3), then*

$$\|u\| \ \leq\ \frac{1}{\beta}\|f\| + \max\{|u(0)|, |\lambda|\}. \tag{4.2.1}$$

Proof. Let us consider the following barrier function

$$\psi^{\pm}(x) = \beta^{-1}\|f\| + \max\{|u(0)|, |\lambda|\} \pm u(x).$$

It is easy to show that $\psi^{\pm}(x)$ is non–negative at $x = 0, 1$. Now from (4.1.3)

$$\begin{aligned} L_\varepsilon \psi^{\pm}(x) &= -(\varepsilon - \delta a(x))\big(\psi^{\pm}(x)\big)'' - a(x)\big(\psi^{\pm}(x)\big)' + b(x)\psi^{\pm}(x) \\ &= b(x)\Big[\beta^{-1}\|f\| + \max\{|u(0)|, |\lambda|\}\Big] \pm L_\varepsilon u(x) \\ &\geq \big[\|f\| \pm f(x)\big] + b(x)\max\{|u(0)|, |\lambda|\} \\ &\geq 0. \end{aligned}$$

Thus by applying the maximum principle (Lemma 4.2.1), we can conclude that $\psi^{\pm}(x) \geq 0, \forall x \in \overline{\Omega}$, which is the required result. ∎

Lemma 4.2.3. *The derivatives $u^{(k)}$ of the solution u of (4.1.3) satisfy the following bound*

$$\|u^{(k)}\| \leq C\big(\varepsilon + \delta\alpha\big)^{-k}, \quad k = 1, 2, 3, \tag{4.2.2}$$

where C depends on $\|a\|$, $\|a'\|$, $\|b\|$, $\|b'\|$ and on the boundary conditions.

Proof. Define a neighborhood $R_x = \big(r, r + \varepsilon + \delta\alpha\big)$, where r is a positive constant to be chosen in such a way that for any $x \in \Omega$, $R_x \subset \Omega$. Now applying the mean value theorem, we can find a point $\xi \in R_x$ for which

$$u'(\xi) = \frac{u(r + (\varepsilon + \delta\alpha)) - u(r)}{\varepsilon + \delta\alpha},$$

and hence,

$$|(\varepsilon + \delta\alpha)u'(\xi)| \leq 2\|u\|. \tag{4.2.3}$$

By integrating the differential equation (4.1.3) from ξ to x, we have

$$(\varepsilon + \delta\alpha)|u'(x)| \leq (\varepsilon + \delta\alpha)|u'(\xi)| + |x - \xi|(\|f\| + \|b\|\|u\|) + \int_\xi^x |a(t)u'(t)|dt. \tag{4.2.4}$$

We know that

$$\int_\xi^x |a(t)u'(t)|dt \leq 2(\|a\| + \|a'\|)\|u\|. \tag{4.2.5}$$

Substituting (4.2.3) and (4.2.5) in (4.2.4), we obtain

$$(\varepsilon + \delta\alpha)|u'(x)| \leq \big[2(\|a\| + \|a'\|) + 2 + \|b\|\,|x - \xi|\big]\|u\| + |x - \xi|\|f\|. \tag{4.2.6}$$

From which, we obtain

$$\|u'\| \leq C\big(\varepsilon + \delta\alpha\big)^{-1},$$

where $C = \|f\| + (2 + 2(\|a\| + \|a'\|) + \|b\|)(\beta^{-1}\|f\| + \max\{|u(0)| + |\lambda|\})$, which is independent of ε and δ. Similarly, from (4.1.3), we have

$$(\varepsilon - \delta a)u'' = bu - au' - f \text{ and } \big((\varepsilon - \delta a)u''\big)' = (bu - au' - f)',$$

from which we can obtain successively the required bounds on the second and third derivatives. ■

Remark 4.2.4. *The derivatives of $u(x)$ of (4.1.3) satisfy the following pointwise sharper bounds*

$$|u^k(x)| \le C\big(\varepsilon + \delta\alpha\big)^{-k} \exp\left(\frac{-\alpha x}{\varepsilon + \delta\alpha}\right), \quad \text{for } k = 1, 2, 3. \tag{4.2.7}$$

Proof. *Following the technique of [28] for the one parameter problem, we can get the required result.* ■

4.3 Discrete Problem

This section presents the numerical scheme and the generation of the adaptive grid for solving the BVP (4.1.3).

4.3.1 The difference scheme

Consider the difference approximations of (4.1.3) on a nonuniform mesh

$$\Omega_N = \{0 = x_0 < x_1 < x_2 < \ldots < x_{N-1} < x_N = 1\},$$

and denote $h_j = x_j - x_{j-1}$. Without loss of generality, we will assume that N is even.

The upwind finite difference discretization of (4.1.3) takes the form

$$\begin{cases} L_\varepsilon^N U_j \equiv -(\varepsilon - \delta a_j)D^+D^-U_j - a_j D^+U_j + b_j U_j = f_j\,, \quad 1 \le j \le N-1, \\ U_0 \approx \gamma(0) = \gamma_0, \quad U_N = \lambda\,, \end{cases} \tag{4.3.1}$$

where U_j denotes the approximation of $u(x_j)$, $a_j = a(x_j)$ and b_j, f_j are defined in a similar fashion. Equation (4.3.1) can be expressed in the following form of system of algebraic equations

$$\begin{cases} -r_j^- U_{j-1} + r_j^c U_j - r_j^+ U_{j+1} = f_j, \quad j = 1, \ldots, N-1, \\ U_0 = \gamma_0, \quad U_N = \lambda, \end{cases} \tag{4.3.2}$$

where

$$r_j^- = \frac{2(\varepsilon - \delta a_j)}{h_j(h_j + h_{j+1})}, \quad r_j^c = \frac{2(\varepsilon - \delta a_j)}{h_j h_{j+1}} + \frac{a_j}{h_{j+1}} + b_j, \quad r_j^+ = \frac{2(\varepsilon - \delta a_j)}{h_{j+1}(h_j + h_{j+1})} + \frac{a_j}{h_{j+1}}\ .$$

One can easily see that

$$r_j^- > 0,\ r_j^+ > 0 \text{ and } \quad r_j^c + r_j^- + r_j^+ \ge 0, \quad \text{for} \quad j = 1, \ldots, N-1, \tag{4.3.3}$$

which imply that the stiffness matrix is an M-matrix.

4.3.2 Grid equidistribution

Here, we consider the arc–length monitor function

$$M\big(u(x),x\big) = \sqrt{1+(u'(x))^2}. \tag{4.3.4}$$

We construct the mesh as the solution of the following nonlinear system of equations:

$$\begin{cases} (x_{j+1}-x_j)^2 + (U_{j+1}-U_j)^2 = (x_j - x_{j-1})^2 + (U_j - U_{j-1})^2, \ j = 1,\ldots,N-1. \\ x_0 = 0, \quad x_N = 1. \end{cases} \tag{4.3.5}$$

The system of equations (4.3.1) and (4.3.5) are solved simultaneously to obtain the solution U_j and the grids x_j. The details of the adaptive grid technique are discussed in Section 2.3 of Chapter 2 and the choice of the adaptive criteria remains the same here.

4.4 Error Analysis

The bound of the truncation error, stability estimates and the ε-uniform error estimates are derived in this section.

4.4.1 Local truncation error

The local truncation error of the difference scheme (4.3.1) at the node x_j is given by

$$\tau_j = L_\varepsilon^N U_j - (L_\varepsilon u)(x_j), \tag{4.4.1}$$

where u and U denote the exact solution of (4.1.3) and (4.3.1) respectively.

Lemma 4.4.1. *The truncation error can be bounded as below*

$$|\tau_j| \le \frac{C\ell}{(\varepsilon+\delta\alpha)N} \exp\left(\frac{-\alpha x_j}{\varepsilon+\delta\alpha}\right). \tag{4.4.2}$$

Proof. Using the Taylor series expansion and Lemma 2.5.1, the truncation error (4.4.1) can be expressed as

$$\begin{aligned} \tau_j \quad = \frac{-2(\varepsilon-\delta a_j)}{h_j+h_{j+1}} \Bigg[\frac{1}{h_{j+1}} \int_{x_j}^{x_{j+1}} (s-x_{j+1})^2 u'''(s)ds \\ - \frac{1}{h_j} \int_{x_{j-1}}^{x_j} (s-x_{j-1})^2 u'''(s)ds \Bigg] + \frac{a_j}{h_{j+1}} \int_{x_j}^{x_{j+1}} (s-x_{j+1}) u''(s)ds, \end{aligned} \tag{4.4.3}$$

from which we obtain the bound

$$|\tau_j| < (\varepsilon+\delta\alpha) \int_{x_{j-1}}^{x_{j+1}} |u'''(s)|ds + C \int_{x_{j-1}}^{x_{j+1}} |u''(s)|ds. \tag{4.4.4}$$

Using the bound of the derivative of the continuous solution (4.2.2) in the first term, the above expression can be written as

$$|\tau_j| < C \int_{x_{j-1}}^{x_{j+1}} |u''(s)| ds. \tag{4.4.5}$$

Using the bound of the solution (4.2.7), we have

$$\begin{aligned} |\tau_j| &\leq \frac{C}{(\varepsilon+\delta\alpha)^2} \int_{x_{j-1}}^{x_{j+1}} \exp\left(\frac{-\alpha s}{\varepsilon+\delta\alpha}\right) ds \\ &\leq \frac{C}{\alpha(\varepsilon+\delta\alpha)} \left[\exp\left(\frac{-\alpha x_{j+1}}{\varepsilon+\delta\alpha}\right) - \exp\left(\frac{-\alpha x_{j-1}}{\varepsilon+\delta\alpha}\right)\right]. \end{aligned}$$

Now, for any $0 \leq t \in \mathbb{R}$, using the inequality $\exp(-t) \leq 1+t$, we obtain

$$\begin{aligned} |\tau_j| &\leq \frac{C}{\alpha(\varepsilon+\delta\alpha)} \left[\left(1+\frac{\alpha x_{j+1}}{\varepsilon+\delta\alpha}\right) - \left(1+\frac{\alpha x_{j-1}}{\varepsilon+\delta\alpha}\right)\right] \\ &\leq \frac{C}{(\varepsilon+\delta\alpha)^2} \left[x_{j+1} - x_{j-1}\right] \\ &\leq \frac{C}{(\varepsilon+\delta\alpha)^2} \int_{\xi_{j-1}}^{\xi_{j+1}} \left(\frac{\ell}{\sqrt{1+(u'(s))^2}}\right) ds \\ &\leq \frac{C}{(\varepsilon+\delta\alpha)^2} \int_{\xi_{j-1}}^{\xi_{j+1}} \left(\frac{\ell}{u'(x_j^*)}\right) ds \\ &\leq \frac{C\ell}{(\varepsilon+\delta\alpha)N} \exp\left(\frac{-\alpha x_j}{\varepsilon+\delta\alpha}\right), \end{aligned}$$

which is the desired result. ∎

4.4.2 Bound on maximum point-wise error

Before deriving the error estimate for the numerical solution of (4.3.1), we provide here some lemmas which are the prerequisites for the main result.

Lemma 4.4.2. (Discrete Comparison Principle) *The system $L_\varepsilon^N \mathcal{V}_j = F_j$ with $\mathcal{V}_0$ and $\mathcal{V}_N$ specified has a unique solution. If $L_\varepsilon^N \mathcal{V}_j < L_\varepsilon^N \mathcal{Z}_j$, for $1 \leq j \leq N-1$ with $\mathcal{V}_0 < \mathcal{Z}_0$ and $\mathcal{V}_N < \mathcal{Z}_N$, then $\mathcal{V}_j < \mathcal{Z}_j$, for $1 \leq j \leq N$.*

Proof. From (4.3.3), it is clear that the matrix associated with the discrete operator L_ε^N is an irreducible M-matrix and therefore has a positive inverse and hence, the result follows. ∎

Lemma 4.4.3. *We define a mesh function S_j by*

$$S_0 = 1, \quad S_j = \prod_{k=1}^{j} \left(1+\frac{\alpha h_k}{\varepsilon+\delta\alpha}\right)^{-1}, \quad j = 1, 2, \ldots, N. \tag{4.4.6}$$

Then, for $j = 1, 2, \ldots, N-1$, there exists a constant C such that

$$L_\varepsilon^N S_j \geq \frac{C}{\max\{\varepsilon+\delta\alpha, h_{j+1}\}} S_j \ . \tag{4.4.7}$$

Proof. We have

$$\frac{S_j - S_{j-1}}{h_j} = -\frac{\alpha}{\varepsilon + \delta\,\alpha} S_j \ .$$

Now

$$\begin{aligned} L_\varepsilon^N S_j &= -\frac{2(\varepsilon - \delta a_j)}{h_j + h_{j+1}}\left[\frac{S_{j+1} - S_j}{h_{j+1}} - \frac{S_j - S_{j-1}}{h_j}\right] - a_j\left[\frac{S_{j+1} - S_j}{h_{j+1}}\right] + b_j S_j \\ &\geq -\frac{2\alpha(\varepsilon - \delta a_j)h_{j+1}}{(\varepsilon + \delta\alpha)(h_j + h_{j+1})}\left[\frac{S_j - S_{j+1}}{h_{j+1}}\right] + \frac{\alpha a_j}{\varepsilon + \delta\alpha} S_{j+1} \\ &\geq \left(\frac{\alpha}{\varepsilon + \delta\alpha + \alpha h_{j+1}}\right)\left[a_j - \frac{2\alpha(\varepsilon - \delta a_j)h_{j+1}}{(\varepsilon + \delta\alpha)(h_j + h_{j+1})}\right] S_j \\ &\geq \frac{C}{\max\{\varepsilon + \delta\alpha, h_{j+1}\}} S_j \ , \end{aligned}$$

which is the desired bound. ∎

Remark 4.4.4. *The function S_j is the piecewise (0,1)–Padé approximation of* $\exp\left(\frac{-\alpha x_j}{\varepsilon + \delta\alpha}\right)$.

The following lemma provides a two-sided bound for S_j, which will be used later.

Lemma 4.4.5. *The grid function S_j defined in (4.4.6) satisfy*

$$\exp(-\alpha x_j/(\varepsilon + \delta\alpha)) < S_j < C\exp(-\alpha x_j/(\varepsilon + \delta\alpha)), \quad j = 1, 2, \ldots, N-1. \tag{4.4.8}$$

Proof. We can express the nodes x_j as $x_j = \sum_{k=1}^{j} h_k$. Therefore,

$$\begin{aligned} \exp\left(-\frac{\alpha x_j}{\varepsilon + \delta\alpha}\right) &= \exp\left(\sum_{k=1}^{j} \frac{-\alpha h_k}{\varepsilon + \delta\alpha}\right) \\ &= \prod_{k=1}^{j} \exp\left(-\frac{\alpha h_k}{\varepsilon + \delta\alpha}\right). \end{aligned}$$

For any real value of $\theta > 0$, we have $\exp(-\theta) < (1+\theta)^{-1}$. Thus, the above expression becomes

$$\exp\left(-\frac{\alpha x_j}{\varepsilon + \delta\alpha}\right) = \prod_{k=1}^{j}\left(1 + \frac{\alpha h_k}{\varepsilon + \delta\alpha}\right)^{-1} < S_j.$$

Now we have to find the upper bound for S_j. We know from (2.3.6) that

$$\begin{aligned} h_j &= \int_{\xi_{j-1}}^{\xi_j} \frac{\ell}{\sqrt{1 + (u'(x))^2}} ds \\ &\leq \int_{\xi_{j-1}}^{\xi_j} \frac{\ell}{u'(x)} ds \\ &\leq \frac{\ell}{N u'(x_j)}. \end{aligned}$$

Again from (4.2.7), we can see that

$$|u'(x_j)| \leq C(\varepsilon+\delta\alpha)^{-1}\exp\left(\frac{-\alpha x_j}{\varepsilon+\delta\alpha}\right).$$

Hence, we have

$$h_j \leq \frac{(\varepsilon+\delta\alpha)\ell}{\alpha N}\exp\left(\frac{\alpha x_j}{\varepsilon+\delta\alpha}\right). \tag{4.4.9}$$

Observe that

$$\begin{aligned}\ln\left[\prod_{k=1}^{j}\left(1+\frac{\alpha h_k}{\varepsilon+\delta\alpha}\right)\right] &\geq \sum_{k=1}^{j}\left[\frac{\alpha h_k}{\varepsilon+\delta\alpha}-\frac{1}{2}\left(\frac{\alpha h_k}{\varepsilon+\delta\alpha}\right)^2\right]\\ &\geq \frac{\alpha x_j}{\varepsilon+\delta\alpha}-\frac{1}{2}\sum_{k=1}^{j}\left(\frac{\alpha h_k}{\varepsilon+\delta\alpha}\right)^2. \end{aligned}\tag{4.4.10}$$

Now using (4.4.9) and for some $\tilde{x}$ in the layer region, *i.e*, $\tilde{x}\in(0, x_{_K})$, we can have

$$\begin{aligned}\sum_{j=1}^{K}\left(\frac{\alpha h_j}{\varepsilon+\delta\alpha}\right)^2 &\leq C(\varepsilon+\delta\alpha)^{-1}N^{-1}\sum_{k=1}^{j}\exp\left(\frac{\alpha h_k}{\varepsilon+\delta\alpha}\right)\\ &\leq C(\varepsilon+\delta\alpha)^{-1}N^{-1}\int_0^{\tilde{x}}\exp\left(\frac{\alpha s}{\varepsilon+\delta\alpha}\right)ds\\ &\leq CN^{-1}\left[\exp\left(\frac{\alpha\tilde{x}}{\varepsilon+\delta\alpha}\right)-1\right]\\ &\leq C\,.\end{aligned}$$

Then, from (4.4.6) and (4.4.10), we obtain that

$$\prod_{k=1}^{j}\left(1+\frac{\alpha h_k}{\varepsilon+\delta\alpha}\right)^{-1} \leq C\exp\left(\frac{-\alpha x_j}{\varepsilon+\delta\alpha}\right),$$

and hence

$$S_j \leq C\exp\left(\frac{-\alpha x_j}{\varepsilon+\delta\alpha}\right).$$

This completes the proof. ∎

The following theorem gives the ε–uniform convergence of the proposed scheme (4.3.1).

Theorem 4.4.6. *Let $u(x)$ and U_j be respectively the exact solution of (4.1.3) and the discrete solution of (4.3.1) on the grids defined by (4.3.5). Then, there exists a constant C, independent of N, ε and δ such that*

$$\max_{0\leq j\leq N}|u(x_j)-U_j| \leq CN^{-1}, \qquad j=0,\ldots,N. \tag{4.4.11}$$

Proof. We already know from (4.4.2) that the bound of the truncation error is given by

$$|\tau_j| \leq \frac{C\ell}{(\varepsilon+\delta\alpha)N} \exp\left(\frac{-\alpha x_j}{\varepsilon+\delta\alpha}\right).$$

Let us apply the discrete comparison principle as given in Lemma 4.4.2 to the barrier function $\mathcal{W}_j$ defined by

$$\mathcal{W}_j = CN^{-1}(1+S_j), \quad j = 0, \ldots, N.$$

The truncation error τ_j and the nodal error e_j are related by $L_\varepsilon^N e_j = \tau_j$. Using (4.4.6), we have for $j = 1, \ldots, N-1$,

$$\begin{aligned} L_\varepsilon^N e_j = \tau_j &\leq \frac{C\ell}{(\varepsilon+\delta\alpha)N} \exp\left(\frac{-\alpha x_j}{\varepsilon+\delta\alpha}\right) \\ &\leq \frac{C\ell}{(\varepsilon+\delta\alpha)N} S_j \\ &\leq \frac{C\ell}{(\varepsilon+\delta\alpha)N} L_\varepsilon^N S_j \\ &\leq L_\varepsilon^N \mathcal{W}_j \,. \end{aligned}$$

Since $e_0 \leq \mathcal{W}_0$ and $e_N \leq \mathcal{W}_N$, we conclude that

$$e_j \leq \mathcal{W}_j \leq CN^{-1}, \qquad j = 0, \ldots, N.$$

Now the same argument can be repeated with e_j being replaced by $-e_j$, and hence we have

$$|e_j| \leq CN^{-1}, \qquad j = 0, \ldots, N.$$

which is the required result. ∎

4.4.3 Layer on the right side

Let the convection coefficient $a(x)$ in the differential equation (4.1.1) be such that $a(x) \leq \tilde{\alpha} < 0$ for $x \in \overline{\Omega}$, where $\tilde{\alpha}$ is a constant. This assumption implies that the boundary layer occurs in the neighborhood of $x = 1$, *i.e.,* on the right side of the interval. We have already established the estimates for the solution of the continuous problem and its derivatives in the case when the solution of the problem (4.1.3) exhibits a boundary layer at $x = 0$, *i.e.,* at the left side of the interval $[0, 1]$. One can easily obtain similar estimates for the right boundary layer case. But the main difference in this kind of approach is that the numerical scheme where the first-order derivative is approximated by the backward finite difference operator in place of the forward finite difference operator as we did in case of left side boundary layer. This is mainly to preserve the stability of the upwind scheme.

Hence, the numerical scheme is of the form

$$\begin{cases} L_\varepsilon^N U_j \equiv -(\varepsilon - \delta a_j) D^+ D^- U_j + a_j D^- U_j + b_j U_j = f_j\,, \quad 1 \le j \le N-1, \\ U_0 = \gamma_0, \quad U_N = \lambda\,. \end{cases} \tag{4.4.12}$$

The above equation can be expressed in the form

$$\begin{cases} -r_j^- U_{j-1} + r_j^c U_j - r_j^+ U_{j+1} = f_j, \quad j = 1, \ldots, N-1, \\ U_0 = \gamma_0, \quad U_N = \lambda, \end{cases} \tag{4.4.13}$$

where

$$r_j^- = \frac{2(\varepsilon - \delta a_j)}{h_j(h_j + h_{j+1})} + \frac{a_j}{h_j},\ r_j^c = \frac{2(\varepsilon - \delta a_j)}{h_j h_{j+1}} + \frac{a_j}{h_j} + b_j,\ r_j^+ = \frac{2(\varepsilon - \delta a_j)}{h_{j+1}(h_j + h_{j+1})}\,.$$

One can easily see that the stiffness matrix (4.4.13) is an irreducible M-matrix.

Here, it is significant to observe that one can construct the nonuniform mesh as given in (4.3.5) through the same monitor function defined in (4.3.4) in the case of right boundary layer without any extra care.

4.5 Numerical Results

In this section to validate the theoretical results, the proposed numerical scheme is applied to several test problems with constant and variable coefficients having left and right boundary layers. For computation purposes, the delay parameter δ is chosen as the square of the perturbation parameter ε *i.e.,* $\delta = \varepsilon^2$. The upwind difference scheme on the piecewise-uniform Shishkin mesh is used for comparison of numerical results.

The piecewise-uniform Shishkin mesh $\overline{\Omega}_\sigma$ is constructed by partitioning the domain $[0,1]$ into two subdomains $[0,\sigma)$ and $[\sigma,1]$. Here σ denotes the transition parameter which determines the point of transition from a fine mesh to the coarse mesh and is defined as $\sigma = \min\{1/2, (\varepsilon - \delta\alpha)\ln N/\alpha\}$, where α is defined earlier. The definition of σ guarantees the existence of some points inside the layer region. Now $N/2$ numbers of subintervals are placed in each of the subdomains. Hence the Shishkin mesh will be of the form

$$\overline{\Omega}_\sigma = \{x_i : x_i = 2\sigma i/N,\ i \le N/2; \quad x_i = x_{i-1} + 2(1-\sigma)/N,\ N/2 < i \le N\}.$$

Note that σ depends on N, if it is chosen independently of N, then the ε-uniform convergence of the upwind scheme can not be guaranteed [28]. Similarly for right boundary layer problems, the corresponding Shishkin mesh can be formed by dividing the domain $[0,1]$ into two subdomains $[0, 1-\sigma]$ and $(1-\sigma, 1]$.

Example 4.5.1. *Consider the constant coefficient problem*

$$\begin{cases} -\varepsilon u''(x) - u'(x-\delta) + u(x) = 0, \quad x \in \Omega\,, \\ u(x) = 1, \quad -\delta \le x \le 0, \qquad u(1) = 1. \end{cases} \tag{4.5.1}$$

The approximate differential equation of Example 4.5.1 is of the form

$$\begin{cases} -(\varepsilon-\delta)u''(x) - u'(x) + u(x) = 0, \quad x \in \Omega\,, \\ u(x) \approx u(0) = 1, \quad -\delta \le x \le 0, \qquad u(1) = 1. \end{cases} \tag{4.5.2}$$

The exact solution of (4.5.2) is given by

$$u(x) = C_1 \exp(m_1 x) + C_2 \exp(m_2 x)\,,$$

where

$$m_{1,2} = \frac{-1 \mp \sqrt{1+4(\varepsilon-\delta)}}{2(\varepsilon-\delta)},\ C_1 = \frac{1-\exp(m_2)}{\exp(m_1)-\exp(m_2)},\ C_2 = \frac{\exp(m_1)-1}{\exp(m_1)-\exp(m_2)}.$$

This solution has a boundary layer at $x = 0$.

Example 4.5.2. *Consider the following variable coefficient delay differential equation*

$$\begin{cases} -\varepsilon u''(x) - \exp(-x)u'(x-\delta) + xu(x) = 0, \quad x \in \Omega\,, \\ u(x) = 1, \quad -\delta \le x \le 0, \qquad u(1) = 1. \end{cases}$$

Here the boundary layer occurs at $x = 0$ and the exact solution is not known.

Example 4.5.3. *Consider the constant coefficient problem with right hand side boundary layer*

$$\begin{cases} \varepsilon u''(x) - u'(x-\delta) - u(x) = 0, \quad x \in \Omega\,, \\ u(x) = 1, \quad -\delta \le x \le 0, \qquad u(1) = -1. \end{cases}$$

The above problem has a boundary layer near $x = 1$. The exact solution of the approximated BVP is given by

$$u(x) = C_3 \exp(m_3 x) - C_4 \exp(m_4 x),$$

where

$$m_{3,4} = \frac{1 \mp \sqrt{1+4(\varepsilon+\delta)}}{2(\varepsilon+\delta)},\ C_3 = \frac{1+\exp(m_4)}{\exp(m_4)-\exp(m_3)},\ C_4 = \frac{\exp(m_3)+1}{\exp(m_4)-\exp(m_3)}.$$

Example 4.5.4. *The final example is the non-constant coefficient problem*

$$\begin{cases} \varepsilon u''(x) - (1+x)u'(x-\delta) - \exp(-x)u(x) = 1, \quad x \in \Omega\,, \\ u(x) = 1, \quad -\delta \le x \le 0, \qquad u(1) = -1. \end{cases}$$

In this BVP, the boundary layer is at $x = 1$ and the exact solution is not known.

Figure 4.2(a) represents the movement of mesh after each iteration and Figure 4.2(b) provides the final computed mesh corresponding to the solution of Example 4.5.1. It is prominent from these figures that the mesh starts to move towards the boundary layer and clusters as many points required for the layer region. So this kind of approach has the advantage that without any prior knowledge of the location of the boundary layer, we are able to generate some points inside the layer region. In Figure 4.3(a) and Figure 4.3(b), we present the effect of δ on the solution of the Example 4.5.1 and finally Figure 4.4(a) and Figure 4.4(b) represent the corresponding solution and the error. Also we plot similar graphs in the case when the boundary layer is located at right side of the domain *i.e.,* for Example 4.5.3. In the Figure 4.5(a), we present the movement of the mesh towards right and Figures 4.6(a) and Figures 4.6(b) represent the effect of δ on the right boundary layer where as Figure 4.7 represent the computed solution along with the error.

For any value of N and ε, the maximum point-wise errors E_ε^N and the corresponding rate of convergence r_ε^N are determined by same way described in Chapter 2. In Table 4.2 and Table 4.4, we present the maximum pointwise error and the corresponding order of convergence for the Example 4.5.1 and 4.5.3 respectively.

The exact solutions are not available for Examples 4.5.2 and 4.5.4. In order to calculate the maximum point-wise error G_ε^N and the rate of convergence q_ε^N, the idea of interpolation is used. Define $\overline{U}^{8192}$ as the piecewise linear interpolation to U^N in Ω_N. Define,

$$G_\varepsilon^N = \max_{x_i \in \overline{\Omega}^N} |U^N - \overline{U}^{8192}| \quad \text{and} \quad q_\varepsilon^N = \log_2 \left(\frac{G_\varepsilon^N}{G_\varepsilon^{2N}} \right).$$

The maximum pointwise error and the corresponding order of convergence for the Examples 4.5.2 and 4.5.4 are provided in Tables 4.3 and 4.5, respectively.

The computational results using the adaptive mesh are compared with the computational results of the Shishkin mesh and are shown in Tables 4.6 and 4.7 for Examples 4.5.2 and 4.5.4, respectively. From these results, one can observe that the adaptive mesh gives comparative results with the Shishkin mesh through the same monitor function as defined in (4.3.4) in the case of left or right boundary layers which shows the advantage of such adaptive grid over the Shishkin mesh.

In order to visualize the order of convergence, the loglog plot of the maximum error is shown in Figures 4.8(a) and 4.8(b) for Examples 4.5.1 and 4.5.3 respectively. From these figures and the numerical results shown in tables, one can conclude that the proposed method is ε–uniform convergent of order one.

4.6 Conclusion

In this chapter, a numerical method is proposed to solve singularly perturbed delay differential equations of the form (4.1.3). The upwind finite difference scheme is applied on a nonuniform mesh generated adaptively from the equidistribution principle. The equidistribution is done with the help of a positive monitor function which contains the first-derivative of the solution. The error analysis is carried out for the numerical solution which shows the first-order ε-uniform convergence of the proposed method. From the graphs and the tables shown here help us to conclude that the errors converge at the rate of first-order, independent of the small perturbation parameters. Hence the key result established here is that if the mesh is generated adaptively, it is possible to obtain approximate solutions that converge uniformly without depending on the small parameters.

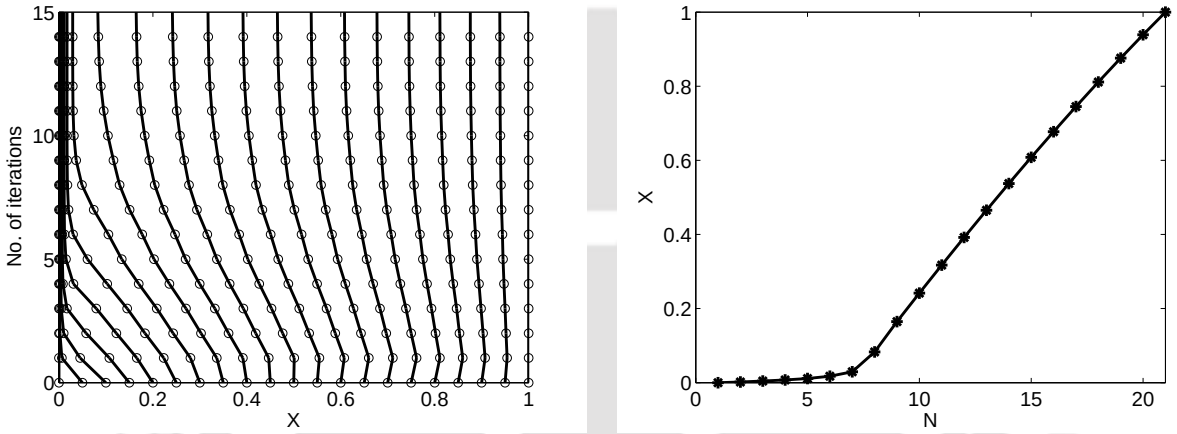

(a) Mesh movement towards left. *(b) Final computed mesh.*

Figure 4.2: *Movement of the mesh points towards left for Example 4.5.1 with* $\varepsilon = 1e-2,\ \delta = 1e-8$ *and* $N = 20$.

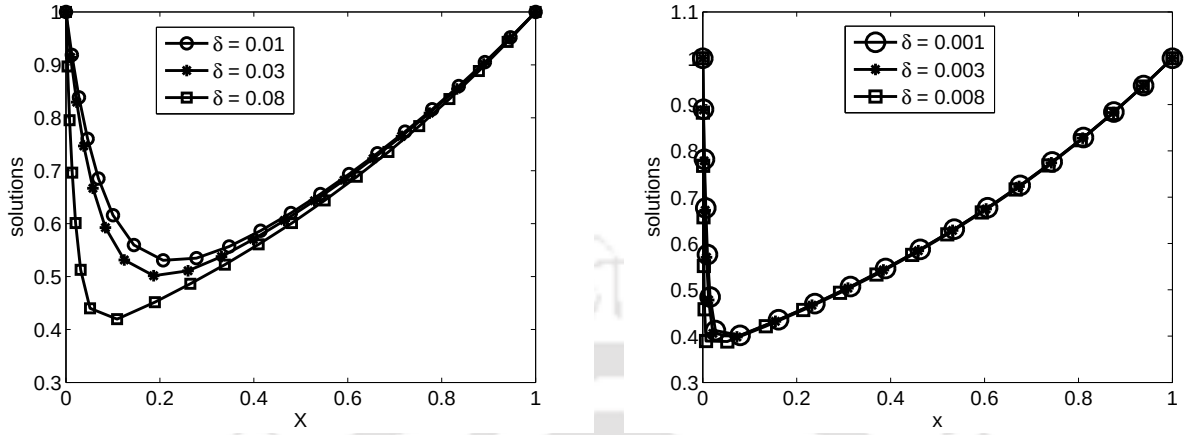

(a) $\varepsilon = 1e-1$. *(b)* $\varepsilon = 1e-2$.

Figure 4.3: *Effect of* δ *on the solution of Example 4.5.1 for* $N = 20$ *with different values of* ε.

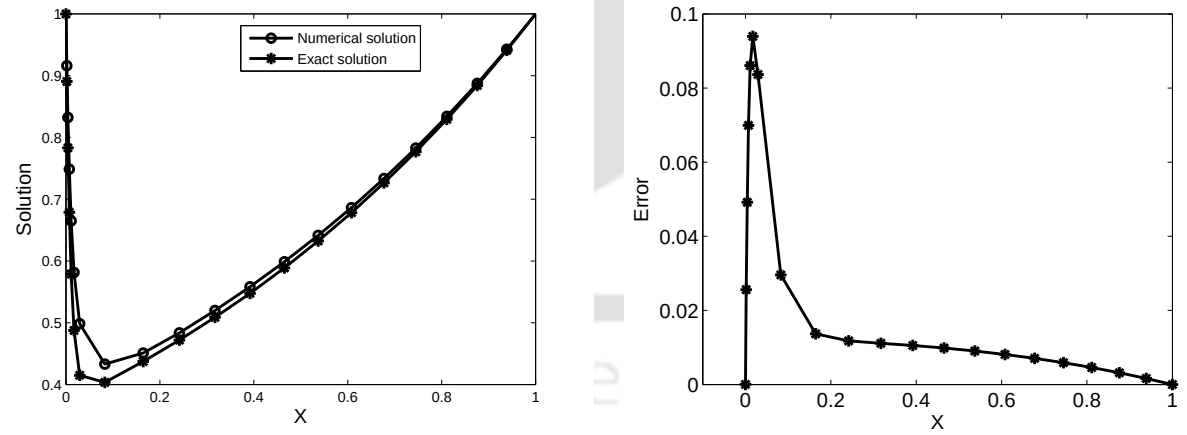

(a) Solution. *(b) Error.*

Figure 4.4: *Numerical solution with exact solution and the corresponding error of Example 4.5.1 for* $\varepsilon = 1e-2,\ \delta = 1e-8$ *and* $N = 20$.

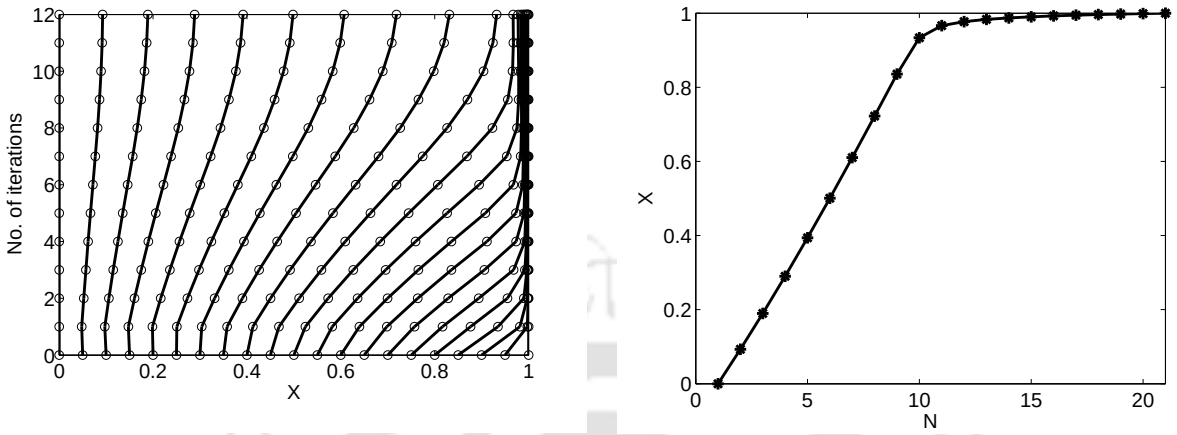

(a) Mesh movement towards right. *(b) Final computed mesh.*

Figure 4.5: *Movement of the mesh points towards right for Example 4.5.3 with* $\varepsilon = 1e-2,\ \delta = 1e-8$ *and* $N = 20$.

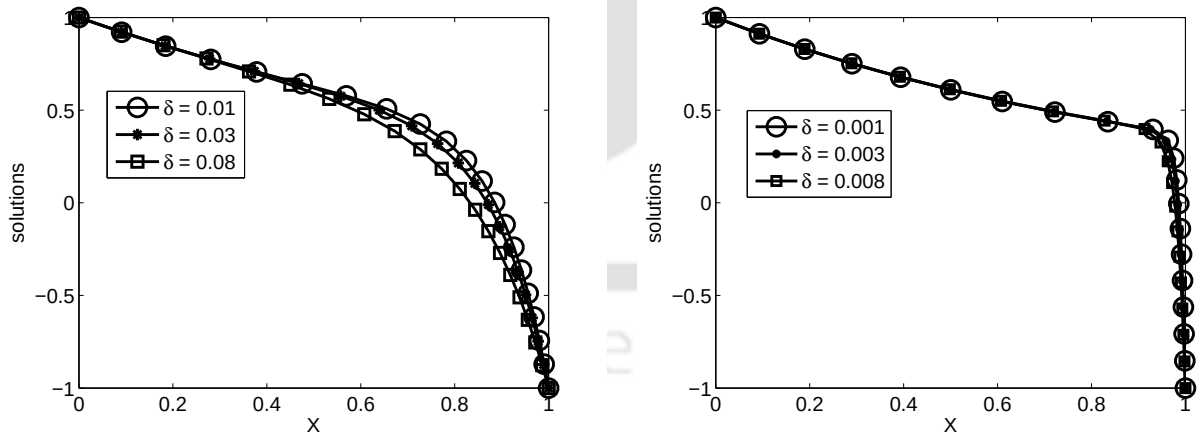

(a) $\varepsilon = 1e-1$. *(b)* $\varepsilon = 1e-2$.

Figure 4.6: *Effect of* δ *on the solution of Example 4.5.3 for* $N = 20$ *with different values of* ε.

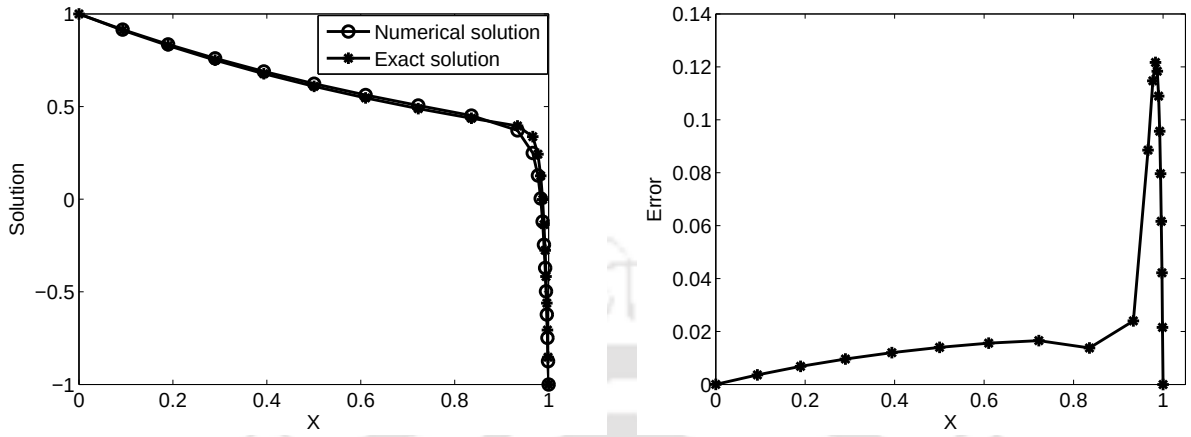

(a) Solution. *(b) Error.*

Figure 4.7: *Numerical solution with exact solution and the corresponding error for Example 4.5.3 with* $\varepsilon = 1e-2,\ \delta = 1e-8$ *and* $N = 20$.

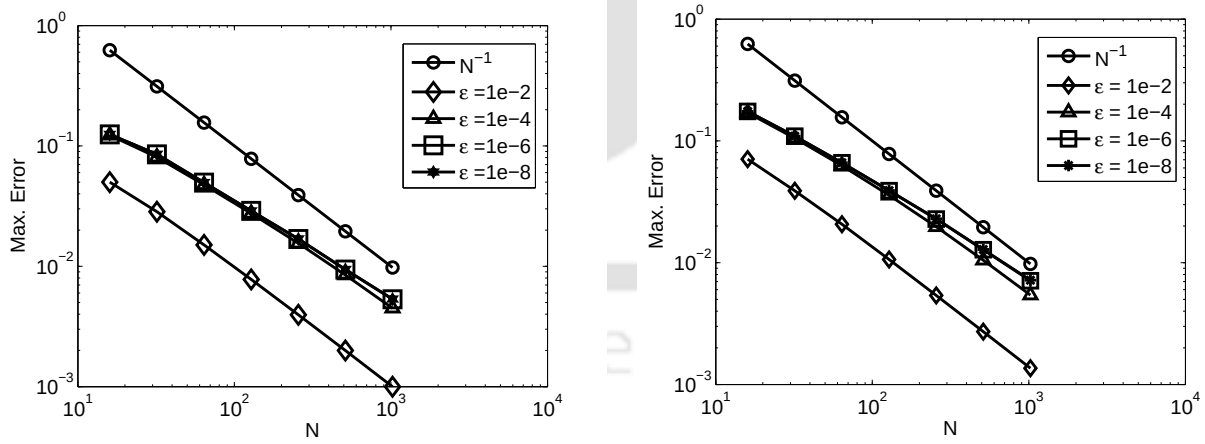

(a) Example 4.5.1. *(b) Example 4.5.3.*

Figure 4.8: *Loglog plot of the maximum error for different values of* ε.

Table 4.2: *Maximum point-wise errors E_ε^N and the rate of convergence r_ε^N for Example 4.5.1.*

ε	Number of intervals N						
	16	32	64	128	256	512	1024
1	3.0659e-3	1.5556e-3	7.8448e-4	3.9372e-4	1.9723e-4	9.8711e-5	4.9379e-5
	0.9788	0.9877	0.9946	0.9973	0.9986	0.9993	
$1e-2$	1.0806e-1	6.5947e-2	3.8353e-2	2.1065e-2	1.1113e-2	5.7156e-3	2.8937e-3
	0.7125	0.7820	0.8645	0.9226	0.9593	0.9820	
$1e-4$	1.2463e-1	8.4308e-2	4.9399e-2	2.8705e-2	1.6724e-2	9.2803e-3	5.1829e-3
	0.5640	0.7712	0.7831	0.7794	0.8497	0.8404	
$1e-8$	1.2485e-1	8.5355e-2	4.9662e-2	2.8857e-2	1.6891e-2	9.4111e-3	5.3383e-3
	0.5486	0.7813	0.7832	0.7727	0.8438	0.8180	
$1e-10$	1.2485e-1	8.5353e-2	4.9660e-2	2.8861e-2	1.6891e-2	9.4096e-3	5.3377e-3
	0.5487	0.7814	0.7830	0.7728	0.8441	0.8179	

Table 4.3: *Maximum point-wise errors G_ε^N and the rate of convergence q_ε^N for Example 4.5.2.*

ε	Number of intervals N						
	16	32	64	128	256	512	1024
1	1.1255e-3	5.5409e-4	2.7353e-4	1.3420e-4	6.4849e-5	3.0251e-5	1.2971e-5
	1.0224	1.0184	1.0273	1.0492	1.1001	1.2217	
$1e-2$	1.3551e-1	8.0474e-2	4.4173e-2	2.2810e-2	1.0904e-2	4.4767e-3	1.8415e-3
	0.7518	0.8654	0.9535	1.0648	1.2843	1.2816	
$1e-4$	8.2523e-2	5.7914e-2	3.9768e-2	2.3760e-2	1.3183e-2	7.4077e-3	3.4080e-3
	0.5109	0.5423	0.7431	0.8499	0.8316	1.1201	
$1e-8$	6.7670e-2	5.5369e-2	3.6724e-2	2.4701e-2	1.4268e-2	6.9121e-3	3.7731e-3
	0.2894	0.5924	0.5722	0.7918	1.0456	0.8734	
$1e-10$	8.1067e-2	5.6218e-2	3.9495e-2	2.2684e-2	1.2954e-2	6.0157e-3	2.4715e-3
	0.5281	0.5094	0.8000	0.8083	1.1066	1.2833	

Table 4.4: *Maximum point-wise errors E_ε^N and the rate of convergence r_ε^N for Example 4.5.3 .*

ε	Number of intervals N						
	16	32	64	128	256	512	1024
1	5.6304e-3	2.9283e-3	1.4940e-3	7.5461e-4	3.7920e-4	1.9007e-4	9.5157e-5
	0.9432	0.9709	0.9854	0.9928	0.9964	0.9982	
$1e-2$	1.4267e-1	8.5082e-2	4.7691e-2	2.5498e-2	1.3224e-2	6.7357e-3	3.6940e-3
	0.7457	0.8351	0.9033	0.9473	0.9732	0.8666	
$1e-4$	1.7424e-1	1.0885e-1	6.5746e-2	3.8706e-2	2.2167e-2	1.2374e-2	6.7611e-3
	0.6787	0.7274	0.7643	0.8042	0.8410	0.8720	
$1e-8$	1.7484e-1	1.0929e-1	6.6127e-2	3.9070e-2	2.2929e-2	1.2822e-2	7.1847e-3
	0.6779	0.7248	0.7592	0.7689	0.8385	0.8357	
$1e-10$	1.7461e-1	1.0933e-1	6.6169e-2	3.9106e-2	2.2958e-2	1.2527e-2	7.0556e-3
	0.6755	0.7244	0.7588	0.7684	0.8740	0.8282	

Table 4.5: *Maximum point-wise errors G_ε^N and the rate of convergence q_ε^N for Example 4.5.4.*

ε	Number of intervals N						
	16	32	64	128	256	512	1024
1	9.3312e-3	4.9243e-3	2.5101e-3	1.2515e-3	6.0855e-4	2.8368e-4	1.2042e-4
	0.9221	0.9721	1.0041	1.0402	1.1011	1.2362	
$1e-2$	1.0985e-1	6.5425e-2	3.6239e-2	1.7269e-2	6.2503e-3	3.2809e-3	1.7116e-3
	0.7476	0.8523	1.0694	1.4662	0.9298	0.9387	
$1e-4$	5.4976e-2	3.6507e-2	2.7036e-2	1.8143e-2	1.1740e-2	6.6864e-3	3.4611e-3
	0.5906	0.4333	0.5755	0.6280	0.8121	0.9500	
$1e-8$	1.7226e-1	8.9547e-2	3.8862e-2	1.9892e-2	1.0979e-2	6.1047e-3	3.2755e-3
	0.9439	1.2043	0.9662	0.8574	0.8468	0.8982	
$1e-10$	1.5374e-1	7.2108e-2	3.7251e-2	1.7697e-2	1.0527e-2	5.5295e-3	2.1111e-3
	1.0923	0.9529	1.0738	0.7494	0.9289	1.3892	

Table 4.6: *Comparison of computational results with the Shishkin mesh for Example 4.5.2.*

N	$\varepsilon = 1e-4$		$\varepsilon = 1e-8$	
	Shishkin mesh	**Adaptive grid**	**Shishkin mesh**	**Adaptive grid**
16	9.1183e-2	8.2523e-2	9.1050e-2	6.7670e-2
	0.7689	0.5109	0.9463	0.2894
32	5.3514e-2	5.7914e-2	4.7252e-2	5.5369e-2
	0.4572	0.5423	0.9820	0.5924
64	3.8978e-2	3.9768e-2	2.3922e-2	3.6724e-2
	0.3263	0.7431	1.0084	0.5722
128	3.1089e-2	2.3760e-2	1.1892e-2	2.4701e-2
	0.2387	0.8499	1.0399	0.7918
256	2.6349e-2	1.3183e-2	5.7837e-3	1.4268e-2
	0.2247	0.8316	1.0955	1.0456
512	2.2549e-2	7.4077e-3	2.7066e-3	6.9121e-3
	0.3259	1.1201	1.2189	0.8734
1024	1.7990e-2	3.4080e-3	1.1628e-3	3.7731e-3
	–	–	–	–

Table 4.7: *Comparison of computational results with the Shishkin mesh for Example 4.5.4.*

N	$\varepsilon = 1e-4$		$\varepsilon = 1e-8$	
	Shishkin mesh	**Adaptive grid**	**Shishkin mesh**	**Adaptive grid**
16	6.5329e-2	5.4976e-2	6.5499e-2	1.7226e-1
	0.9476	0.5906	0.5906	0.9439
32	3.3874e-2	3.6507e-2	3.4127e-2	8.9547e-2
	0.9772	0.4333	0.4333	1.2043
64	1.7207e-2	2.7036e-2	1.7300e-2	3.8862e-2
	0.1440	0.5755	0.5755	0.9662
128	1.5572e-2	1.8143e-2	8.6037e-3	1.9892e-2
	0.0373	0.6280	0.6280	0.8574
256	1.5174e-2	1.1740e-2	4.1850e-3	1.0979e-2
	0.1060	0.8121	0.8121	0.8468
512	1.4100e-2	6.6864e-3	1.9579e-3	6.1047e-3
	0.2489	0.9500	0.9501	0.8982
1024	1.1865e-2	3.4611e-3	8.4012e-4	3.2755e-3
	–	–	–	–

Chapter 5

A Uniformly Accurate Finite Difference Approximation of Singularly Perturbed Differential-Difference Equation

In this chapter, the adaptive grid idea discussed in Chapter 4 is extended to solve a class of singularly perturbed differential-difference equations having both the delay and the shift terms. A numerical method comprising of upwind finite difference operator on an adaptive grid which is formed by equidistributing the arc-length monitor function, is constructed for approximating the solution. The method is proved to be robust, in the sense that the discrete solution obtained converges in the maximum norm to the exact solution uniformly with respect to the perturbation parameters. Parameter-uniform error bounds for the numerical approximations are established. Numerical examples are in well agreement with the theoretical results.[2]

5.1 Introduction

Consider the following singularly perturbed differential–difference equation (SPDDE) in the domain $\Omega = (0, 1)$:

$$\begin{cases} \mathcal{L}_\varepsilon u_\varepsilon(x) \equiv -\varepsilon u_\varepsilon''(x) - p(x)u_\varepsilon'(x) - \alpha(x)u_\varepsilon(x-\delta) + q(x)u_\varepsilon(x) - \beta(x)u_\varepsilon(x+\eta) = F(x), \\ u_\varepsilon(x) = \phi(x), \quad -\delta \le x \le 0, \\ u_\varepsilon(x) = \gamma(x), \quad 1 \le x \le 1+\eta, \end{cases} \tag{5.1.1}$$

where $0 < \varepsilon \ll 1$ is the perturbation parameter, the functions $p(x), \alpha(x), q(x), \beta(x)\ F(x), \phi(x)$ and $\gamma(x)$ are sufficiently smooth and the delay parameter δ and the shift parameter η are such that $0 < \delta, \eta \ll 1$, both are of $o(\varepsilon)$. These equations are also known as SPDDE and are widespread

[2]Some portion of this chapter is published in *Int. J. Numer. Meth. Biomed. Engng., DOI:10.1002/cnm.1370.*

in many branches of sciences and have been used for many years in control theory, biophysics, mechanics, etc. ([89], [93]). The SPDDEs provide more realistic models than the conventional singularly perturbed differential equations. For example, in population dynamics, these small parameters display time-lag or after-effect and hence play an important role in modelling the real-life phenomena.

Without loss of generality, we assume that $p(x) > 0$. Again if the BVP (5.1.1) is considered without the delay and the shift terms, *i.e.,* $\alpha(x) = \beta(x) = 0$, then (5.1.1) reduces to an ordinary differential equation (ODE) with boundary layer at $x = 0$, which can be solved by using the standard procedure of singular perturbation.

For $\delta = \eta = \kappa\varepsilon > 0$, where κ is sufficiently small, the technique discussed in Chapter 4 is followed. To tackle the delay and the shift terms, the delay and the shift arguments are expanded through the Taylor's series expansion assuming sufficient smoothness condition on the solution of (5.1.1) so that the BVP (5.1.1) reduces to a standard singular perturbation problem. Expanding the delay and the shift terms, we obtain that

$$\begin{cases} u_\varepsilon(x-\delta) \approx u_\varepsilon(x) - \delta u'_\varepsilon(x) + \delta^2 u''_\varepsilon(x)/2 + \ldots, & \text{as } \varepsilon \to 0 \\ u_\varepsilon(x+\eta) \approx u_\varepsilon(x) + \eta u'_\varepsilon(x) + \eta^2 u''_\varepsilon(x)/2 + \ldots, & \text{as } \varepsilon \to 0. \end{cases} \tag{5.1.2}$$

Now using the first three terms of the expansions (5.1.2) in the SPDDE (5.1.1), we obtain the following BVP:

$$\begin{cases} L_\varepsilon u(x) \equiv -R_\varepsilon(x)u''(x) - P_\varepsilon(x)u'(x) + Q(x)u(x) = F(x), & x \in \Omega, \\ u(x) \approx \phi(0) = \phi_0, & -\delta \le x \le 0, \\ u(x) \approx \gamma(1) = \gamma_1, & 1 \le x \le 1+\eta, \end{cases} \tag{5.1.3}$$

where $R_\varepsilon(x) = \varepsilon + \big(\alpha(x)\delta^2 + \beta(x)\eta^2\big)/2 \ge 0$, $P_\varepsilon(x) = p(x) - \alpha(x)\delta + \beta(x)\eta$ and $Q(x) = q(x) - \alpha(x) - \beta(x)$. Furthermore, the coefficients $\alpha(x)$, $\beta(x)$ are chosen in such a way that $K^* \ge P_\varepsilon(x) \ge K > 0$ and $Q(x) \ge \lambda > 0$, for some positive constants K, K^* and λ, $\forall x \in \overline{\Omega}$. Under these assumptions, the solution of the BVP (5.1.3) exhibits layer behavior on the left side of the domain near $x = 0$. The layer behavior will remain for sufficiently small non-zero values of $\delta(\varepsilon)$ and $\eta(\varepsilon)$.

It is worthwhile to mention that the BVP (5.1.3) is an approximate differential equation which differ from the original equation (5.1.1) by a term which is of $O(\delta^3 u'''_\varepsilon, \eta^3 u'''_\varepsilon)$. Since (5.1.3) is an approximation of (5.1.1), we have used only $u(x)$ as a different notation for $u_\varepsilon(x)$.

If the delay and the shift are sufficiently small, then one can expect that $u(x)$ will provide a good approximation to $u_\varepsilon(x)$. The crucial question is for what order of magnitude of δ and η for small ε, does $u(x)$ as a solution of (5.1.3) provide a leading order approximation to the solution $u_\varepsilon(x)$ of (5.1.1). To answer this, the procedure as discussed in Chapter 4 for the delay differential equations

is followed by applying an asymptotic approach first for a constant coefficient homogeneous problem *i.e.,* by setting $F(x) \equiv 0$ and then, by solving (5.1.1) numerically by introducing a direct numerical scheme.

Let us take $\delta(\varepsilon) = \tau\varepsilon^m$, $\eta(\varepsilon) = \mu\varepsilon^m$, where $m > 0$ will be determined later. Now (5.1.3) can be written as

$$-\varepsilon\big(1 + R\varepsilon^{2m-1}\big)u''(x) - (p - P\varepsilon^m)u'(x) + Qu(x) = 0, \tag{5.1.4}$$

where

$$R = (\alpha\tau^2 + \beta\mu^2)/2, \quad P = \alpha\tau - \beta\mu, \quad Q = q - \alpha + \beta.$$

Then the exact solution of (5.1.4) is of the form

$$u(x) = \exp(Ax)\left[C_1\cos(Bx) + C_2\sin(Bx)\right],$$

where

$$A = \frac{P\varepsilon^m - p}{2\varepsilon(1 + R\varepsilon^{2m-1})}, \quad B = \frac{\sqrt{(P^2 + 4RQ)\varepsilon^{2m} + 2\varepsilon(2Q - Pp\varepsilon^{m-1}) + p^2}}{2\varepsilon(1 + R\varepsilon^{2m-1})}.$$

For all $m \geq 1$, A and B are of $O(\varepsilon^{-1})$; therefore $\delta^n u^{(n)}$ and $\eta^n u^{(n)}$ are both of $O(\varepsilon^{n(m-1)})$ if C_1 and C_2 are of $O(1)$. It is also known that for a singular perturbation problem, the derivatives $u^{(n)}$ of the solution are of order $O(\varepsilon^{-n})$ and if δ and η are of the same order of ε, then the higher-order terms in the expansion (5.1.2) cannot be neglected. In other words, for $m = 1$, all higher-order derivative terms that have been omitted from (5.1.3) upon expansion of the delay and the shift terms given by (5.1.2) are of the same order of magnitude of those that have been kept. Since the approximated differential equation (5.1.3) of (5.1.1) is of $O(\delta^3 u''', \eta^3 u''')$ which will at least give us $O(\varepsilon^3)$ order approximation by choosing $m \geq 2$.

The original BVP (5.1.1) with the delay and the shift terms, is solved numerically by the following direct scheme:

$$\begin{cases} \mathcal{L}_\varepsilon^N \widehat{\mathcal{U}}_j \equiv -\varepsilon D^+D^-\widehat{\mathcal{U}}_j - p_j D^+\widehat{\mathcal{U}}_j - \alpha_j\widehat{\mathcal{U}}_{j-N} + q_j\widehat{\mathcal{U}}_j - \beta_j\widehat{\mathcal{U}}_{j+N} = F_j\,, \quad 1 \leq j \leq N-1, \\ \widehat{\mathcal{U}}_0 = \phi(0), \quad \widehat{\mathcal{U}}_N = \gamma(0)\,, \end{cases} \tag{5.1.5}$$

where $\widehat{\mathcal{U}}_{j-N} = \phi_j$ and $\widehat{\mathcal{U}}_{j+N} = \gamma_j$. Here, the delay and shift terms are approximated numerically. The numerical solution of the BVP (5.1.5) with large number of mesh points is treated as the exact solution of the original BVP (5.1.1). The numerical solution obtained by the proposed method (5.3.1) is compared with the numerical solution of the BVP (5.1.5).

To solve initial-value problems for first-order ODEs with delay terms, Amiraliyev and Erdogan proposed a similar numerical scheme in [2].

In order to calculate the maximum point-wise error $\widehat{E}_\varepsilon^N$ and the rate of convergence $\widehat{r}_\varepsilon^N$, the idea of interpolation is used. Define $\widehat{\mathcal{U}}^{8192}$ as the piecewise linear interpolation to $\widehat{\mathcal{U}}_j$ of (5.1.5) in

Ω_N. Define

$$\widehat{E}_\varepsilon^N = \max_{x_i \in \overline{\Omega}^N} |U^N - \widehat{\mathcal{U}}^{8192}| \quad \text{and} \quad \widehat{r}_\varepsilon^N = \log_2 \left(\frac{\widehat{E}_\varepsilon^N}{\widehat{E}_\varepsilon^{2N}} \right),$$

where U^N is the numerical solution obtained by our proposed method (5.3.1).

The solution of the proposed method (5.3.1) is compared with the solution of (5.1.5) in Figure 5.1 and in Table 5.1. From these graphs and the numerical results, one can conclude that the solution obtained by the proposed scheme (5.3.1) very well approximates the solution of (5.1.1) by the direct scheme (5.3.1).

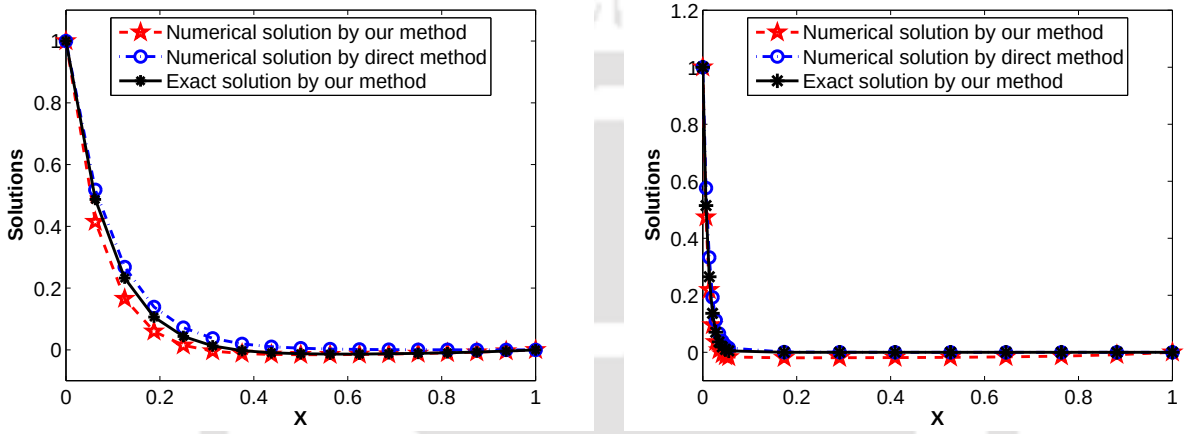

(a)$\varepsilon = 1e-01$. *(b)* $\varepsilon = 1e-02$.

Figure 5.1: *Comparison of solutions obtained by the direct numerical scheme (5.1.5) and our proposed scheme (5.3.1) for Example 5.5.1.*

Table 5.1: *Maximum point-wise errors* $\widehat{E}_\varepsilon^N$ *and the rate of convergence* $\widehat{r}_\varepsilon^N$ *for Example 5.5.1.*

ε	Number of intervals N					
	16	32	64	128	256	512
$1e-4$	1.0128e-1	6.8815e-2	4.3960e-2	2.6383e-2	1.5194e-2	8.3922e-3
	0.5575	0.6465	0.7366	0.7961	0.8563	
$1e-8$	1.0001e-1	6.8541e-2	4.3913e-2	2.6379e-002	1.5197e-2	8.3956e-3
	0.5451	0.6423	0.7352	0.7956	0.8561	

Hence, in summary of the constant coefficient case, one can conclude that the solution of the approximated equation (5.1.3) provides a leading order solution to (5.1.1) up to δ and η are both of $o(\varepsilon)$.

The layout of the rest of this chapter is as follows: In Section 5.2, the maximum principle, the stability result and some *a priori* estimates on the solution and its derivatives are established.

Section 5.3 presents the upwind finite difference discretization and provides the generation of the nonuniform grids through the equidistribution principle. The bounds for the local truncation error and for the maximum point-wise error are obtained in Section 5.4. Finally, several numerical examples are provided in Section 5.5 to illustrate the applicability of the proposed method.

5.2 Continuous Problem

This section provides the bounds of the solution of the BVP (5.1.3) and its derivatives which will be used later in deriving the error estimates.

Lemma 5.2.1. (Maximum Principle) *Let $\mathcal{V}$ be a smooth function satisfying $\mathcal{V}(0) \geq 0,\ \mathcal{V}(1) \geq 0$ and $L_\varepsilon \mathcal{V}(x) \geq 0,\ \forall x \in\ \Omega$. Then $\mathcal{V}(x) \geq 0,\ \forall x \in\ \overline{\Omega}$.*

Proof. Let $x^* \in \overline{\Omega}$ be such that $\mathcal{V}(x^*) = \min\limits_{x\in\overline{\Omega}} \mathcal{V}(x)$ and assume that $\mathcal{V}(x^*) < 0$. Clearly $x^* \notin \{0, 1\}$ and $\mathcal{V}'(x^*) = 0$ and $\mathcal{V}''(x^*) \geq 0$. Now consider

$$L_\varepsilon \mathcal{V}(x^*) \equiv -R_\varepsilon(x^*)\mathcal{V}''(x^*) - P_\varepsilon(x^*)\mathcal{V}'(x^*) + Q(x^*)\mathcal{V}(x^*) < 0$$

which is a contradiction to our assumption. Hence, $\mathcal{V}(x) \geq 0, \forall x \in\ \overline{\Omega}$. ∎

Lemma 5.2.2. *If u is the solution of the BVP (5.1.3), then*

$$\|u\| \ \leq\ \lambda^{-1}\|F\| + \max\{|\phi_0|, |\gamma_1|\}. \tag{5.2.1}$$

Proof. Applying the maximum principle as given in Lemma 5.2.1 to the following barrier function

$$\psi^{\pm}(x) = \lambda^{-1}\|F\| + \max\{|\phi_0|, |\gamma_1|\} \pm u(x),$$

one can obtain the required result. ∎

Lemma 5.2.3. *The solution $u(x)$ of the BVP (5.1.3) and its derivatives satisfy the following bounds:*

$$\begin{aligned} |u(x)| \quad &\leq \quad C\left[1 + \exp\left(\frac{-Kx}{R_\varepsilon}\right)\right], \\ |u^{(i)}(x)| \quad &\leq \quad CR_\varepsilon^{-i} \exp\left(\frac{-Kx}{R_\varepsilon}\right), \quad i = 1, 2, 3, \qquad x \in \overline{\Omega}. \end{aligned} \tag{5.2.2}$$

Proof. One can prove this lemma by following the method of proof as given in Chapter 4. ∎

Let us decompose the solution of (5.1.3) into regular and singular parts as follows:

$$u(x) = v_\varepsilon(x) + w_\varepsilon(x).$$

Define $R_\varepsilon = \varepsilon + \alpha\delta^2 + \beta\eta^2$ where α, β are respectively the bounds for $\alpha(x), \beta(x)$ in Ω. Now $v_\varepsilon(x)$ can be written in an asymptotic expansion as

$$v_\varepsilon(x) = v_0(x) + R_\varepsilon v_1(x) + R_\varepsilon^2 v_2(x),$$

where v_0, v_1 and v_2 are defined as the solutions of the following differential equations:

$$\begin{cases} P_\varepsilon(x)v_0'(x) - Q(x)v_0(x) = -F(x), & v_0(1) = u(1), \\ P_\varepsilon(x)v_1'(x) - Q(x)v_1(x) = -v_0''(x), & v_1(1) = 0, \\ L_\varepsilon(v_2(x)) = \dfrac{R_\varepsilon(x)}{R_\varepsilon} v_1''(x), & v_2(0) = 0, v_2(1) = 0. \end{cases} \tag{5.2.3}$$

Hence, the regular component of the solution satisfies

$$L_\varepsilon v_\varepsilon(x) = F(x), \quad v_\varepsilon(0) = v_0(0) + R_\varepsilon v_1(0),\ v_\varepsilon(1) = u(1), \tag{5.2.4}$$

and the layer component satisfies the BVP:

$$L_\varepsilon w_\varepsilon(x) = 0, \quad w_\varepsilon(0) = u(0) - v_\varepsilon(0),\ w_\varepsilon(1) = 0. \tag{5.2.5}$$

Lemma 5.2.4. *For sufficiently small ε and $0 \le i \le 3$, the derivatives of v_ε and w_ε satisfy the following bounds:*

$$\begin{aligned} \|v_\varepsilon^{(i)}\| &\le C\left[1 + \left(R_\varepsilon\right)^{2-i}\right], \\ |w_\varepsilon^{(i)}(x)|_{\overline{\Omega}} &\le C\left(R_\varepsilon\right)^{-i} \exp\left(-\frac{Kx}{R_\varepsilon}\right), \quad \forall x \in \overline{\Omega}. \end{aligned} \tag{5.2.6}$$

Proof. One can get this result following the proof as done in Chapter 4. ∎

5.3 Discrete Problem

The difference scheme and the generation of the adaptive grid are discussed in this section.

Consider the difference approximations of (5.1.3) on a non-uniform mesh $\Omega^N = \{x_j\}_{j=0}^N$ and denote $h_j = x_j - x_{j-1}$. The upwind finite difference discretization of (5.1.3) takes the form

$$\begin{cases} L_\varepsilon^N U_j \equiv -R_{\varepsilon,j} D^+D^- U_j - P_{\varepsilon,j} D^+ U_j + Q_j U_j = F_j\,, \quad 1 \le j \le N-1, \\ U_0 = \phi_0, \quad U_N = \gamma_1\ . \end{cases} \tag{5.3.1}$$

Here U_j denotes the approximation of $u(x_j)$, $R_{\varepsilon,j} = R_\varepsilon(x_j)$ and $P_{\varepsilon,j}$, Q_j, F_j are defined in a similar fashion. Equation (5.3.1) can be expressed in the following tri-diagonal system of algebraic equations:

$$\begin{cases} -r_j^- U_{j-1} + r_j^c U_j - r_j^+ U_{j+1} = F_j, \quad j = 1, \ldots, N-1, \\ U_0 = \phi_0, \quad U_N = \gamma_1, \end{cases} \tag{5.3.2}$$

where

$$r_j^- = \frac{2R_{\varepsilon,j}}{h_j(h_j + h_{j+1})}, \quad r_j^c = \frac{2R_{\varepsilon,j}}{h_j h_{j+1}} + \frac{P_{\varepsilon,j}}{h_{j+1}} + Q_j, \quad r_j^+ = \frac{2R_{\varepsilon,j}}{h_{j+1}(h_j + h_{j+1})} + \frac{P_{\varepsilon,j}}{h_{j+1}} \ .$$

In the tri-diagonal system (5.3.2), the off-diagonal entries have the following properties.

$$r_j^- > 0, \ r_j^+ > 0,$$

and

$$r_j^c + r_j^- + r_j^+ \geq 0, \quad \text{for} \quad j = 1, \ldots, N-1, \tag{5.3.3}$$

which imply that the stiffness matrix is an M-matrix.

5.3.1 Adaptive grid

Here, to generate the adaptive grid the following arc-length monitor function is considered

$$M\big(u(x), x\big) = \sqrt{1 + (u'(x))^2}. \tag{5.3.4}$$

The adaptive grid can be constructed as the solution of the following nonlinear system of equations:

$$\begin{cases} (x_{j+1} - x_j)^2 + (U_{j+1} - U_j)^2 = (x_j - x_{j-1})^2 + (U_j - U_{j-1})^2, \ j = 1, \ldots, N-1. \\ x_0 = 0, \quad x_N = 1. \end{cases} \tag{5.3.5}$$

The system of equations (5.3.1) and (5.3.5) are solved simultaneously to obtain the solution U_j and the grids x_j.

5.4 Error Analysis

This section presents the bound of the truncation error and the ε-uniform error of the proposed scheme (5.3.1).

5.4.1 Local truncation error

The local truncation error of the difference scheme (5.3.1) at the node x_j is given by

$$\tau_j = L_\varepsilon^N U_j - (L_\varepsilon u)(x_j), \tag{5.4.1}$$

where u and U_j denote the solution of (5.1.3) and (5.3.1) respectively.

Lemma 5.4.1. *The required bound for the truncation error is given by*

$$|\tau_j| \leq \frac{C}{R_\varepsilon N} \exp\left(\frac{-Kx_j}{R_\varepsilon}\right). \tag{5.4.2}$$

Proof. Using the Taylor series expansion and Lemma 2.5.1, the truncation error (5.4.1) can be expressed as

$$\begin{aligned}\tau_j \quad &= \frac{-R_{\varepsilon,j}}{h_j + h_{j+1}}\left[\frac{1}{h_{j+1}}\int_{x_j}^{x_{j+1}} (x_{j+1}-s)^2 u'''(s)ds - \frac{1}{h_j}\int_{x_{j-1}}^{x_j} (s-x_{j-1})^2 u'''(s)ds\right] + \\ &\quad + \frac{P_{\varepsilon,j}}{h_{j+1}}\int_{x_j}^{x_{j+1}} (x_{j+1}-s)u''(s)ds,\end{aligned} \tag{5.4.3}$$

from which we obtain the following bound

$$|\tau_j| < R_{\varepsilon,j}\int_{x_{j-1}}^{x_{j+1}} |u'''(s)|ds + C\int_{x_{j-1}}^{x_{j+1}} |u''(s)|ds. \tag{5.4.4}$$

If we invoke the derivative bounds of the continuous solution in the first term, the above expression becomes

$$|\tau_j| < C\int_{x_{j-1}}^{x_{j+1}} |u''(s)|ds. \tag{5.4.5}$$

From (2.3.6), we have

$$\begin{aligned}|\tau_j| \quad &\leq \quad C\ell \int_{\xi_{j-1}}^{\xi_{j+1}} \frac{|u''(x)|}{\sqrt{1+u'(x)^2}}d\xi \\ &\leq \quad \frac{C}{R_\varepsilon}\int_{\xi_{j-1}}^{\xi_{j+1}} \frac{|u'(x)|}{\sqrt{1+u'(x)^2}}d\xi.\end{aligned} \tag{5.4.6}$$

From Lemma 5.2.3, we know that $|u'(x)| = O(1/R_\varepsilon)$. Again, using the bound of the solution (5.2.2) and the proof provided in [82], we have

$$\frac{C_1}{R_\varepsilon}\exp\left(\frac{-K^*x}{R_\varepsilon}\right) \leq u'(x) \leq \frac{C_2}{R_\varepsilon}\exp\left(\frac{-Kx}{R_\varepsilon}\right).$$

Now using these bounds in (5.4.6), we have

$$\begin{aligned}|\tau_j| \quad &\leq \quad \frac{C}{R_\varepsilon}\int_{\xi_{j-1}}^{\xi_{j+1}} \frac{\frac{C_2}{R_\varepsilon}\exp\left(\frac{-Kx}{R_\varepsilon}\right)}{\sqrt{1+(\frac{C_1}{R_\varepsilon})^2\exp\left(\frac{-2K^*x}{R_\varepsilon}\right)}}d\xi \\ &\leq \quad \frac{C}{R_\varepsilon N}\frac{\frac{C_2}{R_\varepsilon}\exp\left(\frac{-Kx_j}{R_\varepsilon}\right)}{\sqrt{1+(\frac{C_1}{R_\varepsilon})^2\exp\left(\frac{-2K^*x_j}{R_\varepsilon}\right)}} \\ &\leq \quad J_j\exp\left(\frac{-\omega x_j}{R_\varepsilon}\right),\end{aligned} \tag{5.4.7}$$

where $0 < \omega < 1$ is independent of ε, N and $J_j = \dfrac{C}{R_\varepsilon N}\dfrac{(C_2/R_\varepsilon)\exp\left(-(K-\omega)x_j/R_\varepsilon\right)}{\sqrt{1+(C_1/R_\varepsilon)^2\exp\left(-2K^*x_j/R_\varepsilon\right)}}$.

Let us denote $y_j = (C/R_\varepsilon)\exp\left(-Kx_j/R_\varepsilon\right)$, $g(y) = y/\sqrt{1+y^2}$, which is an increasing function in $[0, y^*]$, where $y^* = \sqrt{(1-\omega)/\omega}$. Since $\omega = O(1)$, we have $y^* = O(\omega)$ and hence $g(y^*) = O(1)$. Therefore, we can express

$$J_j \leq \frac{C}{R_\varepsilon N} g(y_j) \leq \frac{C}{R_\varepsilon N} g(y^*) \leq \frac{C}{R_\varepsilon N} \ ,$$

and hence,

$$|\tau_j| \leq \frac{C}{R_\varepsilon N} \exp\left(\frac{-Kx_j}{R_\varepsilon}\right),$$

which is the required result. ∎

Before deriving the error estimate for the numerical solution of (5.3.1), we provide here some lemmas which are the prerequisites for the main result.

Lemma 5.4.2. (Discrete Comparison Principle) *If $L_\varepsilon^N \mathcal{V}_j < L_\varepsilon^N \mathcal{Z}_j$ for $1 \leq j \leq N-1$ with $\mathcal{V}_0 < \mathcal{Z}_0$ and $\mathcal{V}_N < \mathcal{Z}_N$, then $\mathcal{V}_j < \mathcal{Z}_j$ for $1 \leq j \leq N$.*

Proof. From (5.3.3), it is clear that the matrix associated with the discrete operator L_ε^N is an irreducible M-matrix and therefore has a positive inverse. Hence, the result follows. ∎

Lemma 5.4.3. *Let the mesh function S_j be*

$$S_0 = 1, \quad S_j = \prod_{k=1}^{j} \left(1 + \frac{Kh_k}{R_\varepsilon}\right)^{-1}, \quad j = 1, \ldots, N. \tag{5.4.8}$$

Then, for $j = 1, \ldots, N-1$, there exists a constant C such that

$$L_\varepsilon^N S_j \geq \frac{C}{\max\{R_\varepsilon, h_{j+1}\}} S_j \ . \tag{5.4.9}$$

Proof. From the definition of S_j, it is clear that

$$\frac{S_j - S_{j-1}}{h_j} = -\frac{K}{R_\varepsilon} S_j \ .$$

Now

$$\begin{aligned}
L_\varepsilon^N S_j &= -\frac{2R_{\varepsilon,j}}{h_j + h_{j+1}} \left[\frac{S_{j+1} - S_j}{h_{j+1}} - \frac{S_j - S_{j-1}}{h_j}\right] - P_{\varepsilon,j} \left[\frac{S_{j+1} - S_j}{h_{j+1}}\right] + Q_j S_j \\
&\geq -\frac{2KR_{\varepsilon,j} h_{j+1}}{R_\varepsilon (h_j + h_{j+1})} \left[\frac{S_j - S_{j+1}}{h_{j+1}}\right] + \frac{K\, P_{\varepsilon,j}}{R_\varepsilon} S_{j+1} \\
&\geq \left(\frac{K}{R_\varepsilon + Kh_{j+1}}\right) \left[P_{\varepsilon,j} - \frac{2KR_{\varepsilon,j} h_{j+1}}{R_\varepsilon (h_j + h_{j+1})}\right] S_j \\
&\geq \frac{C}{\max\{R_\varepsilon, h_{j+1}\}} S_j \ .
\end{aligned}$$

∎

Remark 5.4.4. *The function S_j is the piecewise (0,1)–Padé approximation of $\exp(-Kx_j/R_\varepsilon)$. A similar comparison function was used originally by Kellogg and Tsan [46] to analyze the methods on uniform grids and more recently by Qiu et al. [82] and Stynes and Roos [92] for analysis on nonuniform grids.*

The following lemma provides a two-sided bound for S_j, which will be used later.

Lemma 5.4.5. *The grid function S_j defined in (5.4.8) satisfy*

$$\exp\left(\frac{-Kx_j}{R_\varepsilon}\right) < S_j < C\exp\left(\frac{-Kx_j}{R_\varepsilon}\right), \quad j = 1, \ldots, N-1. \tag{5.4.10}$$

Proof. We can express the nodes x_j as

$$x_j = \sum_{k=1}^{j} h_k \ .$$

Therefore,

$$\begin{aligned}\exp\left(-\frac{Kx_j}{R_\varepsilon}\right) &= \exp\left(\sum_{k=1}^{j}\frac{-Kh_k}{R_\varepsilon}\right)\\ &= \prod_{k=1}^{j}\exp\left(-\frac{Kh_k}{R_\varepsilon}\right).\end{aligned}$$

For any real value of $\lambda > 0$, we have $\exp(-\lambda) < (1+\lambda)^{-1}$. Therefore,

$$\exp\left(-\frac{Kx_j}{R_\varepsilon}\right) < \prod_{k=1}^{j}\left(1+\frac{Kh_k}{R_\varepsilon}\right)^{-1} \le S_j.$$

Now we have to find the upper bound for S_j. We know from (2.3.6) that

$$\begin{aligned}h_j &= \int_{\xi_{j-1}}^{\xi_j}\frac{\ell}{\sqrt{1+(u'(s))^2}}ds\\ &\le \int_{\xi_{j-1}}^{\xi_j}\frac{\ell}{u'(s)}ds\\ &\le \frac{\ell}{Nu'(x_j)}.\end{aligned}$$

From (5.2.2), we can see that

$$|u'(x_j)| \le CR_\varepsilon^{-1}\exp\left(\frac{-Kx_j}{R_\varepsilon}\right).$$

Hence, we have

$$h_j \le \frac{R_\varepsilon\ell}{KN}\exp\left(\frac{Kx_j}{R_\varepsilon}\right). \tag{5.4.11}$$

Observe that

$$\begin{aligned}\ln\Big[\prod_{k=1}^{j}\Big(1+\frac{Kh_k}{R_\varepsilon}\Big)\Big] &\geq \sum_{k=1}^{j}\Big[\frac{Kh_k}{R_\varepsilon}-\frac{1}{2}\Big(\frac{Kh_k}{R_\varepsilon}\Big)^2\Big]\\ &\geq \frac{Kx_j}{R_\varepsilon}-\frac{1}{2}\sum_{k=1}^{j}\Big(\frac{Kh_k}{R_\varepsilon}\Big)^2 \qquad (5.4.12)\end{aligned}$$

Now using (5.4.11) and for some $\tilde{x}$ in the layer region *i.e.*, $\tilde{x}\in(0,x_{_K})$, we can write

$$\begin{aligned}\sum_{j=1}^{K}\Big(\frac{Kh_j}{R_\varepsilon}\Big)^2 &\leq CR_\varepsilon^{-1}N^{-1}\sum_{k=1}^{j}\exp\Big(\frac{Kh_k}{R_\varepsilon}\Big)\\ &\leq CR_\varepsilon^{-1}N^{-1}\int_0^{\tilde{x}}\exp\Big(\frac{Ks}{R_\varepsilon}\Big)ds\\ &\leq C\,.\end{aligned}$$

Then, from (5.4.8) and (5.4.12), we obtain that

$$\prod_{k=1}^{j}\Big(1+\frac{Kh_k}{R_\varepsilon}\Big)^{-1}\leq C\exp\Big(\frac{-Kx_j}{R_\varepsilon}\Big),$$

and hence

$$S_j\leq C\exp\Big(\frac{-Kx_j}{R_\varepsilon}\Big).$$

The main result namely, the ε-uniform convergence of the upwind scheme is given in the following theorem.

Theorem 5.4.6. *Let $u(x)$ and U_j be respectively the solution of (5.1.3) and the discrete solution of (5.3.1) on the grids defined by (5.3.5). Then, there exists a constant C, independent of N, ε, δ and η such that*

$$\max_{0\leq j\leq N}|u(x_j)-U_j|\leq CN^{-1},\qquad j=0,\ldots,N. \qquad (5.4.13)$$

Proof. We already know from (5.4.2) that the bound of the truncation error is given by

$$|\tau_j|\leq\frac{C}{R_\varepsilon N}\exp\Big(\frac{-Kx_j}{R_\varepsilon}\Big).$$

Let us apply the discrete comparison principle (Lemma 5.4.2) to the barrier function $\mathcal{W}_j$ defined by

$$\mathcal{W}_j=CN^{-1}(1+S_j),\quad j=0,\ldots,N.$$

The truncation error τ_j and the nodal error e_j are related by $L_\varepsilon^N e_j = \tau_j$. Using (5.4.10), we have for $j = 1, \ldots, N-1$,

$$\begin{aligned} L_\varepsilon^N e_j = \tau_j &\leq \frac{C}{R_\varepsilon N} \exp\left(-\frac{K x_j}{R_\varepsilon}\right) \\ &\leq \frac{C}{R_\varepsilon N} S_j \\ &\leq \frac{C}{R_\varepsilon N} L_\varepsilon^N S_j \\ &\leq L_\varepsilon^N \mathcal{W}_j \ . \end{aligned}$$

Since $e_0 \leq \mathcal{W}_0$ and $e_N \leq \mathcal{W}_N$, we can conclude that

$$e_j \leq \mathcal{W}_j \leq CN^{-1}, \quad j = 0, \ldots, N.$$

Now the same argument can be repeated with e_j being replaced by $-e_j$ and hence we have

$$|e_j| \leq CN^{-1}, \quad j = 0, \ldots, N.$$

which is the required result. ■

Remark 5.4.7. *Now we assume that the convection coefficient $P_\varepsilon(x)$ in the differential equation (5.1.3) is such that $P_\varepsilon \leq \tilde{K} < 0$ for $x \in \overline{\Omega}$ where $\tilde{K}$ is a constant. This assumption implies that the boundary layer occurs in the neighborhood of $x = 1$,* i.e., *on the right hand side of the interval. We have already established the estimates for the solution of the continuous problem and its derivatives in the case when the solution of the problem (5.1.3) exhibits a boundary layer at $x = 0$,* i.e., *at the left side of the interval $[0, 1]$. One can easily obtain similar estimates for the right boundary layer case. But the main difference in this kind of approach is the numerical scheme, where the first-order derivative is approximated by the backward finite difference operator in place of the forward finite difference operator as we did in the case of left side boundary layer. This is mainly to preserve the stability of the upwind scheme. Here it is significant to observe that the non-uniform mesh as given in (5.3.5) can be constructed through the same monitor function as defined in (5.3.4) in the case of the right boundary layer.*

Also for the adaptive mesh, the error estimate is of first-order accurate whereas in the case of Shishkin mesh, it will be of first-order upto a logarithmic factor.

5.5 Numerical Results

In this section to validate the theoretical results, the proposed numerical scheme is applied to several test problems with constant and variable coefficients having left and right boundary layers with $\delta = \eta = \varepsilon^2$. The results obtained on the adaptive grid are compared with the numerical results obtained by using the upwind difference scheme on the piecewise-uniform Shishkin mesh.

Example 5.5.1. *Consider the constant coefficient problem*

$$\begin{cases} -\varepsilon u''(x) - u'(x) + 2u(x-\delta) + 5u(x) - u(x+\eta) = 0, \quad x \in (0,1), \\ u(x) = 1, \quad -\delta \le x \le 0, \qquad u(x) = 0, \quad 1 \le x \le 1+\eta. \end{cases}$$

The exact solution is given by $u(x) = \dfrac{\exp(m_1 x + m_2) - \exp(m_1 + m_2 x)}{\exp(m_2) - \exp(m_1)}$, where

$$m_{1,2} = \big(- P_\varepsilon \pm \sqrt{P_\varepsilon^2 - 4QR_\varepsilon}\big)/2R_\varepsilon \quad \text{and} \quad R_\varepsilon = \varepsilon + (\eta^2 - 2\delta^2)/2,\ P_\varepsilon = 1 + 2\delta + \eta,\ Q = 6.$$

This BVP has a boundary layer near the left end at $x = 0$.

For boundary layer on the left, the piecewise-uniform Shishkin mesh $\overline{\Omega}_\varepsilon$ is constructed by partitioning the domain $[0,1]$ into two subdomains $[0,\sigma)$ and $[\sigma,1]$. Here, σ is the the point of transition from a fine mesh to the coarse mesh and is defined as $\sigma = \min\{1/2, \sigma_0 R_\varepsilon \ln N\}$, $\sigma_0 = 1/K$, where K is the lower bound of $P_\varepsilon(x)$. The definition of σ guarantees the existence of some points inside the layer region. Without loss of generality, assume that N is even. Now $N/2$ numbers of subintervals are placed in each of the subdomains. The corresponding Shishkin mesh for the right boundary layer can be constructed in a similar fashion by dividing the domain into two subdomains $[0, 1-\sigma]$ and $(1-\sigma, 1]$ and placing N/2 number of intervals in each subdomain.

Example 5.5.2. *Consider the constant coefficient problem with right hand side boundary layer*

$$\begin{cases} -\varepsilon u''(x) + u'(x) - 2u(x-\delta) + 5u(x) - u(x+\eta) = 0, \quad x \in (0,1), \\ u(x) = 1, \quad -\delta \le x \le 0, \qquad u(x) = -1, \quad 1 \le x \le 1+\eta. \end{cases}$$

The above problem has a boundary layer near $x = 1$. The exact solution is given by

$$u(x) = \frac{(1+\exp(m_2))\exp(m_1 x) - (1+\exp(m_1))\exp(m_2 x)}{\exp(m_2) - \exp(m_1)},$$

where $m_{1,2}$ is defined earlier with $R_\varepsilon = \varepsilon + (2\delta^2 + \eta^2)/2$, $P_\varepsilon = \eta - 2\delta - 1$, $Q = 2$.

For any value of N and ε, we calculate the maximum point-wise errors E_ε^N and the ε-uniform error E^N for Examples 5.5.1 and 5.5.2 by

$$E_\varepsilon^N = \max_{0 \le j \le N} |u(x_j) - U_j| \text{ and } E^N = \max_{0 < \varepsilon \le 1} E_\varepsilon^N, \tag{5.5.1}$$

where u is the exact solution and U_j is the numerical solution. The corresponding rate of convergence is calculated by

$$r_\varepsilon^N = \log_2\left(\frac{E_\varepsilon^N}{E_\varepsilon^{2N}}\right) \text{ and } r^N = \log_2\left(\frac{E^N}{E^{2N}}\right). \tag{5.5.2}$$

In Table 5.2 and Table 5.3, we present the maximum pointwise error and the corresponding order of convergence for Example 5.5.1 and 5.5.2 respectively, which clearly shows that the proposed method is uniform convergent of order one.

Example 5.5.3. *Consider the following variable coefficient problem for $x \in \Omega$;*

$$\begin{cases} \varepsilon u''(x) - (1+\exp(x^2))u'(x) - x\exp(x)u(x-\delta) - x^2u(x) - (1-\exp(-x))u(x+\eta) = 1, \\ u(x) = 1, \quad -\delta \le x \le 0, \qquad u(x) = -1, \quad 1 \le x \le 1+\eta, \end{cases}$$

Here, this BVP has a boundary layer is at $x = 1$ and the exact solution is not known.

The exact solution is not available for Example 5.5.3. In order to calculate the maximum pointwise error G_ε^N and the rate of convergence q_ε^N, we use the interpolation as discussed in Chapter 4. The quantities G^N and q^N are defined analogously to E^N and r^N as defined in (5.5.1) and (5.5.2). The maximum pointwise error and the corresponding order of convergence for Example 5.5.3 is provided in Table 5.4.

Figure 5.2(a) represents the movement of mesh after each iteration and Figure 5.2(b) shows the final computed mesh corresponding to the solution of Example 5.5.1. It is clear from these two figures that the mesh starts to move towards the boundary layer and clusters as many points required for the layer region. Figures 5.3(a) and 5.3(b) provide the corresponding solution obtained on the adaptive grid and the error respectively. Also similar graphs are plotted for the case when boundary layer is located at the right *i.e.,* for Example 5.5.2. The Figure 5.4(a) shows the movement of the mesh towards right and Figure 5.4(b) shows the corresponding mesh while Figure 5.5 shows the computed solution along with the error.

The computational results using the adaptive mesh are also compared with the computational results using the Shishkin mesh which are shown in Table 5.5 for $\varepsilon = 1e-4$ and $\varepsilon = 1e-8$ for Example 5.5.1. From these results, one can observe that the adaptive mesh produces errors almost of the same order as produced by using the Shishkin mesh. The advantage of this approach is that without any prior knowledge of the location of the boundary layer, we are able to generate an appropriate non–uniform mesh suitable for the layer type problems. Similarly the comparison for Example 5.5.2 is also shown in Table 5.6 in the case of the right boundary layer.

In order to have proper visualization of the order of convergence, the loglog plots of the maximum error are shown in Figures 5.6(a) and 5.6(b) for Examples 5.5.1 and 5.5.2 respectively. These figures and the numerical results shown in tables help us to conclude that the proposed method is ε-uniform convergent of order one.

5.6 Conclusion

This chapter presents the convergence analysis for the first-order upwind finite difference approximation of the singularly perturbed differential-difference equation with the delay as well as the shift terms. The solution obtained on a nonuniform mesh, generated adaptively from the equidistribution principle which is done with the help of a positive monitor function depending on the

solution. The error analysis is carried out for the numerical solution and it has been shown both theoretically and computationally that the proposed scheme is ε-uniformly convergent and is of first-order accurate.

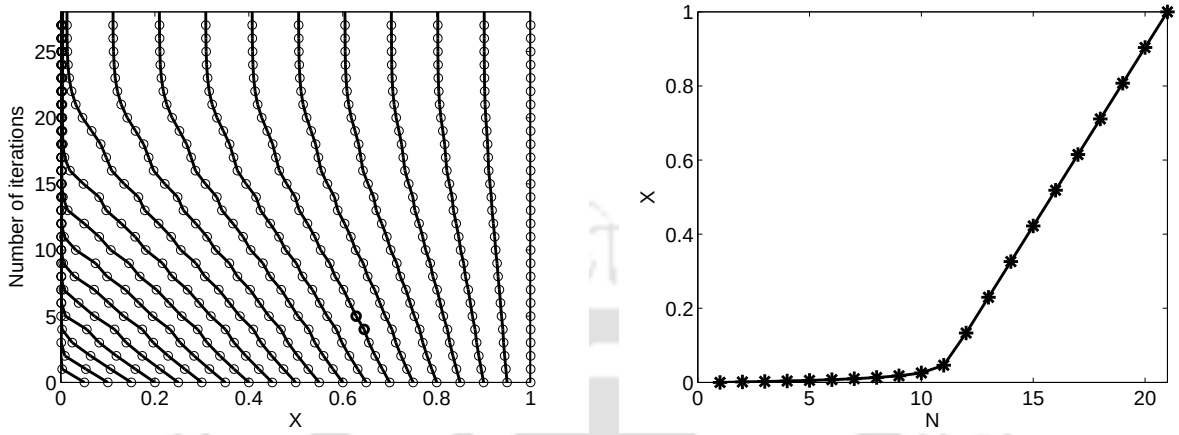

(a) Mesh movement towards left. *(b) Final computed mesh.*

Figure 5.2: *Movement of the mesh points towards left for Example 5.5.1 for* $\varepsilon = 1e-2$ *and* $N = 20$.

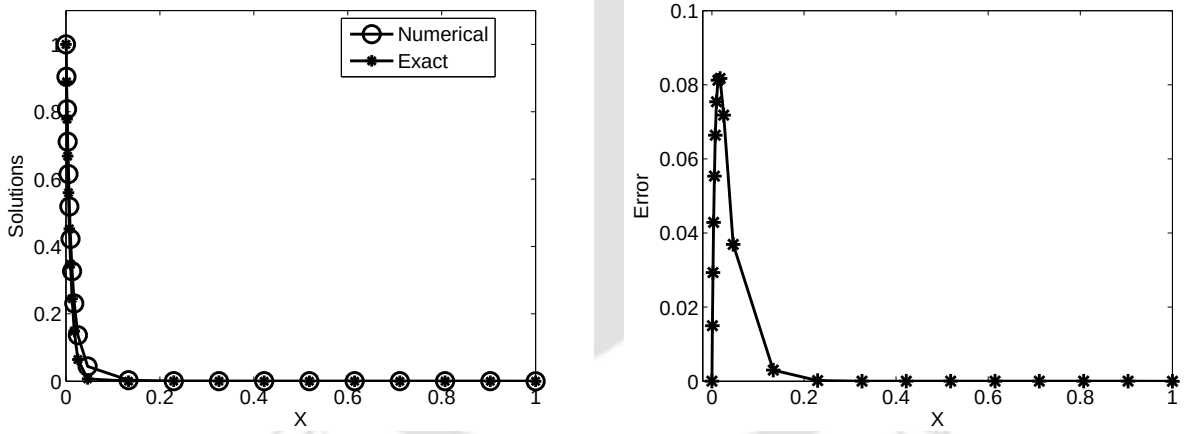

(a) Solution. *(b) Error.*

Figure 5.3: *Numerical solution with exact solution and the corresponding error of Example 5.5.1 for* $\varepsilon = 1e-2$ *and* $N = 20$.

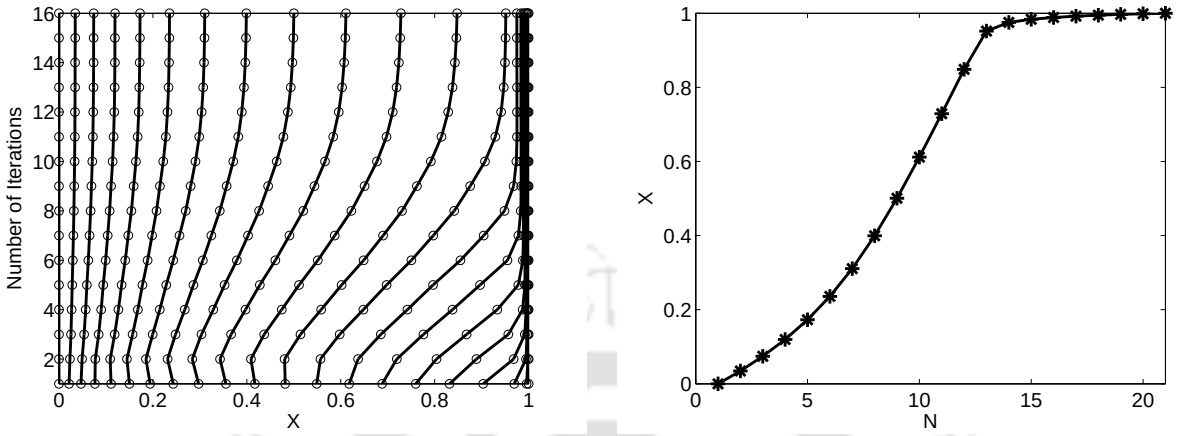

(a) Mesh movement towards right. *(b) Final computed mesh.*

Figure 5.4: *Movement of the mesh points towards right for Example 5.5.2 with* $\varepsilon = 1e-2$ *and* $N = 20$.

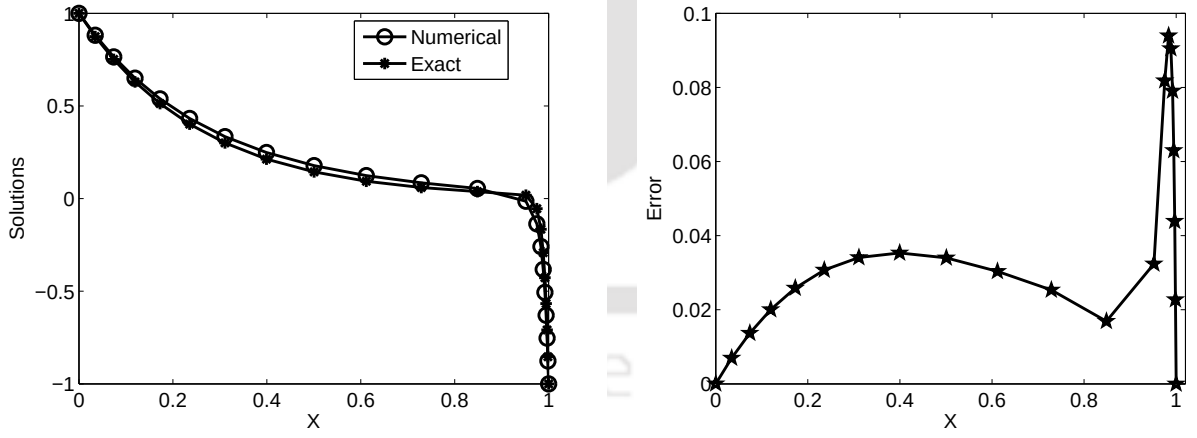

(a) Solution. *(b) Error.*

Figure 5.5: *Numerical solution with exact solution and the corresponding error of Example 5.5.2 for* $\varepsilon = 1e-2$ *and* $N = 20$.

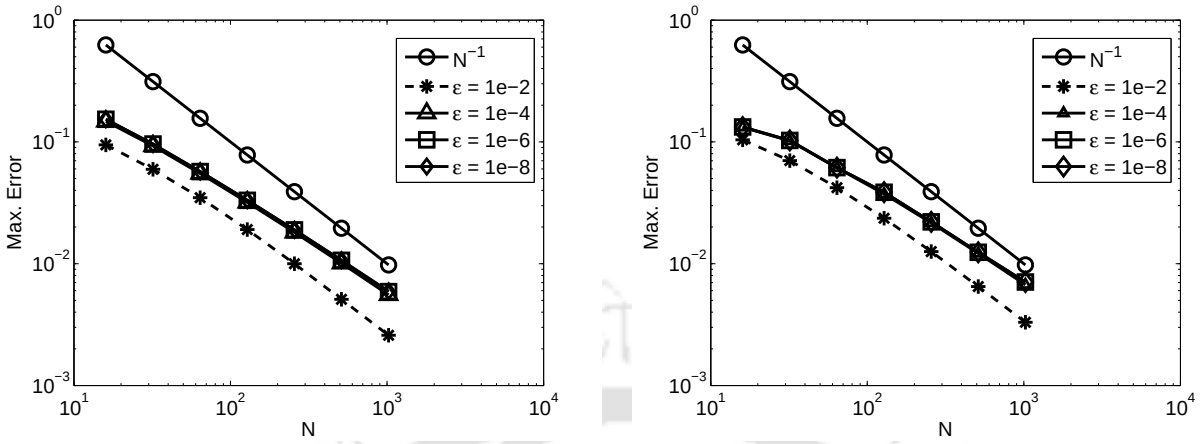

(a) Example 5.5.1. *(b) Example 5.5.2.*

Figure 5.6: *Loglog plot of the maximum error for different values of ε.*

Table 5.2: *Maximum point-wise errors E_ε^N and the rate of convergence p_ε^N for Example 5.5.1.*

ε	Number of intervals N						
	16	32	64	128	256	512	1024
$1e-0$	1.8954e-2	1.0127e-2	5.2399e-3	2.6665e-3	1.3450e-3	6.7547e-4	3.3848e-4
	0.9043	0.9506	0.9746	0.9873	0.9937	0.9968	
$1e-2$	9.4554e-2	5.9631e-2	3.4797e-2	1.9060e-2	9.9959e-3	5.0997e-3	2.5832e-3
	0.6651	0.7771	0.8684	0.9311	0.9709	0.9813	
$1e-4$	1.4746e-1	9.2545e-2	5.5074e-2	3.1902e-2	1.8077e-2	1.0086e-2	5.5420e-3
	0.6721	0.7488	0.7877	0.8195	0.8418	0.8639	
$1e-8$	1.5356e-1	9.6126e-2	5.7165e-2	3.3247e-2	1.8984e-2	1.0684e-2	5.9443e-3
	0.6758	0.7498	0.7819	0.8084	0.8293	0.8459	
$1e-10$	1.5356e-1	9.6126e-2	5.7165e-2	3.3247e-2	1.8984e-2	1.0685e-2	5.9444e-3
	0.6758	0.7498	0.7819	0.8084	0.8293	0.8459	
E^N	1.5356e-1	9.6126e-2	5.7165e-2	3.3247e-2	1.8984e-2	1.0685e-2	5.9444e-3
p^N	0.6758	0.7498	0.7819	0.8084	0.8293	0.8459	

Table 5.3: *Maximum point-wise errors E_ε^N and the rate of convergence p_ε^N for Example 5.5.2.*

ε	Number of intervals N						
	16	32	64	128	256	512	1024
$1e-0$	2.0603e-3	1.2275e-3	6.6488e-4	3.4538e-4	1.7591e-4	8.8764e-5	4.4585e-5
	0.7471	0.8845	0.9449	0.9734	0.9868	0.9934	
$1e-2$	1.0395e-1	7.0133e-2	4.2061e-2	2.3625e-2	1.2576e-2	6.4954e-3	3.3004e-3
	0.5677	0.7376	0.8321	0.9097	0.9532	0.9768	
$1e-4$	1.3205e-1	1.0180e-1	6.1182e-2	3.7373e-2	2.1588e-2	1.2143e-2	6.7179e-3
	0.3753	0.7346	0.7111	0.7918	0.8301	0.8540	
$1e-8$	1.3247e-1	1.0273e-1	6.1537e-2	3.8636e-2	2.2077e-2	1.2395e-2	7.0772e-3
	0.3668	0.7393	0.6715	0.8074	0.8328	0.8085	
$1e-10$	1.3240e-1	1.0270e-1	6.1535e-2	3.8643e-2	2.2079e-2	1.2284e-2	7.0207e-3
	0.3664	0.7390	0.6712	0.8075	0.8459	0.8071	
E^N	1.3247e-1	1.0273e-1	6.1537e-2	3.8643e-2	2.2077e-2	1.2395e-2	7.0772e-3
p^N	0.3668	0.7393	0.6712	0.8074	0.8328	0.8085	

Table 5.4: *Maximum point-wise errors G_ε^N and the rate of convergence q_ε^N for Example 5.5.3.*

ε	Number of intervals N						
	16	32	64	128	256	512	1024
$1e-0$	2.5615e-2	1.3405e-2	6.8223e-3	3.3955e-3	1.6455e-3	7.6147e-4	3.1774e-4
	0.9342	0.9745	1.0066	1.0451	1.1116	1.2609	
$1e-2$	1.5346e-1	8.9743e-2	4.6893e-2	1.9818e-2	9.8145e-3	5.3983e-3	2.5123e-3
	0.7740	0.9364	1.2426	1.0138	0.8624	1.1035	
$1e-4$	8.2696e-2	5.6596e-2	3.7338e-2	2.4148e-2	1.3842e-2	7.5110e-3	3.5319e-3
	0.5471	0.6001	0.6287	0.8028	0.8820	1.0886	
$1e-8$	1.4572e-1	6.1728e-2	4.2696e-2	2.2476e-2	1.5602e-2	6.8759e-3	2.7374e-3
	1.2392	0.5318	0.9257	0.5266	1.1821	1.3287	
$1e-10$	1.0185e-1	6.5577e-2	3.8680e-2	2.2737e-2	9.3969e-3	4.9449e-3	2.2735e-3
	0.6352	0.7616	0.7665	1.2748	0.9262	1.1210	
G^N	1.5346e-1	8.9743e-2	4.6893e-2	2.4148e-2	1.5602e-2	7.5110e-3	3.5319e-3
q^N	0.7740	0.9364	0.9575	0.6302	1.0547	1.0886	

Table 5.5: *Comparison of numerical results with the Shishkin mesh for Example 5.5.1.*

N	$\varepsilon = 1e-4$		$\varepsilon = 1e-8$	
	Shishkin mesh	**Adaptive grid**	**Shishkin mesh**	**Adaptive grid**
16	7.4585e-2	1.4746e-1	7.4959e-2	1.5356e-1
	0.4953	0.6721	0.4915	0.6758
32	5.2913e-2	9.2545e-2	5.3316e-2	9.6126e-2
	0.7042	0.7488	0.6974	0.7498
64	3.2478e-2	5.5074e-2	3.2878e-2	5.7165e-2
	0.8094	0.7877	0.7971	0.7819
128	1.8532e-2	3.1902e-2	1.8921e-2	3.3247e-2
	0.8660	0.8195	0.8434	0.8084
256	1.0168e-2	1.8077e-2	1.0545e-2	1.8984e-2
	0.9099	0.8418	0.8675	0.8293
512	5.4116e-3	1.0086e-2	5.7796e-3	1.0684e-2
	0.9624	0.8639	0.8814	0.8459
1024	2.7773e-3	5.5420e-3	3.1373e-3	5.9443e-3
	–	–	–	–

Table 5.6: *Comparison of numerical results with the Shishkin mesh for Example 5.5.2.*

N	$\varepsilon = 10^{-4}$		$\varepsilon = 10^{-8}$	
	Shishkin mesh	**Adaptive grid**	**Shishkin mesh**	**Adaptive grid**
16	7.6481e-2	1.3205e-1	7.6565e-2	1.3247e-1
	0.6858	0.3753	0.6838	0.3668
32	4.7544e-2	1.0180e-1	4.7665e-2	1.0273e-1
	0.6589	0.7346	0.6572	0.7393
64	3.0113e-2	6.1182e-2	3.0225e-2	6.1537e-2
	0.7774	0.7111	0.7744	0.6715
128	1.7568e-2	3.7373e-2	1.7671e-2	3.8636e-2
	0.8332	0.7918	0.8287	0.8074
256	9.8610e-3	2.1588e-2	9.9489e-3	2.2077e-2
	0.8639	0.8301	0.8564	0.8328
512	5.4182e-3	1.2143e-2	5.4952e-3	1.2395e-2
	0.8855	0.8540	0.8726	0.8085
1024	2.9329e-3	6.7179e-3	3.0013e-3	7.0772e-3
	–	–	–	–

Chapter 6

Richardson Extrapolation Technique for Singularly Perturbed Delay Differential Equation

Richardson extrapolation is a well-known post-processing technique where two computed solutions are approximated by an average quantity to provide better approximation. This technique is widely used because of its simple construction and it can be extended to problems in more than one dimension. It is well-known that the classical upwind scheme yields solutions that are first-order accurate. This chapter is devoted to the study of a post-processing method for solving singularly perturbed delay differential equations of the form (6.1.1) on the piecewise-uniform Shishkin mesh and to convert the almost first-order convergence of the upwind scheme to almost second-order convergence measured in the discrete supremum norm. First, the problem is solved by using the upwind finite difference scheme on the Shishkin mesh and obtain an optimal order of convergence *i.e.,* error is of the order $O(N^{-1}\ln N)$. Then, the Richardson extrapolation technique is applied on the computed solution fixing the transition parameter of the Shishkin mesh. It is proved both theoretically and computationally that the extrapolation technique improves the almost first-order convergence of the simple upwinding to almost second-order convergence.[3]

6.1 Introduction

Consider the following singularly perturbed delay differential equation

$$\begin{cases} \mathscr{L}_\varepsilon u_\varepsilon(x) \equiv -\varepsilon u_\varepsilon''(x) + a(x)u_\varepsilon'(x-\delta) + b(x)u_\varepsilon(x) = f(x), \quad x \in \Omega = (0,1), \\ u_\varepsilon(x) = \gamma(x), \quad -\delta \le x \le 0, \\ u_\varepsilon(1) = \lambda\,, \end{cases} \tag{6.1.1}$$

where $0 < \varepsilon \ll 1$ is a small parameter and the delay parameter δ is such that $0 < \delta \ll 1$, which is of $o(\varepsilon)$. The functions $a(x), b(x), f(x)$ and $\gamma(x)$ are sufficiently smooth and λ is a given constant.

[3]Some portion of this chapter is published in *Neural Parallel Sci. Comput., Vol-16, pp.353-370, 2008.*

It is also assumed that $b(x) \geq 0, \forall x \in \overline{\Omega}$. Depending upon the sign of $a(x)$, *i.e.,* if $a(x) > 0$ (or $a(x) < 0$), a boundary layer is located at right (or left) end of the domain. The layer is maintained for sufficiently small δ with $\delta \neq 0$ and $\delta = o(\varepsilon)$.

Without loss of generality, we will assume that $a(x) > 0$. When $\delta \equiv 0$, the equation (6.1.1) reduces to a singularly perturbed differential equation with boundary layer at $x = 1$ and one can follow the standard procedure of singular perturbation analysis to find the solution in this case.

For $\delta = \kappa\varepsilon > 0$, where κ is sufficiently small, the technique discussed in Chapter 4 is followed. Expanding the delay term through Taylor's series expansion, we have

$$u'_\varepsilon(x-\delta) = u'_\varepsilon(x) - \delta u''_\varepsilon(x) + \ldots, \quad \text{as } \delta \to 0. \tag{6.1.2}$$

Now, using the leading two terms of the expansion (6.1.2) in (6.1.1), we obtain the following BVP:

$$\begin{cases} L_\varepsilon u(x) \equiv -\big(\varepsilon + \delta a(x)\big)u''(x) + a(x)u'(x) + b(x)u(x) = f(x), & x \in \Omega = (0,1) \\ u(x) = \gamma(x), \qquad -\delta \leq x \leq 0, \\ u(1) = \lambda\,. \end{cases} \tag{6.1.3}$$

Here, we assume that

$$2\alpha^* \geq a(x) > 2\alpha > 0 \quad \text{and} \quad \big(\varepsilon + \delta a(x)\big) > 0, \qquad \forall x \in \overline{\Omega}.$$

Under these assumptions, the BVP (6.1.3) has a unique solution exhibiting the layer on the right side of the domain at $x = 1$.

It is worthwhile to mention that the BVP (6.1.3) is an approximate differential equation of the original BVP (6.1.1). In Chapter 4, we have already proved that the expansion (6.1.2) is a valid expansion. Through the asymptotic approach and by proposing a direct numerical scheme, it has been shown both asymptotically and numerically that the solution $u(x)$ of (6.1.3) provides a leading order approximation to the solution $u_\varepsilon(x)$ of (6.1.1) which differs by a term $O(\varepsilon)$ for sufficiently small value of δ. Hence, the same argument is valid here. One can refer Chapter 4 for more details.

Kadalbajoo and Ramesh [39] applied the upwind finite difference scheme on the piecewise-uniform Shishkin mesh for solving the BVP (6.1.3) and shown $O(N^{-1}\ln^2 N)$ as the order of convergence which is not optimal. Further, they used a hybrid finite difference scheme to increase the order of convergence from almost first-order to almost second-order. Here, our aim is to provide an *optimal* order of convergence *i.e.,* approximation of the order $O(N^{-1}\ln N)$ by applying the upwind scheme on the Shishkin mesh for the BVP (6.1.3). Then, through a simple post-processing technique to enhance the rate of convergence of the order $O(N^{-2}\ln^2 N)$.

This chapter is organized as follows. Section 6.2 establishes the maximum principle, stability result and some a priori estimates on the solution and its derivatives of the BVP (6.1.3). Section 6.3

presents the upwind finite difference scheme and the convergence of the standard upwind method where we obtain the error *i.e.,* $O(N^{-1}\ln N)$ which is optimal for the BVP of type (6.1.3). In Section 6.4, the Richardson extrapolation is applied on the computed solution and it is proved that the extrapolated solution is almost second-order convergent measured in maximum norm. Finally, some numerical examples are provided in Section 6.5 to illustrate the applicability of the present method and the maximum point-wise error and the corresponding rate of convergence are shown in terms of tables and figures.

6.2 Continuous Problem

This section presents the maximum principle, the stability estimate and *a priori* bounds on the analytical solution of the BVP (6.1.3) and its derivatives. Also, a decomposition of the solution $u(x)$ into regular and singular components and their bounds are discussed in this section.

6.2.1 Properties of the solution and its derivatives

Lemma 6.2.1. (Maximum Principle) *Let $\mathcal{V}$ be a smooth function satisfying $\mathcal{V}(0) \geq 0$, $\mathcal{V}(1) \geq 0$ and $L_\varepsilon \mathcal{V}(x) \geq 0$ $\forall x \in \Omega$. Then $\mathcal{V}(x) \geq 0$, $\forall x \in \overline{\Omega}$.*

Proof. Let $x^* \in \overline{\Omega}$ be such that $\mathcal{V}(x^*) = \min_{x\in\overline{\Omega}} \mathcal{V}(x)$ and assume that $\mathcal{V}(x^*) < 0$. Clearly $x^* \notin \{0,1\}$ and $\mathcal{V}'(x^*) = 0$ and $\mathcal{V}''(x^*) \geq 0$. Now consider

$$L_\varepsilon \mathcal{V}(x^*) \equiv -\big(\varepsilon + \delta a(x^*)\big)\mathcal{V}''(x^*) + a(x^*)\mathcal{V}'(x^*) + b(x^*)\mathcal{V}(x^*) < 0,$$

which contradicts our assumption. Hence, $\mathcal{V}(x) \geq 0, \forall x \in \overline{\Omega}$. ∎

An immediate consequence of the maximum principle is the following stability estimate.

Lemma 6.2.2. *If u is the solution of the boundary value problem (6.1.3), then*

$$\|u\| \;\leq\; \frac{1}{\alpha}\|f\| + \max\{|u(0)|, |\lambda|\}. \tag{6.2.1}$$

Proof. Let us consider the following barrier function

$$\psi^{\pm}(x) = \frac{1+x}{2\alpha}\|f\| + \max\{|u(0)|, |\lambda|\} \pm u(x).$$

It easy to show that $\psi^{\pm}(x)$ is non–negative at $x = 0, 1$. Now from (6.1.3)

$$\begin{aligned}
L_\varepsilon \psi^{\pm}(x) &= -(\varepsilon + \delta a(x))\big(\psi^{\pm}(x)\big)'' + a(x)\big(\psi^{\pm}(x)\big)' + b(x)\psi^{\pm}(x) \\
&= \frac{a(x)}{2\alpha}\|f\| + b(x)\left[\frac{1+x}{2\alpha}\|f\| + \max\{|\gamma(0)|, |\lambda|\}\right] \pm L_\varepsilon u(x) \\
&\geq \frac{a(x)}{2\alpha}\|f\| \pm f(x) \\
&\geq 0.
\end{aligned}$$

Thus by applying the maximum principle as given in Lemma 6.2.1, we can conclude that $\psi^{\pm}(x) \geq 0, \forall x \in \overline{\Omega}$ and hence the required result. ∎

Lemma 6.2.3. *Let $0 \leq k \leq 5$ be a positive integer. Assume that $f \in \mathcal{C}^k[0,1]$, then the derivatives $u^{(k)}$ of the solution u of (6.1.3) satisfy the following bound*

$$|u^{(k)}| \leq C\left[1 + (\varepsilon + \delta\alpha)^{-k} \exp\left(\frac{-\alpha(1-x)}{\varepsilon + \delta\alpha}\right)\right], \tag{6.2.2}$$

where C depends on $\|a\|$, $\|a'\|$, $\|b\|$, $\|b'\|$ and on the boundary conditions.

Proof. For $0 \leq k \leq 3$, the detailed proofs are similar to the proofs given in Chapter 4. By differentiating (6.1.3) twice and following the same argument given in Chapter 4, one can obtain the result for $k = 4, 5$. ∎

6.2.2 Solution decomposition

To show that a numerical method is ε–uniform convergent, some prior information of the solution are required. Let us decompose the solution of (6.1.3) into regular and singular parts as follows:

$$u(x) = v(x) + w(x).$$

Now $v(x)$ can be written in an asymptotic expansion as

$$v(x) = v_0(x) + (\varepsilon + \delta\alpha)v_1(x) + (\varepsilon + \delta\alpha)^2 v_2(x),$$

where v_0, v_1 and v_2 are defined as the solution of the following differential equations:

$$\begin{cases} a(x)v_0'(x) + b(x)v_0(x) = f(x), & v_0(0) = u(0), \\ a(x)v_1'(x) + b(x)v_1(x) = (\varepsilon + \delta a(x))v_0''(x)/(\varepsilon + \delta\alpha), & v_1(0) = 0, \\ L_\varepsilon v_2(x) = (\varepsilon + \delta a(x))v_1''(x)/(\varepsilon + \delta\alpha), & v_2(0) = 0, v_2(1) = 0. \end{cases} \tag{6.2.3}$$

Hence the regular component v satisfies the BVP

$$L_\varepsilon v(x) = f(x), \quad v(0) = v_0(0) + (\varepsilon + \delta\alpha)v_1(0) = u(0),\ v(1) = u(1), \tag{6.2.4}$$

and the layer component satisfies

$$L_\varepsilon w(x) = 0, \quad w(0) = 0,\ |w(1)| \leq C. \tag{6.2.5}$$

Lemma 6.2.4. *Let $u(x)$ be the solution of (6.1.3) and $u(x) = v(x) + w(x)$. For sufficiently small ε and $0 \leq k \leq 4$, the derivatives of $v(x)$ and $w(x)$ satisfy the following bounds:*

$$\|v^{(k)}\| \leq C\big(1 + (\varepsilon + \delta\alpha)^{3-k}\big), \tag{6.2.6}$$

$$|w^{(k)}(x)| \leq C\big(\varepsilon + \delta\alpha\big)^{-k} \exp\left(\frac{-\alpha(1-x)}{\varepsilon + \delta\alpha}\right), \quad x \in \overline{\Omega}. \tag{6.2.7}$$

Proof. From (6.2.3), we observe that v_0 is independent of ε and δ. Similarly, v_1 involves the quantity $(\varepsilon + \delta a(x))/(\varepsilon + \delta\alpha)$ which is bounded above as $a(\cdot)$ is bounded in Ω. Again, v_2 is the solution of the class of problem similar to (6.1.3) and hence, using Lemma 6.2.3 for $0 \le k \le 3$, we have the bounds

$$\|v^{(k)}\| \le C\big(1 + (\varepsilon + \delta\alpha)^{3-k}\big).$$

For $k = 4$, one can write $\Big((\varepsilon + \delta a(x))v''(x)\Big)'' = \Big(b(x)v(x) + a(x)v'(x) - f(x)\Big)''$ which leads to the bound $\|v^{(4)}\| \le C(\varepsilon + \delta\alpha)^{-1}$.

To obtain the required bound on $w(x)$ and its derivatives, we consider the barrier function

$$\psi^{\pm}(x) = C\exp\left(\frac{-\alpha(1-x)}{\varepsilon + \delta\alpha}\right) \pm w(x).$$

It is easy to show that $\psi^{\pm}$ is nonnegative at $x = 0, 1$. Using (6.2.2), we have

$$L_\varepsilon\psi^{\pm}(x) = \left(\frac{C\alpha}{\varepsilon + \delta\alpha}\right)\left[a(x) - \frac{\alpha(\varepsilon + \delta a(x))}{\varepsilon + \delta\alpha} + \frac{\varepsilon + \delta\alpha}{C\alpha}b(x)\right] \ge 0.$$

Thus by applying the maximum principle of Lemma 6.2.1, we can conclude that $\psi^{\pm}(x) \ge 0$. From this result, we can obtain the required pointwise bound on $w(x)$ and its derivatives. ∎

6.3 Discrete Problem

This section contains the piecewise-uniform Shishkin mesh, the upwind scheme and the convergence analysis of the upwind scheme on the Shishkin mesh. It also provides a few technical results which are used later in deriving the error estimate of the extrapolation method.

6.3.1 The Shishkin mesh

To solve the BVP (6.1.3) numerically, the piecewise-uniform Shishkin mesh is used. This mesh has a transition point $1 - \sigma$, where

$$\sigma = \min\left\{\frac{1}{2}, \frac{2(\varepsilon + \delta\alpha)}{\alpha}\ln N\right\}.$$

Now divide the subinterval $[0, 1-\sigma]$ into $N/2$ equal subdivisions of width H, where $H = 2(1-\sigma)/N$. Similarly divide the subinterval $(1-\sigma, 1]$ into $N/2$ equal subdivisions of width h, where $h = 2\sigma/N = 4(\varepsilon + \delta\alpha)\ln N/\alpha N$. Then the Shishkin mesh $\Omega_{N,\sigma} = \{x_i\}_{i=0}^{N}$, where $x_0 = 0, x_N = 1$ and the mesh width $h_i := x_i - x_{i-1}$ satisfy $h_i = H$ for $i = 1, \ldots, N/2$ and $h_i = h$ for $i = N/2 + 1, \ldots, N$. Here the piecewise-uniform mesh is entirely determined by the two chosen parameters N and σ.

6.3.2 The upwind scheme

The upwind finite difference scheme for (6.1.3) takes the form

$$\begin{cases} L_\varepsilon^N U_i^N \equiv -(\varepsilon + \delta a_i) D^+ D^- U_i^N + a_i D^- U_i^N + b_i U_i^N = f_i\,, \quad 1 \le i \le N-1, \\ U_0^N = \gamma(0) = \gamma_0, \quad U_N^N = \lambda\,, \end{cases} \tag{6.3.1}$$

where U_i^N denotes the approximation of $u(x_i)$, $a_i = a(x_i)$ and b_i, f_i are defined in a similar fashion. Equation (6.3.1) can be expressed in the following form of system of algebraic equations

$$\begin{cases} -r_i^- U_{i-1}^N + r_i^c U_i^N - r_i^+ U_{i+1}^N = f_i, \quad i = 1, \ldots, N-1, \\ U_0^N = \gamma_0, \quad U_N^N = \lambda\,, \end{cases} \tag{6.3.2}$$

where

$$r_i^- = \frac{2(\varepsilon + \delta a_i)}{h_i(h_i + h_{i+1})} - \frac{a_i}{h_i}, \quad r_i^c = \frac{2(\varepsilon + \delta a_i)}{h_i h_{i+1}} + \frac{a_i}{h_i} + b_i, \quad r_i^+ = \frac{2(\varepsilon + \delta a_i)}{h_{i+1}(h_i + h_{i+1})}\ .$$

One can easily see that

$$r_i^- > 0,\ r_i^+ > 0 \quad \text{and} \quad r_i^c + r_i^- + r_i^+ \ge 0, \quad \text{for} \quad i = 1, \ldots, N-1, \tag{6.3.3}$$

which imply that the stiffness matrix is an M–matrix.

Lemma 6.3.1. (Discrete Comparison Principle) *The system of equations $L_\varepsilon^N \mathcal{V}_j = F_j$ for given $\mathcal{V}_0$ and $\mathcal{V}_N$ has a unique solution. If $L_\varepsilon^N \mathcal{V}_j < L_\varepsilon^N \mathcal{Z}_j$ for $1 \le j \le N-1$ with $\mathcal{V}_0 < \mathcal{Z}_0$ and $\mathcal{V}_N < \mathcal{Z}_N$, then $\mathcal{V}_j < \mathcal{Z}_j$ for $1 \le j \le N$.*

Proof. From (6.3.3), it is clear that the matrix associated with the discrete operator L_ε^N is an irreducible M-matrix and therefore has a positive inverse. Hence, the result follows. ∎

6.3.3 Convergence of the upwind scheme

The local truncation error of the difference scheme (6.3.1) at the node x_i is given by

$$\tau_i = L_\varepsilon^N U_i^N - (L_\varepsilon u)(x_i), \tag{6.3.4}$$

where u and U_i^N denote the exact solution of (6.1.3) and (6.3.1) respectively.

Using Taylor series expansion, the truncation error (6.3.4) can be expressed as

$$\tau_i = \frac{-2(\varepsilon + \delta a_i)}{h_i + h_{i+1}} \left[\frac{1}{h_{i+1}} \int_{x_i}^{x_{i+1}} (s - x_{i+1})^2 u'''(s) ds - \frac{1}{h_i} \int_{x_{i-1}}^{x_i} (s - x_{i-1})^2 u'''(s) ds \right] + \\ + \frac{a_i}{h_i} \int_{x_{i-1}}^{x_i} (x_{i-1} - s) u''(s) ds, \tag{6.3.5}$$

from which we obtain the bound

$$|\tau_i| < (\varepsilon + \delta\alpha)\int_{x_{i-1}}^{x_{i+1}} |u'''(s)|ds + C\int_{x_{i-1}}^{x_{i+1}} |u''(s)|ds. \tag{6.3.6}$$

The following theorem provides the *optimal* order error estimate of the upwind scheme on the Shishkin mesh.

Theorem 6.3.2. *Let u be the solution of the BVP (6.1.3) and U^N be the solution of (6.3.1) computed on $\Omega_{N,\sigma}$. Then we have the following ε–uniform convergence result:*

$$|U^N - u(x_i)| \leq CN^{-1}\ln N, \quad \forall x_i \in [0,1].$$

Proof. The discrete solution U^N is decomposed as $U^N = V^N + W^N$, where V^N is the solution of the BVP

$$L_\varepsilon^N V^N = f, \quad V_0^N = v(0),\ V_N^N = v(1), \tag{6.3.7}$$

and W^N is the solution of the following BVP

$$L_\varepsilon^N W^N = 0, \quad W_0^N = w(0),\ W_N^N = w(1). \tag{6.3.8}$$

Now the error can be written as $(U^N - u)(x_i) = (V^N - v)(x_i) + (W^N - w)(x_i)$. We will find out the error of the individual components in the two different region $[0, 1-\sigma]$ and $(1-\sigma, 1]$. Now

$$\begin{aligned} L_\varepsilon^N(V^N - v)(x_i) &= f(x_i) - L_\varepsilon^N v(x_i) \\ &= L_\varepsilon v(x_i) - L_\varepsilon^N v(x_i) \\ &= (L_\varepsilon - L_\varepsilon^N)v(x_i) \\ &= -(\varepsilon + \delta a(x_i))\left(\frac{d^2}{dx^2} - D^+D^-\right)v(x_i) + a(x_i)\left(\frac{d}{dx} - D^-\right)v(x_i). \end{aligned} \tag{6.3.9}$$

Now using bound as given in Lemma 2.5.1 of Chapter 2 in (6.3.9), we have

$$L_\varepsilon^N(V^N - v)(x_i) \leq (x_{i+1} - x_{i-1})\left(\frac{\varepsilon + \delta a(x_i)}{3}\right)\|v'''\| + \frac{a(x_i)}{2}\|v''\|. \tag{6.3.10}$$

Since $(x_{i+1} - x_{i-1}) \leq 2N^{-1}$ and using the bounds of $\|v'''\|$ and $\|v''\|$ given in Lemma 6.2.4, we obtain that

$$L_\varepsilon^N(V^N - v)(x_i) \leq CN^{-1}, \quad \forall x_i \in \Omega_{N,\sigma}. \tag{6.3.11}$$

Applying the discrete comparison principle as given in Lemma 6.3.1 to the function $(V^N - v)(x_i)$, we have

$$|(V^N - v)(x_i)| \leq C \max_{1\leq i\leq N-1} |L_\varepsilon^N(V^N - v)(x_i)|,$$

and hence

$$|(V^N - v)(x_i)| \leq CN^{-1}. \tag{6.3.12}$$

Now we have to find the error in the singular component. Without loss of generality, assume that $\sigma = 2(\varepsilon + \delta\alpha)\ln N/\alpha < 1/2$. Applying the same argument as we did for the regular part, we will reach at

$$|L_\varepsilon^N(W^N - w)(x_i)| \leq (x_{i+1} - x_{i-1})\left(\frac{\varepsilon + \delta a(x_i)}{3}\right)\|w'''\| + \frac{a(x_i)}{2}\|w''\|\,.$$

From the bound of the derivative of $w(x)$ as given in Lemma 6.2.4, we have

$$(\varepsilon + \delta a(x_i))|w'''(x)| \leq |w''(x)|\,.$$

On simplification,

$$|L_\varepsilon^N(W^N - w)(x_i)| \leq C(x_{i+1} - x_{i-1})\|w''\|\,.$$

Now using the bound of $w''(x)$ given in (6.2.7), we have

$$|w''(x_i)| \leq C(\varepsilon + \delta\alpha)^{-2}\exp(-\alpha(1-x)/(\varepsilon + \delta\alpha))\,.$$

Substituting $1 - x = 2(\varepsilon + \delta\alpha)\phi(t)$, where the mesh generating function ϕ is piecewise continuously differentiable for some arbitrary $t \in [x_{i-1}, x_{i+1}]$ on the fine part of the mesh as defined in [83], we obtain

$$|L_\varepsilon^N(W^N - w)(x_i)| \leq C(\varepsilon + \delta\alpha)^{-2}\int_{x_{i-1}}^{x_{i+1}}\exp(-2\phi(t))\phi'(t)dt.$$

Again, we have $x_i - x_{i-1} = h_i = 2(\varepsilon + \delta\alpha)N^{-1}\ln N$. Therefore,

$$\begin{aligned}\exp(-\phi(t)) \leq \exp(-(1-x_{i-1})/2(\varepsilon+\delta\alpha)) &\leq \exp(-(1-x_i)/2(\varepsilon+\delta\alpha))\exp(h_i/2(\varepsilon+\delta\alpha)) \\ &\leq C\exp(-(1-x_i)/2(\varepsilon+\delta\alpha)).\end{aligned}$$

Hence,

$$|L_\varepsilon^N\left(W^N - w\right)(x_i)| \leq C(\varepsilon + \delta\alpha)^{-1}N^{-1}\ln N\int_{x_{i-1}}^{x_{i+1}}\exp(-(1-x_i)/2(\varepsilon+\delta\alpha))dx.$$

Thus, by applying the discrete comparison principle as given in Lemma 6.3.1, we obtain

$$|\left(W^N - w\right)(x_i)| \leq CN^{-1}\ln N\,. \tag{6.3.13}$$

Now combining the error bounds of the regular component given in (6.3.12) and the singular component given in (6.3.13), we get the required result. ∎

Before moving to the extrapolation analysis, here two more lemmas are provided which are needed in the next section.

For $i = 0, 1, \ldots, N$, define the mesh functions on $\Omega_{N,\sigma}$ as

$$S_0 = \bar{S}_0 = 1, \quad S_i = \prod_{j=1}^{i}\left(1 + \frac{\alpha h_j}{\varepsilon + \delta\alpha}\right), \quad \bar{S}_j = \prod_{j=1}^{i}\left(1 + \frac{\alpha h_j}{2(\varepsilon + \delta\alpha)}\right). \tag{6.3.14}$$

Lemma 6.3.3. *There exists a positive constant C_2 such that for $i = 1, \ldots, N-1$,*

$$L_\varepsilon^N S_i \geq \frac{C_2}{\varepsilon + \delta\alpha + \alpha h_i} S_i \quad \text{and} \quad L_\varepsilon^N \bar{S}_i \geq \frac{C_2}{2(\varepsilon + \delta\alpha) + \alpha h_i} \bar{S}_i \,. \tag{6.3.15}$$

Moreover, we can get a positive constant C_3 such that for which $i = N/2+1, \ldots, N-1$, we have

$$L_\varepsilon^N S_i \geq C_3(\varepsilon + \delta\alpha)^{-1} S_i \quad \text{and} \quad L_\varepsilon^N \bar{S}_i \geq C_3(\varepsilon + \delta\alpha)^{-1} \bar{S}_i \,. \tag{6.3.16}$$

Proof. Define $\widehat{S}_i = \prod_{j=1}^{i} \left(1 + \frac{\bar{\alpha} h_j}{\varepsilon + \delta\alpha}\right)$, where $\bar{\alpha}$ can be either α or $\alpha/2$. Now

$$\begin{aligned} L_\varepsilon^N \widehat{S}_i &= -\frac{2(\varepsilon + \delta a_i)}{h_i + h_{i+1}} \left[\frac{\widehat{S}_{i+1} - \widehat{S}_i}{h_{i+1}} - \frac{\widehat{S}_i - \widehat{S}_{i-1}}{h_i}\right] + a_i \left[\frac{\widehat{S}_i - \widehat{S}_{i-1}}{h_i}\right] + b_i \widehat{S}_i \\ &\geq \left(\frac{\varepsilon + \delta a(x_i)}{\varepsilon + \delta\alpha + \bar{\alpha} h_i}\right)\left(a_j \bar{\alpha} - 2\bar{\alpha}^2 \widehat{S}_j\right) \\ &\geq \frac{C_2}{\varepsilon + \delta\alpha + \bar{\alpha} h_i} \widehat{S}_j \,. \end{aligned}$$

for some C_2, since $a(x) \geq 2\alpha \geq 2\bar{\alpha}$ and $h = O(\varepsilon)$. Hence the required results (6.3.15) and (6.3.16) are obtained. ∎

Lemma 6.3.4. *Let $\Omega_{N,\sigma} = \{x_i\}_{i=0}^N$ with $h_i = x_i - x_{i-1}$. Then there exists a positive constant C_4 such that*

$$N^{-1} \leq \prod_{j=N/2+1}^{N} \left(1 + \frac{\alpha h_j}{2(\varepsilon + \delta\alpha)}\right)^{-1} \leq C_4 N^{-1} \quad \text{and} \quad \prod_{j=N/2+1}^{N} \left(1 + \frac{\alpha h_j}{\varepsilon + \delta\alpha}\right)^{-1} \leq C_4 N^{-2}. \tag{6.3.17}$$

Proof. We have

$$\prod_{j=N/2+1}^{N} \left(1 + \frac{\alpha h_j}{2(\varepsilon + \delta\alpha)}\right)^{-1} = \left(1 + \frac{2\ln N}{N}\right)^{-N/2} \leq C_4 N^{-1} \,.$$

Using the inequality $\ln(1+x) \leq x - x^2/4$ for $0 \leq x \leq 1$, we have

$$\ln\left[\prod_{j=N/2+1}^{N} \left(1 + \frac{\alpha h_j}{2(\varepsilon + \delta\alpha)}\right)^{-1}\right] = \ln\left(1 + \frac{2\ln N}{N}\right)^{-N/2} \geq -\ln N + \frac{\ln^2 N}{2N},$$

and hence the first inequality holds. The proof of the second inequality is given in [92]. ∎

6.4 Richardson Extrapolation Technique

The main goal of this chapter is to improve the accuracy of the upwind scheme which can be obtained *via* the Richardson extrapolation. The solution U^N is computed on the mesh $\Omega_{N,\sigma}$. Now we can solve the same problem on $\Omega_{2N,\sigma} = \{\widetilde{x}_i\}_{i=0}^{2N}$ with $2N$ number of subintervals by keeping the

same transition point $1-\sigma$. Thus on $\Omega_{2N,\sigma}$: $\widetilde{x}_i - \widetilde{x}_{i-1} = H/2$ for $\widetilde{x}_i \in [0, 1-\sigma]$ and $\widetilde{x}_i - \widetilde{x}_{i-1} = h/2$ for $\widetilde{x}_i \in (1-\sigma, 1]$. From Theorem 6.3.2, we know that

$$U^N(x_i) - u(x_i) = C_5 N^{-1} \ln N + R_N(x_i) = C_5 N^{-1} \left(\frac{\alpha\sigma}{2(\varepsilon + \delta\alpha)} \right) + R_N(x_i), \ \forall x_i \in \Omega_{N,\sigma}, \quad (6.4.1)$$

where C_5 is a fixed constant and the remainder R_N is of $o(N^{-1} \ln N)$. Similarly, one can have

$$U^{2N}(x_i) - u(x_i) = C_5 (2N)^{-1} \left(\frac{\alpha\sigma}{2(\varepsilon + \delta\alpha)} \right) + R_{2N}(x_i), \quad \forall x_i \in \Omega_{2N,\sigma}, \quad (6.4.2)$$

where U^{2N} denotes the solution of discrete problem (6.3.1) on $\Omega_{2N,\sigma}$ and the remainder R_{2N} is of $o(N^{-1} \ln N)$. Eliminating the first term (which is of $O(N^{-1})$) from the above two equations, we obtain

$$u(x_i) - (2U^{2N}(x_i) - U^N(x_i)) = R_N(x_i) - R_{2N}(x_i) = o(N^{-1} \ln N), \quad \forall x_i \in \Omega_{N,\sigma}. \quad (6.4.3)$$

That is, $(2U^{2N}(x_i) - U^N(x_i))$ is a better approximation of $u(x_i)$ which is more accurate than $U^N(x_i)$ and $U^{2N}(x_i)$ on $\Omega_{N,\sigma}$. Hence, we use the extrapolation formula

$$(2U^{2N}(x_i) - U^N(x_i)) \quad \text{for } x_i \in \Omega_{N,\sigma}. \quad (6.4.4)$$

From the decomposition of the solution U^N on $\Omega_{N,\sigma}$ given in (6.3.7) and (6.3.8), one can set

$$U^N - u = (V^N - v) + (W^N - w) \quad \text{and} \quad U^{2N} - u = (V^{2N} - v) + (W^{2N} - w).$$

Let $\xi(x) = a(x)v''(x)/2$, $\forall x \in [0, 1]$. The following lemma provides the bound of the truncation error of v.

Lemma 6.4.1. *Under the assumption $\varepsilon \leq CN^{-1}$ and for all $x_i \in (0, 1)$, we have*

$$L_\varepsilon^N (V^N - v)(x_i) = \xi(x_i) h_i + O(H^2).$$

Proof. From Lemma 6.2.4, we know that $|v'''| \leq C$. Now using the assumption $\varepsilon \leq N^{-1} \leq H$ and Lemma 2.5.1 given in Chapter 2, we can prove this lemma. ∎

For all $x \in (0, 1)$, define the function $E(x)$ as the solution of the BVP

$$L_\varepsilon E(x) = \xi(x), \quad E(0) = E(1) = 0. \quad (6.4.5)$$

One can decompose E as $E = \eta + \vartheta$, where η, ϑ are the smooth and layer parts of E. Now using Lemma 6.2.4, we have the following bounds:

$$|\eta^{(k)}(x)| \leq C(1 + (\varepsilon + \delta\alpha)^{2-k}), \qquad 0 \leq k \leq 3, \quad (6.4.6)$$

$$|\vartheta^{(k)}(x)| \leq C(\varepsilon + \delta\alpha)^{-k}) \exp(-\alpha(1-x)/(\varepsilon + \delta\alpha)), \quad 0 \leq k \leq 3, \quad (6.4.7)$$

with $x \in \Omega$

$$\begin{cases} L_\varepsilon \eta(x) = \xi(x), \quad \eta(0) = \vartheta(0) = 0, \\ L_\varepsilon \vartheta(x) = 0, \qquad \eta(1) = -\vartheta(1). \end{cases} \tag{6.4.8}$$

In the following lemma, we determine the error in the smooth part V^N.

Lemma 6.4.2. *We have*

$$V^N(x_i) - v(x_i) = HE(x_i) + O(N^{-2}), \quad \forall x_i \in [0, 1-\sigma].$$

Proof. Fix $x_i \in (0,1)$. Now from the truncation error, we have

$$L_\varepsilon^N \eta(x_i) = L_\varepsilon \eta(x_i) + L_\varepsilon^N \eta(x_i) - L_\varepsilon \eta(x_i) = L_\varepsilon \eta(x_i) + O(H).$$

So

$$HL_\varepsilon^N \eta(x_i) = H\xi(x_i) + O(H^2).$$

Using the fact that $h_i \le H$, Lemma 6.4.1 yields

$$\begin{aligned} L_\varepsilon^N (V^N - v - H\eta)(x_i) &= \begin{cases} O(H^2), & x_i \in (0, 1-\sigma) \\ (h-H)\xi(x_i) + O(H^2), & x_i \in (1-\sigma, 1), \end{cases} \\ &= \begin{cases} O(H^2), & x_i \in (0, 1-\sigma) \\ O(H), & x_i \in (1-\sigma, 1). \end{cases} \end{aligned} \tag{6.4.9}$$

Define the mesh function

$$Z_i = C_6 \left[N^{-2}(1+x_i) + H\bar{S}_i \prod_{j=1}^{N} \left(1 + \frac{\alpha h_j}{2(\varepsilon + \delta\alpha)} \right)^{-1} \right], \quad \text{for } i = 0, \ldots, N,$$

where the constant C_6 has to be determined later. Then

$$L_\varepsilon^N Z_i \ge C_6 \left[2\alpha N^{-2} + H \prod_{j=1}^{N} \left(1 + \frac{\alpha h_j}{2(\varepsilon + \delta\alpha)} \right)^{-1} L_\varepsilon^N \bar{S}_i \right], \quad \text{for } i = 1, \ldots, N-1.$$

Using (6.3.15) and $\varepsilon \le N^{-1}$ for $0 < i \le N/2$, it follows that

$$L_\varepsilon^N Z_i \ge C_6 \alpha N^{-2} \ge C_6 \alpha H^2/4, \tag{6.4.10}$$

and for $0 < i \le N/2$,

$$L_\varepsilon^N Z_i \ge C_6 C_3 H (\varepsilon + \delta\alpha)^{-1} \prod_{j=1}^{N} \left(1 + \frac{\alpha h_j}{2(\varepsilon + \delta\alpha)} \right)^{-1} \ge C_6 C_3 H. \tag{6.4.11}$$

It is easy to check that $Z_0 \geq 0 = |V^N(0) - v(0) - H\eta(0)|$ and $Z_N \geq C_5 = |V^N(1) - v(1) - H\eta(1)|$. If we choose sufficiently large C_5, then Z_i plays the role of a barrier function for $\pm[V^N(x_i) - v(x_i) - H\eta(x_i)]$. Hence, by using the discrete comparison principle as given in Lemma 6.3.1 on Z_i, we have

$$Z_i \geq V^N(x_i) - v(x_i) - H\eta(x_i), \quad \forall x_i \in (0, 1-\sigma).$$

But for $i = 1, \ldots, N/2$, we have from (6.3.17),

$$Z_i \leq C_6\left[2\alpha N^{-2} + H\prod_{j=1}^{N}\left(1 + \frac{\alpha h_j}{2(\varepsilon + \delta\alpha)}\right)^{-1}\right] \leq C\left(N^{-2} + hN^{-1}\right) \leq CN^{-2}. \tag{6.4.12}$$

Thus, for $i = 1, \ldots, N/2$, we have

$$\begin{aligned} |V^N(x_i) - v(x_i) - HE(x_i)| &\leq |V^N(x_i) - v(x_i) - H\eta(x_i)| + |H\vartheta(x_i)| \\ &\leq Z_i + 2N^{-1}|\vartheta(x_i)| \leq CN^{-2}. \end{aligned} \tag{6.4.13}$$

Now we are in a position to show that extrapolation improves the accuracy of V^N on $(0, 1-\sigma]$.

Lemma 6.4.3. *For all $x_i \in [0, 1-\sigma]$, we have the following estimate:*

$$|v(x_i) - (V^{2N}(x_i) - V^N(x_i))| \leq CN^{-2}.$$

Proof. From Lemma 6.4.2, we have for $x_i \in [0, 1-\sigma]$

$$V^N(x_i) - v(x_i) = HE(x_i) + O(N^{-2}).$$

Note that the subinterval mesh widths of $\Omega_{2N,\sigma}$ is half of $\Omega_{N,\sigma}$ and the function $E(x)$ defined in (6.4.5) depend only on σ. Hence

$$V^{2N}(x_i) - v(x_i) = \frac{H}{2}E(x_i) + O(N^{-2}).$$

So from the above two relations we can conclude that

$$v(x_i) - (V^{2N}(x_i) - V^N(x_i)) = -2(V^{2N} - v)(x_i) + (V^N - v)(x_i) = O(N^{-2}),$$

for $1 \leq i \leq N/2$. ∎

The following lemma shows the error of $V^N(x_i)$ after the extrapolation on $(1-\sigma, 1]$.

Lemma 6.4.4. *For all $x_i \in (1-\sigma, 1]$, we have for some constant C*

$$|v(x_i) - (V^{2N}(x_i) - V^N(x_i))| \leq CN^{-2}\ln N.$$

Proof. Let us define the function $G(x)$ on $[1-\sigma, 1]$ as the solution of the BVP

$$L_\varepsilon G(x) = 0, \quad G(1-\sigma) = 1, \quad G(1) = 0.$$

On $\Omega_{N,\sigma}$, define a discrete approximation G^N of G by

$$L_\varepsilon^N G^N(x_i) = 0, \quad G^N(1-\sigma) = 1, \quad G^N(1) = 0.$$

From the convergence of the upwind scheme given in Theorem 6.3.2, we have

$$|G(x_i) - G^N(x_i)| \leq CN^{-1} \ln N, \quad \text{for } N/2 \leq i \leq N. \tag{6.4.14}$$

Define $\omega(x_i) = V^N(x_i) - v(x_i) - (HE(1-\sigma))G^N(x_i)$ for $N/2 \leq i \leq N$. Then $\omega(x_{N/2}) = O(N^{-2})$, $\omega(x_N) = 0$ and $L_\varepsilon^N \omega(x_i) = O(h_i) + O(H^2) = O(N^{-2} \ln N)$. Now using the barrier function $C(1+x_i)N^{-2}$, we can get

$$|\omega(x_i)| \leq CN^{-2} \ln N, \quad \text{for } N/2 \leq i \leq N. \tag{6.4.15}$$

Observe that $|E(1-\sigma)| \leq C$, so we obtain

$$V^N(x_i) - v(x_i) = (HE(1-\sigma))G^N(x_i) + O(N^{-2} \ln N), \quad \text{for } N/2 \leq i \leq N. \tag{6.4.16}$$

Similarly, on the mesh $\Omega_{2N,\sigma}$, one has

$$V^{2N}(\tilde{x}_i) - v(\tilde{x}_i) = (H/2)E(1-\sigma)G^N(\tilde{x}_i) + O(N^{-2} \ln N), \quad \text{for } N \leq i \leq 2N. \tag{6.4.17}$$

But $\tilde{x}_{2i} = x_i$ for $N/2 \leq i \leq N$. Now combining (6.4.16) and (6.4.17), we obtain

$$v(x_i) - (2V^{2N} - V^N)(x_i) = 2(v - V^{2N})(x_i) - (v - V^N)(x_i) = O(N^{-2} \ln N),$$

for $N \leq i \leq 2N$. ∎

Now in the following lemmas, the Richardson extrapolation technique is applied on W^N in $\Omega_{N,\sigma}$. First, the error $W^N(x_i) - w(x_i)$ is calculated in the subintervals $[0, 1-\sigma]$ and $(1-\sigma, 1]$ separately.

Lemma 6.4.5. *For all $x_i \in [0, 1-\sigma]$, we have*

$$|w(x_i) - (W^{2N}(x_i) - W^N(x_i))| \leq CN^{-2}.$$

Proof. One can prove this lemma by following the same procedure as done in Lemma 3.5 of [72]. ∎

Now let us define $F(x)$ on $[1-\sigma, 1]$ as the solution of the following BVP:

$$L_\varepsilon F(x) = \frac{2}{\alpha} a(x) w''(x), \quad F(1-\sigma) = F(1) = 0. \tag{6.4.18}$$

The following lemma shows the error in the singular component in the inner region of $\Omega_{N,\sigma}$.

Lemma 6.4.6. *We have*

$$W^N(x_i) - w(x_i) = (N^{-1} \ln N)F(x_i) + O(N^{-2} \ln N), \quad \forall x_i \in (1-\sigma, 1].$$

Proof. From the bound of the layer part, we know that

$$|F^{(k)}(x)| \le C(\varepsilon+\delta\alpha)^{-k}\exp(-\alpha(1-x)/(\varepsilon+\delta\alpha)), \quad \text{for } 0 \le k \le 3.$$

By using the Taylor series expansion at the point $x_i \in [1-\sigma, 1]$, we get

$$L_\varepsilon^N F(x_i) = L_\varepsilon F(x_i) + O\bigg((\varepsilon+\delta\alpha)^{-1}N^{-1}\ln N\exp(-\alpha(1-x)/(\varepsilon+\delta\alpha))\bigg).$$

Now for some $\tilde{x}_1 \in (x_i, x_{i+1})$ and $\tilde{x}_2, \tilde{x}_3 \in (x_i, x_{i+1})$, we have

$$\begin{aligned} L_\varepsilon^N(W^N-w)(x_i) &= \frac{(\varepsilon+\delta\alpha)}{4!}[w^{(4)}(\tilde{x}_1)+w^{(4)}(\tilde{x}_2)]h^2 + \frac{a(x_i)}{2}\left[\frac{w'''(\tilde{x}_3)}{3}h^2 + w''(x_i)h\right] \\ &= -\frac{2}{\alpha}((\varepsilon+\delta\alpha)^{-1}N^{-1}\ln N)a(x_i)w''(x_i) + \\ &+ O\bigg((\varepsilon+\delta\alpha)^{-1}N^{-2}\ln^2 N\exp(-\alpha(1-x)/(\varepsilon+\delta\alpha))\bigg). \end{aligned} \tag{6.4.19}$$

Hence from the above two equations, we have

$$\begin{aligned} (N^{-1}\ln N)L_\varepsilon^N F(x_i) &= (N^{-1}\ln N)L_\varepsilon F(x_i) + O\bigg((\varepsilon+\delta\alpha)^{-1}N^{-2}\ln^2 N\exp(-\alpha(1-x)/(\varepsilon+\delta\alpha))\bigg) \\ &= L_\varepsilon^N(W^N-w)(x_i) + O\bigg((\varepsilon+\delta\alpha)^{-1}N^{-2}\ln^2 N\exp(-\alpha(1-x)/(\varepsilon+\delta\alpha))\bigg). \end{aligned}$$

That is, $\forall x \in (1-\sigma, 1)$,

$$|L_\varepsilon^N(W^N - w - (N^{-1}\ln N)F)(x_i)| \le C_7(\varepsilon+\delta\alpha)^{-1}N^{-2}\ln^2 N\exp(-\alpha(1-x)/(\varepsilon+\delta\alpha)), \tag{6.4.20}$$

for some constant C_7. For $i = N/2, \ldots, N$, consider the mesh function

$$\Gamma_i = C_8\left[N^{-2}(1+x_i) + (N^{-2}\ln^{-2}N)S_i\prod_{j=1}^{N}\left(1+\frac{\alpha h_j}{2(\varepsilon+\delta\alpha)}\right)^{-1}\right],$$

where C_8 has to be chosen later. From (6.3.15), we have

$$L_\varepsilon^N\Gamma_i \ge C_3C_8(\varepsilon+\delta\alpha)^{-1}N^{-2}\ln^2 N\prod_{j=1}^{N}\left(1+\frac{\alpha h_j}{2(\varepsilon+\delta\alpha)}\right)^{-1}. \tag{6.4.21}$$

For $i \ge N/2$, we can have

$$\begin{aligned} \exp(-\alpha(1-x_{i+1})/(\varepsilon+\delta\alpha)) &= \exp(\alpha h_{i+1}/(\varepsilon+\delta\alpha))\prod_{j=i+1}^{N}\exp(-\alpha h_j/(\varepsilon+\delta\alpha)) \\ &\le \exp(4N^{-1}\ln N)\prod_{j=i+1}^{N}\left(1+\frac{\alpha h_j}{\varepsilon+\delta\alpha}\right)^{-1} \\ &\le \exp(4)\prod_{j=i+1}^{N}\left(1+\frac{\alpha h_j}{\varepsilon+\delta\alpha}\right)^{-1}, \end{aligned} \tag{6.4.22}$$

provided $C_8 \geq \exp(4)C_7/C_3$. Hence from (6.4.21) and (6.4.22), we can get

$$L_\varepsilon^N \Gamma_i \geq |L_\varepsilon^N (W^N - w - (N^{-1}\ln N)F)(x_i)| \quad \text{for } x_i \in (1-\sigma, 1).$$

It is easy to show that $\Gamma_N \geq 0 = |W^N(1) - w(1) - (N^{-1}\ln N)F(1)|$. From Lemma 6.4.5, we have $|(w - W^N)(1-\sigma)| \leq C_9 N^{-2}$. So $\Gamma_{N/2} \geq C_8 N^{-2} = |(W^N - w - (N^{-1}\ln N)F)(1-\sigma)|$ provided $C_8 \geq C_9$. Now choosing $C_8 = \max\{\exp(4)C_7/C_3, C_9\}$, we can show that Γ_i is a barrier function for $\pm[W^N(x_i) - w(x_i) - (N^{-1}\ln N)F(x_i)]$ for $x_i \in [1-\sigma, 1]$. Hence applying the discrete comparison principle as given in Lemma 6.3.1, we can conclude that

$$|W^N(x_i) - w(x_i) - (N^{-1}\ln N)F(x_i)| \leq \Gamma_i \leq C_8 N^{-2}\ln^2 N.$$

In the next lemma, we will obtain the second-order error bound for the extrapolation of the singular component.

Lemma 6.4.7. *For some constant C and $\forall x_i \in (1-\sigma, 1]$, we have*

$$|w(x_i) - (2W^{2N}(x_i) - W^N(x_i))| \leq CN^{-2}\ln^2 N.$$

Proof. From Lemma 6.4.6, we have

$$\begin{aligned} W^N(x_i) - w(x_i) &= N^{-1}\ln N F(x_i) + O(N^{-2}\ln^2 N) \\ &= N^{-1}(\sigma\alpha/(\varepsilon + \delta\alpha))F(x_i) + O(N^{-2}(\sigma\alpha/(\varepsilon+\delta\alpha))^2). \end{aligned} \tag{6.4.23}$$

Similarly,

$$W^{2N}(x_i) - w(x_i) = N^{-1}(\sigma\alpha/(\varepsilon + \delta\alpha))F(x_i) + O(N^{-2}(\sigma\alpha/(\varepsilon+\delta\alpha))^2). \tag{6.4.24}$$

Replacing the first term from (6.4.23) and (6.4.24), we have

$$w(x_i) - (2W^{2N} - W^N)(x_i) = 2(w - W^{2N})(x_i) - (w - W^N)(x_i) = O(N^{-2}\ln^2 N),$$

Hence the desired result is obtained. ∎

The main result of this chapter is stated in the following theorem, which provides the ε-uniform second-order convergent result of the Richardson extrapolation technique applied to the BVP (6.1.3).

Theorem 6.4.8. *Assume that $\varepsilon \leq N^{-1}$, then there exists a positive constant C such that*

$$|u(x_i) - (2U^{2N}(x_i) - U^N(x_i))| \leq CN^{-2}\ln^2 N, \quad \forall x_i \in \Omega_{N,\sigma}.$$

Proof. For each $x_i \in \Omega_{N,\sigma}$, we have

$$|u(x_i) - (2U^{2N}(x_i) - U^N(x_i))| \leq |v - (2V^{2N} - V^N)(x_i)| + |w - (2W^{2N} - W^N)(x_i)|.$$

Combining the results of Lemmas 6.4.3 and 6.4.4 for the first term and the results of Lemmas 6.4.5 and 6.4.7 for the second term of the above equation, we will obtain the required result. ∎

6.5 Numerical Results

In this section, to validate the theoretical results, the proposed numerical scheme is applied to the following singularly perturbed delay differential equations with constant and variable coefficients.

Example 6.5.1. *Consider the constant coefficient problem*

$$\begin{cases} -\varepsilon u''(x) + u'(x-\delta) + u(x) = 0, \quad x \in \Omega = (0,1), \\ u(x) = 1, \ -\delta \leq x \leq 0, \qquad u(1) = -1. \end{cases} \tag{6.5.1}$$

The solution of this BVP exhibits a boundary layer at $x = 1$. Now using the Taylor series expansion, we obtain the following BVP:

$$\begin{cases} -(\varepsilon+\delta)u''(x) + u'(x) + u(x) = 1, \quad x \in \Omega\,, \\ u(0) = 1, \ -\delta \leq x \leq 0, \qquad u(1) = -1. \end{cases} \tag{6.5.2}$$

The exact solution to the approximated BVP is given by $u(x) = C_1 \exp(m_1 x) - C_2 \exp(m_2 x)$, where

$$m_{1,2} = \frac{1 \mp \sqrt{1 + 4(\varepsilon+\delta)}}{2(\varepsilon+\delta)}, \ C_1 = \frac{1 + \exp(m_2)}{\exp(m_2) - \exp(m_1)}, \ C_2 = \frac{\exp(m_1) + 1}{\exp(m_2) - \exp(m_1)}.$$

For any value of N, the maximum pointwise errors E_ε^N are calculated by $E_\varepsilon^N = \max |u - U^N|$ where u is the exact solution and U^N is the numerical solution. The double mesh method is used to compute the rate of convergence as $r_\varepsilon^N = \log_2 \left(E_\varepsilon^N / E_\varepsilon^{2N} \right)$.

Example 6.5.2. *Consider the variable coefficient problem*

$$\begin{cases} -\varepsilon u''(x) + (1+x)u'(x-\delta) + xu(x) = 1, \quad x \in \Omega\,, \\ u(x) = 0, \ -\delta \leq x \leq 0, \qquad u(1) = 0. \end{cases}$$

Here, the boundary layer is at $x = 1$ and the exact solution is not known for this problem.

In the absence of the exact solution, to obtain the accuracy of the numerical solution and to show the ε–uniform convergence of the proposed method, the idea of interpolation is used which

is described as follows. Let $\overline{U}^{8192}$ be the piecewise linear interpolant of U^N in Ω_N. Define, the maximum point-wise error G_ε^N and the rate of convergence q_ε^N as,

$$G_\varepsilon^N = \max_{x_i \in \overline{\Omega}^N} |U^N - \overline{U}^{8192}| \quad \text{and} \quad q_\varepsilon^N = \log_2 \left(\frac{G_\varepsilon^N}{G_\varepsilon^{2N}} \right).$$

For computational purposes, the delay parameter δ is taken as the square of the perturbation parameter ε, *i.e.,* $\delta = \varepsilon^2$ and the bound of the convective coefficient to be equal to one. Figure 6.1(a) presents the solutions of (6.5.2) by the upwind scheme before and after extrapolation along with the exact solution. It shows that the steep boundary layer is located on the right side of the domain. The corresponding errors are shown in Figure 6.1(b). One can easily mark that the solution due to extrapolation is a better approximation than the solution obtained by the upwind scheme. In Figure 6.2, the number of mesh intervals and the maximum point-wise errors are presented using loglog scale along with the theoretical rate of convergence. Clearly, these figures show that the computed errors decreases approximately at the same rates which is proved theoretically and the rate of convergence of the upwind scheme is doubled after extrapolation.

In Table 6.1, the maximum pointwise error before and after extrapolation are presented for a range of values of ε and N and the corresponding order of convergence. The maximum pointwise error and the corresponding order of convergence for Example 6.5.2 is provided in Table 6.2. From these computational results, one can observe the ε-uniform convergence of the scheme before and after extrapolation.

6.6 Conclusion

In this chapter, the Richardson extrapolation technique is applied for singularly perturbed delay differential equations on Shishkin mesh. First, the BVP (6.1.3) is solved by the upwind finite difference scheme to get U^N and the convergence analysis is carried out to obtain the optimal error of order $O(N^{-1} \ln N)$. By keeping the transition parameter fixed on the Shishkin mesh, the numerical solution U^{2N} is calculated. Then the Richardson extrapolation is implemented. It is shown both theoretically and computationally that after extrapolation, the rate of convergence of the upwind scheme is raised from almost first-order *i.e.,* $O(N^{-1} \ln N)$ to almost second-order *i.e.,* $O(N^{-2} \ln^2 N)$.

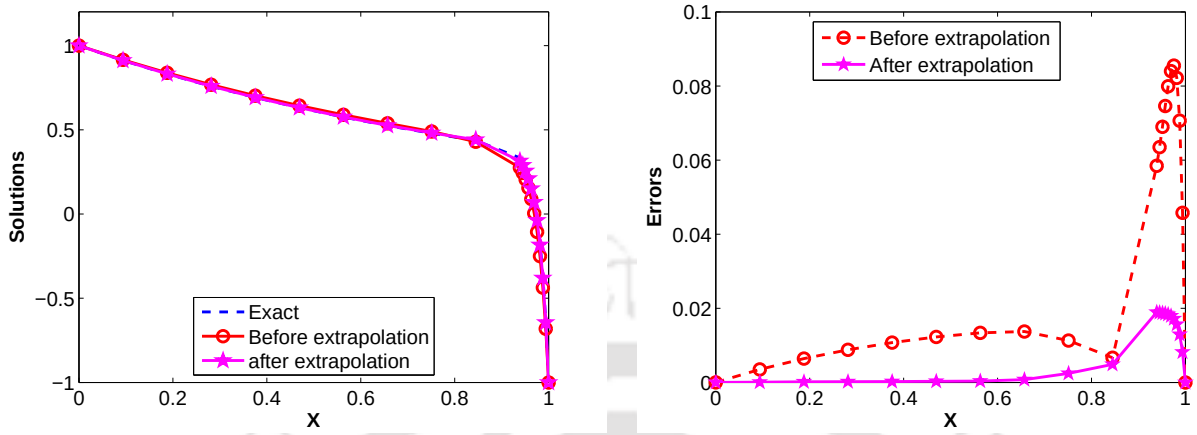

(a) Solutions. (b) Errors.

Figure 6.1: *Numerical solution and the error due to the upwind scheme before and after extrapolation of Example 6.5.1 for* $\varepsilon = 1e-2$ *and* $N = 20$.

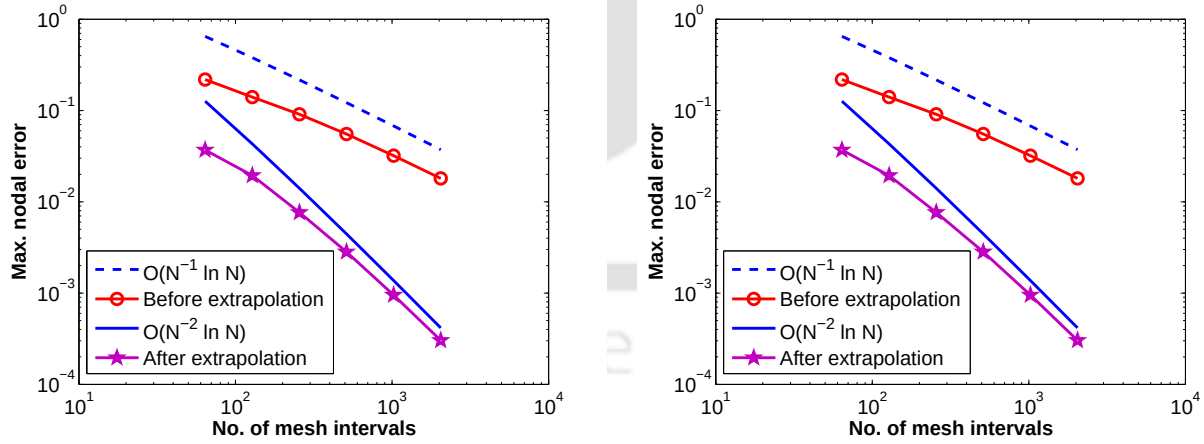

(a) For $\varepsilon = 1e-4$. (b) For $\varepsilon = 1e-8$.

Figure 6.2: *Loglog plot of the maximum errors before and after extrapolation for Example 6.5.1.*

Table 6.1: *Maximum point-wise errors E_ε^N and the rate of convergence r_ε^N before and after extrapolation for Example 6.5.1*

ε	Extrapolation	Number of intervals N					
		32	64	128	256	512	1024
	before	1.4785e-3	7.4410e-4	3.7334e-4	1.8698e-4	9.3568e-5	4.6804e-5
	rate	0.9905	0.9950	0.9976	0.9988	0.9994	
1	after	9.7307e-6	2.4617e-6	6.1892e-7	1.5518e-7	3.8843e-8	9.7491e-9
	rate	1.9829	1.9918	1.9958	1.9982	1.9943	
	before	8.6354e-2	5.6101e-2	3.4222e-2	2.0195e-2	1.1593e-2	6.5208e-3
	rate	0.6222	0.7131	0.7609	0.8008	0.8301	
$1e-2$	after	7.3194e-3	3.0500e-3	1.1405e-3	3.9703e-4	1.3022e-4	4.1064e-5
	rate	1.2629	1.4192	1.5223	1.6083	1.6650	
	before	8.7003e-2	5.6261e-2	3.4226e-2	2.0163e-2	1.1576e-2	6.5127e-3
	rate	0.6289	0.7170	0.7634	0.8006	0.8298	
$1e-4$	after	7.9395e-3	3.1993e-3	1.1760e-3	4.0513e-4	1.3199e-4	4.1408e-5
	rate	1.3113	1.4439	1.5374	1.6179	1.6725	
	before	8.7014e-2	5.6265e-2	3.4227e-2	2.0163e-2	1.1576e-2	6.5126e-3
	rate	0.6290	0.7171	0.7634	0.8006	0.8298	
$1e-6$	after	7.9572e-3	3.2064e-3	1.1791e-3	4.0641e-4	1.3254e-4	4.1636e-5
	rate	1.3113	1.4433	1.5366	1.6165	1.6706	
$1e-8$	before	8.7015e-2	5.6265e-2	3.4227e-2	2.0163e-2	1.1576e-2	6.5126e-3
to	rate	0.6290	0.7171	0.7634	0.8006	0.8298	
$1e-10$	after	7.9574e-3	3.2065e-3	1.1791e-3	4.0641e-4	1.3254e-4	4.1624e-5
	rate	1.3113	1.4433	1.5367	1.6165	1.6709	

Table 6.2: *Maximum point-wise errors G_ε^N and the rate of convergence q_ε^N before and after extrapolation for Example 6.5.2*

ε	Extrapolation	Number of intervals N					
		32	64	128	256	512	1024
	before	3.3487e-2	1.7279e-2	8.7870e-3	4.4309e-3	2.2249e-3	1.1148e-3
	rate	0.9546	0.9756	0.9878	0.9938	0.9969	
1	after	1.1737e-3	3.1343e-4	8.1080e-5	2.0626e-5	5.2019e-6	1.3062e-6
	rate	1.9049	1.9507	1.9749	1.9873	1.9936	
	before	2.1872e-1	1.4031e-1	9.0775e-2	5.5255e-2	3.2016e-2	1.8060e-2
	rate	0.6405	0.6283	0.7162	0.7873	0.8260	
$1e-4$	after	3.6932e-2	1.9431e-2	7.6571e-3	2.8299e-3	9.5231e-4	3.0311e-4
	rate	0.9265	1.3435	1.4361	1.5712	1.6516	
	before	2.1869e-1	1.4031e-1	9.0768e-2	5.5245e-2	3.2012e-2	1.8058e-2
	rate	0.6403	0.6283	0.7164	0.7872	0.8260	
$1e-8$	after	3.6936e-2	1.9428e-2	7.6569e-3	2.8296e-3	9.5222e-4	3.0310e-4
	rate	0.9268	1.3433	1.4361	1.5712	1.6515	

Chapter 7

Defect-Correction Method for Singularly Perturbed Delay Differential Equation

This chapter is dealt with the study of a defect-correction method based on the finite difference scheme for solving a singularly perturbed delay differential equation. It is well-known that the classical upwind scheme on the piecewise-uniform Shishkin mesh yields solutions that are first-order accurate measured in the discrete supremum norm. Here, our main aim is to design a numerical method using the principle of the defect-correction on the Shishkin mesh to get better result from the almost first-order convergence to almost second-order convergence. The defect-correction technique is studied by several researchers ([31], [32], [34]) in the literature to improve the accuracy of the solution of the one-dimensional singularly perturbed convection-diffusion equation. Here, the same technique is applied to solve singularly perturbed delay differential equations on the Shishkin mesh. First, the equation is solved by the upwind finite difference scheme on the piecewise-uniform Shishkin mesh, then the defect-correction technique is applied which combines the stability of the upwind scheme and the higher-order accuracy of the central difference scheme. The method is shown to be uniformly convergent with respect to the perturbation parameter and almost second-order convergent measured in the discrete maximum norm.[4]

7.1 Introduction

This chapter considers the following singularly perturbed delay differential equation:

$$\begin{cases} \mathscr{L}_\varepsilon u_\varepsilon(x) \equiv -\varepsilon u_\varepsilon''(x) + a(x)u_\varepsilon'(x-\delta) + b(x)u_\varepsilon(x) = f(x), \quad x \in \Omega = (0,1), \\ u_\varepsilon(x) = \gamma(x), \ \ -\delta \le x \le 0, \qquad u_\varepsilon(1) = \lambda\,, \end{cases} \tag{7.1.1}$$

where $0 < \varepsilon \ll 1$ and $0 \le \delta(\varepsilon) \ll 1$. The parameter ε is known as the perturbation parameter and δ (which is of $o(\varepsilon)$) as the delay parameter. Moreover, the functions $a(x), b(x), f(x)$ and $\gamma(x)$ are

[4]Some portion of this chapter will appear in *Int. J. Comput. Methods. (In Press)*

sufficiently smooth and λ is a constant. It is also assumed that $b(x) \geq 0, \forall x \in \overline{\Omega} = [0,1]$.

Without loss of generality, we will assume that $a(x) > 0$. Expanding the delay term in the Taylor's series expansion, we obtain that

$$u'_\varepsilon(x-\delta) = u'_\varepsilon(x) - \delta u''_\varepsilon(x) + \delta^2 u'''_\varepsilon(x) + \ldots, \quad \text{as } \delta \to 0. \tag{7.1.2}$$

Now using the first two terms of the expansion (7.1.2) in the DE (7.1.1), we have the following BVP:

$$\begin{cases} L_\varepsilon u(x) \equiv -\big(\varepsilon + \delta a(x)\big)u''(x) + a(x)u'(x) + b(x)u(x) = f(x), \ x \in \Omega = (0,1), \\ u(x) = \gamma(x), \quad -\delta \leq x \leq 0, \qquad u(1) = \lambda\,. \end{cases} \tag{7.1.3}$$

Since (7.1.3) is an approximation of (7.1.1), we have used $u(x)$ as a different notation for $u_\varepsilon(x)$. For convenience, we have taken $\gamma(x) \equiv$ constant (see [53], [56]). Here, we assume that $a(x) > \alpha > 0, \forall x \in \overline{\Omega}$. Under these assumptions, the BVP (7.1.3) has a unique solution which exhibits an exponential layer on the right side of the domain at $x = 1$. The layer behavior remains for sufficiently small non-zero values of $\delta(\varepsilon)$.

The outline of this chapter is as follows. In Section 7.2, the maximum principle, stability result and some *a priori* estimates on the solution and its derivatives of the BVP (7.1.3) are established. Section 7.3 presents the upwind finite difference scheme and the convergence of the standard upwind method where we obtain the first-order error estimate *i.e.*, $O(N^{-1}\ln N)$ which is optimal for the BVP (7.1.3). In Section 7.4, the defect-correction method is applied and also it is proved that this method is of almost second-order convergent *i.e.*, $O(N^{-2}\ln^3 N)$ measured in the discrete supremum norm. Finally, numerical examples are provided in Section 7.5 to illustrate the applicability of the present method with the maximum point-wise error and the rate of convergence which are shown in tables and figures.

7.2 Continuous Problem

7.2.1 Properties of the solution

Lemma 7.2.1. (Maximum Principle) *Let $\mathcal{V}$ be a smooth function satisfying $\mathcal{V}(0) \geq 0,\ \mathcal{V}(1) \geq 0$ and $L_\varepsilon \mathcal{V}(x) \geq 0\ \forall x \in\ \Omega$. Then $\mathcal{V}(x) \geq 0,\ \forall x \in\ \overline{\Omega}$.*

Proof. The proof is given in Lemma 6.2.1 of Chapter 6. ∎

Lemma 7.2.2. *The solution $u(x)$ of the BVP (7.1.3) satisfies the following stability estimate*

$$\|u\| \ \leq \ \frac{1}{\alpha}\|f\| + \max\{|u(0)|, |\lambda|\}. \tag{7.2.1}$$

Proof. The proof is given in Lemma 6.2.2 of Chapter 6. ∎

Lemma 7.2.3. *Let $0 \leq k \leq 4$ be a positive integer. Assuming $f \in \mathcal{C}^k(\overline{\Omega})$, the derivatives $u^{(k)}$ of the solution u of (7.1.3) satisfy the following bound:*

$$|u^{(k)}(x)| \leq C\left[1 + (\varepsilon + \delta\alpha)^{-k} \exp\left(\frac{-\alpha(1-x)}{\varepsilon + \delta\alpha}\right)\right], \tag{7.2.2}$$

where C depends on $\|a\|$, $\|a'\|$, $\|b\|$, $\|b'\|$ and on the boundary conditions.

Proof. One can refer Lemma 6.2.3 of Chapter 6 for the proof. ∎

7.2.2 Solution decomposition

To show that a numerical method is ε–uniform convergent, some prior information of the solution is required. Let us decompose the solution $u(x)$ of (7.1.3) into regular (v) and singular (w) components as follows:

$$u(x) = v(x) + w(x).$$

The regular component $v(x)$ can be written in an asymptotic expansion as

$$v(x) = v_0(x) + (\varepsilon + \delta\alpha)v_1(x) + (\varepsilon + \delta\alpha)^2 v_2(x) + (\varepsilon + \delta\alpha)^3 v_3(x),$$

where v_0, v_1 and v_2 are respectively the solutions of the following differential equations:

$$\begin{cases} a(x)v_0'(x) + b(x)v_0(x) = f(x), & v_0(0) = u(0), \\ a(x)v_1'(x) + b(x)v_1(x) = (\varepsilon + \delta a(x))v_0''(x)/(\varepsilon + \delta\alpha), & v_1(0) = 0, \\ L_\varepsilon v_2(x) = (\varepsilon + \delta a(x))v_1''(x)/(\varepsilon + \delta\alpha), & v_2(0) = 0, v_2(1) = 0. \end{cases} \tag{7.2.3}$$

Hence, the regular component of the solution satisfies the BVP:

$$L_\varepsilon v(x) = f(x), \quad v(0) = v_0(0) = u(0),\ v(1) = v^*(1), \tag{7.2.4}$$

and the singular component satisfies

$$L_\varepsilon w(x) = 0, \quad w(0) = 0,\ w(1) = u(1) - v^*(1), \tag{7.2.5}$$

where $v^*(1)$ depends on v and its derivatives which are bounded uniformly in ε (for more details, see [34]).

Lemma 7.2.4. *Let $u(x)$ be the solution of BVP (7.1.3) and $u(x) = v(x) + w(x)$. For sufficiently small ε and $0 \leq k \leq 4$, the derivatives of $v(x)$ and $w(x)$ satisfy the following bounds:*

$$\|v^{(k)}\| \leq C\big(1 + (\varepsilon + \delta\alpha)^{3-k}\big), \tag{7.2.6}$$

$$|w^{(k)}(x)| \leq C\big(\varepsilon + \delta\alpha\big)^{-k} \exp\left(\frac{-\alpha(1-x)}{\varepsilon + \delta\alpha}\right), \quad x \in \overline{\Omega}. \tag{7.2.7}$$

Proof. The detailed proof is given in Lemma 6.2.4. ∎

7.3 Discrete Problem

This section presents the Shishkin mesh, the difference scheme and the convergence of the upwind scheme on the Shishkin mesh. It also provides the bounds of the decomposition of the numerical solution.

7.3.1 The Shishkin mesh

Without loss of generality, we assume that N is even. To solve (7.1.3) numerically, the piecewise-uniform Shishkin mesh is used containing $N+1$ number of points. This mesh has a transition point $1-\sigma$, where

$$\sigma = \min\left\{\frac{1}{2}, \frac{\sigma_0(\varepsilon+\delta\alpha)}{\alpha}\ln N\right\}.$$

Now divide the subinterval $[0, 1-\sigma]$ into $N/2$ equal subdivisions of width H where $H = 2(1-\sigma)/N$. Similarly divide the subinterval $(1-\sigma, 1]$ into $N/2$ equal subdivisions of width h where $h = 2\sigma/N = 2\sigma_0(\varepsilon+\delta\alpha)\ln N/\alpha N$ with $\sigma_0 \geq 3/\alpha$. Then the Shishkin mesh $\Omega^N = \{x_i\}_{i=0}^N$, where $x_0 = 0, x_N = 1$ and the mesh width $h_i := x_i - x_{i-1}$ satisfy $h_i = H$ for $i = 1, \ldots, N/2$ and $h_i = h$ for $i = N/2+1, \ldots, N$. Here the piecewise-uniform mesh is entirely determined by the two chosen parameters N and σ.

7.3.2 The difference scheme

The upwind finite difference discretization of (7.1.3) takes the form

$$\begin{cases} L_\varepsilon^N U_i^N \equiv -(\varepsilon+\delta a_i)D^+D^-U_i^N + a_i D^-U_i^N + b_i U_i^N = f_i\,, \ 1 \leq i \leq N-1, \\ U_0^N = \gamma_0, \quad U_N^N = \lambda\,, \end{cases} \tag{7.3.1}$$

where U_i^N denotes the approximation of $u(x_i)$, $a_i = a(x_i)$ and b_i, f_i are defined in a similar fashion. Equation (7.3.1) can be expressed in the following form of system of algebraic equations

$$\begin{cases} -r_i^- U_{i-1}^N + r_i^c U_i^N - r_i^+ U_{i+1}^N = f_i, \quad i = 1, \ldots, N-1, \\ U_0^N = \gamma_0, \quad U_N^N = \lambda\,, \end{cases} \tag{7.3.2}$$

where

$$r_i^- = \frac{2(\varepsilon+\delta a_i)}{h_i(h_i+h_{i+1})} + \frac{a_i}{h_i}, \quad r_i^c = \frac{2(\varepsilon+\delta a_i)}{h_i h_{i+1}} + \frac{a_i}{h_i} + b_i, \quad r_i^+ = \frac{2(\varepsilon+\delta a_i)}{h_{i+1}(h_i+h_{i+1})}\ .$$

One can easily see that

$$r_i^- > 0,\ r_i^+ > 0 \text{ and } \quad r_i^c + r_i^- + r_i^+ \geq 0, \quad \text{for} \quad i = 1, \ldots, N-1, \tag{7.3.3}$$

which imply that the stiffness matrix is an M-matrix.

7.3.3 Convergence of the upwind scheme

Lemma 7.3.1. (Discrete Comparison Principle) *The system of equations $L_\varepsilon^N \mathcal{V}_j = F_j$ for given $\mathcal{V}_0$ and $\mathcal{V}_N$ has a unique solution. If $L_\varepsilon^N \mathcal{V}_j < L_\varepsilon^N \mathcal{Z}_j$ for $1 \le j \le N-1$ with $\mathcal{V}_0 < \mathcal{Z}_0$ and $\mathcal{V}_N < \mathcal{Z}_N$, then $\mathcal{V}_j < \mathcal{Z}_j$ for $1 \le j \le N$.*

Proof. From (7.3.3), it is clear that the matrix associated with L_ε^N is an M-matrix and therefore has a positive inverse. Hence, the result follows. ∎

The local truncation error of the difference scheme (7.3.1) at the node x_i is given by

$$\tau_i = L_\varepsilon^N U_i^N - L_\varepsilon u(x_i), \tag{7.3.4}$$

where u and U_i^N denote the exact solution of (7.1.3) and (7.3.1) respectively.

Using Taylor series expansion, the truncation error (7.3.4) can be expressed as

$$\tau_i = \frac{-(\varepsilon+\delta a_i)}{h_i+h_{i+1}}\left[\frac{1}{h_{i+1}}\int_{x_i}^{x_{i+1}}(x_{i+1}-s)^2 u'''(s)ds - \frac{1}{h_i}\int_{x_{i-1}}^{x_i}(s-x_{i-1})^2 u'''(s)ds\right] + \\ + \frac{a_i}{h_i}\int_{x_{i-1}}^{x_i}(s-x_{i-1})u''(s)ds, \tag{7.3.5}$$

from which we obtain the bound

$$|\tau_i| < (\varepsilon+\delta\alpha)\int_{x_{i-1}}^{x_{i+1}}|u'''(s)|ds + C\int_{x_{i-1}}^{x_{i+1}}|u''(s)|ds. \tag{7.3.6}$$

Theorem 7.3.2. *Let u be the solution of (7.1.3) and U_i^N be the solution of (7.3.1) computed on Ω_σ^N, then there exists a constant C such that*

$$|U_i^N - u(x_i)| \le CN^{-1}\ln N, \qquad \forall x_i \in \overline{\Omega}.$$

Proof. The complete proof of this theorem is given in Theorem 6.3.2 of Chapter 6. ∎

7.3.4 Decomposition of the discrete solution

Consider the decomposition of the discrete solution

$$U = V + W.$$

The regular and the singular components respectively satisfy the following equations

$$L^N V = f, \qquad V(0) = v(0), \quad V(1) = v(1), \tag{7.3.7}$$

$$L^N W = 0, \qquad W(0) = w(0), \quad W(1) = w(1), \tag{7.3.8}$$

where the difference operator L^N is defined as follows:

$$L^N Z(x_i) = \begin{cases} L^N_{up} Z(x_i), & \text{if } 1 \le i < N/2 \quad \text{and} \quad \|a\|N^{-1} \ge \varepsilon, \\ L^N_{cd} Z(x_i), & \text{if } 1 \le i < N/2 \quad \text{and} \quad \|a\|N^{-1} < \varepsilon, \\ L^N_{cd} Z(x_i), & \text{if } N/2 \le i < N\,. \end{cases}$$

The central difference operator L^N_{cd} and the upwind difference operator L^N_{up} are defined by

$$L^N_{cd} \equiv -(\varepsilon + \delta a_i) D^+ D^- + a_i D^{\pm} + b_i,$$

$$L^N_{up} \equiv -(\varepsilon + \delta a_i) D^+ D^- + a_i D^{-} + b_i.$$

Lemma 7.3.3. *If $\sigma \neq 0.5$ and $N \ge N_0$, then the error associated with the regular component satisfies*

$$|v(x_i) - V_i| \le \begin{cases} CN^{-1}(1 - x_i), & \text{if } \|a\|N^{-1} \ge \varepsilon \\ CN^{-2}, & \text{if } \|a\|N^{-1} < \varepsilon\,. \end{cases} \tag{7.3.9}$$

Proof. Here the proof is divided into two cases.

Case (i) For $\|a\|N^{-1} \ge \varepsilon$, we know that the regular component satisfies

$$|L^N(V - v)(x_i)| \le CN^{-1},$$

and thus applying the discrete comparison principle as given in Lemma 7.3.1, we have

$$(V - v)(x_i) \le CN^{-1}(1 - x_i)\,.$$

Case (ii) For $\|a\|N^{-1} < \varepsilon$ with $\sigma \neq 0.5$, we have the operator as the central difference operator on a nonuniform mesh. So in this case,

$$|L^N(v(x_i) - V_i)| \le \begin{cases} C(N^{-1}\varepsilon + N^{-2}), & \text{if } i = N/2 \\ CN^{-2}, & \text{otherwise}\,. \end{cases} \tag{7.3.10}$$

In other words, the truncation error is of second-order except at the transition point. In order to show that the bound at the transition point is also of second-order, let us take the following discrete barrier function

$$\psi_i = CN^{-2}\theta(z_i) + CN^{-2}(1 - x_i)\,,$$

where

$$\theta(z_i) = \begin{cases} \dfrac{1 - z_i}{1 - \sigma}, & \text{if } 0 \le z_i \le 1 - \sigma, \\ 1, & \text{if } 1 - \sigma < z_i \le 1. \end{cases} \tag{7.3.11}$$

Using the above function, we can show that

$$(\varepsilon+\delta\alpha)D^+D^-\psi_i \le C\begin{cases} 0, & \text{if } i \ne N/2 \\ \dfrac{N^{-1}(\varepsilon+\delta\alpha)}{1-\sigma}, & \text{if } i = N/2. \end{cases} \tag{7.3.12}$$

Therefore,

$$|L^N(V_i - v(x_i))| \le L^N\psi_i\,,$$

and applying the discrete comparison principle as given in Lemma 7.3.1 yields

$$|V_i - v(x_i)| \le \psi_i \le CN^{-2}\,, \tag{7.3.13}$$

which is the desired bound. ∎

Lemma 7.3.4. *The error in the singular component satisfies*

$$|w(x_i) - W_i| \le \begin{cases} CN^{-3}, & \text{if } x_i \in [0, 1-\sigma] = \Omega^N_{out} \\ CN^{-2}(\ln N)^3, & \text{if } x_i \in (1-\sigma, 1] = \Omega^N_{in}\,. \end{cases} \tag{7.3.14}$$

Proof. From the bound of the singular part, we have

$$|w(x_i)| \le C\exp\left(\frac{-\alpha(1-x_i)}{\varepsilon+\delta\alpha}\right).$$

If $x_i \in \Omega^N_{out}$, then we have

$$|w(x_i)| \le CN^{-3}\,. \tag{7.3.15}$$

Define $\xi(x_i)$ as the solution of (7.3.1) by considering the constant coefficient only, then we must have $\xi(x_i) > 0$. Observe that, for all $N \ge 1$

$$\left(1+\frac{2\sigma_0\ln N}{N}\right)^{-N/2} \le CN^{-\sigma_0}, \text{ if } 2\sigma_0\ln N < N,$$

which is the consequence of the inequality $\ln(1+t) > t(1-t/2)$ for all $0 < t < 1$ and we can deduce $\xi(x_i) \le CN^{-3}$, for $x_i \in \Omega^N_{out}$. Again note that

$$w(0)\xi(0) \ge W(0) \quad \text{and} \quad w(1)\xi(1) \ge W(1).$$

Also $L^N_{up}\xi(x_i) < 0$ and $L^N_{cd}\xi(x_i) < 0$, so using the discrete comparison principle (Lemma 7.3.1), it follows that

$$W(x_i) \le w(0)\xi(x_i) \le CN^{-3}. \tag{7.3.16}$$

Now using the above bounds given in (7.3.15) and (7.3.16), we can claim that

$$|w(x_i) - W_i| \le |w(x_i)| + |W_i| \le CN^{-3}, \quad \text{for } x_i \in \Omega^N_{out}.$$

It remains to show that the required bound for the mesh points inside the layer region, where

$$|L^N(w(x_i) - W_i)| \leq C\frac{h^2}{(\varepsilon + \delta\alpha)^3}, \quad (w - W)(0) = 0, \quad |(w - W)(1 - \sigma)| \leq CN^{-3}. \tag{7.3.17}$$

Using the barrier function

$$\chi_i = \frac{C(1 - \sigma - x_i)h^2}{(\varepsilon + \delta\alpha)^3} + CN^{-3},$$

in the above inequality, we have

$$|w(x_i) - W_i| \leq CN^{-2}(\ln N)^3,$$

which is our desired bound. ∎

7.4 The Defect-Correction Method

The defect–correction method consists of the following: let us define a modified central difference operator (modified at the transition point) as:

$$L^N_{dc}Z(x_i) = \begin{cases} L^N_{cd}Z(x_i), & \text{if } i \neq N/2, \\ -(\varepsilon + \delta a_i)D^+D^-Z(x_i) + a_iD^0Z(x_i) + b_iZ(x_i), & \text{if } i = N/2\,, \end{cases} \tag{7.4.1}$$

where

$$L^N_{cd} \equiv -(\varepsilon + \delta a_i)D^+D^- + a_iD^{\pm} + b_i.$$

The defect τ_{dc} is estimated by means of the central difference scheme as

$$\begin{aligned} L^N\tau_{dc} &= f - L^N_{dc}U \quad \text{in } \Omega, \\ \tau_{dc} &= 0 \quad \text{on } \partial\Omega, \end{aligned} \tag{7.4.2}$$

and the final computed solution is

$$U^{dc} = U + \tau_{dc}\ . \tag{7.4.3}$$

Now the correction τ_{dc} can be decomposed into

$$\tau^v_{dc} + \tau^w_{dc}\,,$$

where these components satisfy the following equations

$$L^N\tau^v_{dc} = f - L^N_{dc}V \quad \text{in } \Omega, \text{ with } \quad \tau^v_{dc} = 0 \text{ on } \partial\Omega, \tag{7.4.4}$$

$$L^N\tau^w_{dc} = -L^N_{dc}W \quad \text{in } \Omega, \text{ with } \quad \tau^w_{dc} = 0 \text{ on } \partial\Omega. \tag{7.4.5}$$

This way we can rewrite the final error committed by the defect–correction method as

$$\|u - U^{dc}\| \leq \|v - (V + \tau^v_{dc})\| + \|w - (W + \tau^w_{dc})\|. \tag{7.4.6}$$

Now the errors in the regular part and in the singular part are calculated separately.

Before calculating the error in the regular part, first the discrete derivative of the error in the regular part is calculated which is defined as follows.

$$e(x_i) = (V - v)(x_i) \tag{7.4.7}$$

$$\tau_v = L^N(V - v)(x_i). \tag{7.4.8}$$

Lemma 7.4.1. *For sufficiently small ε and for $N \geq N_0$, the following inequality holds,*

$$(\varepsilon + \delta\alpha)D^- e(x_i) \leq CN^{-1}, \quad \text{for } x_i \in \Omega^N. \tag{7.4.9}$$

Proof. Using the bound $|v(x_i) - V_i| \leq CN^{-1}(1 - x_i)$, and $\varepsilon \leq CN^{-1}$, we have

$$(\varepsilon + \delta\alpha)|D^- e(x_i)| \leq CN^{-1}(1 - x_i).$$

Now at the transition point $1 - \sigma$, we have

$$\begin{aligned} -2(\varepsilon + \delta\alpha)(D^+ - D^-)e(1-\sigma) &+ a_{N/2}(h+H)D^- e(1-\sigma) + (h+H)b_{N/2}e(1-\sigma) \\ &= (h+H)\tau_v(1-\sigma). \end{aligned}$$

Using the fact that

$$|(h+H)D^- e(1-\sigma)| \leq 2\big[|e(1-\sigma)| + |e(1-\sigma-H)|\big],$$

we have

$$(\varepsilon + \delta\alpha)|D^- e(1-\sigma)| \leq CN^{-1}.$$

Lastly, for the mesh points inside the layer region,

$$-2(\varepsilon + \delta\alpha)(D^+ - D^-)e(x_i) + a_i h D^- e(x_i) + b_i h e(x_i) = h\tau_v(x_i). \tag{7.4.10}$$

Summing from $i = 1, \ldots, N/2$, we obtain that

$$\begin{aligned} \sum_{i=1}^{N/2} a_i D^{\pm} e_i &= a_{N/2-1} D^{\pm}_{N/2-1} e_{N/2-1} + a_{N/2-2} D^{\pm}_{N/2-2} e_{N/2-2} \\ &+ \sum_{i=1}^{N/2-3} (D^{\pm} a_i D^{\pm} e_i \pm D^{\pm} a_{i+2} e_{i+2}) \\ &= a_{N/2} e_{N/2} + a_{N/2-1} e_{N/2-1} \Bigg(\sum_{i=1}^{N/2-3} (a_i - a_{i+2}) e_{i+1} - a_{i+1} e_i - a_i e_{i-1} \Bigg) / 2h \\ &= O(N^{-1}/h). \end{aligned} \tag{7.4.11}$$

Hence, we have

$$(\varepsilon + \delta\alpha)D^- e(x_i) \leq CN^{-1}, \quad \text{for } x_i \in \Omega^N.$$

On a uniform mesh, $D^0 = (D^+ + D^-)/2$. Since the Shishkin mesh is piecewise–uniform, therefore, for $x_i \in (1-\sigma, 1]$ and using $\rho_i = a(x_i)h/(\varepsilon + \delta\alpha) \leq CN^{-1}\ln N$, we obtain

$$\frac{1-\rho_{i/2}}{1+\rho_{i/2}} \leq \frac{1}{1+\rho}, \quad \text{as} \quad 0 < 1-\rho_{i/2} < 1,$$

where $\rho = \alpha h/(\varepsilon + \delta\alpha)$. For $x_i \in \Omega_{in}^N$,

$$|D^- e(x_i)| \leq \left(\frac{1}{1+\rho}\right)|D^- e(x_i)| + c\left(\frac{\rho}{1+\rho}\right)N^{-1}. \tag{7.4.12}$$

Using the above relation recursively, we can get

$$\begin{aligned} |D^- e(1-\sigma-h)| &\leq C(1+\rho)(1+\rho)^{-N/2}|D^+ e(0)| + C\frac{\rho}{1+\rho}N^{-1}\sum_{i=0}^{N/2-1}(1+\rho)^{-i} \\ &\leq C(1+\rho)^{-N/2}|D^+ e(0)| + CN^{-1} \\ &\leq CN^{-1}|D^+ e(0)| + CN^{-1}. \end{aligned} \tag{7.4.13}$$

Now

$$D^+ e(1-\sigma) \leq \frac{\varepsilon + \delta\alpha}{\varepsilon + \delta\alpha + \alpha H}D^- e(1-\sigma) + CN^{-1}\frac{\varepsilon + \delta\alpha}{\varepsilon + \delta\alpha + \alpha H}. \tag{7.4.14}$$

So, we have

$$D^- e(1-\sigma) \leq CN^{-1},$$

hence for all $x_i \in \Omega^N$, we obtain

$$(\varepsilon + \delta\alpha)D^- e(x_i) \leq CN^{-1}. \tag{7.4.15}$$

Now we will find the truncation error in the regular component of the defect-correction method.

Lemma 7.4.2. *The truncation error associated with the regular component of the corrected solution is given by*

$$\|L^N e^{dc}\| \leq CN^{-1}\ln N. \tag{7.4.16}$$

Proof. The truncation error is of the form

$$\begin{aligned} L^N e^{dc} &= L^N e + L^N \tau_{cd} \\ &= L^N e + (f - L_{cd}^N V) \\ &= (L^N - L_{cd}^N)e - L_{cd}^N v + f \\ &= (L^N - L_{cd}^N)e + \tau_{cd}^v, \end{aligned} \tag{7.4.17}$$

where $\tau_{cd}^v = (f - L_{cd}^N v)(x_i)$. Now for $x_i \in \Omega_{out}^N$, we have

$$\begin{aligned}(L^N - L_{cd}^N)e(x_i) &= a_i(D^+ - D^0)e(x_i) \\ &= \frac{a_i h_i}{h_i + h_{i+1}}(D^+ - D^-)e(x_i). \end{aligned} \tag{7.4.18}$$

If $x_i \in \Omega_{in}^N$ and the mesh is uniform, then we have

$$|\tau_{dc}^v| \le CN^{-2}.$$

Similarly if $x_i \in \Omega_{in}^N$, then using Lemma 7.4.1, we have

$$\begin{aligned}L^N e^{dc}(x_i) &\le |\tau_{cd}^v(x_i)| + \frac{a_i}{2}D^- e(x_i) + \frac{a_i}{2}D^+ e(x_{i+1}) \\ &\le CN^{-1}. \end{aligned} \tag{7.4.19}$$

Finally at the transition point $1-\sigma$, as $h/(h+H) = O((\varepsilon + \delta\alpha)\ln N)$, we obtain

$$\begin{aligned}L^N e^{dc}(1-\sigma) &\le |\tau_{cd}^v(1-\sigma)| + \frac{a_{N/2}h}{h+H}D^- e(1-\sigma) + \frac{a_i}{2}D^+ e(1-\sigma) \\ &\le CN^{-1}\ln N, \end{aligned} \tag{7.4.20}$$

and hence the result. ∎

Lemma 7.4.3. *We have the following result*

$$|D^- e^{dc}(x_i)| \le \begin{cases} CN^{-1}\ln N, & \text{if } x_i \in \Omega_{out}^N \\ \dfrac{CN^{-1}\ln N}{\varepsilon + \delta\alpha}, & \text{if } x_i \in \Omega_{in}^N. \end{cases}$$

Proof. The first result holds from the previous lemma. Again, we have

$$(\varepsilon + \delta\alpha)|D^- e^{dc}(x_i)| \le CN^{-1}.$$

Now at the transition point, we have

$$\begin{aligned}D^-(e^{dc}(1-\sigma)) &\le \frac{\varepsilon + \delta\alpha}{\varepsilon + \delta\alpha + \alpha H}|D^- e^{dc}(1-\sigma)| + \frac{CN^{-1}(h+H)}{\varepsilon + \delta\alpha + \alpha H} \\ &+ a_{N/2}\frac{h}{\varepsilon + \delta\alpha + \alpha H}|(D^+ - D^-)(e(1-\sigma))| \\ &\le CN^{-1}\ln N, \end{aligned} \tag{7.4.21}$$

and hence the proof. ∎

Now we are in a stage to find the error in the regular part of the defect-correction method.

Lemma 7.4.4. *Assuming $N \ge N_0$ and $\sigma \ne 0.5$, we have*

$$\|v - (V + \tau_{dc}^v)\| \le CN^{-2}\ln N. \tag{7.4.22}$$

Proof. Let $x_i \in \Omega_{out}^N$. For $i = 1, \ldots, N-1$,

$$-\frac{\varepsilon + \delta\alpha}{H}(D^+ e_i^{dc} - D^- e_i^{dc}) + a_i D^- e_i^{dc} + b_i e_i^{dc} = \tau_i^{dc} + a_i(D^- - D^+)e_i.$$

Summing up, we have

$$\begin{aligned}\sum_{i=1}^{N-1} a_i D^+ e_i^{dc} + b_i e_i^{dc} &= \left(-\frac{\varepsilon + \delta\alpha}{H}(D^- e_{N-1}^{dc} - D^+ e_{i-1}^{dc}) \right) \\ &+ \sum_{i=1}^{N-1} \frac{a_i}{2}(D^- - D^+)e_i + \sum_{i=1}^{N-1} \tau_i^{cd}. \end{aligned} \tag{7.4.23}$$

Here we need to find the bound for the terms in the right hand side of the above expression separately. We know that

$$\begin{aligned}(\varepsilon + \delta\alpha) &\leq CN^{-1}, \\ \left(\frac{\varepsilon + \delta\alpha}{H}\right) D^- e_{i-1}^{dc} &= O(N^{-1} \ln N), \\ \sum_{i=1}^{N-1} \tau_i^{cd} &\leq CN^{-1}. \end{aligned}$$

Similarly,

$$\begin{aligned}\sum_{i=1}^{N-1} a_j(D^+ - D^-)e_i &= a_{N-1} D^- e_{N-1} + \sum_{i=1}^{N-2}(a_i - a_{i-1})D^- e_i - a_i D^- e_i \\ &= O(N^{-1}), \end{aligned} \tag{7.4.24}$$

and hence, we have

$$|e^{dc}| \leq CN^{-2} \ln N.$$

Now one can show that

$$|L^N e^{dc}(x_i)| \leq CN^{-2}, \quad e^{dc}(0) = 0, \quad |e^{dc}(1-\sigma)| \leq CN^{-2} \ln N.$$

Hence, combining the above inequalities, one can obtain the required result. ∎

In the following lemma, the error in the singular part of the corrected solution is calculated.

Lemma 7.4.5. *Assuming $N \geq N_0$ and $\sigma \neq 0.5$, we have*

$$\|w - (W + \tau_{dc}^w)\| \leq CN^{-2}(\ln N)^3. \tag{7.4.25}$$

Proof. From the triangle inequality, we have

$$\begin{aligned} \|w-(W+\tau_{dc}^{w})\| &\leq \|w-W\|+\|\tau_{dc}^{w}\| \\ &\leq CN^{-2}(\ln N)^{3}+\|\tau_{dc}^{w}\|. \end{aligned} \tag{7.4.26}$$

Since L^N satisfy the discrete comparison principle as given in Lemma 7.3.1, it has a positive inverse, or in other words, L^N is uniformly stable. Hence,

$$\|\tau_{dc}^{w}\| \leq \|(L^N)^{-1}\|\|L^N\tau_{dc}^{w}\| \leq \|L_{cd}^{N}W\|.$$

Again for $i \leq N/2$,

$$L_{cd}^{N}W_i = 0 \quad \text{and} \quad L_{u}^{N}W_i = 0.$$

Now

$$\begin{aligned} L_{cd}^{N}W_i &= (L_{cd}^{N}-L_{u}^{N})W_i \\ &= a_i(D^0-D^-)W_i \\ &= a_i\frac{h_i}{h_i+h_{i+1}}(D^+-D^-)W_i. \end{aligned} \tag{7.4.27}$$

Hence,

$$|L_{cd}^{N}W_i| \leq CN\sum_{j=i-1}^{i+1}|W_j|.$$

We have already shown that

$$|W_i| \leq CN^{-3},$$

so it follows that

$$\|\tau_{dc}^{w}\| \leq CN^{-2},$$

and hence the lemma holds. ∎

An immediate consequence of this lemma is the following result which is the parameter–uniform error bound of the defect–correction method.

Theorem 7.4.6. *Assuming that $N \geq N_0$ and $\sigma \neq 0.5$, one can have the error associated with the defect–correction scheme is*

$$\|u-U^{dc}\| \leq CN^{-2}(\ln N)^{3}, \tag{7.4.28}$$

where u is the exact solution of (7.1.3) and U^{dc} is the numerical solution obtained from (7.4.3).

Proof. Combining the results of Lemmas 7.3.3, 7.3.4, 7.4.5 and using the inequality (7.4.6), we can obtain the desired estimate. ∎

7.5 Numerical Results

In this section, the proposed numerical scheme is applied to the following examples to validate the theoretical results.

Example 7.5.1. *Consider the constant coefficient problem*

$$\begin{cases} -\varepsilon u''(x) + u'(x-\delta) + u(x) = 1, \quad x \in \Omega = (0,1), \\ u(x) = 0, \ -\delta \le x \le 0, \\ u(1) = 0. \end{cases} \tag{7.5.1}$$

The solution of this BVP exhibits a boundary layer at $x = 1$. Now using the expansion given in (7.1.2), we obtain the following approximate BVP of (7.5.1):

$$\begin{cases} -(\varepsilon+\delta)u''(x) + u'(x) + u(x) = 1, \quad x \in \Omega\,, \\ u(0) = 0, \ -\delta \le x \le 0, \\ u(1) = 0. \end{cases} \tag{7.5.2}$$

The exact solution to the approximated BVP (7.5.2) is given by

$$u(x) = C_1 \exp(m_1 x) + C_2 \exp(m_2 x) + 1,$$

where

$$m_{1,2} = \frac{1 \mp \sqrt{1+4(\varepsilon+\delta)}}{2(\varepsilon+\delta)}, \ C_1 = \frac{\exp(m_2) - 1}{\exp(m_1) - \exp(m_2)}\,, \ C_2 = \frac{1 - \exp(m_1)}{\exp(m_1) - \exp(m_2)}.$$

Example 7.5.2. *Consider the variable coefficient problem*

$$\begin{cases} -\varepsilon u''(x) + (1+x)u'(x-\delta) + \exp(-x)u(x) = 1, \quad x \in \Omega\,, \\ u(x) = 0, \ -\delta \le x \le 0, \\ u(1) = 0. \end{cases}$$

Here, the boundary layer is at $x = 1$ and the exact solution is not known for this problem. For any value of N and ε, the maximum point-wise errors E_ε^N and the corresponding rate of convergence r_ε^N are determined by the same way as described in Chapter 6. In the absence of the exact solution, to obtain the accuracy of the numerical solution and to show the ε-uniform

convergence of the proposed method, we follow the method of interpolation. The maximum point-wise error G_ε^N and the rate of convergence q_ε^N are also calculated in a similar fashion as described in Chapter 6.

For computation purposes, the delay parameter δ is chosen as the square of the perturbation parameter ε *i.e.,* $\delta = \varepsilon^2$ and the bound of the convective coefficient to be equal to one. Figure 7.1(a) represents the solutions of (7.5.2) by the upwind scheme and the defect-correction method along with the exact solution. It shows that the steep boundary layer is located on the right side of the domain. The corresponding errors are shown in Figure 7.1(b). One can easily mark that the solution due to defect-correction method is a better approximation than the solution obtained by the upwind scheme. In Figure 7.2, the maximum point-wise errors are given using loglog scale along with the theoretical rate of convergence. Clearly, these figures show that the computed errors decrease approximately at the same rates which is proved theoretically and the rate of convergence of the upwind scheme is almost doubled using the defect–correction method.

In Table 7.1, the maximum point-wise errors and the corresponding order of convergence of the upwind scheme and the defect-correction method are presented for a range of values of ε and N. The maximum pointwise errors and the corresponding order of convergence for Example 7.5.2 are provided in Table 7.2. From the computational results shown in these tables, one can see the monotonically decreasing behavior of the parameter-uniform errors obtained for different values of ε and N which ensures the ε-uniform convergence of both the schemes.

7.6 Conclusion

In this chapter, the defect-correction method is applied for singularly perturbed delay differential equations on the Shishkin mesh. The problem is solved first by the upwind finite difference scheme and then by the defect-correction method which combines the stability of the upwind scheme and the higher-order convergence of the central difference scheme. It is shown both theoretically and computationally that by using the defect-correction method, the rate of convergence of the upwind scheme is raised from almost first-order *i.e.*, $O(N^{-1}\ln N)$ to almost second-order *i.e.*, $O(N^{-2}\ln^3 N)$.

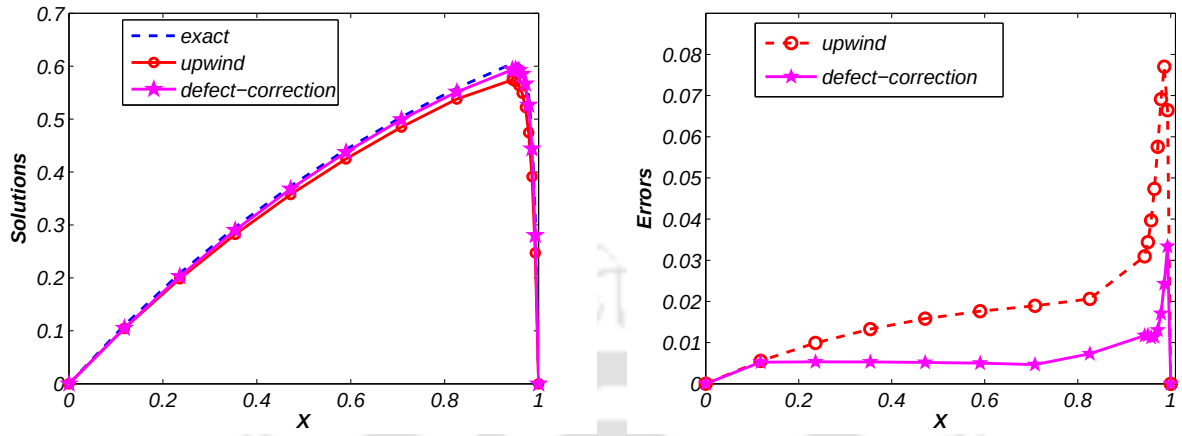

(a) Solutions. (b) Errors.

Figure 7.1: *Numerical solution and the error due to the upwind scheme and the defect-correction method of Example 7.5.1 for* $\varepsilon = 1e-2$ *and* $N = 16$.

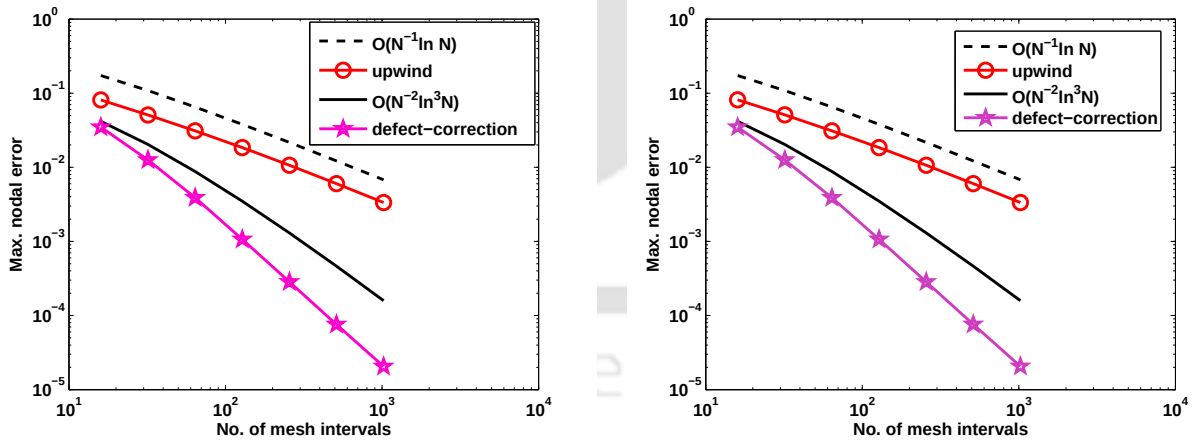

(a) For $\varepsilon = 1e-4$. (b) For $\varepsilon = 1e-8$.

Figure 7.2: *Loglog plot of the maximum errors due to the upwind scheme and the defect-correction method.*

Table 7.1: *Maximum point-wise errors E_ε^N and the rate of convergence r_ε^N of the upwind scheme (up) and the defect-correction method (d-c) for Example 7.5.1.*

ε		Number of intervals N					
		32	64	128	256	512	1024
1	up	4.3534e-4	2.1827e-4	1.0927e-4	5.4668e-5	2.7342e-5	1.3673e-5
		0.9960	0.9982	0.9990	0.9995	0.9997	
	d-c	8.4580e-5	2.1297e-5	5.3435e-6	1.3383e-6	3.3488e-7	8.3757e-8
		1.9896	1.9948	1.9974	1.9987	1.9993	
$1e-2$	up	4.8573e-2	2.9856e-2	1.7789e-2	1.0281e-2	5.8129e-3	3.2333e-3
		0.7021	0.7470	0.7909	0.8227	0.8462	
	d-c	1.2255e-2	3.8264e-3	1.0374e-3	2.7176e-4	7.1859e-5	1.9419e-5
		1.6793	1.8830	1.9326	1.9191	1.8877	
$1e-4$	up	5.0894e-2	3.0989e-2	1.8430e-2	1.0635e-2	6.0106e-3	3.3411e-3
		0.7157	0.7497	0.7932	0.8232	0.8471	
	d-c	1.2564e-2	3.8842e-3	1.0649e-3	2.8375e-4	7.5699e-5	2.0541e-5
		1.6936	1.8669	1.9080	1.9063	1.8817	
$1e-6$	up	5.0920e-2	3.1002e-2	1.8437e-2	1.0639e-2	6.0129e-3	3.3424e-3
		0.7158	0.7497	0.7932	0.82321	0.8471	
	d-c	1.2568e-2	3.8851e-3	1.0654e-3	2.8408e-4	7.5844e-5	2.0607e-5
		1.6937	1.8666	1.9070	1.9052	1.8799	
$1e-8$	up	5.0921e-2	3.1002e-2	1.8438e-2	1.0639e-2	6.0130e-3	3.3424e-3
to		0.7158	0.7497	0.7932	0.8232	0.8471	
$1e-10$	d-c	1.2568e-2	3.8851e-3	1.0654e-3	2.8408e-4	7.5842e-5	2.0603e-5
		1.6937	1.8666	1.907	1.9052	1.8801	

Table 7.2: *Maximum point-wise errors G_ε^N and the rate of convergence q_ε^N of the upwind scheme (up) and the defect-correction method (d-c) for Example 7.5.2.*

ε		Number of intervals N					
		32	64	128	256	512	1024
1	up	1.7693e-3	8.9267e-4	4.4672e-4	2.2292e-4	1.1065e-4	5.4463e-5
		0.9870	0.9987	1.0028	1.0105	1.0227	
	d-c	1.3527e-3	3.4802e-4	8.7103e-5	2.0645e-5	5.0937e-6	1.2314e-6
		1.9586	1.9984	2.0769	2.0190	2.0484	
$1e-4$	up	1.5311e-1	1.1320e-1	7.3230e-2	4.9273e-2	3.0231e-2	1.7648e-2
		0.4357	0.6283	0.5716	0.7047	0.7765	
	d-c	1.1923e-1	6.6787e-2	3.5554e-2	1.4605e-2	4.5041e-3	1.2678e-3
		0.8361	0.9095	1.2836	1.6971	1.8289	
$1e-8$	up	1.5312e-1	1.1323e-1	7.3251e-2	4.9288e-2	3.0240e-2	1.7654e-2
		0.4354	0.6283	0.5716	0.7047	0.7764	
	d-c	1.1924e-1	6.6809e-2	3.5567e-2	1.4610e-2	4.5059e-3	1.2694e-3
		0.8357	0.9095	1.2836	1.6971	1.8277	

Chapter 8

Summary and Future Scopes

This chapter is completely devoted to a brief summary of the results highlighting the contributions made in this thesis and also of the techniques used in deriving these results. It also provides information for the scope of possible extensions of the present work and future investigations.

8.1 Summary of the Results

The main theme of this thesis revolves around developing, analyzing and optimizing the ε-uniform upwind based fitted mesh methods resolving the convection-dominated layer type problems. Here, some ε-uniform numerical methods are discussed for solving SPPs using the piecewise-uniform *Shishkin mesh* and the *adaptive grid*. The results of this thesis with some important observations are briefly described below:

- A uniformly convergent upwind finite difference scheme is analyzed for solving singularly perturbed convection-diffusion BVP. The global solution and approximation to the global normalized flux are obtained on a suitable nonuniform mesh which is formed by equidistributing the arc-length monitor function depending on the numerical solution. It is shown that the discrete solution obtained by the upwind scheme and the global solution obtained *via* interpolation converge uniformly with respect to the perturbation parameter ε. In addition, the uniform first-order (*optimal*) convergence of the weighted derivative of the numerical solution on this nonuniform mesh and the uniform convergence of the global normalized flux on the whole domain are proved. The results obtained by using the adaptive grid are compared with the results obtained on the Shishkin mesh which show the advantage of using such adaptive grids.

- Then, the idea of adaptive grid is extended for solving singularly perturbed convection-diffusion problems with Robin boundary conditions. The error analysis for the numerical solution is carried out and an *optimal* order error estimate *i.e.*, $O(N^{-1})$ is obtained which is

independent of the singular perturbation parameter.

- In the literature, so far there exists no result where the adaptive grid is used for solving singularly perturbed differential-difference equations. Here, in this thesis, a uniformly accurate numerical method comprising of the standard upwind scheme with adaptively generated grid is proposed for solving singularly perturbed differential equations having the delay and the shift terms. The maximum principle, the stability results and some *a priori* estimates on the solution and its derivatives are established. The error analysis for the numerical solution is carried out which shows the ε-uniform convergence of the proposed method and an *optimal* first-order error estimate *i.e.,* convergence of order $O(N^{-1})$ is achieved. The theoretical and numerical results help us to conclude that the errors converge at the rate of first-order, independent of the small perturbation parameters.

- Next, a post-processing technique known as the Richardson extrapolation technique is analyzed for solving singularly perturbed delay differential equation with layer behaviour, on the piecewise-uniform Shishkin mesh. It is proved both theoretically and computationally that after extrapolation, the rate of convergence of the upwind scheme is raised from almost first-order to almost second-order measured in the discrete supremum norm.

- Finally, a defect-correction method based on the finite difference scheme is studied for solving a singularly perturbed delay differential equation on the Shishkin mesh. The problem is solved by using the upwind finite difference scheme and then by the defect-correction method. The defect-correction method combines the stability of the upwind scheme and the higher-order convergence of the central differences scheme. It is shown both theoretically and numerically that by using the defect-correction method, the rate of convergence of the upwind scheme is increased from almost first-order to almost second-order.

8.2 Future Scopes

Here, in this thesis some efficient numerical methods and post-processing techniques are discussed for solving singularly perturbed BVPs exhibiting layer behaviors. But the chances of examining the potential of these methods are still open for studying more complex problems with smooth and non-smooth data. We now present some observations pertaining the possible extensions of our results to different problems. A brief outline of some interesting problems which can be taken up in future are also described below:

The upwind numerical scheme is analyzed on a suitable nonuniform mesh generated adaptively by equidistributing a positive monitor function depending on the computed solution for standard convection-diffusion problem with Dirichlet and Robin type boundary conditions in **Chapter** 2

and **Chapter** 3, respectively. Again a post-processing technique is discussed in **Chapter** 6 on piecewise-uniform Shishkin mesh. Now one can combine both the ideas to solve the following model convection-diffusion BVP:

$$\begin{cases} Lu(x) \equiv -\varepsilon u''(x) + a(x)u'(x) + b(x)u(x) = f(x), \ x \in \Omega = (0,1), \\ u(0) = A, \quad u(1) = B, \end{cases} \tag{8.2.1}$$

where $0 < \varepsilon \ll 1$, the functions $a(x), b(x), f(x)$ are sufficiently smooth and A, B are given constants. Assuming $a(x) > 0$ and $b(x) \geq 0$, the BVP (8.2.1) has a unique solution which exhibits a layer of width $O(\varepsilon)$ at $x = 1$. Now the BVP (8.2.1) can be solved by using the upwind scheme on the adaptive grid and then, one can apply the extrapolation idea to enhance its order of accuracy.

Table 8.1: *Maximum point-wise errors and the rate of convergence before and after extrapolation using adaptive grid*

ε	Extrapolation	Number of intervals N					
		32	64	128	256	512	1024
	before	1.8509e-3	9.3607e-4	4.7074e-4	2.3605e-4	1.1820e-4	5.9143e-5
	rate	0.9835	0.9917	0.9958	0.9979	0.9990	
1	after	2.0880e-5	5.3227e-6	1.3433e-6	3.3744e-7	8.4559e-8	2.1159e-8
	rate	1.9719	1.9864	1.9931	1.9966	1.9987	
	before	3.9379e-2	2.0655e-2	1.0596e-2	5.3714e-3	2.7030e-3	1.3559e-3
	rate	0.9309	0.9629	0.9802	0.9908	0.9953	
$1e-2$	after	1.4700e-3	3.9418e-4	1.0254e-4	2.6154e-5	6.6000e-6	1.6578e-6
	rate	1.8989	1.9426	1.9711	1.9865	1.9932	
	before	7.5909e-2	4.2486e-2	2.2706e-2	1.1768e-2	5.9881e-3	3.0266e-3
	rate	0.8373	0.9039	0.9482	0.9747	0.9844	
$1e-4$	after	3.8180e-3	1.9927e-3	6.6807e-4	2.0793e-4	5.7826e-5	1.5365e-5
	rate	0.9381	1.5767	1.6839	1.8463	1.9121	

This idea is experimented on a test problem by considering $a(x) = 1$, $b(x) = f(x) = 0$ with the boundary conditions $A = 0, B = 1$. The maximum point-wise error and the corresponding order of convergence for the BVP (8.2.1) before and after extrapolation are provided in Table 8.1. Though the numerical results are given here, the problem to provide the detailed convergence analysis of the Richardson extrapolation on the adaptive grid is still open. One may also think of using the method of defect–correction on these adaptive grids for solving problem of type (8.2.1).

Again the adaptive grid may be used to solve the following nonlinear singularly perturbed BVP:

$$\begin{cases} \varepsilon u''(x) = f(x, u, u') = -a(x, u)u'(x) + b(x, u), \ x \in \Omega = (0,1), \\ u(0) = A, \quad u(1) = B, \end{cases} \tag{8.2.2}$$

One can follow the method of Newton's quasi-linearized process ([21], [97]) for solving the BVP (8.2.2) and then, the upwind scheme can be applied on the adaptive grid.

The analysis in this thesis has focused only on one-dimensional problems. However, most realistic applications involve multi-dimensional singular perturbation problems. One may think to extend the adaptive grid idea to solve the following model convection-diffusion equation:

$$\begin{cases} -\varepsilon \triangle u_\varepsilon - \underline{a}.\nabla u_\varepsilon = f(x,y), & (x,y) \in \Omega = (0,1)^2, \\ u_\varepsilon = 0, & (x,y) \in \partial\Omega, \end{cases} \tag{8.2.3}$$

where $\underline{a} = (a_1, a_2)$ such that the constants $a_1, a_2 \gg \varepsilon > 0$. The source term f is sufficiently smooth and define the inflow and outflow boundaries as

$$\partial\Omega_{\text{in}} = \{(x,y) \in \partial\Omega : y = 1\} \cup \{(x,y) \in \partial\Omega : x = 1\}$$

and

$$\partial\Omega_{\text{out}} = \{(x,y) \in \partial\Omega : y = 0\} \cup \{(x,y) \in \partial\Omega : x = 0\}$$

respectively. The BVP (8.2.3) is the two-dimensional extension of the BVP (2.1.1) and the solution of (8.2.3) has boundary layers normal to $\partial\Omega_{\text{out}}$ and is smooth away from these layers.

Lastly, these ideas can be extended to solve one-dimensional time dependent parabolic problem with a delay term where the model can be described as follows:

Let $\Omega = (0,1)$, $D = \Omega \times (0,T]$ and $\Gamma = \Gamma_l \cup \Gamma_b \cup \Gamma_r$, where Γ_l and Γ_r are the left and the right sides of the rectangle D corresponding to $x = 0$ and 1 respectively, $\Gamma_b = [0,1] \times [-\delta, 0]$. The model singularly perturbed delay parabolic equation with Dirichlet boundary conditions on Γ is given by

$$\begin{cases} \left(\dfrac{\partial u_\varepsilon}{\partial t} - \varepsilon \dfrac{\partial^2 u_\varepsilon}{\partial x^2} - a u_\varepsilon\right)(x,t) = -b(x,t) u_\varepsilon(x, t-\delta) + f(x,t), & (x,t) \in D, \\ u_\varepsilon(x,t) = \phi_l(t), \quad (x,t) \in \Gamma_l, \qquad u_\varepsilon(x,t) = \phi_r(t), \quad (x,t) \in \Gamma_r \\ u_\varepsilon(x,t) = \phi_b(x,t), \quad (x,t) \in \Gamma_b, \end{cases} \tag{8.2.4}$$

where $0 < \varepsilon \ll 1$ and $\delta > 0$ (note that $T = k\delta$ for some integer $k > 1$). The functions $a(x,t)$, $b(x,t)$, $f(x,t)$, $(x,t) \in \overline{D}$ and $\phi_l(t)$, $\phi_b(x,t)$, $\phi_r(t)$, $(x,t) \in \Gamma$ are sufficiently smooth which satisfy

$$a(x,t) \geq 0 \quad \text{and} \quad b(x,t) \geq \beta \geq 0, \qquad (x,t) \in \overline{D}.$$

Under these assumptions, the BVP (8.2.4) has a unique solution which exhibits layers at Γ_l and Γ_r. For more details, one can refer [3].

Moreover, it is important to observe that the model problems and their convergence analysis provided in this thesis are based upon solving BVPs with smooth data. It will be a more challenging work to establish these results for problems with non-smooth data resulting in strong interior layers.

Bibliography

[1] L.R. Abrahamsson and S. Osher. Monotone difference schemes for singular perturbation problems. SIAM *J. Numer. Anal.*, **19**(5):979–992, 1982.

[2] G.M. Amiraliyev and F. Erdogan. Uniform numerical method for singularly perturbed delay differential equations. *Comput. Math. Appl.*, **53**(5):1251–1259, 2007.

[3] A.R. Ansari, S.A. Bakr, and G.I. Shishkin. A parameter-robust finite difference method for singularly perturbed delay parabolic partial differential equations. *J. Comput. Appl. Math.*, **205**(1):552–566, 2007.

[4] A.R. Ansari and A.F. Hegarty. Numerical solution of a convection diffusion problem with Robin boundary conditions. *J. Comput. Appl. Math.*, **156**(5):221–238, 2003.

[5] N.S. Bakhvalov. On the optimization of methods for solving boundary-value problems with boundary layers. *J. Numer. Meth. Math. Phys.*, **9**(4):841–859, 1969.

[6] R.K. Bawa and S. Natesan. A computational method for self-adjoint singular perturbation problems using quintic spline. *Comput. Math. Appl.*, **50**(8-9):1371–1382, 2005.

[7] M.G. Beckett. *The robust and efficient numerical solution of a singularly perturbed boundary value problems using grid adaptivity.* PhD thesis, University of Strathclyde, 1998.

[8] M.G. Beckett and J.A. Mackenzie. Convergence analysis of finite differences approximations on equidistribted grids to a singularly perturbed boundary value problem. *Appl. Numer. Math.*, **35**(166):87–109, 2000.

[9] M.G. Beckett and J.A. Mackenzie. On a uniformly accurate finite difference approximation of a singularly perturbed reaction-diffusion problem using grid equidistribution. *J. Comput. Appl. Math.*, **131**:381–405, 2001.

[10] C.M. Bender and S.A. Orszag. *Advance Mathematical Methods for Scientists and Engineers.* McGraw-Hill, New York, 1978.

[11] A.E. Berger, J.M. Solomon, and M. Ciment. An analysis of a uniformly accurate difference method for a singular perturbation problem. *Math. Comp.*, **37**:79–94, 1981.

[12] A.E. Berger, J.M. Solomon, M. Ciment, S.H. Leventhal, and B.C. Weinberg. Generalized operator comapct implicit schemes for boundary layer problems. *Math. Comp.*, **35**:695–731, 1980.

[13] A.W. Bush. *Perturbation Methods for Engineers and Scientists*. CRC Press, London, 1992.

[14] X. Cai and F. Liu. Uniform convergence difference schemes for singularly perturbed mixed boundary problems. *J. Comput. Appl. Math.*, **166**:31–54, 2004.

[15] Y. Chen. Uniform pointwise converenges for a singularly perturbed problem using arc-length equidistribution. *J. Comput. Appl. Math.*, **159**:25–34, 2003.

[16] Y. Chen. Uniform convergence analysis of finite difference approximations for singularly perturbation problems on an adapted grid. *Adv. Comput. Math.*, **24**:197–212, 2006.

[17] C. Clavero, R.K. Bawa, and S. Natesan. A robust second-order numerical method for global solution and global normalized flux for singularly perturbed self-adjoint boundary value problems. *Int. J. Comput. Math.*, **86**(10-11):1731–1745, 2009.

[18] G. Das and S. Pattanayak. *Fundamentals of Mathematical Analysis*. Tata McGraw-Hill, New Delhi, 1987.

[19] D.N. de G Allen and R.V. Southwell. Relaxation methods applied to determine the motion, in $2D$, of a viscous fluid past a fixed cylinder. *Quart. J. Mech. Appl. Math.*, **VIII**(2):129–145, 1955.

[20] R.B. Dingle. *Asymptotic Expansions: Their Derivation and Interpretation*. Academic Press, New York, 1973.

[21] E.P. Doolan, J.J.H. Miller, and W.H.A. Schildrers. *Uniform Numerical Methods for Problems with Initial and Boundary Layers*. Boole Press, Dublin, 1980.

[22] M. Van Dyke. *Perturbation Methods in Fluid Mechanics*. Academic Press, New York, 1964.

[23] W. Eckhaus. *Matched Asymptotic Expansions and Singular Perturbations*. North Holland, Amsterdam, 1973.

[24] W. Eckhaus. *Asymptotic Analysis of Singular Perturbations*. North Holland, Amsterdam, 1979.

[25] A. Erdelyi. *Asymptotic Expansions*. Dover, New York, 1956.

[26] V. Ervin and W. Layton. On the approximation of the derivatives of singularly perturbed boundary value prblems. SIAM *J. Sci. Comput.*, **8**(3):265–277, 1987.

[27] P.A. Farrell. Sufficient conditions for the uniform convergence of a class of difference schemes for a singularly perturbed problem. IMA. *J. Numer. Anal.*, **7**(4):459–472, 1987.

[28] P.A. Farrell, A.F. Hegarty, J.J.H. Miller, E. O'Riordan, and G.I. Shishkin. *Robust Computational Techniques for Boundary Layers*. Chapman & Hall/CRC Press, Boca Raton, FL, 2000.

[29] R. Föβmeier. On Richardson extrapolation for finite difference methods on regular grids. *Numer. Math.*, **55**:451–462, 1989.

[30] K.O. Friedrichs and W. Wasow. Singular perturbations of nonlinear oscillations. *Duke Math. J*, **13**:367–381, 1946.

[31] A. Fröhner, T. Linβ, and H.G. Roos. Defect correction on Shishkin-type meshes. *Numer. Algorithms*, **26**:281–299, 2001.

[32] A. Fröhner and H.G. Roos. The ε-uniform convergence of a defect correction method on a Shishkin mesh. *Appl. Numer. Math.*, **37**:79–94, 2001.

[33] E.C. Gartland. Graded-mesh difference schemes for singularly perturbed two point boundary-value problems. *Math. Comp.*, **51**:631–657, 1988.

[34] J.L. Gracia and E. O'Riordan. A defect-correction parameter-uniform numerical method for a singularly perurbed convection-diffusion problem in one dimension. *Numer. Algorithms*, **41**:359–385, 2006.

[35] P.W. Hemker and J.J.H. Miller. *Numerical Analysis of Singular Perturbation Problems*. Academic Press, London, 1979.

[36] M.H. Holmes. *Introduction to Perturbation Methods*. Springer, Berlin, 1995.

[37] M.K. Kadalbajoo and K.C. Patidar. A survey of numerical techniques for solving singularly perturbed ordinary differential equations. *Appl. Math. Comput.*, **130**:457–510, 2002.

[38] M.K. Kadalbajoo and K.C. Patidar. Singularly perturbed problems in partial differential equations - a survey. *Appl. Math. Comput.*, **134**(2-3):371–429, 2003.

[39] M.K. Kadalbajoo and V.P. Ramesh. Hybrid method for numerical solution of singularly perturbed delay differential equations. *Appl. Math. Comput.*, **187**:797–814, 2007.

[40] M.K. Kadalbajoo and V.P. Ramesh. Numerical methods on Shishkin mesh for singularly perturbed delay differential equations with a grid adaptation strategy. *Appl. Math. Comput.*, **188**:1816–1831, 2007.

[41] M.K. Kadalbajoo and K.K. Sharma. An ε-uniform fitted operator method for solving boundary-value problems for singularly perturbed delay differential equations: layer behavior. *Int. J. Comput. Math.*, **80**(10):1261–1276, 2003.

[42] M.K. Kadalbajoo and K.K. Sharma. Numerical analysis of singularly perturbed delay differential equations with layer behavior. *Appl. Math. Comput.*, **157**:11–28, 2004.

[43] M.K. Kadalbajoo and K.K. Sharma. A numerical method based on finite difference for boundary value problems for singularly perturbed delay differential equations. *Appl. Math. Comput.*, **197**:692–707, 2008.

[44] S. Kaplaun. *Fluid Mechanics and Singular Perturbations*. Academic Press, New York, 1967.

[45] H.B. Keller. Accurate difference methods for linear ordinary differential systems subject to linear constraints. SIAM *J. Numer. Anal.*, **6**(1):8–30, 1969.

[46] R.B. Kellogg and A. Tsan. Analysis of some difference approximations for a singular perturbation problem without turning point. *Math. Comp.*, **32**(144):1025–1039, 1978.

[47] J. Kevorkian and J.D. Cole. *Perturbation Methods in Applied Mathematics*. Springer-Verlag, New York, 1981.

[48] J. Kevorkian and J.D. Cole. *Multiple Scale and Singular Perturbation Methods*. Springer-Verlag, New York, 1996.

[49] N. Kopteva and M. Stynes. Approximation of derivatives in a convection-diffusion two-point boundary value problem. *Appl. Numer. Math.*, **39**:47–60, 2001.

[50] N. Kopteva and M. Stynes. A robust adaptive method for a quasilinear one dimensional convection–diffusion problem. SIAM *J. Numer. Anal.*, **39**(4):1446–1467, 2001.

[51] P.A. Lagerstrom. *Matched Asymptotic Expansions*. Springer-Verlag, New York, 1988.

[52] P.A. Lagerstrom and R.G. Casten. Basic concepts underlying singular perturbations techniques. SIAM *Review*, **14**(1):63–120, 1972.

[53] C.G. Lange and R.M. Miura. Singular perturbation analysis of boundary-value problems for differential-difference equations. SIAM *J. Appl. Math.*, **42**(3):502–531, 1982.

[54] C.G. Lange and R.M. Miura. Singular perturbation analysis of boundary-value problems for differential-difference equations. II. rapid oscillations and resonances. SIAM *J. Appl. Math.*, **45**(5):687–707, 1985.

[55] C.G. Lange and R.M. Miura. Singular perturbation analysis of boundary-value problems for differential-difference equations. III. turning point problems. SIAM *J. Appl. Math.*, **45**(5):708–734, 1985.

[56] C.G. Lange and R.M. Miura. Singular perturbation analysis of boundary-value problems for differential-difference equations. V. small shifts with layer behavior. SIAM *J. Appl. Math.*, **54**(1):249–272, 1994.

[57] C.G. Lange and R.M. Miura. Singular perturbation analysis of boundary-value problems for differential-difference equations. VI. small shifts with rapid oscillations. SIAM *J. Appl. Math.*, **54**(1):273–283, 1994.

[58] T. Linβ. Uniform pointwise convergence of finite difference schemes using grid equidistribution. *Computing*, **66**:27–39, 2001.

[59] J. Mackenzie. Uniform convergence analysis of an upwind finite difference approximation of a convection-diffusion boundary value problem on an adaptive grid. IMA *J. Numer Anal.*, **19**:233–249, 1999.

[60] J.J.H. Miller. Sufficient conditions for the convergence, uniformly in ε, of a three-point difference scheme for a singular perturbation problem. *Lecture Notes in Mathematics*, (No. 679):55–91, 1978.

[61] J.J.H. Miller, E. O'Riordan, and G.I. Shishkin. On piecewise-uniform meshes for upwind and central-difference operators for solving singularly perturbed problems. IMA *J. Numer. Anal.*, **15**:89–99, 1995.

[62] J.J.H. Miller, E. O'Riordan, and G.I. Shishkin. *Fitted Numerical Methods for Singular Perturbation Problems*. World Scientific, Singapore, 1996.

[63] K.W. Morton. *Numerical Solution of Convection-Diffusion Problems*. Chapman & Hall, London, 1996.

[64] J.D. Murray. *Mathematical Biology*. Springer-Verlag, New York, 1989.

[65] S. Natesan, R.K. Bawa, and C. Clavero. Second-order numerical scheme for singularly perturbed reaction-diffusion Robin problems. JNAIAM *J. Numer. Anal. Ind. Appl. Math.*, **2**(3-4):177–192, 2007.

[66] S. Natesan, R.K. Bawa, and C. Clavero. Uniformly convergent compact numerical scheme for the normalized flux of singularly perturbed reaction-diffusion problems. *Int. J. Inf. Syst. Sci.*, **3**(2):207–221, 2007.

[67] S. Natesan and N. Ramanujam. 'Shooting method' for singular perturbation problems arising in chemical reactor theory. *Inter. J. Comp. Math.*, **70**(2):251–262, 1998.

[68] S. Natesan and N. Ramanujam. A "booster method" for singular perturbation problems arising in chemical reactor theory. *Appl. Math. Comput.*, **100**:27–48, 1999.

[69] S. Natesan and N. Ramanujam. Booster method for singularly perturbed one-dimensional convection-diffusion Neumann problems. *J. Optim. Theory Appl.*, **99**(1):53–72, 1999.

[70] S. Natesan and N. Ramanujam. Improvement of numerical solution of self-adjoint singular perturbation problems by incorporation of asymptotic approximations. *Appl. Math. Comput.*, **98**:199–137, 1999.

[71] S. Natesan and N. Ramanujam. An asymptotic-numerical method for singularly perturbed Robin problems-I. *Appl. Math. Comput.*, **126**(1):97–107, 2002.

[72] M.C. Natividad and M. Stynes. Richardson extrapolation for a convection-diffusion problem using Shishkin mesh. *Appl. Numer. Math.*, **45**:315–329, 2003.

[73] A.H. Nayfeh. *Perturbation Methods*. John Wiley & Sons, New York, 1973.

[74] A.H. Nayfeh. *Introduction to Perturbation Methods*. John Wiley & Sons, New York, 1981.

[75] R.E. O'Malley. *Introduction to Singular Perturbations*. Academic Press, New York, 1974.

[76] R.E. O'Malley. *Singular Perturbation Methods for Ordinary Differential Equations*. Springer, New York, 1991.

[77] K.C. Patidar and K.K. Sharma. Uniformly convergent non-standard finite difference methods for singularly perturbed differential-difference equations with delay and advance. *Int. J. Numer. Meth. Eng.*, **66**:272–296, 2006.

[78] K.C. Patidar and K.K. Sharma. ε-uniformly convergent non-standard finite difference methods for singularly perturbed differential difference equations with small delay. *Appl. Math. Comput.*, **175**:864–890, 2006.

[79] V. Pereyra and E.G. Sewell. Mesh selection for discrete solution of boundary problems in ordinary differential equations. *Numer. Math.*, **23**:261–268, 1975.

[80] L. Prandtl. Über Flussigkeitsbewegung bei sehr kleiner Reibung. In *Verhandlungen, III Inter. Math. Kongresses, Tuebner, Leipzig*, pages 484–491, 1905.

[81] Y. Qiu and D.M. Sloan. Analysis of difference approximations to a singularly perturbed two point boundary–value problem on an adaptively generated grid. *J. Comput. Appl. Math.*, **101**:1–25, 1999.

[82] Y. Qiu, D.M. Sloan, and T. Tang. Numerical solution of a singularly perturbed two point boundary–value problem using equidistribution: analysis of convergence. *J. Comput. Appl. Math.*, **116**:121–143, 2000.

[83] H.G. Roos and T. Linβ. Sufficient conditions for uniform convergence on layer-adapted grids. *Computing*, **63**:27–45, 1999.

[84] H.G. Roos, M. Stynes, and L. Tobiska. *Numerical Methods for Singularly Perturbed Differential Equations*. Springer, Berlin, 1996.

[85] R.D. Russell and J. Christiansen. Adaptive mesh selection strategies for boundary-value problems. SIAM *J. Numer. Anal.*, **15**(1):59–80, 1978.

[86] G.I Shishkin. A difference scheme on a non–uniform mesh for a differential equation with small parameter in thehighest derivative. *USSR Comput. Maths. Math. Phys.*, **23**(4):59–66, 1983.

[87] G.I. Shishkin and L.P. Shishkina. *Difference Methods For Singular Perturbation Problems*. Chapman & Hall/CRC Press, Boca Raton, FL, 2009.

[88] D.R. Smith. The multivariable method in singular perturbation analysis. SIAM *Review*, **17**(2):221–273, 1975.

[89] R.B. Stein. Some models of neuronal variability. *Biophysical Journal*, **7**:37–68, 1967.

[90] M. Stynes. Steady-state convection-diffusion problems. *Acta Numerica*, **31**:445–508, 2005.

[91] M. Stynes and E. O'Riordan. A finite element method for a singularly perturbed boundary-value problem. *Numer. Math.*, **50**:1–15, 1986.

[92] M. Stynes and H.G. Roos. The midpoint upwind scheme. *Appl. Numer. Math.*, **23**:361–374, 1997.

[93] H. Tian. The exponential asymptotic stability of singularly perturbed delay differential equations with bounded lag. *J. Math. Anal. Appl.*, **270**:143–149, 2002.

[94] F. Verhulst. *Methods and Applications of Singular Perturbations*. Springer, New York, 2005.

[95] J. Vigo-Aguiar and S. Natesan. A parallel boundary value technique for singularly perturbed two-point boundary value problems. *J. Supercomput.*, **27**(2):195–206, 2004.

[96] J. Vigo-Aguiar and S. Natesan. An efficient numerical method for singular perturbation problems. *J. Comput. Appl. Math.*, **192**(1):132–141, 2006.

[97] R. Vulanović. Finite difference schemes for qualsilinear singular perturbation problems. *J. Comput. Appl. Math.*, 26:345–365, 1989.

[98] R. Vulanović, D. Herceg, and N. Petrović. On the extrapolation for a singularly perturbed boundary-value problem. *Computing*, **36**:69–79, 1986.

[99] W. Wasow. *On boundary layer problems in the theory of ordinary differential equations*. PhD thesis, New York University.

[100] A.B. White. On selection of equidistributing meshes for two-point boundary-value problems. SIAM *J. Numer. Anal.*, **16**(3):472–502, 1979.

List of published and communicated papers

Based on the work in this thesis, the following research articles are published or communicated.

1. **J. Mohapatra** and S. Natesan, "Uniformly convergent numerical method for singularly perturbed differential-difference equation using grid equidistribution", *Int. J. Numer. Meth. Biomed. Engng.*, *DOI:10.1002/cnm.1370*.
2. **J. Mohapatra** and S. Natesan, "The parameter-robust numerical method based on defect-correction technique for singularly perturbed delay differential equations with layer behavior", *Int. J. Comput. Methods*, *(In Press)*.
3. **J. Mohapatra** and S. Natesan, "Uniform convergence analysis of finite difference scheme for singularly perturbed delay differential equation on an adaptively generated grid", *Numer. Math. Theory Methods Appl.*, **16**(1), 1–22, 2010.
4. **J. Mohapatra** and S. Natesan, "Uniformly convergent second-order numerical method for a singularly perturbed delay differential equations", *Neural Parallel Sci. Comput.*, **16**, 353–370, 2008.
5. **J. Mohapatra** and S. Natesan, "Numerical solution of a convection-diffusion problem with Robin boundary conditions on an adaptively generated grid", *Resubmitted to J. Appl. Math. Comput. after minor revision*.
6. **J. Mohapatra** and S. Natesan, "Parameter-uniform numerical methods for global solution and global normalized flux of singularly perturbed boundary value problems using grid equidistribution", *Communicated*.

Conference Proceedings

1. **J. Mohapatra** and S. Natesan, "ε-uniform convergent numerical scheme for singularly perturbed delay differential equation on an adaptively generated grid", 53^{rd} *CONGRESS OF ISTAM (An International Meet), Osmania University, Hyderbad, Dec., 2008* .
2. **J. Mohapatra** and S. Natesan, "Parameter-uniform convergence analysis of finite difference scheme for two-parameter singular perturbation problems on the equidistributed grids", 35^{th} *National Conference, Odisha Mathematical Society, Bhubaneswar, Feb., 2008*.